

Oncogene driver mutations and copy number variation as markers for predicting drug resistance and disease outcome in NSCLC

Thesis submitted for the degree of

Doctor of Philosophy

At the University of Leicester

By

Almahdi Jaber MRes (Newcastle upon Tyne)

Department of Cancer Studies

University of Leicester

September 2016

Abstract

Oncogene driver mutations and copy number variation as markers for predicting drug resistance and disease outcome in NSCLC

Almahdi Jaber

Introduction: Worldwide, lung cancer is the leading cause of death. Non-small cell lung cancer (NSCLC) patients with *KRAS* mutations have a poor prognosis and show drug resistance, with *MCL-1* implicated in this mechanism via evasion of apoptosis. This study is aimed at evaluating the relationship between key oncogene driver mutations, *MCL-1* regulation and *MCL-1*-induced drug resistance.

Methods: We analysed 39 adenocarcinomas (ADCs), 38 squamous cell carcinomas (SCCs), two large cell lung carcinomas (LCCs) and cell lines. A PNA-LNA-based TaqMan qPCR approach was performed for eight *KRAS*, one *BRAF*, three *PIK3CA* and one *EGFR* mutations. *MCL-1*, *PIK3CA* and *SOX2* were analysed for copy number variation (CNV). Immunohistochemistry (IHC) and *in situ* hybridization (ISH) was performed for protein and mRNA, respectively. Alamar blue assay was used to evaluate drug responses.

Results: *KRAS* mutations were detected in 36% of ADCs and 0% of SCCs, whereas *PIK3CA* mutation was most common in SCC (15.7%) and found in 5% of ADCs. *MCL-1*, *PIK3CA* and *SOX2* amplification were detected in 13%, 74% and 86.6% of SCCs respectively, and were detected in 2.5%, 25.9% and 13.3% of ADCs respectively. *MCL-1*-amplified tumours demonstrated high expression of *MCL-1* mRNA compared to non-amplified ($p < 0.05$). Cases with high phospho-ERK and phospho-AKT also showed high expression of *MCL-1* mRNA. No growth inhibition was detected in cell lines treated with 5 μ M of SH-4-54 inhibitor; however, 10 μ M caused 99.9% growth inhibition. *Ex vivo* experiments mimicking the *in vivo* tumour environment demonstrated that NSCLCs are sensitive to cisplatin, one of which was *MCL-1*-amplified.

Conclusion: We have shown that *KRAS* mutation is common in ADC, whereas *PIK3CA* is more common in SCC. Importantly, we have highlighted that CNV of *MCL-1* may be an important driver in resistance to chemotherapy. The JAK/STAT pathway was the key regulator for *MCL-1* transcription. Resistance to cisplatin was observed in the *KRAS* mutant cell, *MCL-1*-amplified cell, cells harbouring *MCL-1* gain and Chr1 polysomy but not the *SOX2*-amplified cell.

Acknowledgements

Thanks are due to Allah for granting me the ability to complete this study.

It would have been impossible to complete this research project without the scholarship granted to me by the Libyan Government and I will be extremely grateful to them for the rest of my life.

I would like to state my sincere thanks to my supervisors Dr Howard Pringle and Dr David Guttery for unrestrained support. I would also like to express my appreciation to Linda Potter, Angie Gillies, Lindsay Primrose, Janine, Abdulrazag Ehdode, Ellie Karekla and Wen-Jing Liao.

I would like also to thank Professor Jacqui Shaw and Professor Don Jones for their support and all the postgraduate students and researchers in my department who took part in our study, in particular the students in the Department of Cancer studies.

I carried out all the experimental work for this thesis except for the explant studies which were performed and analysed by Ellie Karekla and Wen-Jing Liao.

I would like to express my appreciation to my friends for their help and support to settle well in the United Kingdom.

Many thanks also go to my daughters Alzahra and Fatima and my sons Mohammed and Abdulrahman for their presence and their sense of humour, which encouraged me to go on. Many thanks again to my brothers and sisters in my home country who have all the time encouraged me to complete this research project.

I would also like to express my sincere thanks and appreciation to my mother and my wife for their permanent support and encouragement and for the sacrifice they have made and for the care they have continually granted. So, I would like to dedicate this work to them.

Finally, I must express my many thanks to everybody that encouraged, helped and supported me whilst I have been engaged in writing this project.

Table of contents

Abstract.....	I
Acknowledgements.....	II
Table of contents.....	IV
List of Tables	IX
List of Figures	X
List of abbreviations	XIII
Chapter 1. Introduction.....	1
1.1 Epidemiology of lung cancer	2
1.2 Risk factors.....	4
1.2.1 Smoking	4
1.2.2 Air pollution.....	6
1.2.3 Role of genetic factors in lung cancer development.....	6
1.2.4 Gender determining pathogenesis and treatment response in NSCLC.....	7
1.2.5 Occupational exposure to carcinogens	7
1.2.6 Passive smoking.....	8
1.2.7 Alcohol consumption	8
1.2.8 Chronic lung disease	8
1.2.9 Ionizing radiation	9
1.2.10 Lack of physical activity and type of diet.....	9
1.3 Histological classification of lung cancer	10
1.3.1 Small cell lung cancer	11
1.3.2 Non-small cell lung cancer	12
1.3.3 Diffuse idiopathic pulmonary neuroendocrine cell hyperplasia (DIPNECH)	16
1.4 Molecular genetic alterations in NSCLC	16
1.4.1 Lung cancer susceptibility genes	17
1.5 MCL-1 regulation and apoptosis regulatory pathways	21
1.6 Diagnosis and current survival.....	24
1.7 Diagnostic molecular methods for <i>ALK</i> and <i>EGFR</i> mutations in NSCLC	27
1.7.1 Quantitative polymerase chain reaction (qPCR)	27

1.7.2	Next generation sequencing.....	28
1.7.3	Fluorescent <i>in situ</i> hybridisation.....	29
1.7.4	IHC.....	29
1.8	Therapeutic targets for NSCLC	30
1.8.1	Targeting of KRAS	30
1.8.2	Targeting of EGFR	31
1.8.3	Targeting of PIK3CA.....	32
1.8.4	Targeting of MCL-1.....	32
1.8.5	Targeting of STAT.....	33
1.8.6	Targeting of SOX2.....	34
1.9	2D and 3D cell culture models.....	34
1.10	Hypothesis.....	35
1.11	Aim and objectives.....	35
Chapter 2.	Materials and methods	36
2.1	Materials.....	37
2.1.1	q-PCR.....	37
2.1.2	Control DNAs	39
2.1.3	Tumour samples.....	39
2.1.4	DNA extraction.....	40
2.1.5	Immunostaining	41
2.1.6	Cell culture.....	43
2.1.7	<i>In-situ</i> hybridization.....	45
2.1.8	RNA extraction	46
2.1.9	Reverse transcription	46
2.1.10	Cell viability assessment.....	46
2.2	Methods.....	47
2.2.1	q-PCR.....	47
2.2.2	DNA extraction.....	53
2.2.3	Immunohistochemistry	54
2.2.4	Culture of cell lines.....	56
2.2.5	<i>In situ</i> hybridization for RNA expression in cell lines and lung tissues...57	
2.2.6	Gene expression.....	59
2.2.7	Cell viability assessment.....	61
2.2.8	Explant tissue culture and analysis	62

2.2.9	Statistical analysis	62
Chapter 3.	Genetic alterations in non-small cell lung cancer	63
3.1	Introduction	64
3.2	Aims and objectives	64
3.3	Results	65
3.3.1	Oncogene driver mutation analysis.....	65
3.3.2	Analysis of copy number changes	74
3.4	Discussion	87
3.5	Conclusions	91
Chapter 4.	Analysis of protein expression and gene transcription using immunohistochemistry and <i>in situ</i> hybridization, respectively	92
4.1	Introduction	93
4.2	Aims and objectives	93
4.3	Results	94
4.3.1	Assessment of p-ERK expression in NSCLC.....	94
4.3.2	Assessment of p-AKT expression in NSCLC.....	98
4.3.3	MCL-1 expression analysis	101
4.3.4	<i>In situ</i> hybridization for MCL-1 mRNA detection	105
4.4	Discussion	109
4.4.1	Analysis of p-ERK.....	109
4.4.2	Analysis of p-AKT.....	110
4.4.3	Analysis of MCL-1	111
4.5	Conclusion.....	113
Chapter 5.	MCL-1 status is linked to oncogene driver mutations, copy number variation and protein expression.	114
5.1	Introduction	115
5.2	Aims and objectives	115
5.3	Results	116
5.3.1	Concurrent <i>MCL-1</i> and <i>PIK3CA</i> / <i>SOX2</i> amplification in NSCLC.....	116
5.3.2	Correlation between oncogene driver mutations and <i>MCL-1</i> amplification.....	116
5.3.3	Expression levels of the MCL-1 protein and MCL-1 mRNA in tumours harbouring mutations	118
5.3.4	Comparison of MCL-1 protein and MCL-1 mRNA levels with p-ERK and p-AKT levels	119

5.4	Discussion	121
5.5	Conclusion.....	122
Chapter 6. <i>in vitro</i> study of MCL-1 regulation and MCL-1-induced drug resistance.....		123
6.1	Introduction	124
6.2	Aim and objectives.....	124
6.3	Results	125
6.3.1	Culture of cell lines	125
6.3.2	Inhibition of JAK/STAT, PI3K/AKT/mTOR and MAPK pathways	125
6.3.3	Targeting the MCL-1 regulatory pathways in KP-2 and RERF-LC-Sq1 cell lines.....	127
6.3.4	Investigation of heat shock protein 90 (HSP90) effects on MCL-1mRNA expression	129
6.3.5	Response of <i>MCL-1</i> -amplified cell lines and other NSCLCs to cisplatin.....	130
6.3.6	Evaluation of cell viability in <i>MCL-1</i> -amplified and non-amplified cell lines after treatment with inhibitors for 24, 48 and 72 hours	132
6.3.7	Response of the cell lines to 5 μ M and 10 μ M of the inhibitors	134
6.3.8	Response to combinations of inhibitor and cisplatin	136
6.3.9	Evaluation of growth inhibition using 10 μ M cisplatin with increased doses of inhibitors.....	137
6.4	Discussion	139
6.5	Conclusion.....	144
Chapter 7. Evaluation of drugs in NSCLC explants.....		145
7.1	Introduction	146
7.2	Results	147
7.2.1	Response of NSCLC explants harbouring oncogene mutations to cisplatin.....	147
7.2.2	Response of NSCLC explants with copy number changes to cisplatin ..	148
7.2.3	Evaluating the effect of MEK inhibitor (U0126) on NSCLC explants with <i>MCL-1</i> gain.....	149
7.2.4	Evaluation of patient outcome	155
7.3	Discussion	158
7.4	Conclusion.....	160
Chapter 8. Discussion and future work		162
8.1	Discussion	163

8.2	Conclusion.....	167
8.3	Future directions.....	168
	Appendices.....	170
	References.....	175

List of Tables

Table 1.1 Mortality rates of different types of cancer and their projections from 1990 to 2030. ...	4
Table 1.2 Survival rates of patients with NSCLC in different stages represented by the 7th edition of the TNM staging system.	27
Table 2.1 List of <i>KRAS</i> primers and <i>KRAS</i> -specific probes used in mutation analysis.	37
Table 2.2 List of allele specific <i>KRAS</i> primers with tags.	38
Table 2.3 List of <i>KRAS</i> LNA primers.	39
Table 2.4 List of <i>PIK3CA</i> primers.	36
Table 2.5 List of <i>BRAF</i> (V600E) LNA primers, <i>EGFR</i> (L858R) primers and <i>ALU</i> repeat assay.	37
Table 2.6 List of copy number analysis and gene expression assays.	38
Table 2.7 List of positive and negative control DNA.	39
Table 2.8 Clinicopathological features of NSCLC tissues.	40
Table 2.9 List of reagents and equipment used for DNA extraction.	41
Table 2.10 List of reagents and equipment used for immunostaining.	42
Table 2.11 list of antibodies used for immunostaining.	43
Table 2.12 List of equipment and reagents used for cell culture.	43
Table 2.13 List of grown cell lines in this study.	44
Table 2.14 Reagents and equipment used for cyto block preparation.	45
Table 2.15 List of materials used for ISH.	45
Table 2.16 Material used for RNA extraction.	46
Table 2.17 List of reagents and equipment used for reverse transcription.	46
Table 2.18 Listed of the used drug in this study.	47
Table 2.19 List of materials used for cell viability assessment.	47
Table 3.1 Examples of mutations detected in tumour samples.	71
Table 3.2 Focal amplification of <i>MCL-1</i> in lung cancer cell lines.	78
Table 3.3 <i>MCL-1</i> copy number gain in lung cancer cell lines.	79
Table 3.4 Copy number variation in NSCLC.	86
Table 4.1 Expression of p-AKT in NSCLC.	100
Table 4.2. Expression of MCL-1 protein in NSCLC.	104
Table 4.3. Expression levels of <i>MCL-1</i> mRNA in NSCLC.	108
Table 5.1 Co-existence of <i>MCL-1</i> , <i>PIK3CA</i> and <i>SOX2</i> amplification.	116
Table 5.2 Expression levels of MCL-1 and MCL-1 mRNA in NSCLC cases.	118
Table 7.1 Patient characteristics and outcomes.	155
Table 9.1 Summary table of all cases.	171
Table 9.2 proteins and <i>MCL-1</i> mRNA expression levels.	174

List of Figures

Figure 1.1 Lung cancer incidences.....	3
Figure 1.2 Pathogenesis and development of lung cancer.	6
Figure 1.3 Histological appearance of the major lung cancer types.	10
Figure 1.4 Regulation of MCL-1 at the cellular level.....	22
Figure 1.5 Regulation of apoptosis via the MAPK and PI3K pathways.....	24
Figure 1.6 Lung cancer stages.....	26
Figure 2.1 Locations of the designed assay for <i>MCL-1</i> and reference genes.....	50
Figure 2.2 Duplex ratio test for gain and amplification analysis.	50
Figure 2.3 Cycling condition of qPCR.....	51
Figure 2.4 Standard curve for DNA concentration measurement. R	52
Figure 3.1 Probe method for mutation analysis.	67
Figure 3.2 Tagged specific primer vs LNA specific primer.....	68
Figure 3.3 PNA clamping.	69
Figure 3.4 Detection of low mutant DNA using the PNA clamping technique.....	69
Figure 3.5 Validation of <i>PIK3CA</i> assays.	70
Figure 3.6 Frequencies of oncogene driver mutations in NSCLC.	72
Figure 3.7 Frequency of KRAS mutations.....	73
Figure 3.8 Frequencies of <i>PIK3CA</i> mutations in NSCLC.	74
Figure 3.9 <i>MCL-1</i> copy number changes in lung cancer cell lines.	76
Figure 3.10 <i>MCL-1</i> amplification and gain in lung cancer cell lines.....	77
Figure 3.11 Amplification vs gain in tumour samples.	81
Figure 3.12 <i>MCL-1</i> amplification and gain in tumour samples..	82
Figure 3.13 <i>PIK3CA</i> and <i>SOX2</i> amplifications in tumour samples.	84
Figure 3.14 <i>PIK3CA</i> and <i>SOX2</i> gain in tumour samples..	85
Figure 4.1 Histology of Lung cancer.	94
Figure 4.2 Expression of p-ERK across lung tissue.....	95
Figure 4.3 p-ERK expression in tumour microenvironment.....	95
Figure 4.4 p-ERK expression in NSCLC. T	97
Figure 4.5 Expression of p-ERK according to stage of the disease..	98
Figure 4.6 Expression of p-AKT in normal and tumour samples..	99
Figure 4.7 Expression of p-AKT in cancer cells.....	101
Figure 4.8 Assessment and optimisation of MCL-1 Ab (S-19) using tonsil specimens.	102
Figure 4.9 Assessment of MCL-1 Ab (S-19) specificity using MCL-1 amplified cell line.....	102
Figure 4.10 Expression of MCL-1 in normal and tumour lung tissue.	103

Figure 4.11 Expression of <i>MCL-1</i> mRNA in <i>MCL-1</i> -amplified cell line (H1395) and <i>MCL-1</i> non-amplified cell line (H1355).....	105
Figure 4.12 <i>MCL-1</i> expression in tumour samples.....	106
Figure 4.13 <i>MCL-1</i> expression in normal diploid and amplified tumour cells.....	107
Figure 5.1 Analysis of <i>MCL-1</i> amplification in cell lines harbouring oncogene driver mutations.....	117
Figure 5.2 <i>MCL-1</i> and <i>MCL-1</i> mRNA expression level in mutant cases of NSCLC.	119
Figure 5.3 <i>MCL-1</i> overexpression correlates with MAP and PI3K pathways in NSCLC.....	120
Figure 5.4 <i>MCL-1</i> and <i>MCL-1</i> mRNA expression levels in NSCLC.	121
Figure 6.1 Expression levels of <i>MCL-1</i> mRNA in cell lines treated with targeted therapies...	127
Figure 6.2 Response of <i>KRAS</i> mutant cell lines to the inhibitor..	128
Figure 6.3 Response of the RERF-LC-Sq1 cell line to targeted therapies.....	129
Figure 6.4 Effect of HSP90 on <i>MCL-1</i> mRNA in normal control and <i>MCL-1</i> -amplified cell lines.....	130
Figure 6.5 Response of NSCLC cell line to cisplatin.	131
Figure 6.6 Responses of SCC cell line and ADC cell lines to cisplatin.	132
Figure 6.7 Responses of cell lines to inhibitors.	133
Figure 6.8 Response of the cell lines to a 5 μ M concentration of the inhibitors.....	135
Figure 6.9 Response of the cell lines to a 10 μ M concentration of the inhibitors.....	135
Figure 6.10 Responses of H1355 and H1395 cell lines to combined therapy.....	136
Figure 6.11 Response of the NSCLC cell line to combined therapy using 50 μ M cisplatin. ...	137
Figure 6.12 Growth inhibition at 5 μ M inhibitor concentrations combined with cisplatin.....	138
Figure 6.13 Response of cell lines to 10 μ M inhibitor concentrations alone, and combined with 10 μ M cisplatin.	139
Figure 7.1 Response of NSCLC explants with oncogene mutations to 50 μ M cisplatin.	147
Figure 7.2 Response of NSCLC explants harbouring <i>PIK3CA</i> amplification, <i>MCL-1</i> amplification and <i>SOX2</i> amplification and chromosome 1 polysomy to 50 μ M cisplatin.....	148
Figure 7.3 Response of NSCLC explants to U0126.....	149
Figure 7.4 Responses of NSCLC explants to cisplatin according to <i>MCL-1</i> status.....	151
Figure 7.5 Responses of NSCLC explants to cisplatin according to <i>MCL-1</i> status.....	152
Figure 7.6 <i>MCL-1</i> and <i>MCL-1</i> mRNA are not associated to drug resistance in the explant system.....	152
Figure 7.7 Response of NSCLC explants to cisplatin according to p-ERK expression.....	153
Figure 7.8 Response of NSCLC explants to cisplatin according to p-AKT expression.....	154
Figure 7.9 p-ERK and p-AKT not correlated to drug resistance.....	154
Figure 7.10 Correlation between patient survival and <i>MCL-1</i> and <i>MCL-1</i> mRNA expression.	157

Figure 7.11 Correlation between patient survival and p-ERK and p-AKT expression..... 157

List of abbreviations

A	Adenine
AAH	Atypical adenomatous hyperplasia
ADC	Adenocarcinoma
AIS	Adenocarcinoma <i>in situ</i>
AIS	Adenocarcinoma in situ
AKT	v-akt murine thymoma viral oncogene homolog
Amp	Amplification
AP1	Activator protein1
ATS	American thoracic society
BAX	BCL-2 associated X protein
BCL-2	B-cell lymphoma2
BRAF	v-raf murine sarcoma viral oncogene homolog B1
C	Cytosine
CAPN7	Calpain 7
CCT3	Chaperonin Containing TCP1, Subunit 3 genes
cDNA	Complimentary DNA
Chr	Chromosome
CIS	Carcinoma <i>in situ</i>
CNV	Copy number variation
COPD	Chronic obstructive pulmonary disease
CT	Cycle threshold
DAB	Diaminobenzidine
DapB	Bacterial dap gene
DIPNECH	Diffuse idiopathic pulmonary neuroendocrine cell hyperplasia

DMF	Dimethylformamide
DMSO	Dimethyl sulfoxide
DNA	Deoxyribonucleic acid
EDTA	Ethylenediaminetetraacetic acid
<i>EGFR</i>	Epidermal growth factor receptor
EPIC	European prospective investigation into cancer and nutrition
ERK	Extracellular-signal-regulated kinase
ERS	European respiratory society
F	Forward
FBS	Foetal bovine serum
FTIs	Farnasyl transferase inhibitors
G	Guanine
GAPDH	Glyceraldehyde 3-phosphate dehydrogenase
GATA2	GATA binding protein 2
Glu	Glutamine
GTPase	Guanosine triphosphate hydrolase
H&E	Haematoxylin and Eosin
<i>H6PD</i>	Hexose-6-Phosphate Dehydrogenase gene
HCl	Hydrochloric acid
IASLC	International association for the study of lung cancer
IC50	Half maximal inhibitory concentration
IHC	Immunohistochemistry
IMS	Industrial methylated spirits
ISH	<i>In situ</i> hybridization
JAK	Janus kinase

<i>KRAS</i>	Kirsten Rat Sarcoma Viral Oncogene
LCC	Large cell lung carcinoma
LNA	Locked nucleic acid
LOD	Limit of detection
MAPK	Mitogen activated protein kinase
MCL1	Myeloid cell leukaemia 1
MDM2	Mouse double minute 2 homolog
MEK	Mitogen-activated protein kinase kinase
MGB	Minor groove binder
MIA	Minimally invasive adenocarcinoma
mRNA	Messenger RNA
mTOR	Mammalian target of rapamycin
MUT	Mutant
NaCl	Sodium chloride
NaOH	Sodium hydroxide
NNK	Nicotine-derived nitrosamine ketone
NRAS	Neuroblastoma RAS viral (v-ras) oncogene homolog
NSCLC	Non-small cell lung cancer
PAHs	Polycyclic aromatic hydrocarbons
p-AKT	Phospho-AKT
PBS	Phosphate buffer saline
Pen-strep	Penicillin streptomycin
p-ERK	Phospho-ERK
PI3K	Phosphoinositide 3-kinase
<i>PIK3CA</i>	Phosphatidylinositol -4, 5-Biphosphate 3-kinase catalytic subunit alpha

PIP3	Phosphatidylinositol (3, 4, 5) triphosphate
PNA	Peptide nucleic acid
POLR2A	Polymerase (RNA)II subunit A
PTB	Pulmonary tuberculosis
PTEN	Phosphatase and tensin homolog
qPCR	Quantitative real-time PCR
R	Reverse
Ref	Reference
RNA	Ribonucleic acid
ROS	Reactive oxygen species
RT	Reverse transcription
RTK	Tyrosine kinase receptor
SCC	Squamous cell carcinoma
SCLC	Small cell lung cancer
SDS	Sodium dodecyl sulphate
SHS	Second hand smoke
<i>SOX2</i>	Sex determining region Y-box 2
STAT	Signal transducer and activator of transcription
T	Thiamine
TBS	Tris-buffered saline
TE	Trypsin/EDTA
TNM system	Tumour Node Metastasis system
<i>TP53</i>	Tumour protein 53
TS	Tobacco smoke
TTF1	Thyroid transcription factor 1

<i>UBC</i>	Ubiquitin C
UHL	University Hospital of Leicester
UPH2O	Ultra-pure water
WES	Whole exome sequencing
WGS	Whole genome sequencing
WT	Wild type

Chapter 1. Introduction

1.1 Epidemiology of lung cancer

Lung cancer is the leading cause of cancer death worldwide (Imielinski *et al.*, 2012) accounting for approximately 28% of all cancer-related deaths (Huncharek *et al.*, 1999). Annually, over 1.3 million people die from lung cancer (Imielinski *et al.*, 2012), with a large proportion of lung cancers being diagnosed between the ages of 70-74 years (Zhong *et al.*, 2005). Sixty one percent of patients with lung cancer are 70 years old and over (Cancer Research UK, 2016). Non-small cell lung cancer (NSCLC) is the most common type of primary lung cancer, accounting for approximately 85% of new diagnoses every year and can be classified into two major histologic subtypes of NSCLC are adenocarcinoma (ADC) and squamous cell carcinoma (SCC) (Dearden *et al.*, 2013). Five year survival ranges from 25-45% in patients with stage I and stage II of lung cancer, whereas patients with stage IIIb and IIIa have a five year survival of 5% and 15%, respectively, and long-term survival is rare in patients with stage IV or metastatic disease (Huncharek *et al.*, 1999). Figure 1.1 shows the incidence of lung cancer in different age groups of patients.

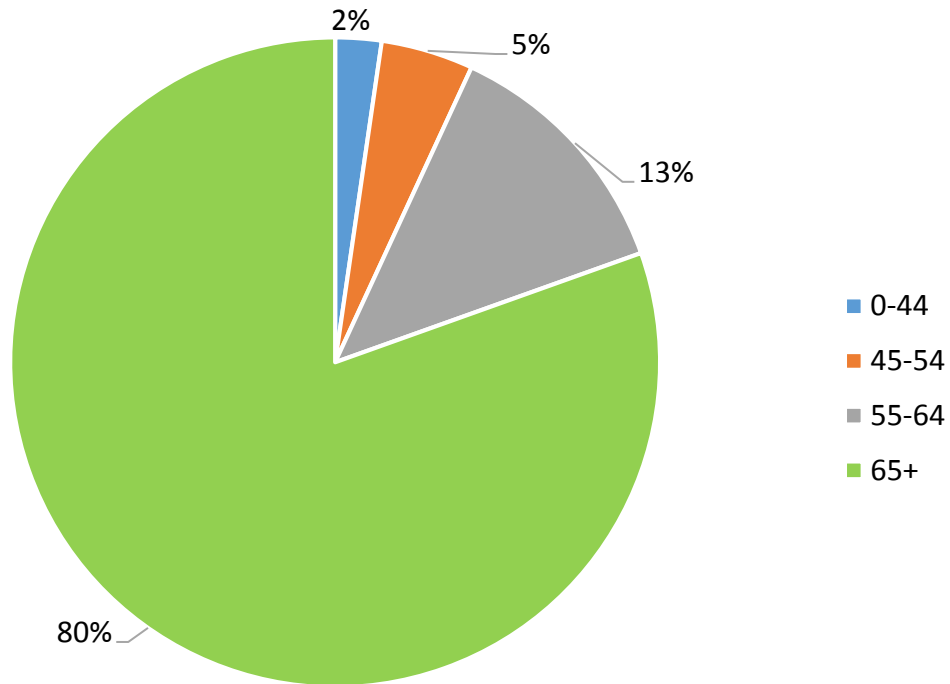


Figure 1.1 Lung cancer incidences. Incidence of lung cancer is higher in people 65 years old and above (80%) and decreases in age groups below 65 years, accounting for 2%, 5% and 13% in age groups of 0-44, 45-54 and 55-64 years, respectively.

Globally, lung cancer incidence and mortality is approximately three-fold higher in men compared to women (Freedman *et al.*, 2008). Cigarette smokers are 15-fold more likely to die from lung malignancies compared to non-smokers (Youlden *et al.*, 2008), with studies indicating that the risk of lung cancer in male smokers is less than in female smokers (Freedman *et al.*, 2008). However, studies are contradictory (Bain *et al.*, 2004). Despite advances in developing chemotherapies, the survival rate and prognosis of the disease is still poor (Youlden *et al.*, 2008). Statistics show that lung cancer is the main cause of cancer death and mortality rates due to lung cancer in the UK will increase in the coming decades (Table 1.1) (Cancer research UK).

Cancer Site	1990	Cancer Site	2010	Cancer Site	2030
Lung	39,176	Lung	34,859	Lung	44,986
Bowel	19,365	Bowel	16,013	Bowel	19,032
Breast	15,141	Breast	11,556	Prostate	16,304
Stomach	9,795	Prostate	10,721	Pancreas	11,449
Prostate	8,926	Pancreas	7,901	Breast	11,133
Pancreas	6,935	Oesophagus	7,610	Oesophagus	10,087
Oesophagus	5,979	Stomach	4,960	Liver	7,918
Bladder	5,468	Bladder	4,907	Bladder	6,272
Ovary	4,528	Leukaemia	4,504	Leukaemia	5,500
Non-Hodgkin Lymphoma	3,998	Non-Hodgkin Lymphoma	4,452	Kidney	5,097

Table 1.1 Mortality rates of different types of cancer and their projections from 1990 to 2030. This table shows the incidence of lung cancer in people between 1990 and 2010, and the projected incidence to 2030. This projected data shows that lung cancer may still be the biggest killer amongst all types of cancers even in 2030 in the UK. Adapted from <http://www.cancerresearchuk.org/health-professional/cancer-statistics/mortality/projections#heading-Four>. [February/2014]

1.2 Risk factors

1.2.1 Smoking

Experimental and epidemiological studies suggest that different types of cancer, such as bladder, pancreatic, oral, cervical, skin and lung cancer can be positively linked to tobacco smoke (TS), which contains over 60 carcinogens, and that approximately 90% of all lung cancers are caused by TS (Zhong *et al.*, 2005). Polycyclic aromatic hydrocarbons (PAHs) and 4-(methyl nitrosamino)-1-(3-pyridyl)-1-butanone (NNK) are constituents of tobacco smoke carcinogens, with the carcinogenicity of PAHs and NKK appearing by metabolic activation; this activation is mediated by cytochrome P450 enzymes. The P450 enzymes

covert the carcinogens to water soluble compounds through the addition of an oxygen atom, with the products further metabolized by a phase two enzyme to highly water soluble compounds (Pfeifer *et al.*, 2002). The disturbance to the balance between metabolic activation and detoxification determine the risk of cancer development (Figure 1.2). This process is controlled by individual variation, with metabolites of PAHs and NKK usually attaching covalently to DNA at adenine and guanine rings, forming a DNA adduct (Hecht, 1999). In this process, tumour suppressor genes and proto-oncogenes can be targeted by activated carcinogens (Pfeifer *et al.*, 2002), with the failure of repair mechanisms and the persistence of the DNA adduct resulting in a permanent mutation (Hecht, 1999). Moreover, tobacco smoke contains carcinogenic metals, radioactive materials, and free radical and oxidative agents. Inhalation of cigarette smoke causes an inflammatory reaction, which in turn leads to formation of additional reactive oxygen species (ROS), and it has been demonstrated that proliferation of pulmonary epithelium and squamous metaplasia are caused by TS in a dose-dependent manner, with mitogen-activated protein kinase (MAPK)/activator protein1 (AP1) being implicated in the pathogenesis of TS-induced lung cancer (Zhong *et al.*, 2005). Sequencing of the NCI-H209 lung cancer cell line genome demonstrated presence of 22,910 somatic mutations, with 134 of these mutations being detected in coding exons and all of them directly resulting from exposure to tobacco carcinogens, with one mutation developing for every 15 cigarettes smoked (Pleasant *et al.*, 2010).

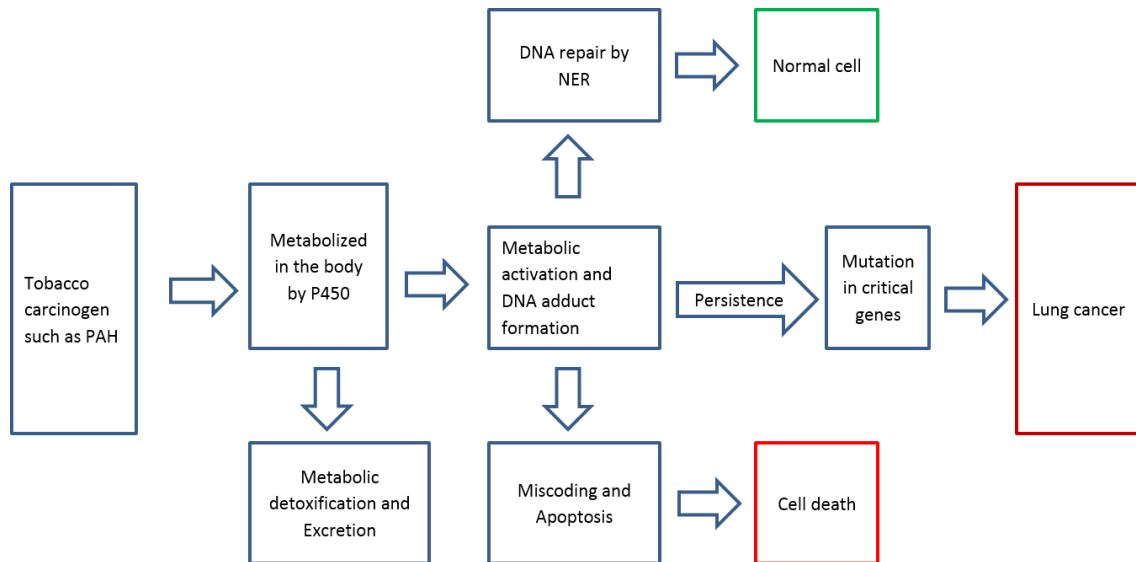


Figure 1.2 Pathogenesis and development of lung cancer. Metabolism of tobacco carcinogens leads to detoxification or metabolic activation of the carcinogens, with their activation resulting in adduct formation and lung cancer development. Adapted and modified from (Hecht, S. S. 1999).

1.2.2 Air pollution

Long-term exposure to polluted air, which contains different carcinogens such as PAH compounds can lead to lung cancer development (Molina *et al.*, 2008). These fine particulates may increase the risk of lung cancer through the generation of reactive oxygen species (ROS), inflammatory injuries, and oxidative damage to DNA (Turner *et al.*, 2011). In Europe, urban air pollution accounts for approximately 11% of lung cancers (Molina *et al.*, 2008). From different countries around the world, epidemiologic studies have revealed that air pollution in industrially polluted zones increases the rate of lung cancer by a factor of 1.5 (Nyberg *et al.*, 2000).

1.2.3 Role of genetic factors in lung cancer development

The hereditary influence of lung cancer development has been known for the last 60 years. Three separate studies have demonstrated the presence of a marker associated with lung cancers on chromosome 15; the marker region contains three genes involved in the coding

of nicotinic acetylcholine receptors, with all three studies showing that the risk of lung cancer development in people who have one extra copy of the marker is about 30% more and 70-80% more in people harbouring two extra copies. All three research groups have suggested that the marker region on chromosome 15 is a risk factor for lung cancer development, and one study suggests that lung cancer is indirectly linked to nicotine addiction (Molina *et al.*, 2008). In addition, Li-Fraumeni syndrome, which is a hereditary syndrome that leads to early development of different cancers, demonstrates the crucial role of genetic risk factors in cancer development. 50-70% of families with Li-Fraumeni syndrome carry the germ line *TP53* mutation, and lung cancer accounts for about 4% among all cancers in these populations (Hwang *et al.*, 2003).

1.2.4 Gender determining pathogenesis and treatment response in NSCLC

Many oncologists believe that lung cancer behaves differently between genders. Regardless of the epidemiological difference, there is also a different therapeutic outcome between males and females with oestrogen and both oestrogen receptors (alpha and beta) seemingly involved in the pathogenesis and development of lung cancer. It has been suggested that the difference in concentration of sex hormones is the best explanation for the gender disparities in lung cancer susceptibility (Paggi *et al.*, 2010).

1.2.5 Occupational exposure to carcinogens

According to the International Agency for Research on Cancer (IARC), 12 occupational exposure factors are classified as carcinogens for lung cancer including arsenic, asbestos, aluminium production, beryllium, cadmium, soot, nickel, coal and coke gasification fumes, crystalline silica, hexavalent chromium, bis-chloromethyl ether and radon gas (Gustavsson *et al.*, 2000). Several studies have suggested that approximately 15% of lung

cancers could be referred to as “occupational exposure-related” lung cancer (Nemery, 1990).

1.2.6 Passive smoking

Passive smoking, which is also known as environmental smoke, has been classified by different governments and authorities as a lung carcinogen (Besaratina and Pfeifer, 2008). Globally, second-hand smoke causes approximately 600,000 deaths per year and the study of the chemical composition of tobacco smoke have suggested that side stream smoke is more toxic than mainstream (Czogala *et al.*, 2014) due to the formation of aromatic amines at low burning temperatures (Besaratina and Pfeifer, 2008). Despite several studies indicating that side stream smoke is more carcinogenic than mainstream smoke, more studies on the mechanisms of carcinogenesis by side stream smoke are required (Lee *et al.*, 2015).

1.2.7 Alcohol consumption

Alcohol increases the risk of lung cancer development through acetaldehyde (an alcohol metabolite), which is classified as a carcinogen by the International Agency of Research on Cancer. Some evidence from a study conducted on Chinese males showed that familial susceptibility to lung cancer has the greatest contribution in lung cancer development in heavy drinkers (Tse *et al.*, 2012). However, other studies indicated that alcohol consumption is a risk factor for lung cancer development in smokers but not in non-smokers (Bagnardi *et al.*, 2009).

1.2.8 Chronic lung disease

Chronic obstructive pulmonary disease (COPD) has been suggested as a lung cancer risk factor for over 30 years, with approximately 50-80% of lung cancer patients being diagnosed with COPD. Chronic inflammation of the air passage plays a key role in lung

cancer development (Schroedl and Kalhan, 2012), with studies suggesting that asthma can increase the risk of lung cancer based on the antigenic stimulation theory (i.e. through chronic inflammation). In contrast, enhanced immune surveillance theory, which is based on detection and elimination of foreign substances and cells via the immune system, suggests that asthma can decrease the risk of lung cancer via increased clearance of the bronchoalveolar cell lining from foreign substances including carcinogens and toxins (Rosenberger *et al.*, 2012).

1.2.9 Ionizing radiation

Ionizing radiation has been suggested to be a carcinogenic factor in lung cancer development in different populations; ionizing radiation carcinogenicity has been demonstrated in atomic bomb survivors from Hiroshima and Nagasaki, uranium miners and patients with Hodgkin's lymphoma who have undergone radiotherapy, and an increased incidence of lung cancer in breast cancer patients who received radiotherapy has also been observed (Neugut *et al.*, 1994).

1.2.10 Lack of physical activity and type of diet

One factor that may reduce the incidence and risk of lung cancer is physical activity, with epidemiological studies demonstrating that physical activity can reduce the risk of lung cancer by 20-30% in women and 20-50% in men (Buffart *et al.*, 2014).

The European Prospective Investigation into Cancer and nutrition (EPIC) study has connected fruit and vegetable intake with the prevalence of lung cancer. This study showed that a high intake of fruit decreases the risk of lung cancer, and that a high consumption of vegetables decreases development of lung cancer in current smokers. In particular, the risk of SCC in current smokers is greatly reduced in those who consumed large amounts of fruit and vegetables (Büchner *et al.*, 2010). Studies have also shown the

potential role of vitamin A and its precursor in chemoprevention, including an inverse effect of beta-carotene on lung cancer (Gallicchio *et al.*, 2008).

1.3 Histological classification of lung cancer

Based on their histology, lung cancers can be divided into two main subtypes: small cell lung cancer (SCLC) and non-small cell lung cancer (NSCLC). NSCLC is further subdivided into three different histological subtypes, namely squamous cell carcinoma (SCC), adenocarcinoma (ADC) and large cell lung carcinoma (LCC) (Johansson *et al.*, 2004). Figure 1.3 demonstrates the major histological types of lung cancer.

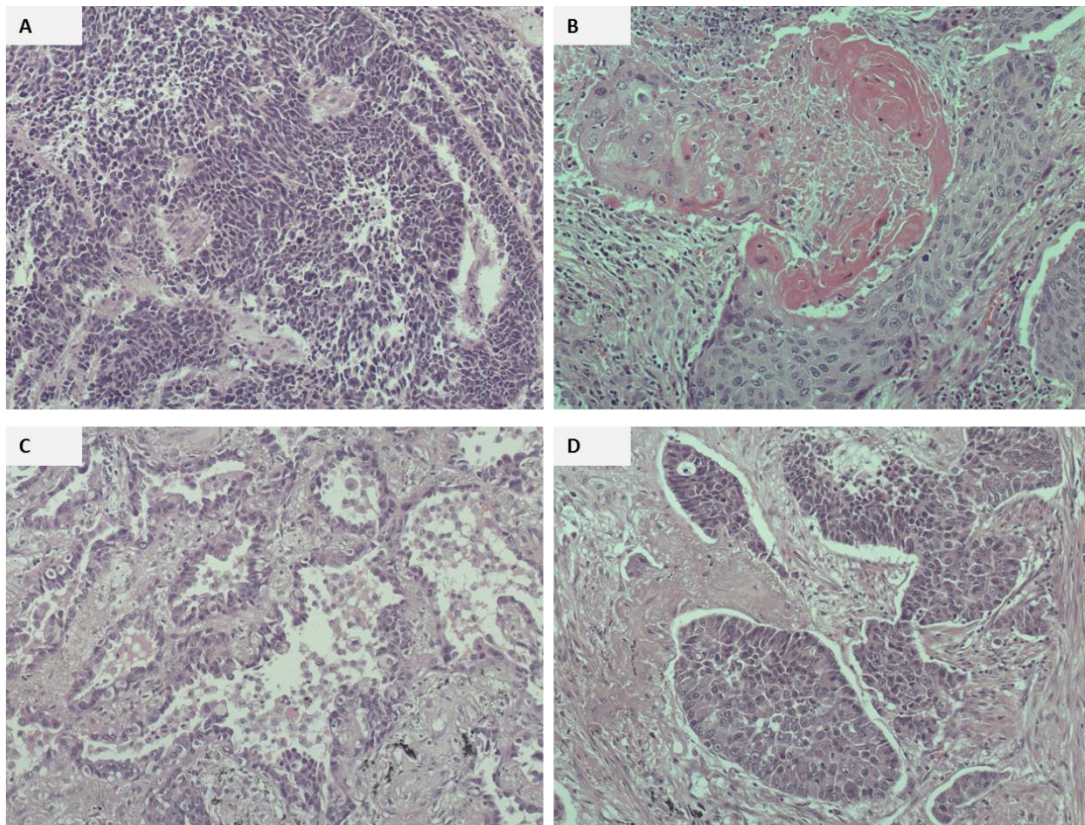


Figure 1.3 Histological appearance of the major lung cancer types. (A) This H&E stain illustrates the histological features of SCLC in which tumour cells appear as small spindle-shaped cells like oats. (B) The histological features of squamous cell carcinoma with the clear presence of keratin in the centre of the tumour. (C) A lepidic predominant type of adenocarcinoma and (D) large cell carcinoma, which appears as a nest of large polygonal cells with prominent nucleoli and vesicular nuclei.

1.3.1 Small cell lung cancer

SCLC is one of the most devastating classes of lung cancer. SCLC belongs to the neuroendocrine subtype, representing 15% of all lung cancers (Zhang and He, 2013) and is usually a disease of heavy smokers (Osann *et al.*, 2000). Small size, round to spindle shape, scant cytoplasm, finely granular nuclear chromatin and indistinctive nucleoli are characteristic features of small cell lung cancer (Travis, 2011). Nearly 75% of SCLCs appear as perihilar nodules. SCLC is usually located in the peribronchial region and then extends to peribronchial tissues and bronchial submucosa; however, endobronchial lesion is rare in SCLC. Bronchial obstruction is usually caused by external pressure (Travis, 2011). Early death and frequent metastasis is observed in SCLC (Zhang and He, 2013), with survival of untreated patients being four to five months, and 9% chance of survival to one year. Patients who respond to *EGFR* tyrosine kinase inhibitors develop resistance after a median of twelve months (Tong and Taira, 2012). SCLC is classified as:

A) Limited stage: the tumour is restricted to one hemithorax and ipsilateral supraclavicular lymph nodes. The main treatment for patients with limited-stage SCLC is a combination of chemotherapy and radiotherapy, which is curative in 20–25% the patients (Kalemkerian, 2011). However, the prognosis for patients with limited disease is poor, with a median survival time of 16-24 months (Tong and Taira, 2012).

B) Extensive stage: the disease is characterized by pericardial effusions or malignant pleural effusion, involvement of supraclavicular or contralateral hilar lymph nodes, and haematogenous metastasis. The extensive-stage of SCLC is incurable (Kalemkerian, 2011), with a median survival time of 7-12 months (Tong and Taira, 2012). However, improvement in quality of life after treatment with chemotherapy has been observed (Kalemkerian, 2011).

1.3.2 Non-small cell lung cancer

1.3.2.1 Squamous cell carcinoma

Squamous cell carcinoma (SCC) usually presents in segmental bronchi and then spreads to lobar and mainstream bronchus. Historically, it has been suggested that two thirds of SCC arise centrally; however, recent studies have demonstrated that roughly 50% of SCC develops in the periphery. This type of lung cancer has been classified into papillary, basaloid and clear cells (Travis, 2011), and accounts for 30% of all lung cancers (Weeden *et al.*, 2015). Intercellular bridge, squamous pearl formation and individual keratin are the morphological features of SCC. However, these characteristics are not present in poorly differentiated types (Travis, 2011). SCC development usually undergoes a series of events before metastasis, starting from reversible precancerous lesions (hyperplasia, metaplasia) (Wistuba, 2007), followed by dysplasia and carcinoma *in situ* until an invasive and metastatic stage (Wistuba, 2012). Genetic instability, such as mutations and deletions, varies from stage to stage in SCC and its precursor lesions (Wistuba, 2007).

Squamous dysplasia arises as a result of multiple cellular and genetic alterations during bronchial carcinogenesis, starting from basal cell hyperplasia, squamous metaplasia to dysplasia and carcinoma *in situ*. Common events include allelic loss at 3p (an early event in 78% of preinvasive bronchial lesions) followed by other events such as telomere reactivation, *TP53* mutation, vascular endothelial growth factor overexpression, P16 inactivation, BCL-2 overexpression and cyclin D1 and E overexpression (Travis *et al.*, 2011). *SOX2* amplification and P16 hypermethylation have also been observed during the progression of SCC (Wistuba *et al.*, 2002).

1.3.2.2 Large cell lung carcinoma

Large cell lung carcinoma (LCC) is as a heterogeneous group of undifferentiated neoplasms arising from different cells (Travis *et al.*, 2015) and is divided into two overarching groups: neuroendocrine and non-neuroendocrine LCLC. Large cell neuroendocrine carcinoma is a rare but aggressive pulmonary neuroendocrine tumour characterized by a high mitotic rates and low nuclear-cytoplasmic ratio (Sakurai and Asamura, 2014). The majority of large cell neuroendocrine carcinomas are located in the lung periphery, but can sometimes be found centrally. Large cell neuroendocrine carcinomas are characterized by the presence of nests and sheets of large polygonal cells with predominant nucleoli and vesicular nuclei. Under the electron microscope, large cell neuroendocrine carcinoma shows features of SCC and adenocarcinoma. However, a small subset of these cells appeared to be poorly differentiated. Similarly, by immunohistochemistry, large cell neuroendocrine carcinoma showed expression of thyroid transcription factor 1 (TTF1), which is a marker for adenocarcinoma, and P63, which is a marker for SCC. A small percentage of these cells can also harbour *KRAS* mutations (Travis *et al.*, 2011).

Non-neuroendocrine LCLC is further divided into a number of sub-groups. The basaloid variant of LCC is characterized by a solid nodular or anastomotic trabecular growth pattern with peripheral palisading. The malignant cell appears as monomorphic cuboidal fusiform with granular chromatin, small nucleoli and moderately hyperchromatic nucleus. Scanty cytoplasm with high mitotic rate was observed in this type of LCC and no squamous differentiation or neuroendocrine markers are observed. (Brambilla *et al.*, 2004). Pulmonary lymphoepithelioma-like carcinoma is a rare type of lung cancer (Liang *et al.*, 2012) consisting of a syncytial growth, large vesicular nucleus, and prominent eosinophilic nucleolus accompanied with heavy lymphocytic infiltration. Epstein Barr

virus particles have also observed in the nucleus of the giant undifferentiated type of the tumour (Brambilla *et al.*, 2004).

Clear cell carcinoma and rhabdoid cell carcinoma also belong to this group of large cell carcinomas. In clear cell carcinoma tumour cells appear as polygonal with water-clear or foamy cytoplasm; whereas large cell carcinoma with a rhabdoid phenotype is characterized by rhabdoid cells containing eosinophilic cytoplasmic globules, which may be positive for vimentin and cytokeratin (Brambilla *et al.*, 2004).

1.3.2.3 Adenocarcinoma

Adenocarcinoma (ADC) ranks as the major histological subtype of lung cancer, accounting for 50% of all lung cancers (Travis, 2011). Adenocarcinoma arises from the alveolar cells of the lung (Park *et al.*, 2012). It represents the most common type of lung cancer in people under 45 years in both smokers and non-smokers. Adenocarcinoma also represents 30% of primary lung cancer amongst male smokers and 40% amongst female smokers.

According to the international association for the study of lung cancer, (IASLC), the American Thoracic Society (ATS) and the European Respiratory Society (ERS) new classification system, adenocarcinoma can be divided into four stages: preinvasive lesion, adenocarcinoma *in situ* (AIS), minimally invasive adenocarcinoma, and invasive adenocarcinoma (Brambilla, 2011). Recently, preinvasive lesions have gained prominence due to their potential for use in lung cancer screening. Preinvasive lesions are classified into four categories: squamous dysplasia/carcinoma *in situ* (CIS), atypical adenomatous hyperplasia (AAH), adenocarcinoma *in situ* (mucinous, nonmucinous or mixed) and diffuse idiopathic pulmonary neuroendocrine cell hyperplasia (DIPNECH) (Travis, 2011). AAH is characterised by proliferation of atypical columnar and cuboidal

cells along the respiratory bronchioles and alveoli, and could be a precursor of well-differentiated adenocarcinoma of the peripheral pulmonary tissue. AAH is predominantly observed in patients with adenocarcinoma (Park *et al.*, 2006), with some studies have described AAH lesions as more common in primary lung cancer (approximately 20% of samples). Histological examination shows the presence of hyperplastic pneumocytes growing along the alveolar wall and changes in the cell range from mild to moderate with hyperchromatic nuclei and prominent nucleoli, in addition to an increase in the nucleus: cytoplasmic ratio. In AAH, mitotic figure is rare and the cells are twice the size of normal adjacent cells, with an atypical nucleus in well-differentiated adenocarcinoma compared to AAH. Moreover, the cells in AAH lesions usually adhere together, and whilst the surrounding tissue is not infiltrated with chronic inflammatory cells, the alveolar wall is mildly thickened with the presence of a few inflammatory cells without scarring (Mori *et al.*, 2001). Despite the controversy around AAH as a precursor lesion for adenocarcinoma (Travis, 2011), the majority of studies have agreed that adenocarcinoma is a result of consequent changes in AAH. The presence of *EGFR* and *KRAS* mutations as an early event in concomitant AAH indicates adenocarcinomas that harbour *EGFR* and *KRAS* mutations develop from the same source.

Adenocarcinoma *in situ* (AIS) is a glandular proliferation with lepidic growth and an absence of invasion, measuring < 3 cm in diameter. The majority of cancer cells are non-mucinous, with Clara cells and type II pneumocytic proliferation. In the instance of the mucinous type (which is rare), cells appear as tall columnar goblet cells containing large amounts of atypical mucin (Travis, 2011). Minimally invasive adenocarcinoma (MIA) has small, solitary nodules with purely lepidic growth, measuring 3 cm in diameter or less, with < 5 mm of invasion. Prognosis of MIA is good, with nearly 100% survival (Van Schil *et al.*, 2012). MIA is usually non-mucinous, however, and the mucinous type is rare

(Travis, 2011). Invasive adenocarcinoma accounts for 70-90% of surgically resected lung cancers and it has recently been classified according to the predominant subtype. The majority of these tumours contain different histologic subtypes (Travis *et al.*, 2011).

1.3.3 Diffuse idiopathic pulmonary neuroendocrine cell hyperplasia (DIPNECH)

DIPNECH is a rare pulmonary disease, which is characterized by diffuse infiltration of hyperplastic neuroendocrine cells in the sub-mucosa, and is classified as a preinvasive lesion for carcinoid tumour (Travis, 2011). Proliferation of this cell proceeds through three forms: generalized proliferation of scattered neuroendocrine cells, small nodules known as neuroendocrine bodies, and proliferation of these cells in a linear manner. Proliferation is restricted to the bronchial and bronchiolar epithelium regions. In cases of extension of neuroendocrine cells beyond the basement membrane, the growth is termed tumourlet, which can be diffuse or localized; whereas, if the tumourlet is more than 5 mm in diameter, it is categorised as carcinoid (Davies *et al.*, 2007). Neuroendocrine cells produce various peptides such as bombesin and gastrin-releasing peptides, which stimulate fibroblasts, bronchoconstriction, and chemotaxis of airway cells, which may in turn cause interstitial and peribronchiolar fibrosis (Nassar *et al.*, 2011).

1.4 Molecular genetic alterations in NSCLC

Lung cancers contain many genetic and epigenetic alterations (Wistuba, 2012), estimating about 200 non-synonymous mutations per tumour (Vogelstein *et al.*, 2013). These abnormalities include activation of proto-oncogenes, and deactivation of tumour suppressor genes (Wistuba, 2012). Different studies have suggested that histologically normal bronchial epithelium and precancerous lesions harbour several genetic and epigenetic alterations, meaning that lung cancers develop due to exposure of normal cells

to multiple genetic and epigenetic changes; many of which are usually associated with tobacco smoking (Sato *et al.*, 2007).

1.4.1 Lung cancer susceptibility genes

1.4.1.1 *KRAS*

KRAS proteins are members of the GTPase family, which regulate signal transduction within the cell and control different cellular activities such as proliferation, survival growth, differentiation and migration (Takashima and Faller, 2013). *RAS* mutation causes persistent activation of the RAF/MAPK/ERK1/2 pathway (Zhong *et al.*, 2005) and is usually linked to cigarette smoke (Boch *et al.*, 2013). Disturbance in *KRAS* protein activity can lead to the development of various diseases, including cancers. Thirty percent of all human cancers harbour *KRAS* mutations, with a frequency of 16-40% in NSCLC (Takashima and Faller, 2013). It has been demonstrated that mutations in *KRAS* usually occur at codons 12, 13 and 61, and constitute 90% of all *RAS* protein family mutations (Sato *et al.*, 2007). *KRAS* mutations of codons 12 and 13 (Okabe *et al.*, 2007) have been previously shown to be more prevalent in ADC (20%) (Paez *et al.*, 2004) compared to SCC (<4%) (Pao and Girard, 2011). In ADC, codon 12 mutations represent 86% of *KRAS* mutations, the most common of which is 34G→T (G12C) (Boch *et al.*, 2013).

Patients with *KRAS* mutation have poor prognosis and overall survival (Nelson *et al.*, 1999). Activation of AKT is associated with *KRAS* mutation, and has been observed in *KRAS* mutant cells at codon 12, but not at codon 13; however, levels of ERK protein have not been correlated with the mutational status of *KRAS* (Davies *et al.*, 2011), despite several studies demonstrating that ERK staining is correlated with patient outcome, other studies have found a relationship between patient outcome and activation of MAPK/ERK (Vicent *et al.*, 2004).

Copy number gain of *KRAS* is also a common event. Gain on chromosome 6 was shown as an early event of tumour pathogenesis in murine lung cancers harbouring a *KRAS* point mutation, with studies also suggesting that deletion of *NRAS* or *HRAS* leads to increased numbers of mutant *KRAS*, which is involved in lung tumourigenesis (To et al., 2013b). Mouse model studies have demonstrated that bronchioalveolar stem cells are putative initiators of *KRAS*-mutated lung adenocarcinomas, with several lung stem cell markers being demonstrated, one of the most significant being CD133, and aldehyde dehydrogenase 1A1 (stem cell marker) expression in non-small cell lung cancer (Wistuba, 2012).

1.4.1.2 EGFR

EGFR and the other members of its family (erbB2, erbB3, and erbB4) show mutations in different types of cancers, including lung cancer (Cho, 2013), and accounts for 4.9% of NSCLC (Boch *et al.*, 2013). The *EGFR* gene is located on chromosome 7 (7p11.2) and is overexpressed in approximately 60% of NSCLCs (da Cunha Santos *et al.*, 2011), which in turn activates the MAPK and PI3K/AKT pathways, as well as the mammalian target of rapamycin (mTOR) pathway (Zhang *et al.*, 2007). The *EGFR* gene can be amplified or mutated (usually exon 18, 19, 20, 21) or both in NSCLC, with exon 19 deletion and exon 21 point mutations being the most common types of *EGFR* mutation in NSCLC (Okabe *et al.*, 2007). Point mutations of *EGFR* are usually associated with pre-invasive lesions while amplifications or gain is considered as a late event in lung cancer and associated with the invasive phenotype of lung cancer (Gazdar and Minna, 2008). Frequency of *EGFR* mutation in smokers (2.7-58.3%) is less than in non-smokers (22.7-72%), however the association between *EGFR* mutation and smoking history is still controversial (Ren *et al.*, 2012).

1.4.1.3 PIK3CA

The *PIK3CA* gene encodes the main catalytic subunit (P110 α) of PI3 kinase proteins (Samuels *et al.*, 2004). *PIK3CA* mutation is detected in approximately 3.7% of NSCLC (Gardizi *et al.*, 2012) with a higher frequency in SCC (5-16%) (Weeden *et al.*, 2015) compared to adenocarcinoma (2.9%) (Scheffler *et al.*, 2015). Exon 9 mutation (Glu542 and Glu545) is more common in lung cancer compared to exon 20 (H1047R) (Scheffler *et al.*, 2015). *PIK3CA* point mutations are detected in all histological types of both early and advanced stages of lung cancer, with *PIK3CA* copy number gain also identified in early stages of the disease, accounting for 9.6%, 42.9% and 16.7% of ADC, SCC and LCC, respectively (Okudela *et al.*, 2007). Poor prognosis in lung cancer patients with mutated *PIK3CA* has been demonstrated in previous studies (Shigaki *et al.*, 2013), however, good outcome was observed in breast cancer patients with *PIK3CA* mutation (Kalinsky *et al.*, 2009).

1.4.1.4 BRAF

The *BRAF* gene encodes a serine/threonine kinase, which is involved in the MAPK pathway via activation of both G-protein coupled receptors and receptor tyrosine kinase (Sasaki *et al.*, 2012). 5-7% of all human lung cancers harbour a *BRAF* mutation, the most common mutation being a valine to glutamate substitution at codon 600 (V600E) (Capper *et al.*, 2011). *BRAF* mutation accounts for 3% of NSCLC, and of these almost all were detected in adenocarcinoma (Brose *et al.*, 2002). Previous studies have demonstrated that *BRAF* mutation is more frequent in ADC (4.9%) compared to SCC (0.3%). Mutation of the *RAF* oncogene in NSCLC is strongly correlated with gender in particular females (Marchetti *et al.*, 2011), as well as those with a history of smoking in NSCLC (Luk *et al.*, 2015).

1.4.1.5 MCL-1

The *MCL-1* gene encodes for the MCL-1 protein (Wei *et al.*, 2012), which is an anti-apoptotic protein, belonging to the BCL-2 family and represents one of the most commonly amplified genes in human cancers (Perciavalle *et al.*, 2012) with a high prevalence in breast and lung cancer (Beroukhim *et al.*, 2010). Sensitivity to chemotherapies has been detected in MCL-1 suppressed cancer cells (Peddaboina *et al.*, 2012)

1.4.1.6 SOX2

The sex-determining region Y-box 2 (*SOX2*) transcription factor is located on the q-arm of chromosome 3 and is involved in self-renewal of adult stem cells and pluri-potency of embryonic stem cells (Maier *et al.*, 2011). Recent studies have demonstrated that *SOX2* is expressed in breast and pancreatic cancer, and is involved in tumour differentiation (Li *et al.*, 2012).

Segmental amplifications of oncogenes have been detected in several types of cancer; 3q alteration accounts for 23% of SCLC (Bass *et al.*, 2009, McCaughan *et al.*, 2010) and has also been found in pre-invasive lesions of SCC (Wilbertz *et al.*, 2011). Overexpression of *SOX2* has been observed in poorly differentiated subtypes of cancers, and has also been identified in subsets of lung adenocarcinoma. Ninety percent of SCLC showed diffuse and strong expression of *SOX2*, while only 20% of ADC demonstrated *SOX2* overexpression, which is associated with poor prognosis (Sholl *et al.*, 2010). *SOX2* overexpression results in poorly differentiated tumours with an aggressive malignant phenotype (Watanabe *et al.*, 2014). Conversely, several studies have shown that *SOX2* overexpression is a marker for a good outcome in patients with SCC (Wilbertz *et al.*, 2011).

1.4.1.7 STAT

Signal transducers and activators of transcription (STAT) factors are a group of proteins that belong to a family of cytoplasmic transcription factors. The STAT family comprises seven members (STAT1, STAT2, STAT3, STAT4, STAT5a, STAT5b and STAT6) encoded by different genes, which are activated and translocated into the nucleus through phosphorylation in the cytoplasm via several receptors, such as receptor for tyrosine kinase (e.g., *EGFR*), receptors associated with tyrosine kinase (e.g., JAKs) and non-receptor protein tyrosine kinase (e.g., BrK) (Furqan *et al.*, 2013). Studies have revealed that STAT signalling plays a critical role in embryogenesis, immunity, cellular differentiation, growth, apoptosis and organ development. STAT proteins are active from a few minutes to several hours under normal physiological conditions, but continuous activation of STAT1, STAT3, and STAT5 has been demonstrated in different types of human cancer (Buettner *et al.*, 2002). STAT3 and STAT5 are the two most important members of the STAT family, and studies have found that tumour progression and development is controlled by STAT3 and STAT5 through inhibition of apoptosis or by inducing cell proliferation (Bowman *et al.*, 2000). In bone marrow, the normal developing pro-lymphoid cells require STAT5 for transcription of the survival factor MCL-1 via IL-7 signalling; however, transcription of MCL-1 through STAT3 rather than STAT5 has been detected in lymphoblastic leukaemia cells with mutant JAK proteins (Ertel *et al.*, 2013).

1.5 MCL-1 regulation and apoptosis regulatory pathways

The MCL-1 protein locates to the outer membrane of mitochondria, and has been implicated in aiding *KRAS*-mutated cells evade apoptosis (Allen *et al.*, 2011). MCL-1 protein sequesters only the BH3-domain-containing pro-apoptotic proteins (Bim, Bak and Noxa) (Zhang *et al.*, 2011). Transcription of MCL-1 is induced via PIK3, MAPK and

Janus (JAK)/signal transducer and activator of transcription (STAT) dependent pathways (Michels *et al.*, 2005). ERK1 and ERK2 contribute in phosphorylation of MCL-1 in the PEST region (amino acid 104-176) at T163 (Zhao *et al.*, 2009) Figure 1.4 demonstrates the different steps of MCL-1 regulation.

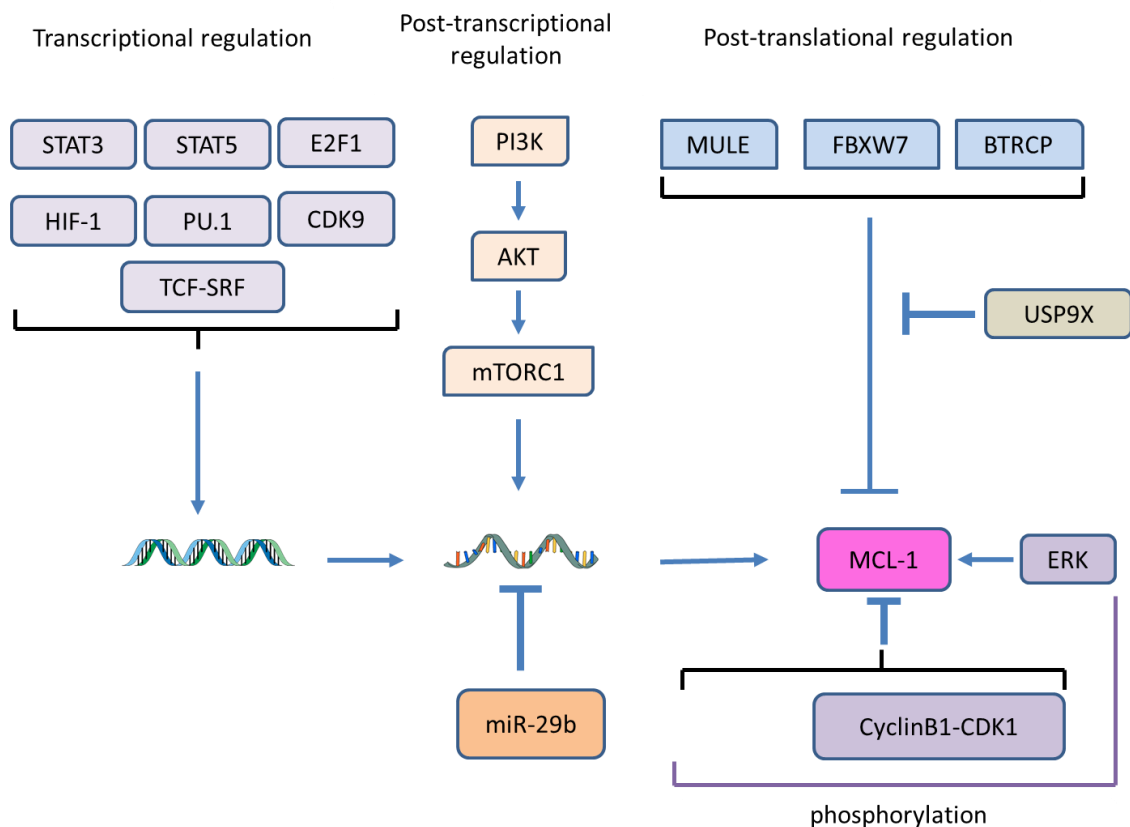


Figure 1.4 Regulation of MCL-1 at the cellular level. MCL-1 transcriptional regulation is controlled by STAT pathways. The MCL-1 post-transcriptional pathway and post-translational regulations are controlled by PI3K pathways and MAPK pathways, respectively. Adapted and modified from (Juin *et al* 2013).

Apoptosis is a genetically controlled physiological cell death, which is essential for normal development in mammals. Inhibition of the apoptosis machinery leads to development of different pathological conditions such as neurodegenerative disease and

cancers. The apoptotic process involves cell shrinkage, chromatin condensation, nuclear fragmentation and membrane blebbing, followed by recognition and engulfment of the damaged cell by macrophages. This process can be initiated by two different mechanisms; the intrinsic and extrinsic pathways (Tait and Green, 2010). Studies have demonstrated that the mitogenic signalling pathway of *RAS* (Shaw *et al.*, 2011) leads to continuous activation of ERK1 and ERK2-promoting phosphorylation of MCL-1 (Zhao *et al.*, 2009). Other studies have shown that stimulation of AKT by PI3K promotes cell survival and inhibition of PI3K prevents phosphorylation of AKT leading to programmed cell death in NSCLC cell lines. It is also believed that AKT up-regulates expression of MDM2, inducing ubiquitination of P53 and decreasing apoptosis (David *et al.*, 2004). Figure 1.5 show regulation of apoptosis via PI3K and MAPK pathway.

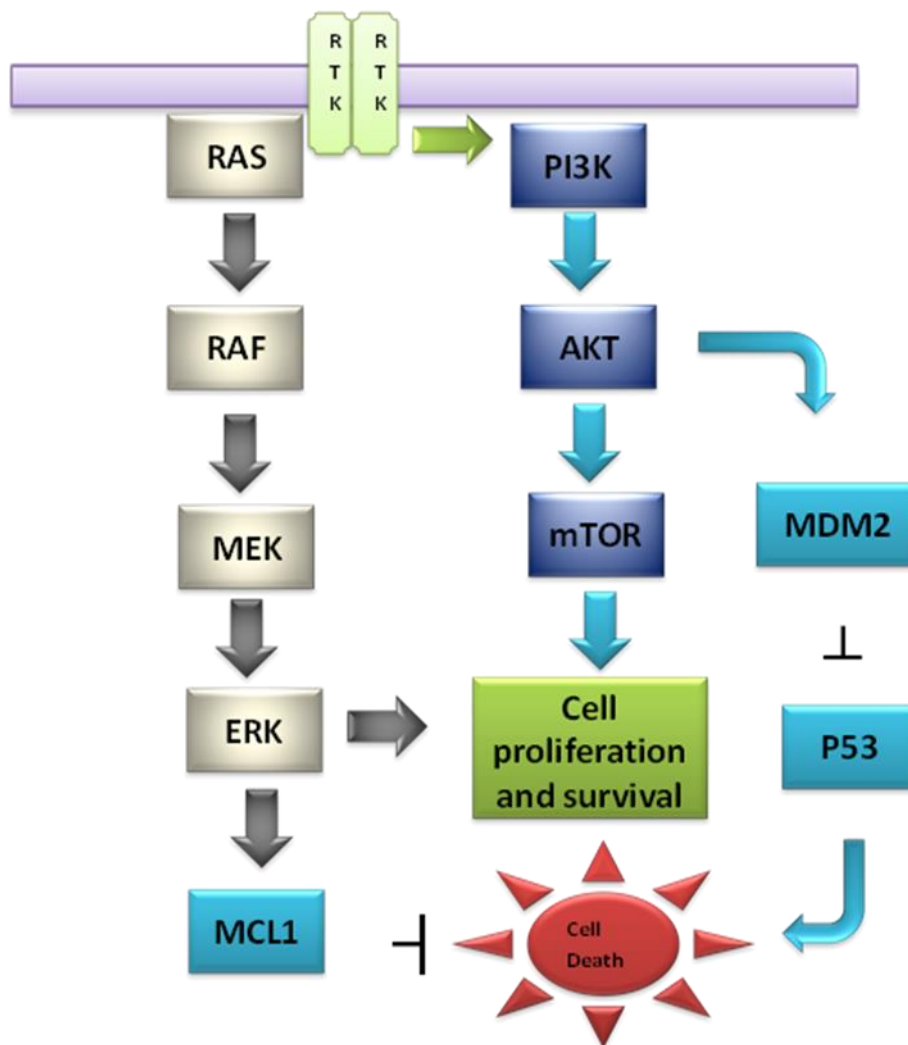


Figure 1.5 Regulation of apoptosis via the MAPK and PI3K pathways. The MAPK and PI3K/AKT pathways are involved in cancer and cell proliferation. Both pathways are also important for cancer cell survival through inhibition of apoptosis; activated ERK causes phosphorylation of MCL-1, which controls cell death through inhibition of pro-apoptotic proteins, whilst the activated AKT controls cell death via activation of the MDM2 protein, which is important in suppression of the P53 protein.

1.6 Diagnosis and current survival

The term ‘tumour stage’ is used to describe the size of the tumour, adjacent lymph node involvement and the migration of the tumour to other parts of the body. In general, lung cancer is classified into stage 1, stage 2, stage 3 and stage 4 (Figure 1.6) and is often

diagnosed in the latter stages of the disease (Table 1.2) (Slatore *et al.*, 2011). In early stages (including stage I and II), the overall survival depends on several factors such as tumour morphology and heterogeneity (Nesbitt *et al.*, 1995) with the literature suggesting that tumours with *KRAS* mutations are poorly differentiated (Slebos *et al.*, 1990). Five-year survival in patients with SCC is higher than in those with adenocarcinoma (Nesbitt *et al.*, 1995) and can be linked to genetic alterations that exist in adenocarcinomas. For example, *RAS* mutation-positive adenocarcinomas are correlated with shorter survival rates (Slebos *et al.*, 1990). However, patients who have mutations in *EGFR* show longer survival rates (Paz-Ares *et al.*, 2010). Five-year survival for patients with localised tumour is approximately 49%, and is only 2% in patients with metastatic disease (Athey *et al.*, 2010).

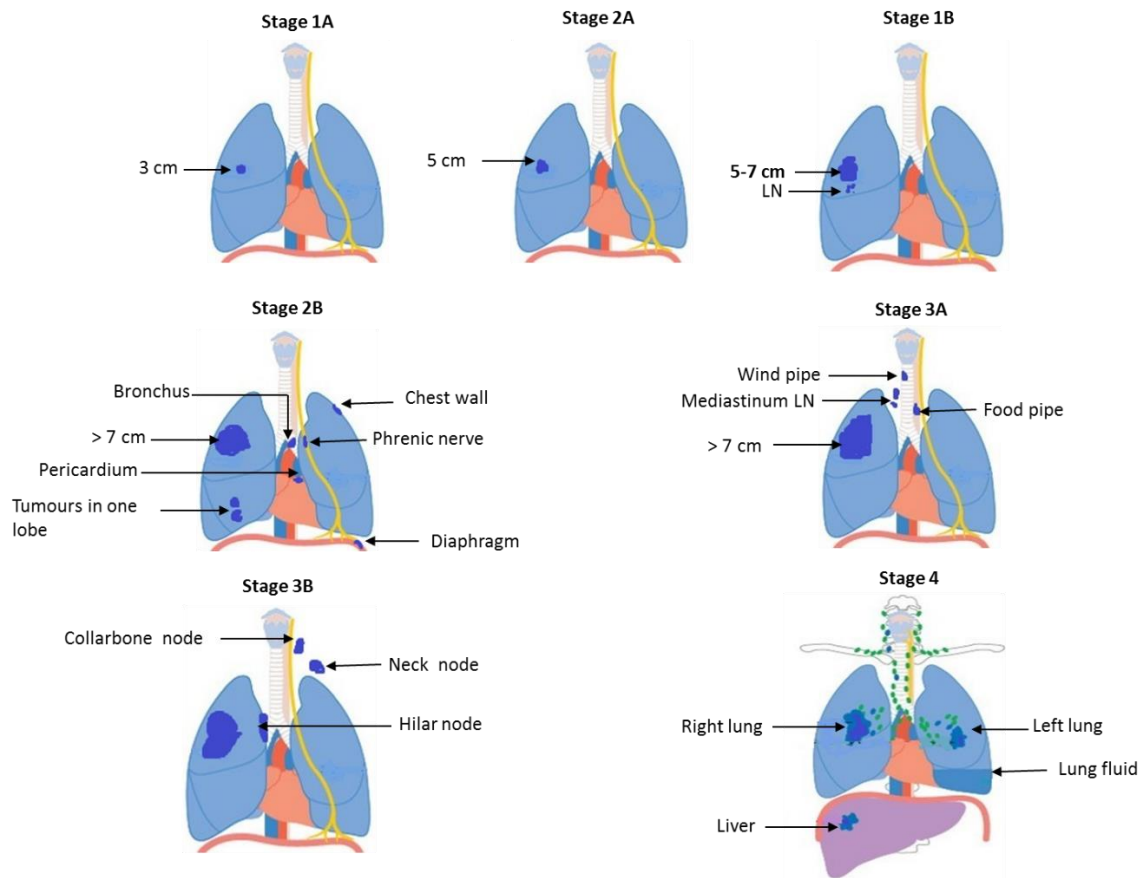


Figure 1.6 Lung cancer stages. This figure shows the stages of lung cancer starting from the non-metastatic stage (stage 1, stage 2 and stage 3) to the metastatic stage (stage 4). Adapted from <http://www.nhsinform.co.uk/health-library/articles/c/cancer-of-the-lung/staging/> accessed on [28/July/2016].

Stage	Est. %	Recommended treatment	Five –year overall survival
IA	14%	Surgical resection	50%
IB	10%	Surgical resection, can consider adjuvant chemotherapy in selected patients (tumour size <4 cm)	43%
IIA	6%	Surgical resection followed by adjuvant chemotherapy	36%
IIB	5%	Surgical resection followed by adjuvant chemotherapy	25%
IIIA	16%	Chemotherapy, radiation +/- surgery	19%
IIIB	8%	Chemotherapy and radiation	7%
IV	41%	Chemotherapy, consider targeted therapies according to driver mutation	2%

Table 1.2 Survival rates of patients with NSCLC in different stages represented by the 7th edition of the TNM staging system. Patients with stage IA of the disease have a 5-years' survival rate of 50%, whilst patients with the late stage (IV) have the lowest 5-years survival rate (2%). NSCLC is usually diagnosed in the late stage, with 41% of patients diagnosed at stage IV. Adapted and modified from (Heist *et al* 2012).

1.7 Diagnostic molecular methods for *ALK* and *EGFR* mutations in NSCLC

1.7.1 Quantitative polymerase chain reaction (qPCR)

Several commercial targeted assays for *EGFR* mutation analysis using quantitative PCR (qPCR) are available including the Cobas assay by Roche, SNaPShot by Applied Biosystems, Therascreen by Qiagen and the Mass ARRAY by Agena Bioscience. The Mass ARRAY system uses PCR amplification based on allele specific single-base primer extension (Khoo *et al.*, 2015). This technology is also developed as a multiplex system to screen a panel of genes including *EGFR* and *ALK* mutations with high throughput and cost-effectiveness (Pearce *et al.*, 2014). The SNaPShot method also can

be used for *EGFR* mutation analysis and uses multiplex PCR and single base primer extension using fluorescent labelled probes. Despite the simplicity of this method and its incorporation in laboratory diagnosis, there are disadvantages of using this method such as an inability to detect insertions, amplifications and deletions. Furthermore, the number of mutations detected with this method are limited compared to the Agena Mass ARRAY, and also there is a limitation to the number of assays that can be multiplexed in the reaction. The Cobas and Therascreen kit for *EGFR* mutation are methods approved by the FDA in the US for clinical diagnosis of *EGFR* mutations. The Cobas test depends on using a specific probe method for mutation analysis and Therascreen uses an allele specific real time PCR assay (Khoo *et al.*, 2015). Both of them are validated for clinical diagnosis; however the Cobas assay has advantages over Therascreen as it detects a higher number of *EGFR* mutations (Kimura *et al.*, 2014).

RT-PCR is another method using for analysis of *EGFR* amplification (Liu *et al.*, 2005) and *ALK* rearrangement. RT-PCR is based on conversion of mRNA to cDNA by reverse transcriptase and is a sensitive, precise and reproducible method for detection of transcripts (Shackelford *et al.*, 2014). The common limitation of RT-PCR is each target requires separate reaction and is also wasteful if insufficient amounts of RNA are available (Bustin and Nolan, 2004).

1.7.2 Next generation sequencing

Next generation sequencing (both whole exome (WES) and whole genome (WGS)) offers a comprehensive method of analysis of the cancer genome from a small tumour biopsy and can be useful in the analysis of *ALK* rearrangement and *EGFR* mutation for personalized medicine (Li *et al.*, 2013). This technology is able to generate huge amounts of data from numerous patient samples; however, it has a limit of detection of 5% mutant allele fraction. One advantage of WES/WGS is its ability to generate large

amounts of data about a patient entire cancer genome, thereby potentially being a powerful tool for patients stratification and guiding therapy. However, next generation sequencing is plagued by false positive and negative variants and must be taken into account when performed (Khoo *et al.*, 2015).

1.7.3 Fluorescent *in situ* hybridisation

Recently, fluorescent *in situ* hybridization has become the gold standard method for gene rearrangement analysis such as *EML4-ALK* fusion and *EGFR* amplification and utilises a specific probe hybridization method to target the region of interest. The Vysis *ALK* Break Apart probe kit is one of the main commercial kits approved by the FDA for laboratory diagnosis of *EML4-ALK* fusions. As inversion and translocation of *ALK* occurs on the same arm of the chromosome, the interpretation of Break Apart FISH is different from other probes, as inversion and translocation occur on the some arm of the chromosome. Although FISH is the gold standard for *EML4-ALK* analysis, compared with IHC, it is relatively expensive and also needs technical expertise for result interpretation, and is prone to false positive results (Khoo *et al.*, 2015).

1.7.4 IHC

Analysis of *ALK* rearrangement using RT-PCR and FISH is a standard method for *EML4-ALK* fusion detection; however, both methods have their own limitations, therefore IHC analysis for evaluation of *ALK* protein expression is also required (To *et al.*, 2013a). *ALK* protein is normally not expressed in lung tissue and based on this observation, application of immunohistochemistry for its protein expression can give an indication of fusion before using the expensive FISH kits for *ALK* fusion detection. The Ventana anti-*ALK* (D5F3) is one of the antibodies developed for detection of *ALK* expression to maximize concordance with *ALK* status as determined by FISH.

Appearance of strong granular cytoplasmic staining is an indication of positive ALK expression in tumour samples.

IHC for ALK expression is only recommended when FISH is available (Khoo *et al.*, 2015). Several IHC tests are available for EGFR analysis including IHC for total EGFR, phosphorylated EGFR and mutant specific. Commercial EGFR mutant specific antibodies are available for the L858R mutation in exon 21 and E746_A750 deletion in exon 19 (Khoo *et al.*, 2015). Although mutant specific EGFR IHC is inferior to molecular genomic methods for EGFR mutation analysis, the advantage of IHC is its cheap and fast workflow with high specificity and can be applied on cytological samples that are not suitable for DNA extraction. Moreover, IHC can be useful for clinical diagnosis where tumour samples are limited when molecular diagnosis is unavailable (Cooper *et al.*, 2013).

1.8 Therapeutic targets for NSCLC

1.8.1 Targeting of KRAS

Although *KRAS* is commonly mutated in lung adenocarcinoma, to date no effective targeted therapy exists (Greulich, 2010). Farnasyl transferase inhibitors (FTIs) target mutated *RAS* protein isoforms through inhibition of prenylation, but it has been suggested that FTIs are not specific for *KRAS* because geranylgeranyl protein transferase works alternatively for Farnasyl protein transferase. Moreover, *KRAS* mutated tumours have shown FTI resistance (Haluska *et al.*, 2002). Targeting BRAF in *KRAS* mutant cells was also ineffective due to activation of the MAPK pathway through CRAF activity (Greulich, 2010).

Studies have demonstrated the potential inhibitory effect of selective BRAF and MEK inhibitors in *KRAS* mutant cells; however, resistance to these inhibitors has also been demonstrated (Hatzivassiliou *et al.*, 2012). Preclinical studies for selumetinib (a MEK1/MEK2 inhibitor) showed significant inhibitory effects on *KRAS* mutant NSCLC tumour xenografts (Jänne *et al.*, 2013). This study showed that treatment response in *KRAS* mutated cells (H1299) is correlated with the type of substitution. For instance, overexpression of G12C-mutant *KRAS* shows high sensitivity to paclitaxel and pemetrexed, and low sensitivity to cisplatin, while G12D mutants revealed sensitivity to sorafinid and are resistant to paclitaxel. In addition, strong sensitivity to cisplatin was demonstrated in G12V mutants compared to wild-type (Karachaliou *et al.*, 2013). The anticancer agent bortezomib, which is usually used for treatment of multiple myeloma, has shown promising results in patients with NSCLC through induction of apoptosis (Voortman *et al.*, 2007). Cell lines harbouring *KRAS* mutations are also more sensitive to the MEK inhibitor PD-0325901.

1.8.2 Targeting of EGFR

EGFR and other ErbB receptor family members are frequently overexpressed in NSCLC (Pal *et al.*, 2010). The small molecule inhibitors erlotinib and gefitinib have shown tumour suppression activity in phase II clinical trials. However, *EGFR* inhibitor resistance has been observed in mutants of the downstream effectors of *EGFR* signalling (Eberhard *et al.*, 2005). The irreversible *EGFR* inhibitor BIWW-2992 has been shown to prolong progression-free survival in lung cancers harbouring *EGFR* mutations, and has also revealed a moderate effect on gefitinib-resistant tumour cells (Regales *et al.*, 2009). BMS690514 has also shown a significant effect on cells harbouring a secondary *EGFR* T790M mutation, which is involved in resistance to erlotinib (Rouge *et al.*, 2007). Cell lines with *EGFR* mutations are also sensitive to the *EGFR* inhibitor BIBW2992.

1.8.3 Targeting of PIK3CA

Various inhibitors have been developed to target isoforms of PI3K. PI3K/mTOR inhibitors have been proposed as effective targeting agents due to their ability to target various proteins both downstream and upstream of the PI3K signalling pathway with potential suppression of some feedback mechanisms involved in AKT regulation. The dual PI3K/mTOR inhibitor NPV-BEZ235 has a low IC₅₀ for p110 α , p110 β and mTOR in mice treated with NPV-BEZ235, showing reduction in p-AKT levels and regression of *PIK3CA*-induced pancreatic carcinoma cells (Payne *et al.*, 2015). Previous reports have demonstrated that the binding of PI3K inhibitors to *EGFR* TKIs overcame resistance to *EGFR* TKIs in the NSCLC cell line. Although several dual PI3K/mTOR inhibitors have shown anticancer effects in preclinical trials, the majority of PI3K/AKT/mTOR inhibitors are still under early development in NSCLC (Villaflor and Salgia, 2013, Yip, 2015). Moreover, progression in clinical trials to evaluate the efficacy of PI3K inhibitors in advanced NSCLC is currently ongoing (Yip, 2015).

1.8.4 Targeting of MCL-1

Overexpression of the MCL-1 protein is one of the strategies that cancer cells use to induce drug resistance via evasion of apoptosis. Despite there being no specific drug to target MCL-1, some drugs, such as BH3-M6, cyclin-dependent kinase inhibitors and deubiquitinase inhibitors, have induced down-regulation of MCL-1; a cyclin-dependent kinase inhibitor (flavopiridol) has shown down-regulation of MCL-1 in B-cell chronic lymphocytic leukaemia. Studies in breast cancer have demonstrated that flavopiridol works synergistically with lapatinib (ERBB1/ERBB2 inhibitor) to potentiate lapatinib toxicity in a MCL-1-dependent manner. Moreover, a synergistic effect of flavopiridol with vorinostat via MCL-1 down regulation was observed in leukaemia cells. The multiple kinase inhibitor sorafenib, which was originally developed to target BRAF, has

also shown induction of apoptosis in leukaemia cells in a MCL-1-dependent manner. The new BH3 mimetic compound BH3-M6 has shown suppression of the interaction between MCL-1 and the pro-apoptotic BH3 proteins, and has been involved in apoptosis induction in lung cancer adenocarcinoma cell line A549 via cytochrome c release from mitochondria (Quinn *et al.*, 2011).

A recent study has identified a small molecular inhibitor of MCL-1, UMI77, which radiosensitises pancreatic cancer cell lines through dissociation of MCL-1 from the pro-apoptotic protein BAK, though treatment of normal small intestine cells with UMI77 did not sensitise intestinal cells to radiotherapy. Previous studies in animal models have also demonstrated the inhibitory effect of UMI77 on pancreatic tumour xenografts without cytotoxic effect on normal tissues in mice (Wei *et al.*, 2015).

1.8.5 Targeting of STAT

The discovery of a *JAK2* mutation in myeloproliferative disorder has led to the development of several inhibitors designed to target STAT3. The JAK2 inhibitor AZD1480 has the ability to deactivate STAT3 in various types of cancers including SCLC and NSCLC, and also has the ability to suppress xenografts with STAT3 hyper activation. Furthermore, ruxolitinib (a JAK1/2 inhibitor) has shown a significant inhibition of xenografted cells of NSCLC in nude mice, and disruption of STAT3 using siRNA has shown suppression of implanted cancer cells in immunocompromised mice (Dutta *et al.*, 2014). Interleukin 6 neutralizing Ab has demonstrated NSCLC tumour cell regression in a xenografted mouse model via suppression of the JAK1/STAT3 signalling pathway (Song *et al.*, 2011). Previous studies have demonstrated that the STAT3/STAT5 inhibitor, OPD 31121, works on cancer cells via inhibition of STAT phosphorylation without any

adverse effect on normal cells, and is considered to be a promising anti-tumour agent (Hayakawa *et al.*, 2013).

1.8.6 Targeting of SOX2

SOX2 and LSD1 (lysine-specific demethylase) co-expression was demonstrated in cancer cells and elevated levels of LSD1 have been identified in tumour cells derived from pluripotent stem cells and SCC overexpressing *SOX2*. Treatment of the NCI-H1434 cell line, which is negative for *SOX2* amplification and the NCI-H520 cell line, which is amplified for *SOX2* with the LSD1 inhibitor, CBB1007, revealed a selective and specific growth inhibition in the *SOX2*-amplified cell line (NCI-H520). Furthermore, targeting the *SOX2*-overexpressing lung cancer cell line A549 and *SOX2* negative lung cancer cell line, H1299, with the LSD1 inhibitor demonstrated the sensitivity of the A549 cell line to the inhibitor, as compared to H1299 cell line. Moreover, targeting LSD1 using siRNA showed growth inhibition in *SOX2*-overexpressed cell lines (A549 and H520), but not in *SOX2* negative cell lines (H1437 and H1299), indicating that *SOX2*-overexpressing lung cancer cells are particularly sensitive to LSD1 suppression (Zhang *et al.*, 2013).

1.9 2D and 3D cell culture models

Conventionally, 2D cell cultures were used to study mammalian cell growth *in vitro*. Typically, researchers depend on 2D cell cultures to study the complex mechanisms of cancer cells for drug discovery (Godugu *et al.*, 2013). Although there are advantages to the 2D cell culture model in terms of its simplicity and reproducibility, *ex vivo* culture (3D) reflects the *in vivo* microenvironment of the patient tumour and should be the more clinically relevant system to screen drug effects on tumour cells (Hsieh *et al.*, 2015). It has been demonstrated that the 3D culture model preserves cellular and organ architecture, as well as maintaining stroma-tumour interaction (Vaira *et al.*, 2010).

Moreover, the hallmark features of cancer cells including angiogenesis, proliferation, self-sufficiency in growth signals, anti-apoptosis mechanisms, invasion and metastasis can be expressed in 3D cell cultures (Godugu *et al.*, 2013).

1.10 Hypothesis

This study tested the hypothesis that oncogene driver mutations potentiate drug resistance in NSCLC via MCL-1 up-regulation

1.11 Aim and objectives

The aim of this study was to determine the significance of selected oncogenic driver mutations (*KRAS*, *EGFR*, *BRAF* and *PIK3CA*), *SOX2*, *PIK3CA* and *MCL-1* amplification) in driving drug resistance and patient outcome in non-small cell lung cancer (NSCLC).

The specific objectives were:

1. To determine the frequency of oncogenic driver mutations in *KRAS*, *PIK3CA*, *EGFR* and *BRAF* in NSCLC cases using PNA-clamping qPCR.
2. To analyse copy number variation of important oncogenes or anti-apoptotic genes such as *PIK3CA*, *SOX2* and *MCL-1* in NSCLC using duplex qPCR.
3. To investigate the importance of the MAPK, PI3K/AKT and JAK/STAT pathways in regulation of MCL-1 in cancer cells using IHC and ISH.
4. To investigate the potential of targeted therapy for NSCLC through culturing cell lines or *ex vivo* NSCLC models.
5. To determine outcomes of patients with NSCLC in relation to MCL-1 and oncogenes.

Chapter 2. Materials and methods

2.1 Materials

2.1.1 q-PCR

2.1.1.1 q-PCR assays

All primers and probes used for DNA quantification, mutation and copy number variation analysis are listed in the tables below.

Table 2.1 List of *KRAS* primers and *KRAS*-specific probes used in mutation analysis.

Primer	Sequence 5'→3'	Length (nt)	Tm (°C)	Exon	Supplier
<i>KRAS</i> F78	AGGCCTGCTGAAAATGACTGA	21	58.5	1	Sigma
<i>KRAS</i> R78	TGTATCGTCAAGGCACTCTTGC	22	59.0	1	
<i>KRAS</i> WT	VIC-CTAC GCCACCAGCTC-MGB	15	69.0	1	
<i>KRAS</i> MUT121	FAM-TACGCCACDAGCTC-MGB	14	-	1	
<i>KRAS</i> MUT 121	FAM-TACGCCADCAGCTC-MGB	14	-	1	
<i>KRAS</i> MUT131	FAM-CTACGCAACCAGCTC-MGB	15	67.0	1	
<i>KRAS</i> MUT132	FAM-CTACGTACCAGCTC-MGB	15	65.0	1	
<i>KRAS</i> _PNA	TACGC CAC CAG CTCC	15	75.5	-	Eurogentec

D is the ambiguity code which represents T or C or A

Table 2.2 List of allele specific *KRAS* primers with tags

Primer	Sequence 5'→3'	Length (nt)	T _m (°C)	Exon	Supplier
<i>KRAS</i> _WT F	<u>CGAATAACA</u> AGTTGGAGCTGGTGG	24	62.7	1	Sigma
<i>KRAS</i> _G34>T	<u>GACTGGAAC</u> TGGTAGTTGGAGCTT	24	58.9	1	
<i>KRAS</i> _G34>C	<u>GACTGGAAC</u> TGGTAGTTGGAGCTC	24	59.3	1	
<i>KRAS</i> _G34>A	<u>GACTGGAAC</u> TGGTAGTTGGAGCTA	24	57.7	1	
<i>KRAS</i> _G35>T	<u>AGACTGTCA</u> GGTAGTTGGAGCTGT	24	57.3	1	
<i>KRAS</i> _G35>C	<u>AGACTGTCA</u> GGTAGTTGGAGCTGC	24	60.0	1	
<i>KRAS</i> _G35>A	<u>AGACTGTCA</u> GGTAGTTGGAGCTGA	24	58.2	1	
<i>KRAS</i> _G37>T	<u>TCTTTGCC</u> TAGTTGGAGCTGGT	23	60.2	1	
<i>KRAS</i> _G38>A	<u>CGAATAACA</u> AGTTGGAGCTGGTGA	24	61.3	1	
<i>KRAS</i> _RP	CATATTCGTCCACAAAATGATTCTG	25	58.5	1	
<i>KRAS</i> _AS_Probe	FAM-CCTTGACGATACAGCTAA-MGB	18	68.0	1	AB

AB: Applied Biosystems. The underlined bases represent tags sequences

Table 2.3 List of *KRAS* LNA primers

Primer	Sequence 5'→3'	Length (nt)	T _m (°C)	Exon	Supplier
<i>KRAS</i> G12C Antisense	CA CTCTTGCCTACGCCACA-LNA	19	57.0	1	Eurogentec
<i>KRAS</i> G12R Antisense	ACTCTTGCCTACGCCACG-LNA	18	56.0	1	
<i>KRAS</i> G12S Antisense	CACTCTTGCCTACGCCACT-LNA	19	55.1	1	
<i>KRAS</i> G12V Antisense	CACTCTTGCCTACGCCAA-LNA	18	54.5	1	
<i>KRAS</i> G12A Antisense	CACTCTTGCCTACGCCAG-LNA	18	54.0	1	
<i>KRAS</i> G12D Antisense	GCACTCTTGCCTACGCCAT-LNA	19	57.5	1	
<i>KRAS</i> G13C Antisense	GGCACTCTTGCCTACGCA-LNA	18	57.1	1	
<i>KRAS</i> G13D Antisense	CAAGGCACTCTTGCCTACGT-LNA	20	54.0	1	
<i>KRAS</i> WT Antisense	AAC TAC CAC AAG TTT ATA-LNA	18	35.3	1	
<i>KRAS</i> probe	FAM-TATAAGGCCTGCTGAAAATGAC-MGB	22	76.0	1	AB
<i>KRAS</i> F	ACTCTTGCCTACGCCAC	17	50.4	1	Sigma

Table 2.4 List of *PIK3CA* primers.

Primer	Sequence 5'→3'	Length (nt)	T _m (°C)	Exon	Supplier
<i>PIK3CA</i> E542K F	GGAAAATGACAAAGAACAGCTCAA	24	58.5	9	Sigma
<i>PIK3CA</i> E542K R	ATCTCCATTTTAGCACTTACCTGT-LNA	24	54.3	9	Eurogentec
<i>PIK3CA</i> E542K WT	VIC-CTCTCTCTGAAATCAC-MGB	16	68.0	9	AB
<i>PIK3CA</i> E542K MUT	FAM-CTCTCTCTAAAATCAC-MGB	16	66.0	9	AB
<i>PIK3CA</i> E542K PNA	CTCTCTCTGAAATCAC	16	65.2		Eurogentec
<i>PIK3CA</i> E545K F	GGAAAATGACAAAGAACAGCTCAA	24	58.5	9	Sigma
<i>PIK3CA</i> E545K R	ATCTCCATTTTAGCACTTACCTGT-LNA	24	54.3	9	Eurogentec
<i>PIK3CA</i> E545K WT	VIC-ATCACTGAGCAGGAGAA-MGB	17	69.0	9	AB
<i>PIK3CA</i> E545K MUT	FAM-ATCACTAAGCAGGAGAA-MGB	17	66.0	9	AB
<i>PIK3CA</i> E545K PNA	TCACTGAGCAGG	12	70.8	9	Eurogentec
<i>PIK3CA</i> H1047R F	CAAGAGGCTTTGGAGTATTTTCATG	24	58.0	9	Sigma
<i>PIK3CA</i> H1047R R	ACAGTGCAGTGTGGAATCCAGA	22	59.0	20	Sigma
<i>PIK3CA</i> H1047R WT	VIC-ATGCACATCATGGTGG-MGB	16	67.0	20	AB
<i>PIK3CA</i> H1047R MUT	FAM-ATGCACGTCATGGTGG-MGB	15	66.0	20	AB
<i>PIK3CA</i> H1047R PNA	ATGCACATCATGGTG	15	74.0	20	Eurogentec

Table 2.5 List of *BRAF* (V600E) LNA primers, *EGFR* (L858R) primers and *ALU* repeat assay.

Primer	Sequence 5'→3'	Length (nt)	T _m (°C)	Exon	Supplier
<i>EGFR</i> F	AACACCGCAGCATGTCAAGA	20	58.9	21	Sigma
<i>EGFR</i> R	CCGCACCCAGCAGTTTG	17	58.3	21	Sigma
<i>EGFR</i> WT	VIC-ACAGATTTTGGGCTGG-MGB	16	64.0	21	AB
<i>EGFR</i> MUT	FAM-CAGATTTTGGGCGGG-MGB	15	64.0	21	AB
<i>EGFR</i> PNA	TGGGCTGGCCAAACTG	16	83.3	-	Eurogentec
<i>BRAF</i> V600E F	TAGGTGATTTTGGTCTAGCTACAGA-LNA	24	55.4	15	Eurogentec
<i>BRAF</i> WT F	TAGGTGATTTTGGTCTAGCTACAGT	24	54.6	15	Eurogentec
<i>BRAF</i> R	ATCCAGACAACGTGTTCAAACGTGATG	25	58.2	15	Sigma
<i>BRAF</i> probe	FAM-AATCTCGATGGAGTGGGT-MGB	18	68.0	15	AB
<i>BRAF</i> PNA	TAGCTACAGTGAAATC	16	71.1	-	Eurogentec
ALU F	GACCATCCCGGCTAAAACG	19	59.0	-	Sigma
ALU R	CCACTACGCCCGGCTAATTT	20	59.9	-	
ALU_ probe	VIC-CCCGTCTCTACTAAA-MGB	15	65.0	-	

Table 2.6 List of copy number analysis and gene expression assays.

Primer	Sequence 5'→3'	Length (nt)	Tm (°C)	Exon	Supplier
<i>MCL-1</i> F	GCATCGAACCATTAGCAGAAAAGT	23	58.5	1	Sigma
<i>MCL-1</i> R	GCCAGTCCCGTTTGTGCCTT	20	59.9	1	Sigma
<i>MCL-1</i> probe	VIC-TCACAGACGTTCTCG-MGB	15	68.0	1	AB
<i>MCL-1</i> probe	FAM-TCACAGACGTTCTCG-MGB	15	68.0	1	AB
<i>CCT3</i> F	FAM-GCATCATTGAAGACTCCTGTGTCT-MGB	24	58.4	6	Sigma
<i>CCT3</i> R	GCATACGTGGATGGGTCACAT	21	59.1	6	Sigma
<i>CCT3</i> probe	FAM-CGTGGAGTCATGATTA-MGB	16	67.0	6	AB
<i>H6PD</i> F	TTCAGGCCAGGAGAGAAGTCTT	22	58.2	5	Sigma
<i>H6PD</i> R	TTGTGCTGGTTGATATGAATGTGT	21	58.1	5	Sigma
<i>H6PD</i> probe	VIC-TTGTGCTGGTTGATATGAATGTGT-MGB	19	68.0	5	AB
<i>PIK3CA</i> F	GTTCGAACAGGTATCTACCATGGA	24	58.1	6	Sigma
<i>PIK3CA</i> R	CTGGGATTGGAACAAGTACTCT	23	57.3	6	Sigma
<i>PIK3CA</i> probe	VIC-AACCCTTATGTGACAATGT-MGB	19	69.0	6	AB
<i>PIK3CA</i> probe	FAM-AACCCTTATGTGACAATGT-MGB	19	69.0	6	AB
<i>CAPN7</i> F	TGGGGCAAGCTACCATTATCA	21	59.0	7	Sigma
<i>CAPN7</i> R	TTGGTGAGGTCTTCTGGTCGT	21	58.2	7	Sigma
<i>CAPN7</i> probe	VIC-AAAACTACATTTTCCAAGTGG-MGB	21	68.0	7	AB
<i>GATA2</i> F	TGCCCTGGCTGGACACAT	18	59.6	7	Sigma
<i>GATA2</i> R	TGTGTCCGGAGTGGCTGAA	19	59.8	7	Sigma
<i>GATA2</i> probe	FAM-CACCTGTGGCCACCT-MGB	16	60.0	7	AB
<i>GAPDH</i> 100F	GGCTAGCTGGCCCGATTT	18	58.8	1	Sigma
<i>GAPDH</i> 100R	GGACACAAGAGGACCTCCATAAA	23	58.1	1	Sigma
<i>GAPDH</i> probe	FAM-ATGCTTTTCTAGATTATTC-MGB	20	69.0	1	AB
<i>UBC</i> F	AGGTGGGATGCAGATCTTCGT	21	59.5	2	Sigma
<i>UBC</i> R	TGTCACTGGGCTCCACCTC	19	58.2	2	Sigma
<i>UBC</i> probe	FAM-ACCCTGACTGGTAAGAC-MGB	17	69.0	2	AB
<i>MCL-1</i> assay 20X	Hs01326481_cn	-	-	1	AB
<i>SOX2</i> assay 20X	Hs02675353_cn	-	-	1	AB
<i>MCL-1</i> assay 20X	Hs01050896_m1MCL-1	-	-	2	AB

2.1.2 Control DNAs

All control DNAs used for mutations and copy number analysis are listed in Table 2.7.

Table 2.7 List of positive and negative control DNA.

Mutated gene		Cell line DNA	Alleles	Type of mutation
<i>KRAS</i>	G12C [G34>T]	H23 or H358	Heterozygous	Point mutation
	G12R [G34>C]	KP-2	Heterozygous	
	G12S [G34>A]	A549	Heterozygous	
	G12V [G35>T]	SW626 or SW480	Heterozygous	
	G12A [G35>C]	SW1116	Heterozygous	
	G12D [G35>A]	GP2D	Heterozygous	
	G13C [G37>T]	H1355	Heterozygous	
G13D [G38>A]	HCT116	Heterozygous		
<i>PIK3CA</i>	E542K [G1624>A]	SW948	Heterozygous	Copy number change
	E545K [G1633>A]	MCF7	Heterozygous	
	H1047R [A 3140>G]	HCT116	Heterozygous	
<i>EGFR</i>	V600E [T2573>G]	H1975	Heterozygous	
<i>BRAF</i>	L858R [T1799>A]	SK-MEL-5	Heterozygous	
<i>MCL-1</i>	1q21.3a	H1395	-	
<i>SOX2</i>	3q26.33b	RERF-LC-Sq1	-	
<i>PIK3CA</i>	3q26.32c	RERF-LC-Sq1	-	
WT DNA	-	HG-DNA	WT alleles	Normal diploid

2.1.3 Tumour samples

A total of 85 NSCLC tissues were obtained from the University Hospital of Leicester (UHL) with consent and clinical outcome. Details of the tissues are listed in Table 2.8. The rare cases were not used due to complexity of the analysis

Table 2.8 Clinicopathological features of NSCLC tissues.

Clinicopathological feature		Total
Tumour type	Adenocarcinoma	39
	Squamous cell carcinoma	38
	Large cell carcinoma	2
	Atypical carcinoid tumour	2
	Adeno-squamous	1
	Combined ADC and SCLC	1
	Combined SCC and SCLC	1
	Combined large cells and small cells	1
Patient gender	Male	45
	Female	42
Patient age	0-44	2
	45-54	3
	55-64	14
	65+	67
Smoking history	Smokers	16
	Ex-smokers	26
	Non-smokers	3
	Unknown	41
Tumour stage	IA	8
	IB	26
	IIA	3
	IIB	21
	IIIA	18
	IIIB	1
	IV	3
	Unknown	7

2.1.4 DNA extraction

All materials used for DNA purification from paraffin-embedded tissues and cell lines are listed in Table 2.9.

Table 2.9 List of reagents and equipment used for DNA extraction

Reagent	Cat No	Supplier
AL buffer	51106	Qiagen
ATL		
AE		
AW1		
AW2		
Proteinase K	03115879001	Roche, Germany
Ethanol	BP28184	Fisher scientific.UK
Tris	BP-152-1	
NaCl	S271-3	
Phenol/chloroform/IAA	P2069	Sigma-Aldrich, UK
Sodium dodecyl sulphate SDS	436142	
Spin column	1011706	Qiagen
Collection tube	1058310	
Eppendorf	211-0015	VWR, USA

2.1.5 Immunostaining

All reagents and equipment used for immunohistochemistry are listed in Table 2.10 and all antibodies are listed in Table 2.11.

Table 2.10 List of reagents and equipment used for immunostaining.

Reagents and equipment	Cat No	Supplier
Novolink polymer detection system kit	RE-7150-K	Leica Biosystems Newcastle Ltd, UK
PBS (Dulbecco A)	BR0014	OXOID limited, Hampshire, England
FBS	EU-000-F	Sera laboratories international Ltd, west sussex.UK
IMS	EC200-578-6	Genta Medical, York, UK.
Xylene	EC215-535-7	
Tris	BP-152-1	Fisher scientific.UK
NaOH	S318-1	
Citric acid monohydrate	C1909	Sigma-Aldrich, UK.
TritonX-100	T-8787	
HCL	H1758	
DPX mounting medium	SEA-1300-00A	Cell Path LTD, Newtown Powys, UK).

Table 2.11 list of antibodies used for immunostaining.

Antibody	description	Host	Detection method	Dilution	Cat No	Supplier
p-ERK	Polyclonal antibody	Rabbit	IHC	1:400	9101S	Cell signalling
p-AKT	Monoclonal antibody	Mouse	IHC	1:100	4060S	Cell signalling
MCL-1 S-19	Polyclonal antibody	Rabbit	IHC	1:2000	SC-819	Santa Cruz biotechnology
MCL-1 G-7	Monoclonal antibody	Mouse	IHC	1:400	SC-74437	Santa Cruz biotechnology

2.1.6 Cell culture

2.1.6.1 Reagents and equipment

Equipment and reagents used for cell culture and maintenance are listed in Table 2.12.

Table 2.12 List of equipment and reagents used for cell culture.

Reagents and equipment	Cat No	Supplier
RPMI 1640	R0883	Sigma-Aldrich, UK.
L-glutamine	G7513	
Trypsin/EDTA	T3924	
Sodium pyruvate	11360070	Gibco, UK.
Hepes	15630106	
Pen-strep	P11-010	PAA
FBS	EU-000-F	Sera laboratories international Ltd, UK.
RPMI-1640	30-2001	ATCC, USA.
Tissue culture flasks	10-126-1 10-126-8	Fisher scientific
Falcon tube	14-432-22	

2.1.6.2 Mammalian cell lines

Mammalian cell lines used in this study were obtained from different sources. The lung adenocarcinoma cell line H1935 was kindly provided by Dr. Sara Busacca, University of Leicester. The pancreatic cell line (KP-2) and lung SCC cell line (RERF-LC-Sq1) were purchased from the Japanese Collection of Research Bioresources Cell Bank (JCRB cell bank, Osaka, Japan), whereas the lung adenocarcinoma cell lines (H1355 and H2342) were supplied by the American Type Culture Collection (ATCC, USA). Cells were kept in the vapour phase of liquid nitrogen until use. Brief information about the cell lines is given in Table 2.13.

Table 2.13 List of grown cell lines in this study.

Cell line	Tissue	Morphology	Ethnicity	Disease	Mutation	Source
KP-2	Pancreas	Epithelial-like	Japanese	Ductal carcinoma	<i>KRAS</i> mutation	JCRB
H1395	Lung	Epithelial	Caucasian	ADC	<i>MCL-1</i> amplification	Dr Busacca UOL
H2342	Lung	Epithelial	Caucasian	ADC	<i>MCL-1</i> gain	ATCC
H1355	Lung	Unknown	Caucasian	ADC	<i>KRAS</i> mutation	ATCC
RERE-LC-Sq1	Lung	Epithelial-like	Japanese	SCC	<i>PIK3CA</i> amplification	JCRB

2.1.6.3 Preparation of cytoblocks

Reagents and equipment used for preparation of cytoblocks are listed in Table 2.14.

Table 2.14 Reagents and equipment used for cytoblock preparation.

Reagents and equipment	Cat No.	Supplier
Shandon Cytoblock System	7401150	Thermofisher Scientific, UK.
haemocytometer	DHC-N01	IN CYTO, Korea.
Shandon cytospin 3 centrifuge	13367	Shandon
IMS	EC200-578-6	Genta Medical, York, UK.
10% formalin	HT501128	Sigma-Aldrich

2.1.7 *In-situ* hybridization

All equipment and reagents used for *in situ* hybridization are listed in Table 2.15.

Table 2.15 List of materials used for ISH.

Reagents and equipment	Cat No	Supplier	
HyEZ hybridization system	HyEZ oven	310010	
	HyEZ Humidity control tray	310012	
	HyEZ humidifying paper	-	
	Slide rack	310014	
Pre-treatment kit	Pre-treat 1	320044	
	Pre-treat 2	320043	
	Pre-treat 3 protease	320045	
RNA scope probes	Target probe (MCL-1)	588851	
	positive control probe (POLR2A)	310451	
	Negative control probe (DapB)	310043	
Detection kit- Brown	Amp1	320451	
	Amp2	320452	
	Amp3	320453	
	Amp4	320454	
	Amp5-Brown	320455	
	Amp6-Brown	320456	
DAB-A	320052	Advanced cell diagnostic Inc. USA.	
DAB-B	320053		
Wash buffer	310091		
Hydrophobic barrier pen	310018		Vector Laboratories, Inc. USA
100% ethanol	BP28184		Fisher scientific.UK
Gill's Haematoxylin I	GHS132		Sigma-Aldrich, UK.
Xylene	EC215-535-7		Genta Medical, York, UK.

2.1.8 RNA extraction

Equipment and reagents used for RNA purification are listed in Table 2.16.

Table 2.16 Material used for RNA extraction.

Reagents and equipment	Cat No	Supplier
Qiagen RNeasy mini kit	RLT buffer	1015762
	RW1 buffer	1015763
	RPE buffer	1018013
	RNase free water	1018017
	RNeasy Mini Spin Column	1011708
	Collection Tubes	1016810
Ethanol	BP28184	Fisher scientific, UK.
β -Mercaptoethanol	M6250	Sigma-Aldrich, UK.

2.1.9 Reverse transcription

All reagent and equipment used for cDNA generation are listed in Table 2.17.

Table 2.17 List of reagents and equipment used for reverse transcription.

Reagents and equipment	Conc	Cat No	Supplier
TaqMan® Reverse Transcription Reagents	RT buffer	10X1.5 ml	100025924
	MgCl ₂	25mM	100020476
	dNTP	10mM	100023382
	RNase inhibitor	20U/ μ L	100021540
	Multiscribe RT	50U/ μ L	100024128
	Oligo d (T) 16	50 μ M	100023441
	Random hexamers	50 μ M	100026484
Genotyping master mix	-	4371355	Applied Biosystems, USA
RNase free water	-	1018017	
RNA	1 μ g	-	-
DNA thermal cycler	-	-	Perkin-Elmer

2.1.10 Cell viability assessment

2.1.10.1 Drugs

All used drugs for viability assessment are listed in Table 2.18.

Table 2.18 Listed of the used drug in this study.

Drug	Target	IC50 (nM)	Storage (°C)	Supplier	Cat No	Vehicle
Cisplatin	DNA	-	-20	Selleckchem, USA.	S1166	DMF
AZD8055	mTORC1/C2	0.08	-20	ChemieTek, USA	CT-A8055	DMSO
U0126	MEK	70	-20	Cell signalling	9903S	
SH-4-54	STATs	300	-80	Selleckchem, USA.	S7337	
Niclosamide	STAT3	700	-20	Santa Cruz biotechnology	SC-250564	
STA9090	HSP90	4	-20	Selleckchem, USA.	S1159	

2.1.10.2 Reagents and equipment

The used reagent and equipment for cell viability assay are listed in Table 2.19.

Table 2.19 List of materials used for cell viability assessment.

Reagents and equipment	Cat No	Supplier
RPMI-1460	30-2001	ATCC, USA.
96 well cell culture(Flat bottom)	3595	Corning incorporated, USA.
Microplate, 96 well black (Clear fat bottom)	655097	Greiner bio-one, GmbH , Germany
DMF	PHR1553	Sigma-Aldrich, UK
DMSO	472301	Sigma-Aldrich, UK
Haemocytometer	DHC-N01	IN CYTO, Korea
Alamar blue	88951	Thermo-scientific, USA.

2.2 Methods

2.2.1 q-PCR

2.2.1.1 Primer design

The Primer 3.0 software (v. 4.0.0) was used to design PCR primers and probes. All probes and primers were blasted on the NCBI databases to ensure their specificity

to the target gene. Primers and probe temperatures were optimized using Primer 3 express (Applied Biosystems). The assays were obtained from the manufacturing company as lyophilized powder, and according to the manufacturer recommendations the powder was dissolved in sterile ultrapure water under sterile conditions to obtain stock primers and probes at concentrations of 100 μM . 10 μM aliquots of primers and 2 μM aliquots of probes were then prepared and stored at -20°C. All used probes were FAM-MGB or VIC-labelled.

2.2.1.1.1 Primer and probe sets for mutation detection

Primer and probe sets were designed to detect different mutations. Specific primers, which contain a mutant base at the 3' end of the sequence and a tag at the 5' end, were designed. Primers were designed to be as short as possible and 8-9 extra bases (Tag) were added at the 5' end to increase the primer melting temperature (Table 2.2 above). Specific mutant hybridizing probes were also designed with ambiguity code (D) which represents the nucleotide A or C or T; all mutant probes were MGB-FAM labelled, and a VIC-labelled wild-type probe was also designed in order to detect the wild-type sequence. This experiment was designed as a duplex reaction containing both wild-type and mutant probes in the same reaction. Two conventional F and R primers were designed on both sides of the specific probe to amplify the reaction. Specific primers with locked nucleic acid (LNA) at the primer 3' end were also designed to increase the specificity of the reaction. LNA primers are described in Table 2.3 above.

2.2.1.1.2 Primers and probes for copy number variation analysis

Prior to primer and probe design, the genes of interest were checked on the Sanger Institute website (https://cancer.sanger.ac.uk/cell_lines/conan/search). Using the

cell line copy number project database (Conan), appropriate cell lines with copy number changes were selected. These amplifications have been validated by the Sanger Institute. Figure 2.1 (brown arrow) shows an example for *MCL-1* amplification on chromosome 1 (Chr1) at 1:150577375-150579530 in a lung cancer cell line represented by the Sanger Institute. After the amplification site was determined, forward primer, reverse primer and two VIC and FAM-labelled MGB probes were designed. Two different reference genes, one on the p-arm and other on the q-arm of the chromosome, with two different label dyes were designed. One of the two reference genes was located on the same arm as the target gene (Figure 2.1, red and green arrows). A duplex ratio test was used to determine copy number changes. Three different master mixes were prepared, each containing a FAM-labelled probe for the target of interest, with the other VIC-labelled for the reference. The reaction was run as follows: target gene vs reference gene 1 (Ref 1), target gene vs reference gene 2 (Ref 2) and Ref 1 vs Ref 2 (Figure 2.2). *MCL-1* amplification was analysed and discriminated from gain as follows:

- $MCL-1$ CT value – $H6PD$ CT value
- $MCL-1$ CT value – $CCT3$ CT value
- $CCT3$ CT value – $H6PD$ CT value

The experiment was run under standard thermo-cycling conditions (40 cycles, 60°C annealing temperature and 95°C denaturing temperature), after which the Δ CT between each gene pair was calculated. The tumour sample was then normalized to the control sample (Human genomic DNA) using $\Delta\Delta$ CT, and a Z-score was analysed using CT values of the normal adjacent tissue against the $\Delta\Delta$ CT.

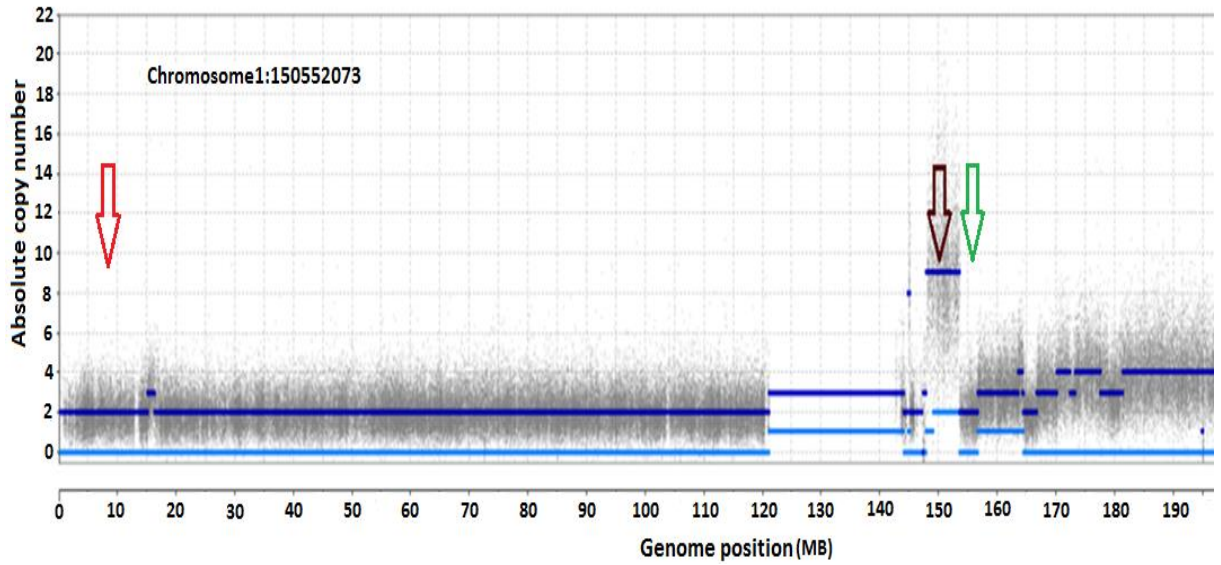


Figure 2.1 Locations of the designed assay for *MCL-1* and reference genes. This figure shows *MCL-1* amplification on chromosome 1 at 1:150577375-150579530 MB (brown arrow) in lung cancer cell line H1395; *MCL-1* assays were designed on this position. The positions of the two selected reference genes are indicated by the red and green arrows.

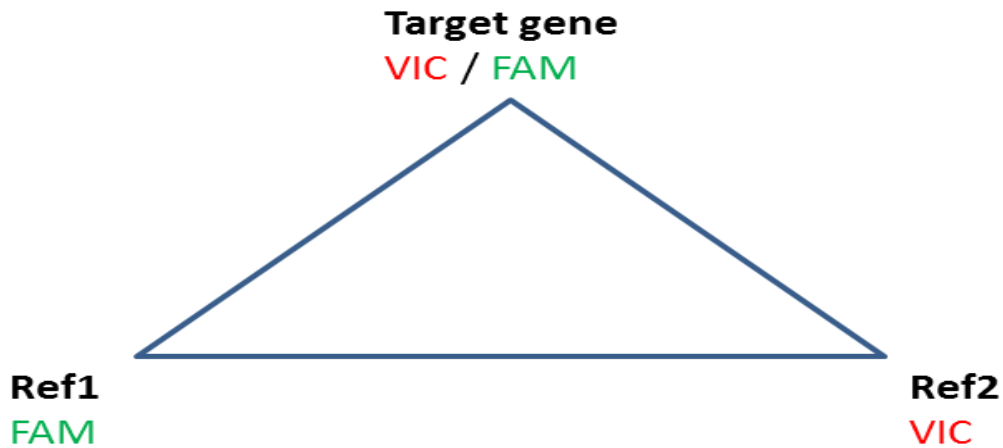


Figure 2.2 Duplex ratio test for gain and amplification analysis. The reaction was run as a duplex test in three different reactions; each reaction contains a FAM-labelled probe and a VIC-labelled probe (VIC-labelled target gene v FAM-labelled Ref1, FAM-labelled target gene v VIC-labelled Ref2 and FAM-labelled Ref1 vs VIC-labelled Ref2).

2.2.1.2 Reaction conditions

Reactions were performed in a final volume of 10 μL comprising 5 μL TaqMan Genotyping Master Mix, 0.6 μL F primer, 0.6 μL R primers, 0.2 μL probe and 0.6 μL H_2O . The primer concentration was 10 μM and the probe concentration was 2 μM . 10 ng of DNA in a volume of 3 μL was added to make up the total volume of the reaction to 10 μL . Reagents and DNA were loaded into 96 well plates; the targeted region of the gene was amplified on a Step One Plus thermocycler (Applied Biosystems) using standard thermal cycling conditions (Figure 2.3). Reactions were run as duplicates or in triplicate according to the amount of DNA obtained from fixed tissues. In duplex tests, the volumes of the primers and probes were reduced by half (to 0.3 μL and 0.1 μL , respectively). Chromosomal polysomy was analysed using the (20X) TaqMan copy number assays containing MCL-1 primers at a concentration of 18 μM and a probe concentration of 5 μM (Table 2.6 above). The 20X assays were diluted to 1X when used to run the reactions, and GAPDH was used as the reference gene. Reactions were run as singleplex.

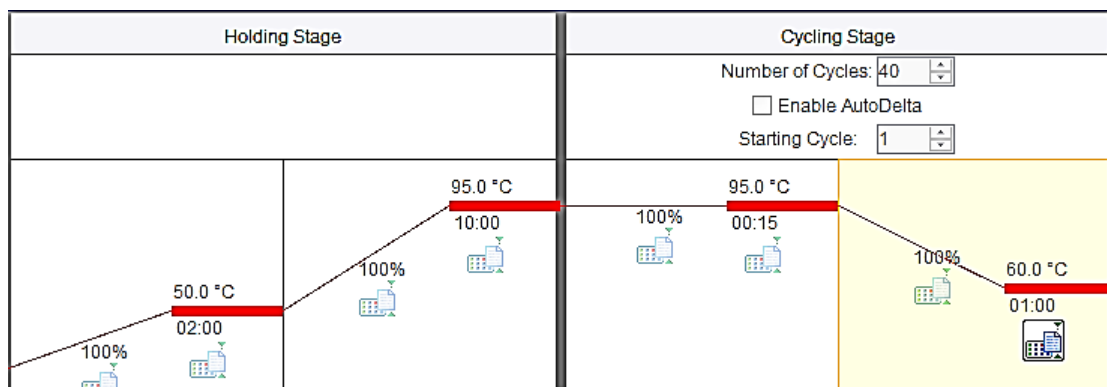


Figure 2.3 Cycling condition of qPCR. The reaction consisted of 40 cycles.

2.2.1.3 DNA quantification

DNA concentrations were measured using qPCR and a standard curve. An ALU repeat assay was used to determine DNA concentrations in all samples. The first standard was 10 ng DNA with six subsequent standards produced using a dilution factor of 1:2 (Figure 2.4).

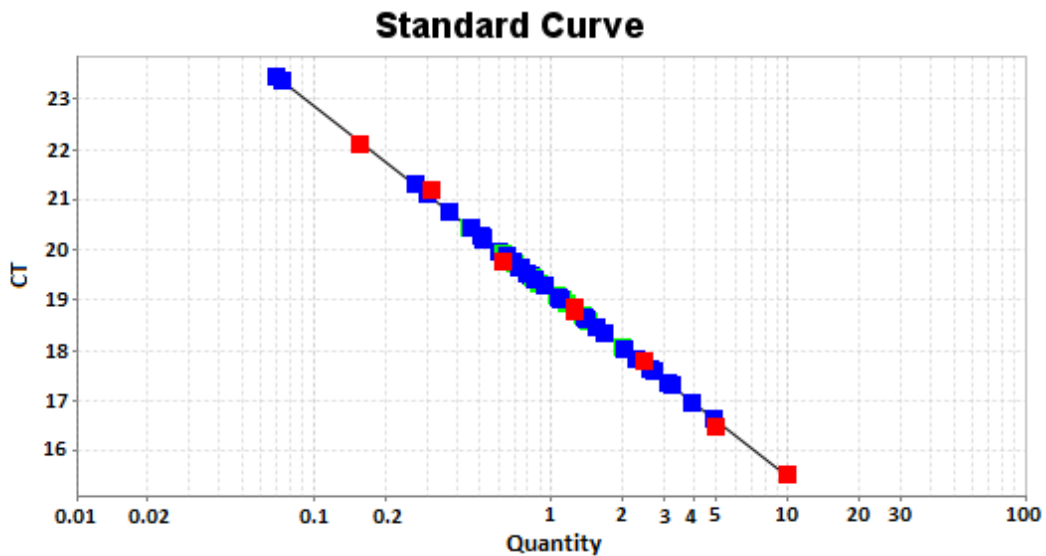


Figure 2.4 Standard curve for DNA concentration measurement. Red squares represent the standards. The blue squares represent concentrations of the tested samples.

2.2.1.4 PNA clamping technique

The development of this technique was based on blocking amplification the WT allele to increase the sensitivity of the reaction to the mutant allele (Behn *et al.*, 2000). A 15-mer or more PNA was designed to cover the targeted region. Experiments were designed as duplex reactions and ran as \pm PNA; the amount of PNA used was included in the 10 μ L total volume of the reaction in each well at a concentration of 0.3 μ M.

2.2.1.5 Sensitivity measurement of the PNA clamping method

Serial dilution for mutant DNA (H23 cell line) into a wild-type DNA background (HG-DNA) was performed. A portion of H23 DNA, which contains 50% of both WT and mutant alleles (G12C), was spiked into a high background wild-type DNA (HG-DNA) which contained 100% wild-type allele. The mixture was then serially diluted (1:2) up to 15 times. The first standard was 10 ng DNA, which contained 2.5 ng of the mutant DNA and 7.5 ng of WT DNA.

2.2.2 DNA extraction

2.2.2.1 DNA extraction from fixed paraffin-embedded tissue

DNA was extracted from NSCLC samples using the QIAamp DNA blood mini kit from Qiagen. The fixed tissue was incubated at 65°C for 5 minutes, followed by immersion in xylene and graded alcohol. The tissue was dried and then scraped into a 1.5 ml eppendorf using an ATL buffer. Ten mg/ml proteinase K was added to the eppendorf and incubated at 56°C for 4 days. AL buffer was then added and the solution transferred to a Safe Lock tube and incubated for 10 minutes at 70°C. Absolute ethanol was then added at room temperature. The mixture was transferred into a QIAamp column and centrifuged for 60 seconds at 8000 rpm, then the collection tube was changed and AW1 added to the column. The column was centrifuged again at the same speed for 1 minute, after which the collection tube was replaced and AW2 was added to the column. The column was centrifuged for 3 minutes at 14000 rpm. After discarding the buffer, the column was centrifuged for 60 seconds at the same speed. To elute the DNA, AE buffer was added to the column and incubated at room temperature for 5 minutes. The column was centrifuged at 8000 rpm for 1 minute and then the eluted DNA was transferred into a new eppendorf and stored at 4°C until required.

2.2.2.2 DNA extraction from cell lines

Cell pellets were suspended in 0.05 M Tris, pH 8.0/0.1% SDS and 10 µl proteinase K (0.5 mg/ml) was added to the cell suspension. The mixture was incubated for 1 hour at 37°C. The sample was mixed thoroughly with an equal volume of Phenol/chloroform/IAA and centrifuged at 14000 rpm for 3 minutes. The upper aqueous layer was transferred to a clean eppendorf without disturbing the interface layer. An equal volume of chloroform/IAA was added to the aqueous phase, mixed thoroughly, and then centrifuged for 3 minutes at 14000 rpm. After centrifugation, the aqueous layer was removed without disturbing the middle layer and mixed with three times the volume of cold ethanol and 1/10 the volume of 1 M sodium chloride. Samples were then incubated at -20°C for 24 hours. After overnight storage, the mixture was centrifuged for 15 minutes at 13000 rpm and 4°C. The pellet was washed in 70% ethanol and then centrifuged again at 13000 rpm for 15 minutes at 4°C. The pellet was air dried, re-suspended in 300 µL ultrapure water, and stored at 4°C until required.

2.2.3 Immunohistochemistry

2.2.3.1 Preparation of wash buffers

2.2.3.1.1 Tris-buffered saline (TBS) and phosphate-buffered saline (PBS)

TBS and PBS were prepared to be used as wash buffer and antibody diluents. TBS was prepared in a fume hood by dissolving Tris(hydroxymethyl) methylalanine and sodium chloride (NaCl) in ultra-pure water (UPH₂O). The pH was then adjusted to 7.65 using concentrated hydrochloric acid (HCL). PBS was prepared by dissolving phosphate-buffered saline tablets (Dulbecco A), pH 7.3 ± 0.2, in UPH₂O and stored at room temperature.

2.2.3.1.2 20X Citrate buffer

42 g of 0.2 M citric acid monohydrate was dissolved in 500 ml UPH₂O in a beaker with a stirrer; 20 g sodium hydroxide (NaOH) pellets were added in 5 g amounts, increasing the pH to 5.8, and the final pH was adjusted to 6.0 using 5 M NaOH. The final volume was made up to 1 litre by adding UPH₂O, and the prepared buffer was stored at 4°C until use.

2.2.3.2 Immunostaining

Paraffin-embedded tissues from NSCLC patients and normal control samples from tumour-adjacent tissue were stained for different cellular proteins and phosphoproteins. Specimens were heated in an incubator for 10 minutes at 65°C and then dewaxed and rehydrated by passing them through xylene and descending graded alcohol, respectively. The antigen retrieval method was citrate buffer/microwave antigen retrieval. A Novolink polymer detection system was used to develop the immuno-staining. Overnight incubation at 4°C was performed for the tested antibody (AB). Rabbit polyclonal antibody (pAB) S-19 and mouse monoclonal antibody (mAB) G-7 (Catalogue No. 74437), P-p44/42 MAPK (T262) or p-ERK (Cat No 4370) and p-AKT (Ser473) Cat No. 4060 were used in this study. Preliminary experiments for the antibodies were performed on tonsil tissues; various dilutions for the antibodies starting from 1:50-1:2000 were tested to obtain appropriate concentrations, and TBS buffer containing 3% FBS/0.1% TritonX-100 was used as an antibody diluent to avoid AB non-specific binding. The optimum dilutions for the p-AKT, p-ERK, MCL-1 (s19), and MCL-1 (G-7) were 1:100, 1:2000, 1:400 and 1:400, respectively. Bright field microscopy (Leica, MD, 2500, Applied Biosystems) was used to analyse the slides. Images were photographed using a Leica DFC 420 camera (Leica Microsystems Ltd., Switzerland). The

tumour area was first marked and then H-score was calculated using Aperio Image Scope software (v.11.1.2.760), with an overall score of 0-300 being stratified into 3 categories of % nuclear staining: weak positive, intermediate positive nuclear staining and strong positive staining nuclear staining (Cohen *et al.*, 2012). Staining level was then categorised according to median of the all staining levels in tumour samples.

2.2.4 Culture of cell lines

2.2.4.1 Growth of cell lines from liquid nitrogen

Cell lines were removed from the liquid nitrogen store and then transferred to a small liquid nitrogen container. In the culture room, cells were transferred from the container to small box containing ice for 1-5 minutes, after which cells were immediately transferred into a water bath at 37°C for 1-3 minutes. Using forceps, the ampule was taken from the water bath and sprayed with 70% IMS. The ampule was opened in a Class-II cabinet, and the contents transferred to a 50 ml Falcon tube and the cells centrifuged at 1000 rpm for 5 minutes. The supernatant was aspirated from the Falcon tube and then the pellet was re-suspended in 5 ml pre-warmed (to 37°C) medium, and the 5 ml suspension transferred to a T25 flask for incubation.

2.2.4.2 Culture condition

Cell lines were cultured in RPMI1640 containing 10% foetal bovine serum (FBS), 5% L-glutamine, 5% sodium pyruvate, 5% HEPES and penicillin-streptomycin (pen-strep). The slower-growing cell line H1395 was grown in a culture medium containing 20% FBS. Cells were incubated at 37°C/5% CO₂ for 3-5 days. When cell confluency reached approximately 80%, the growing cells were then detached

using Trypsin/EDTA (TE) and pelleted by centrifugation at 1000 rpm for 5 minutes at 25°C. The obtained pellets were stored at -20°C until DNA extraction.

2.2.4.3 Cryopreservation of the cell lines

Cell lines were harvested as previously mentioned, and cell counts were performed. The freezing medium was prepared by adding 1 ml 10% FBS and 1 ml dimethylsulfoxide (DMSO) into 18 ml complete medium containing 10% FBS. Cells were centrifuged at 1000 rpm for 5 minutes and then the pellet was re-suspended in the freezing medium at a concentration of $2-5 \times 10^6$ /ml. A 1 ml aliquot of this solution was put into each clearly labelled cryotube. The cryotubes were then wrapped in clean towels and incubated at -80°C for approximately 24 hours, then transferred to liquid nitrogen.

2.2.5 *In situ* hybridization for RNA expression in cell lines and lung tissues.

2.2.5.1 Preparation of cytoblocks

Cell lines were grown in a complete RPMI-1640 medium containing 10% foetal bovine serum (FBS) and penicillin streptomycin (pen-strep). Cells were then harvested and the Shandon Cytoblock System was used to prepare cytoblocks. The harvested cells were counted using a haemocytometer and centrifuged at 800 rpm for 5 minutes. The supernatant was removed, and the cell pellet re-suspended in 10% formalin for 30 minutes at room temperature for fixation. The cell suspension was then centrifuged again for 5 minutes at 800 rpm. A sufficient amount of reagent 2 was added to the pellet after removing the supernatant to obtain a concentration of approximately 5×10^7 cells per 100 μ l. Three drops of reagent 1 were added to the well in the cytoblock board, and cytoblock cassettes and cytofunnels were then assembled in the cytospin clip. 100 μ l of the suspended cells in reagent 2 were

placed in the cytofunnel and centrifuged for 5 minutes at 1500 rpm on 'Lo' acceleration. One drop of reagent 1 was applied to the centre of the cassette well after removing the cassette from the clip, and then the cassette was closed and immersed in 70% IMS prior to embedding into paraffin wax. Cytoblocks were prepared from both treated and control cells, and then fixed on polysene slides.

2.2.5.2 *In situ* hybridization technique

ISH was used to determine the level of *MCL-1*-mRNA expression in NSCLC cases. Paraffin-embedded tissues from patients with NSCLC were analysed for *MCL-1* mRNA expression along with different lung cancer cell lines with *MCL-1* amplification. Slides were heated to 60°C for an hour, and then passed twice through xylene solvent for 10 minutes, followed by merging twice into 100% fresh ethanol or 99% IMS for 3 minutes each time. Sections were dried for 5 minutes at room temperature. A hydrophobic barrier was created around the specimen using an ImmEdge pen (Vector Laboratories, Inc., Cat No. 4000; Burlingame, CA, USA) and then 5-8 drops of pre-treatment 1 were added onto the specimen and incubated at room temperature for 10 minutes. The pre-treatment 1 was decanted and the tissue sections immersed in distilled water with agitation. In a fume hood, pre-treatment 2 was heated to 100-104°C and slides were then transferred into boiling solution for 15 minutes. Samples were removed from the boiling pre-treatment 2 and rinsed in distilled water with agitation, followed by submerging into 100% or 99% IMS. Samples were then treated with pre-treatment 3 and incubated at 40°C for 30 minutes for the lung tissue and for 15 minutes for the cell lines. Samples were washed in distilled water with frequent agitation, which was repeated for 5-15 minutes. Samples were transferred into a warm HyEZ humidity control tray (40°C) containing a slide rack and humidifying paper. Target and control probes

were pre-warmed at 40°C for 10 minutes and 3-4 drops of probe were added to the specimens, which were then incubated for 2 hours at 40°C in a HyEZ oven. 1X wash buffer was used immediately to wash the slides for 2 minutes after 2 hours incubation, and then the wash was repeated in fresh 1X wash buffer with frequent agitation. Following that, amplifiers 1, 2, 3 and 4 were applied to the slides, and the slides were incubated at 40°C for 30, 15, 30 and 15 minutes, respectively. Amplifiers 5 and 6 were then added for 30 and 15 minutes, respectively, and incubated at room temperature followed by washing twice for 2 minutes after each amplifier treatment. Equal amounts of DAB solution A and DAB solution B were mixed and then applied to the tissue sections for 10 minutes at room temperature to develop the signals. Distilled water was then used to wash the DAB chromogene and the slides submerged in 50% haematoxylin for 2 minutes. Fresh water was used to wash the haematoxylin stain, and then the slides were passed through 70% ethanol or 95% IMS once for 2 minutes and twice in 100% ethanol or 99% IMS for 2 minutes, followed by merging into fresh xylene for 5 minutes. Finally, slides were mounted using a DPX mounting medium (Cell Path Ltd., Newtown Powys, UK). Pictures were captured using a Leica DFC 420 camera (Leica Microsystems Ltd., Switzerland) and the staining was analysed using the Aperio Image Scope software (v.11.1.2.760).

2.2.6 Gene expression

2.2.6.1 Cell treatment

Cell lines were seeded at a density of 5×10^5 and grown in RPMI1640 complete medium containing 10% FBS at 37°C/5% CO₂. MEK inhibitor (U0126), mTOR inhibitor (AZD8055) and stat inhibitors (Niclosamide and SH-4-54) were used to target MAPK, PI3K and JAK pathways, respectively, with control cells treated with

DMSO. Cells were treated with inhibitors for 3, 24, 48 and 72 hours. The selected concentrations of the inhibitors for treatment were 70 nM, 700 nM, 0.8 nM, 300 nM and 464 nM to target MEK1, STAT3, mTORC1/2, STAT3 and STAT5, respectively. Cells were then harvested for RNA extraction.

2.2.6.2 RNA extraction from cell lines using the Qiagen RNeasy kit

RNA was prepared from cell lines using the Qiagen RNeasy mini kit (Cat. No 74106) according to manufacturer instructions. Briefly, cell pellets were re-suspended in lysis buffer RLT containing 0.01% β -Mercaptoethanol (BME) and homogenised at room temperature, after which 70% ethanol was added. The mixture was then introduced into the RNeasy column. RNA was eluted using RNase-free water after washes with RW1 and RPE, respectively, and the RNA was stored at -20°C until required.

2.2.6.3 Generation of cDNA by reverse transcription (RT)

TaqMan® Reverse Transcription Reagents (Applied Biosystems, CA, USA) were used to generate cDNA. The reaction was performed in a total volume of 20 μL . A master mix was prepared by combination of 2 μL 10X RT buffer, 1.4 μL MgCl_2 (25 mM), 4 μL dNTP (10 mM; 2.5 mM for each constituent), 1 μL RNase inhibitor (20 U/ μL), 1 μL of 50 U/ μL Multiscribe RT (recombinant Murine Leukemia Virus reverse transcriptase (MuLV RT)), 1 μL Oligo d(T)₁₆ (50 μM) and 1 μL random hexamers (501 μM). At least 1 μg total RNA was added to the pre-mixed reagents. The volume of RNA added was dependent on the RNA concentration in the suspension medium; finally, RNase-free water was used to make up the final volume (20 μL).

For cDNA generation, samples were incubated for 5 minutes at 65°C, incubated at 4°C for 2 minutes, and then left for 5 minutes at room temperature and re-incubated at 37°C and 95°C for 30 minutes and 5 minutes, respectively. Finally, samples were kept at -20°C until use.

2.2.6.4 Gene expression analysis

For the target genes' relative expressions ($\Delta\Delta CT$), target genes were compared to endogenous standards (Glyceraldehyde-3-Phosphate Dehydrogenase (GAPDH) and Ubiquitin C (UBC)). Average threshold (CT) values were obtained, and from this a ΔCT and $\Delta\Delta CT$ was calculated to give a final RQ value from the following equations:

$$\Delta CT = \text{average Ct sample} - \text{average Ct endogenous control}$$

$$\Delta\Delta CT = \Delta CT \text{ sample} - \Delta CT \text{ sample reference.}$$

$$\text{Then: } RQ = 2^{(-\Delta\Delta CT)}$$

2.2.7 Cell viability assessment

The alamarBlue assay was used for determination of cell proliferation and viability in the culture medium. The cell lines were cultured in 96 well plates, and incubated at 37°C. After 24 hours of treatment, 10 μL of alamarBlue solution 10X was added to the seeded cells on the 96 well plates and re-incubated for 1-4 hours; each of the 96 well plates contained 100 μL of the culture medium. The resulting fluorescence was read on a microplate reader (FLUOstar, BMG LABTECH, Germany), and each experiment was repeated 3-4 times.

2.2.8 Explant tissue culture and analysis

After surgery tumour tissues were placed in balanced salt solution and then cut into pieces of 2-3 mm³. Explants were cultured in DMEM medium containing 4.5g/L glucose, 0-5% FCS and 1% penstrep and were incubated at 37°C and 5% CO₂ for 16-20 hours. Explants then transferred into 1.5 ml new culture medium and carrier control or drug were added and incubated for 24 hours to each culture medium. The used cisplatin doses included 0, 1, 10 and 50 µM. After treatment explants were washed with PBS and transferred into 1 ml of 4% paraformaldehyde for 20 hrs. Explants were transferred onto presoaked sponge in 70% ethanol and placed in histology cassette and then embedded into paraffin wax for immunostaining analysis for cPARP (cell death) and Ki67 (cell proliferation). Drug response was evaluated by dividing the value of each treatment by the carrier control to obtain a fold change (Karekla *et al.*, 2016) (submitted to cancer research).

2.2.9 Statistical analysis

All statistical analyses were performed in Graph Pad Prism 6.04. P values of < 0.05 were considered statistically significant.

Chapter 3. Genetic alterations in non-small cell lung cancer

3.1 Introduction

DNA sequencing is the standard method for mutation analysis in tumour samples; however, whole exome (WES) and whole genome (WGS) sequencing is hampered by limited sensitivity and analysis of CNV is challenging. Analysis of 300 individual tumours using next-generation sequencing has shown that *MCL-1* is one of the most commonly amplified genes in human malignancies (Vogler, 2014), with several genetic alterations such as translocations and copy number changes being identified in lung cancer, including amplification of *FGFR1*, *SOX2*, *KRAS*, *MDM2*, *MYC*, *MET*, *EGFR*, *ERBB2*, *BCL2L1*, and *TERT* (Staaf *et al.*, 2013). Furthermore, several oncogenic mutations have been identified in lung cancer (El-Telbany and Ma, 2012).

Quantitative real-time PCR (qRT-PCR) is an extremely sensitive method for detection of somatic mutations (even at single copy frequencies) and copy number alterations, making this an attractive method for screening clinical biopsies and minute lysates from micro-dissected samples. Furthermore, high throughput and low cost assays are other advantages of qRT-PCR, as well as the ability to multiplex (Nicklas and Buel, 2003, Xu *et al.*, 2012). Taken together, this offers a huge advantage over WGS, which is plagued by high costs of consumables, laborious workflows and relatively lower sensitivity (limit of detection 5%). In this chapter, analysis of genetic alterations including point mutations and copy number variation in NSCLC using qRT-PCR was performed.

3.2 Aims and objectives

Due to the high cost of next generation sequencing, and its inferior limits of detection, the aim of this study was to develop a PNA-LNA-clamping assay for low limit detection of oncogenic driver mutations such as *KRAS*, *PIK3CA*, *EGFR* and *BRAF* in NSCLC and develop CNV assays for detection of gene amplification. Specific objectives were:

1. To study oncogene driver mutations and copy number change in a cohort of 85 cases of NSCLC using DNA extracted from FFPE sections by micro-dissection.
2. To analyse hotspot mutation in *KRAS*, *PIK3CA*, *EGFR* and *BRAF* using PNA-LNA-clamping qPCR in NSCLC cases.
3. To validate *MCL-1* amplifications in NSCLC cell lines.
4. To determine the frequency of *MCL-1*, *PIK3CA* and *SOX2* copy number changes in NSCLC cases.

3.3 Results

3.3.1 Oncogene driver mutation analysis

3.3.1.1 Validation of oncogenic mutations in control cell lines.

Mutations were analysed using tagged primers, specific hybridizing probes and LNA primers, as previously mentioned in Table 2.1, 2.2, 2.3, 2.4 and 2.5. The PNA clamping technique was introduced to increase sensitivity of the reactions via suppression of WT alleles. *KRAS* (exon 2), *PIK3CA* (exon 9 and 20), *BRAF* (exon 15), and *EGFR* (exon 21) mutations were analysed in control DNAs (Table 2.7 in Chapter 2). Cell lines were first analysed for mutations using the duplex test, in which each reaction contains specific WT and MUT probes. Figure 3.1 shows an example of a duplex test performed on two cell lines containing the *KRAS* mutation in the first base of codon 12; the specific hybridizing probe for detection of this mutation was described as *KRAS* 121 in Table 2.1. The reaction showed amplification of both WT and MUT alleles, indicating the presence of *KRAS* mutation in codon 12 without discrimination of which nucleotide substitution.

Base substitution was then discriminated using LNA-specific primers. The LNA-specific primers were more precise than tagged specific primers and showed specific

amplification to the exact targeted allele (Figure 3.2). This strategy was also adopted to analyse *BRAF* mutations. The PNA clamping technique increased the sensitivity of the reaction through suppression of the WT alleles (Figure 3.3) with a limit of detection of 0.1% of the mutant allele (Figure 3.4).

PIK3CA and *EGFR* mutations were analysed using only specific hybridizing probes. Each assay showed high specificity to the target sequence, with no concurrent detection of mutants in wild-type DNA. Figure 3.5 shows an example of the reaction using *PIK3CA* assays.

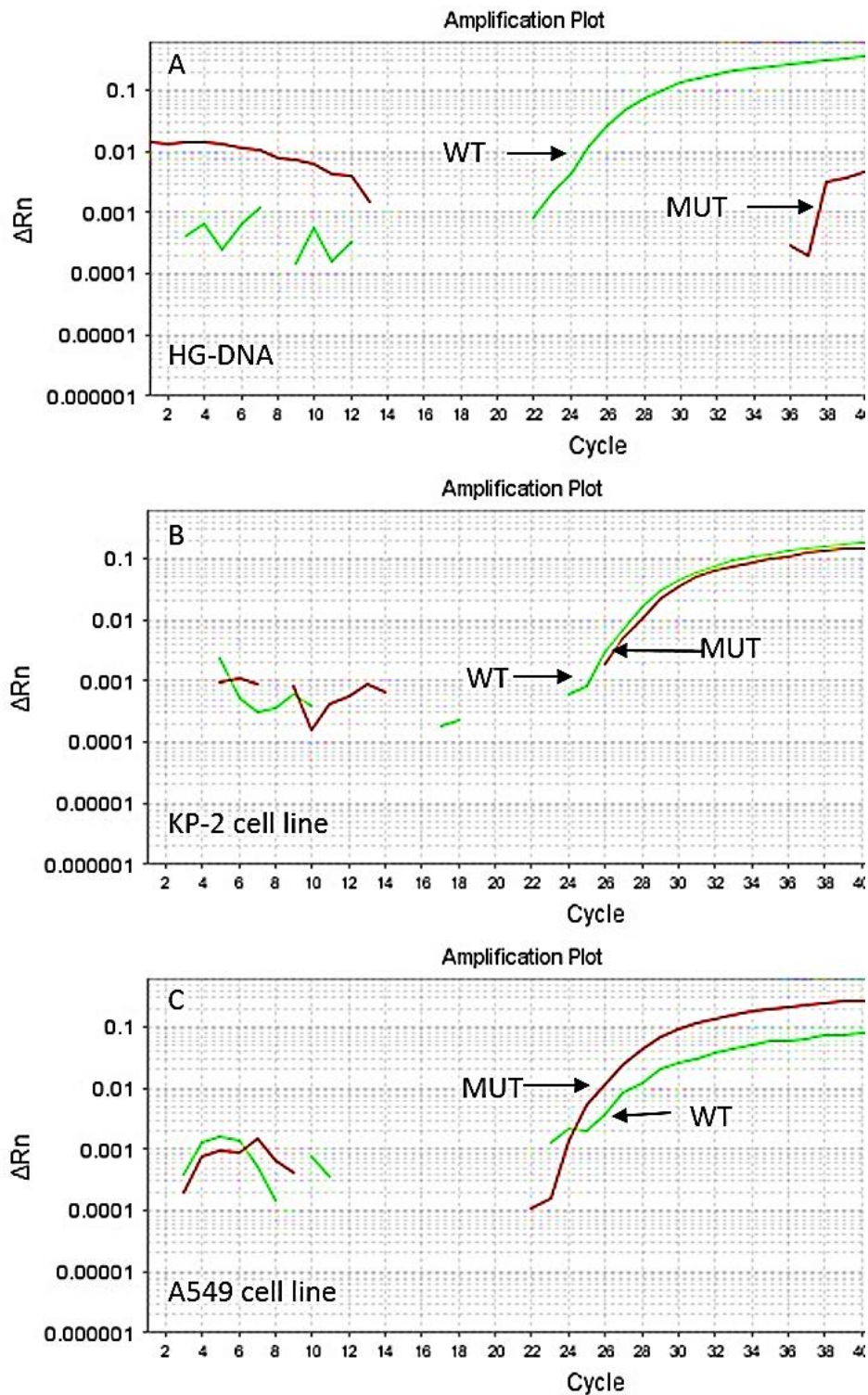


Figure 3.1 Probe method for mutation analysis. A duplex test showing amplification of both WT and mutant (MUT) DNA by specific WT and MUT hybridizing probes. No amplification of the MUT *KRAS121* probe was detected when the normal control HG-DNA used (A). The MUT *KRAS121* probe has detected two different mutations, G12R (B) and G12S (C), in the KP-2 and A549 cell lines, respectively.

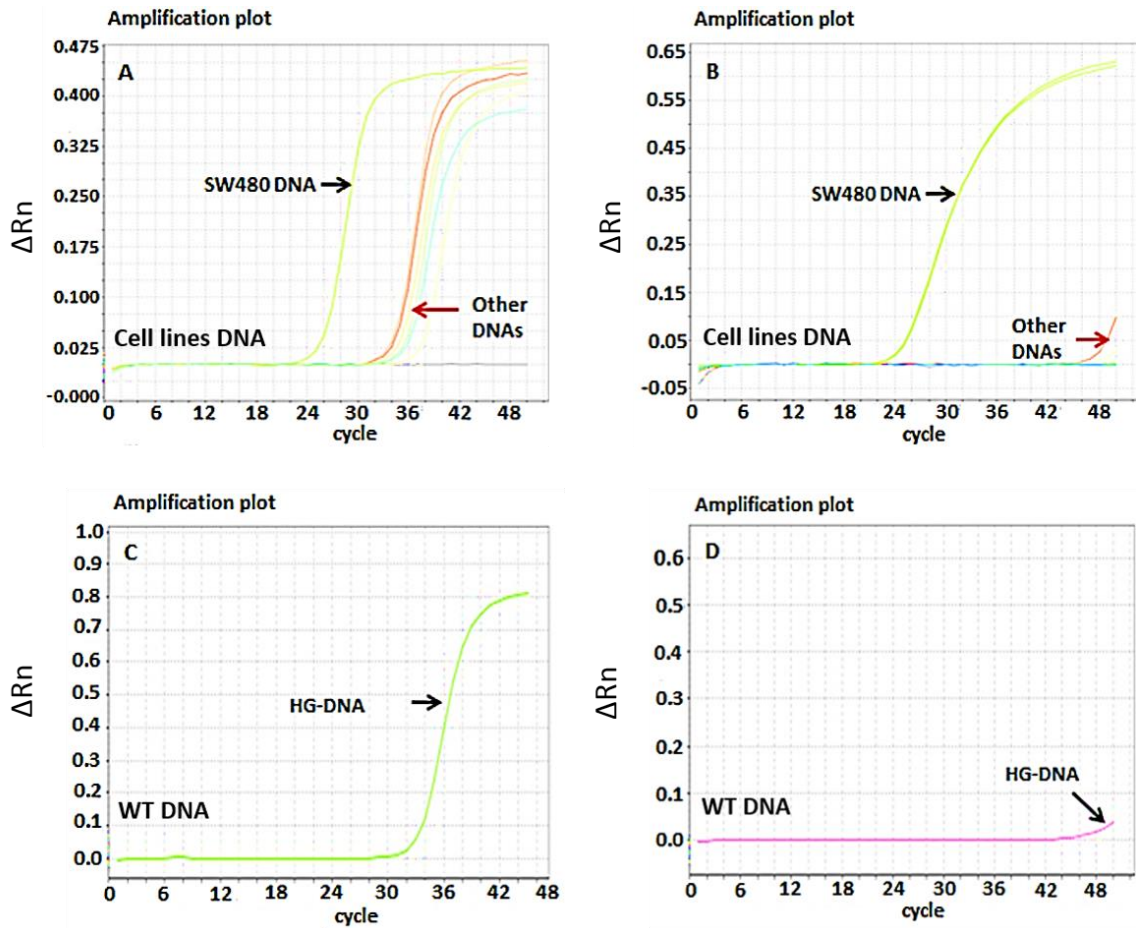


Figure 3.2 Tagged specific primer vs LNA specific primer. The tagged *KRAS* 35G→T primed reaction has a low CT value with SW480 DNA for a cell line which possesses the 35G→T mutation. However, the other *KRAS* mutant cell lines (SW 837, A549, SW1116, GP2D and HCT 116) have high CT values, indicated by red arrow (A). The LNA- 35G→T primed reaction was more specific as all CT values of the other DNAs were over 45 as indicated by red arrow (B). The tagged 35G→T showed amplification of the WT allele with a high CT value (C), while the LNA- 35G→T reaction with WT DNA (HG-DNA) showed complete absence of amplification signal (D).

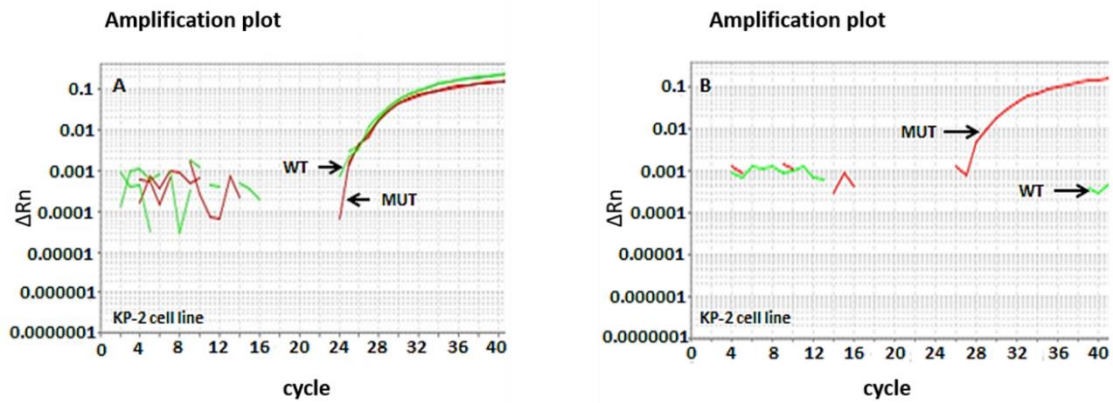


Figure 3.3 PNA clamping. Amplification of both WT and MUT alleles in the KP-2 cell line DNA (A) in a reaction without PNA and a reaction containing PNA showed suppression of the WT allele in the KP-2 cell line DNA (B)

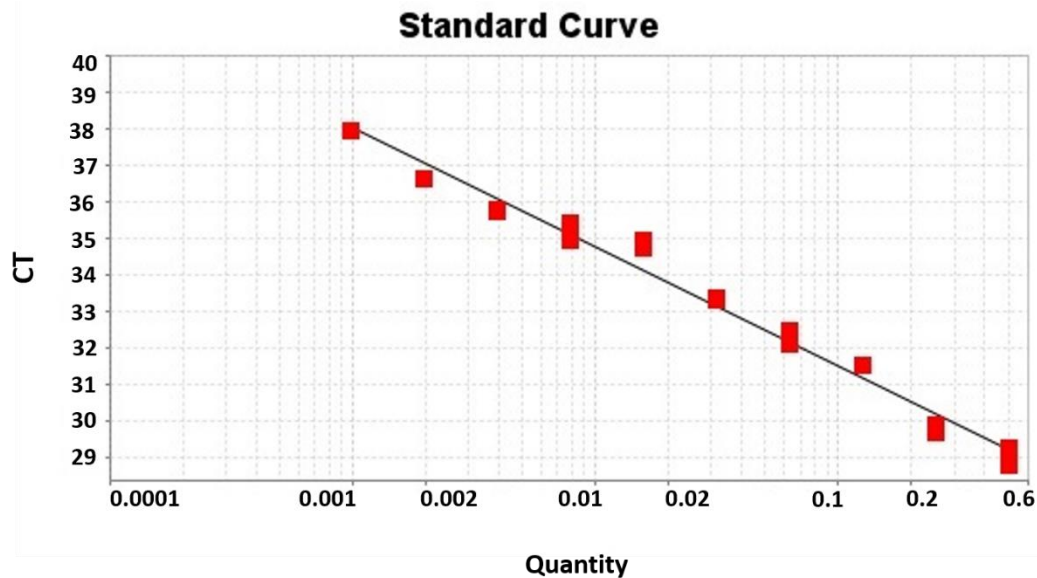


Figure 3.4 Detection of low mutant DNA using the PNA clamping technique. The standard curve shows the detection of a low concentration of mutant DNA (*KRAS* G12C from H358 cell line) within a high background of wild-type allele (HG-DNA). The curve is showing the lowest detected amount of the mutant DNA (*KRAS* G12C), which is about 0.1% of mutant alleles in large background wild-type alleles (HG-DNA). Control reactions with HG-DNA only showed CT values > 40.

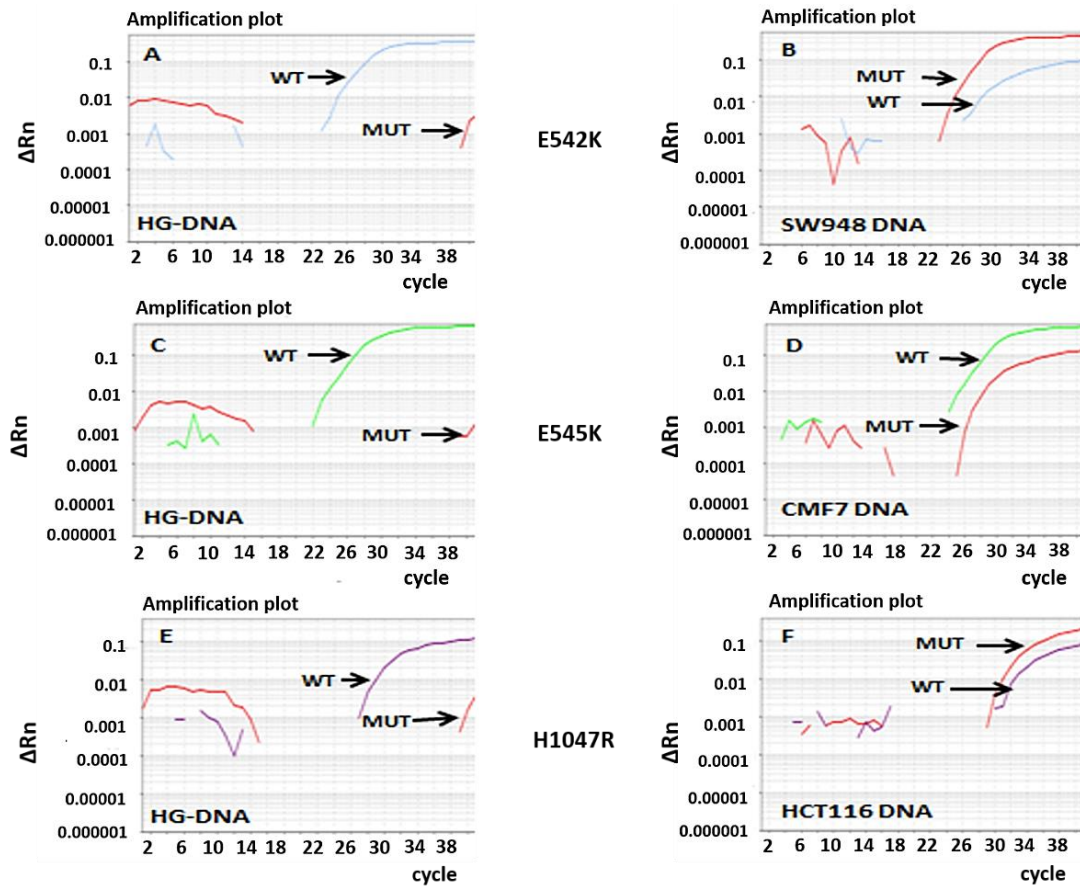


Figure 3.5 Validation of *PIK3CA* assays. The duplex reaction for *PIK3CA* probes E542K, E545K and H1047R showed specific amplification of WT alleles through a WT-specific probe without amplification of the mutant alleles when the reaction was run with HG-DNA (A, C and E). Specific amplification of both WT and MUT alleles were detected in the heterozygous cell line SW948 when the reaction was run with an E542K assay (B). Specific amplifications for WT and MUT alleles were also detected in MCF7 and HCT116 heterozygous cell lines when the reaction was run with E545K and H1047R-specific probes, respectively (D and F).

3.3.1.2 Oncogene driver mutation analysis in tumour samples

Eighty five cases of lung cancer, including 79 cases of NSCLC, were analysed for oncogene mutations. Several oncogene driver mutations were investigated in NSCLC using the PNA clamping technique. Table 3.1 shows some examples for the identified oncogene driver mutation in the screened clinical samples.

Sample	Mutation	CT
Tumour sample LT35	<i>PIK3CA</i> G 1633→A (E545K)	35
MCF7 cell line	<i>PIK3CA</i> G 1633→A (E545K)	30
Tumour sample LT40	<i>KRAS</i> 35G→A (G12D)	33
HCT116 cell line	<i>KRAS</i> 35G→A (G12D)	32
Tumour sample LT51	<i>KRAS</i> 34G→T (G12C)	31
SW837 cell line	<i>KRAS</i> 34G→T (G12C)	27
Tumour sample LT64	<i>EGFR</i> T 2537→G (L858R)	27
H1975 cell line	<i>EGFR</i> T 2537→G (L858R)	26
Negative control HG-DNA	-	Over 45

Table 3.1 Examples of mutations detected in tumour samples. The table shows some examples for *KRAS*, *PIK3CA* and *EGFR* mutation in the analysed tumour samples. The table also shows examples of positive and negative control DNAs used for mutation analysis. The negative control DNA (HG-DNA) showed a CT value of over 45. Tumour samples and cell line with oncogene mutations showed CT values below 40. There are some slight variations between CT values of tumour samples and cell lines due the poor quality of the DNA obtained from paraffin-embedded tissue compared to cell lines.

KRAS mutation was detected in 19% (15/79) of NSCLC and 10% of the cases showed *PIK3CA* mutation, while the frequencies of *BRAF* and *EGFR* mutations were 0% and 5%, respectively. The majority of the *KRAS* mutant alleles were detected in ADC subtypes with a frequency of 36% (14/39), while the frequency of *KRAS* mutation in SCC was 0% (0/38), *KRAS* mutation was also found in 1 case of LCC (1/2). *PIK3CA* mutations were present in 5% (2/39) and 15.7% (6/38) of ADC and SCC, respectively. *BRAF* mutation was not detected in either SCC or ADC. *EGFR* mutation was detected in 10% (4/39) of ADCs but no *EGFR* mutation was identified in SCC (Figure 3.6).

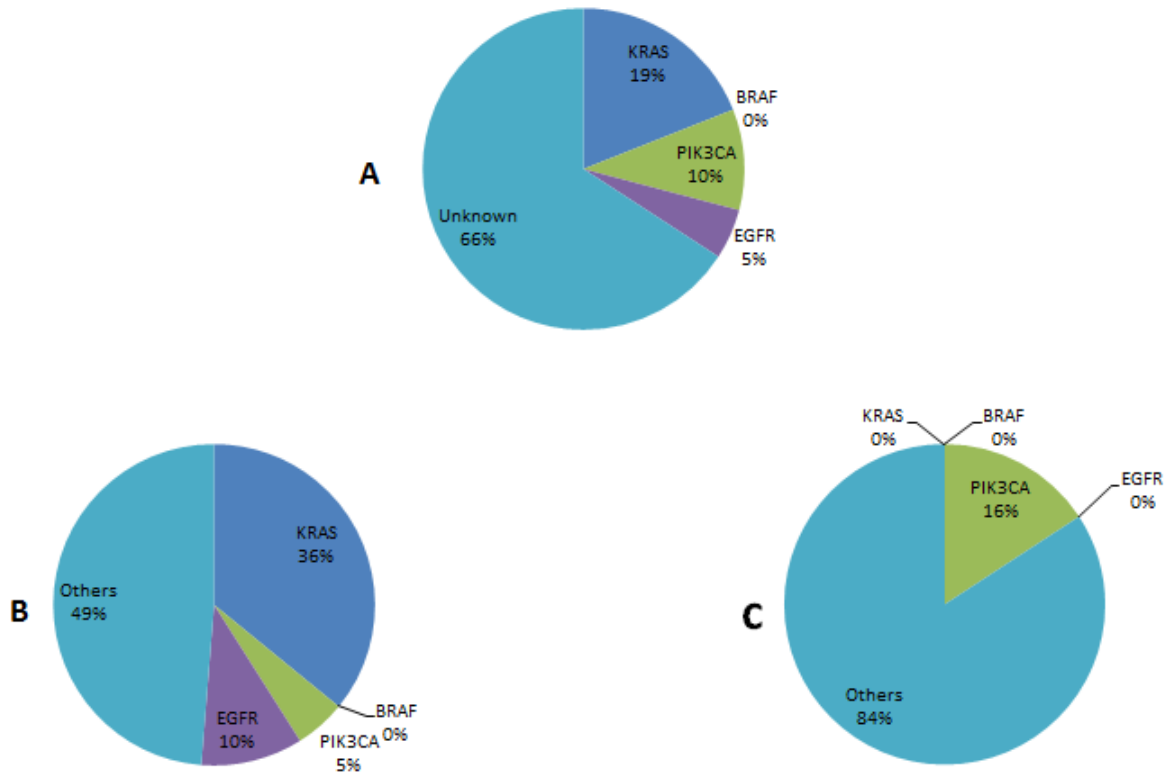


Figure 3.6 Frequencies of oncogene driver mutations in NSCLC. In NSCLC, *KRAS* mutation was the most common type of mutation (19%) compared to *PIK3CA* (10%), *EGFR* (5%) and *BRAF* (0%) (A). The most common type of mutation in ADC was *KRAS* mutation (B), whereas *PIK3CA* mutation was the commonest mutation in SCC (C).

All cases positive for *KRAS* mutation, were in codon 12 mutation, the most common of which 34 G→T (G12C), and was detected in 40% (6/15) of cases. G35>T (G12V) was found in 13% (2/15) of cases, whereas G35>C (G12A) and G35>A (G12D) were present at frequencies of 20% (3/15) and 27% (4/15), respectively. 34 G>A (G12S), 34 G>C (G12R) and codon 13 mutations were not detected (Figure 3.7). One LCC sample also harboured a 35 G>A (G12D) *KRAS* mutation.

Seven of the fourteen patients were smokers, whilst the other seven patients were described as cases with an unknown smoking history. 80% (12/15) of patients who

demonstrated *KRAS* mutations were females. Furthermore *KRAS* mutations were seen at different stages of the disease. One stage IV cancer had *KRAS* mutation, 2/15 samples were identified at stage III, one case was an unknown stage, while 5/15 stages I and 6/15 stage II cases harboured *KRAS* mutations.

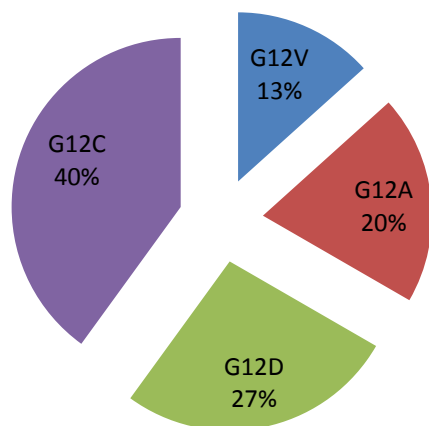


Figure 3.7 Frequency of *KRAS* mutations. Guanine to thymine substitution 34G→T, or G12C, was the most frequent type of base substitution in codon 12 of the *KRAS* gene, whereas 35G→T, or G12V, was the less frequent type of nucleotide substitution among the all detected base changes in codon 12 of *KRAS* gene. Codon 13 substitutions were not detected.

PIK3CA mutations were detected in 8 NSCLC cases (10%) of which 2 were E545K positive, 2 were H1047R and 4 were positive for E542K (Figure 3.8). E542K was identified as the most frequent *PIK3CA* mutation in SCC (4/6), with both E545K and H1047R being detected once. The two detected mutations in ADC were E545K and H1047R. No gender disparity was observed in the frequency of *PIK3CA* mutation, with 57.1% of the cases being females and 42.9% being males. Moreover, *PIK3CA* mutations were detected at all stages of NSCLC.



Figure 3.8 Frequencies of PIK3CA mutations in NSCLC. The highest frequency of PIK3CA mutation was detected at the hotspot E542K, while the other two hotspots (E545K and H1047R) showed equal frequencies in NSCLC.

Mutations in EGFR (L585R) were identified in NSCLC samples. *EGFR* mutant alleles were detected in patients with adenocarcinomas, but not in SCC. A high incidence of *EGFR* mutation was observed in 3/4 women (75%). 2/4 patients with the *EGFR* mutation were at stage I of the disease, while the other two patients were diagnosed with stage III ADC. Three of the patients were smokers, whilst the smoking history of the fourth patient was unknown.

Finally, the most common type of *BRAF* mutation (V600E) was not found in either SCC or ADC.

3.3.2 Analysis of copy number changes

3.3.2.1 Analysis of *MCL-1* amplification and gain in NSCLC cell lines.

Lung cancer cell lines of different histological subtypes were analysed for *MCL-1* gain and amplification. Chaperonin-Containing TCP1, Subunit 3 (*CCT3*) and the hexose-6-

phosphate dehydrogenase (*H6PD*) genes were used as control reference genes. *CCT3* is located on the q arm with *MCL-1* and *H6PD* is located on the p arm.

In the case of focal amplification, *MCL-1* CT values were lower than *CCT3* and *H6PD* CT values, and the Δ CT between two reference genes *H6PD* and *CCT3* is zero, whereas in case of gain, the *MCL-1* CT value is lower than the *H6PD* CT value but not the *CCT3* value, and the Δ CT between *MCL-1* and *CCT3* is zero as they are on the same chromosome. However, the CT value of the *CCT3* reference gene is lower than the *H6PD* CT value (Figure 2.2).

The H1395 cell line was used to validate the assay as it is amplified for *MCL-1*. A commercial human genomic DNA (Roche, UK) was used as a diploid copy number reference. *MCL-1* analysis was performed using the qPCR-duplex ratio test. Multiple copies of *MCL-1* were detected, showing amplification and gain in H1395 and H2342 cell lines, respectively, whereas normal diploid copy number was identified in the H23 cell line (Figure 3.9). Comparative analysis for *MCL-1* against *CCT3* and *CCT3* against *H6PD* showed significant amplification and gain of *MCL-1* in the H1395 and H2342 cell lines, respectively, as determined using a Z score test (Figure 3.10). Tables 3.2 and 3.3 show example cell lines analysed for *MCL-1* amplification and gain, respectively.

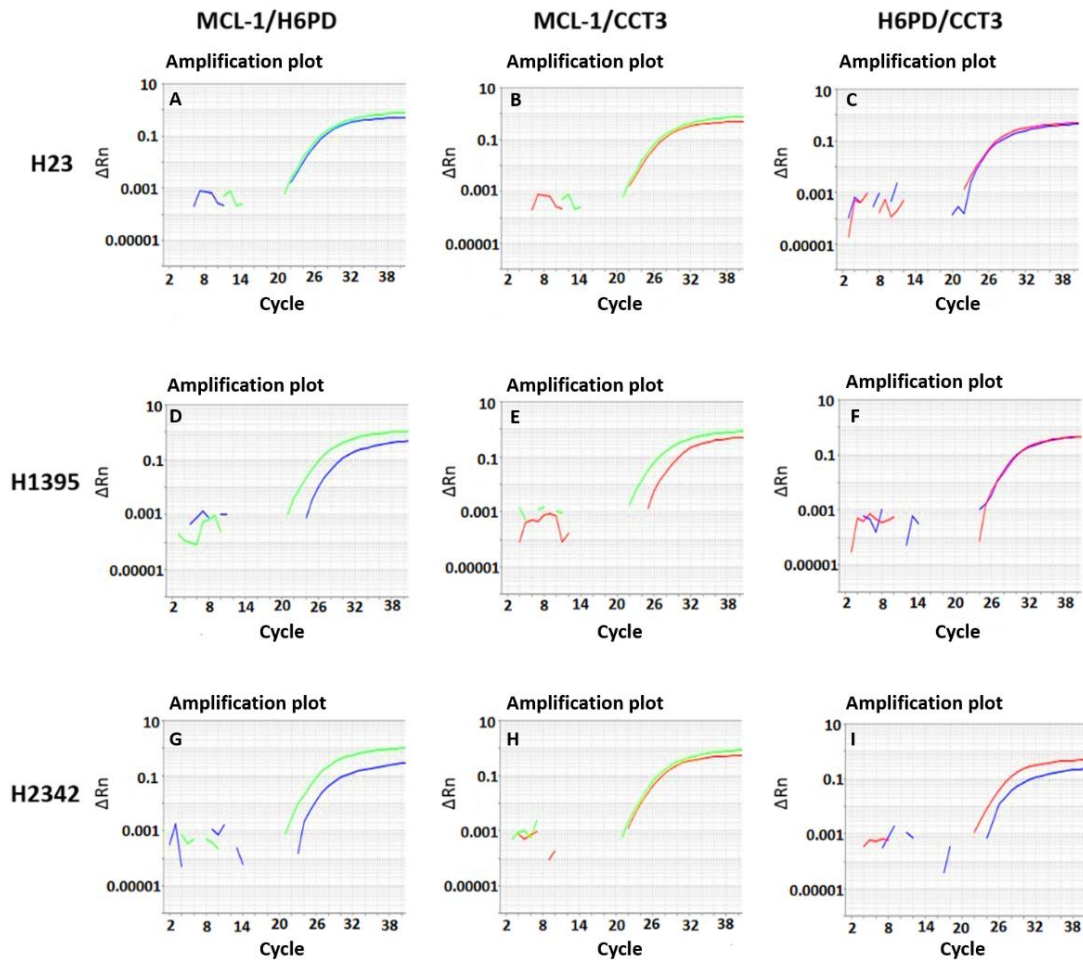


Figure 3.9 *MCL-1* copy number changes in lung cancer cell lines. The normal diploid cell line (H23) showed diploid copies of *MCL-1* (A, B and C). *MCL-1* focal amplification is presented by the adenocarcinoma cell line H1395 as *MCL-1* showed low CT (green curves) compared to the reference genes (blue and red curves) (D and E respectively); the two reference genes have the same CT (F). The H2342 cell line showed gain as the *MCL1* (green curve in G) and *CCT3* gene (red curve in I) showed a lower CT than the *H6PD* gene (blue curve in G and I), but no difference was found between *MCL1* and *CCT3* (H).

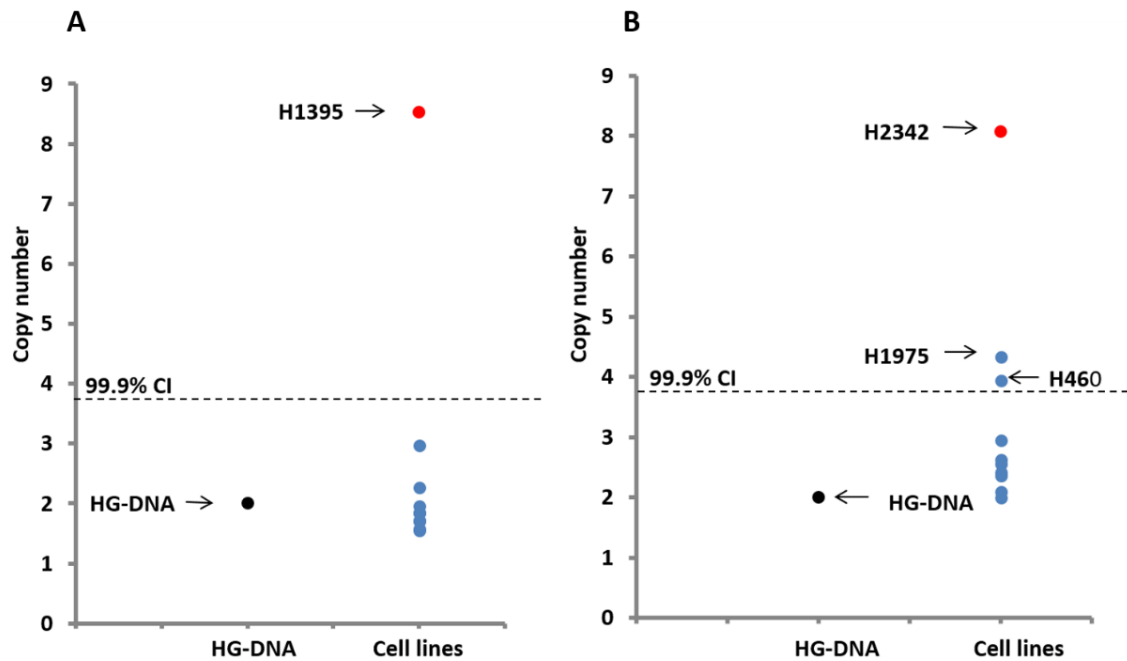


Figure 3.10 *MCL-1* amplification and gain in lung cancer cell lines. The duplex ratio test for *MCL-1* amplification and gain analysis at 99.9% confidence intervals showed massive amplification of *MCL-1* in the H1395 cell line whereas no amplification was identified in H23, A549, H358, H460, H522, H1299, H1975 and H2342 cell lines. HG-DNA was used as a normal diploid control DNA (A). Significant gain was identified in the H2342 cell line; gain was also detected in the H1975 and H460 cell lines, whereas no gain was identified in the H23, A549, H358, H1395, H522 and H1299 cell lines (B).

Cell line	Tissue	Disease	CT	Δ CT	$\Delta\Delta$ CT	RQ	CN amp	Z Score
H23	Lung	ADC	26.30	0.27	0.37	0.77	1.54	-1.62
			26.68					
A549	Lung	ADC	26.36	0.01	0.11	0.92	1.84	-1.87
			26.71					
H358	Lung	BAC	27.81	0.02	0.11	0.92	1.84	-1.87
			27.82					
H460	Lung	LCC	25.09	-0.27	-0.17	1.13	2.26	-2.17
			24.78					
H522	Lung	ADC	28.73	0.11	0.21	0.85	1.71	-1.77
			28.82					
H727	Lung	NE	26.91	-0.67	-0.57	1.48	2.97***	-2.56***
			26.20					
H1299	Lung	NSCLC	30.85	-0.06	0.03	0.97	1.95	-1.96
			30.72					
H1975	Lung	ADC	28.25	0.12	0.22	0.85	1.70	-1.76
			28.33					
H1395	Lung	ADC	28.85	-2.19	-2.09	4.26	8.53*****	-4.08*****
			26.64					
H2342	Lung	ADC	26.37	0.24	0.33	0.79	1.58	-1.65
			26.63					
HG-DNA	-	-	26.94	-0.09	0	1	2	-1.99
			26.90					

Table 3.2 Focal amplification of *MCL-1* in lung cancer cell lines. This table shows example cell lines analysed for *MCL-1* focal amplification using the duplex ratio test. *MCL-1* CT values (blue) and reference gene CT values (black) used to generate Δ CT, $\Delta\Delta$ CT, RQ and CN, and then a Z score test for each sample at CI 99.9% showed significant amplification of *MCL-1* in the H1395 cell line (*p* value 2.20E-05) . H727 has also shown significant amplification compared to the other cell lines at 99.9% CI (*p* value 0.005129). **** Statistically significant.

Cell line	Tissue	Disease	CT	Δ CT	$\Delta\Delta$ CT	RQ	CN gain	Z Score
H23	Lung	ADC	26.10	1.12	-0.39	1.31	2.62	-0.77
			24.99					
A549	Lung	ADC	27.41	0.95	-0.56	1.47	2.95	-0.94
			26.48					
H358	Lung	BAC	27.54	1.24	-0.27	1.20	2.41	-0.65
			26.22					
H460	Lung	LCC	24.97	0.54	-0.97	1.96	3.93	-1.35
			24.44					
H522	Lung	ADC	28.52	1.16	-0.35	1.27	2.55	-0.73
			27.43					
H727	Lung	NE	26.90	1.27	-0.23	1.18	2.36	-0.61
			25.62					
H1299	Lung	NSCLC	30.79	1.52	0.00	0.99	1.99	-0.37
			29.34					
H1975	Lung	ADC	28.13	0.40	-1.11	2.16	4.32	-1.49
			27.72					
H1395	Lung	ADC	29.07	1.45	-0.06	1.04	2.09	-0.44
			27.64					
H2342	Lung	ADC	26.39	-0.49	-2.01	4.03	8.07****	-2.39****
			26.89					
HGDNA	-	-	26.72	1.51	0	1	2	-0.38
			25.24					

Table 3.3 *MCL-1* copy number gain in lung cancer cell lines. This table shows example cell lines analysed for *MCL-1* gain using the duplex ratio test. CN was analysed after generation of CT, Δ CT, $\Delta\Delta$ CT, RQ and CN of the candidate genes (*CCT3* and *H6PD*), and a Z score test for each sample at CI 99.9% was determined, with the result showing significant copy number gain of the *CCT3* gene on the q-arm with *MCL-1* in the H2342 cell line (*p* value 0.008378). However, the other cell lines, including H1395 (amplified for *MCL-1*), did not show *CCT3* copy number gain at 99.9% CI (*p* < 0.01). **** Statistically significant.

3.3.2.2 *MCL-1* copy number variation analysis in tumour specimens

Copy number variation analysis (amplification and gain) for *MCL-1*, *PIK3CA* and *SOX2* was performed using qPCR. Each tumour tissue was analysed using $\Delta\Delta\text{CT}$ and a Z score test was used to analyse the significance of the gain and amplification in the tumour samples at a confidence interval (CI) of 99.9%. Figure 3.11 shows an example amplification plot of *MCL-1* copy number change (amplification and gain) in tumour samples, whilst Figure 3.12 demonstrates cases with significant *MCL-1* gain and *MCL-1* focal amplification at a 99.9% CI.

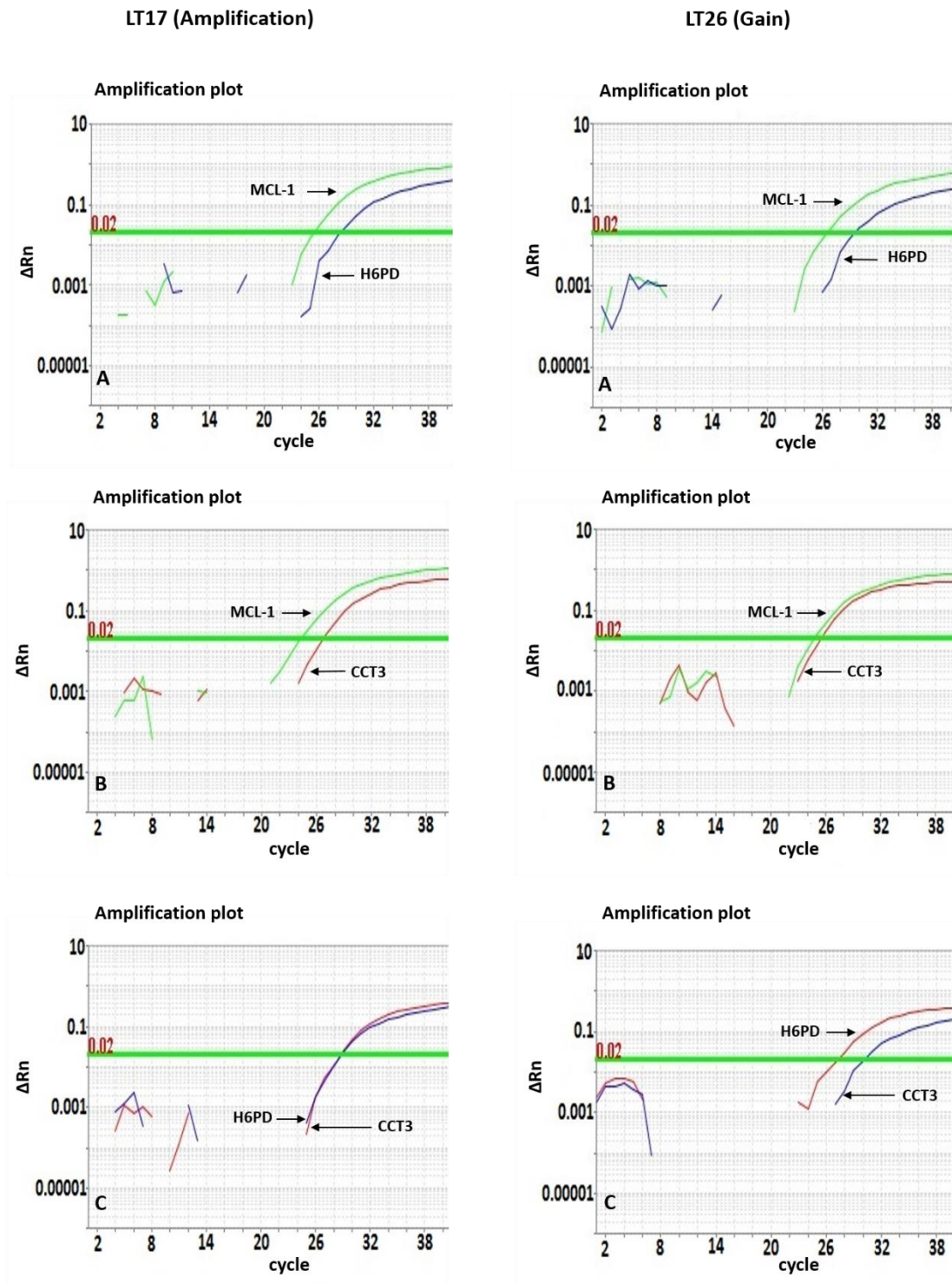


Figure 3.11 Amplification vs gain in tumour samples. The top three amplification plots show amplification of the *MCL-1* gene in SCC sample (T17), while the bottom three amplification plots show the presence of gain in the ADC sample (T26). The blue curves on the amplification plots (A) show *MCL-1*, the green curves on the amplification plots (B) also show *MCL-1*, whilst on the amplification plots (C), *CCT3* and *H6PD* were designated by orange and pink curves, respectively

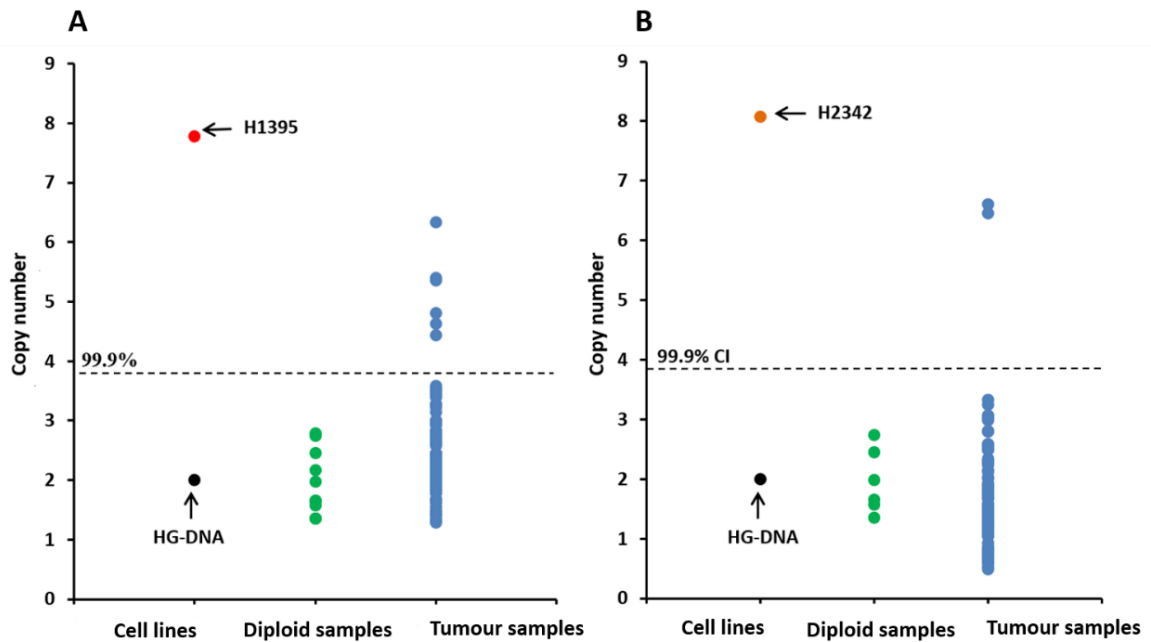


Figure 3.12 *MCL-1* amplification and gain in tumour samples. *MCL-1* amplification was significant in tumour samples LT5, LT7, LT8, LT9, LT17 and LT38 at a 99.9% confidence interval, diploid samples (tumour adjacent tissues) and HG-DNA did not show significant *MCL-1* amplification, whereas the positive control DNA from the H1395 cell line showed significant *MCL-1* amplification ($p < 0.001$) and showed about eight copies of *MCL-1* (A). *MCL-1* gain was significant in tumour samples LT7 and LT26 at a 99.9% confidence interval; control tumour samples and HG-DNA did not show significant *MCL-1* gain, whereas positive control DNA from the H2342 cell line showed very significant *MCL-1* gain ($p < 0.001$) (B).

MCL-1 amplification was found in 7.5% (6/79) of NSCLC cases. *MCL-1* amplification was found in 5/38 (13%) of SCC, however one patient with ADC demonstrated *MCL-1* amplification. Gain was detected only in two cases of NSCLC, one SCC and one ADC. *MCL-1* amplification was detected in both early and late stages of NSCLC without correlation to stages of the disease; 3/6 patients were stage I and II, while the last case was stage III.

There was no significant difference between gains and amplifications according to the stage of the disease. Furthermore, extra copies of chromosome 1 were detected in different stages of NSCLC, in both males and females, and both smokers and non-smokers showed *MCL-1* amplifications. However, males had a higher frequency of *MCL-1* amplification (4/5) compared to females (1/5), without links to a smoking history. Genetic and chromosomal aberrations were identified in the all age groups of NSCLC patients (53-84 years old).

3.3.2.3 Analysis of *PIK3CA* and *SOX2* copy number variation

PIK3CA copy number change was evaluated through qPCR; high copy numbers of *PIK3CA* and *SOX2* were first validated in the SCC cell line (RERF-LC-Sq1), which was used as a positive control for amplification in tumour samples. *CAPN7* (on the p-arm of chromosome 3) and *GATA2* (on the q-arm of chromosome 3 with *PIK3CA* and *SOX2*) were used as reference genes for both *SOX2* and *PIK3CA* amplification analysis and gain discrimination.

Amplification of *PIK3CA* was detected in 34% (27/79) of NSCLC. 20/27 (74%) of the cases were SCCs and 7/27 (25.9%) were ADC. 15/79 (18%) of NSCLC showed amplification of *SOX2*. The majority of the cases with *SOX2* copy number change were SCCs 13/15 (86.6%), whereas *SOX2* amplification was detected in 13.3% (2/15) of ADCs. Figure 3.13 demonstrates cases with significant *PIK3CA* and *SOX2* focal amplification at a 99.9% CI. *SOX2* and *PIK3CA* were detected in all stages of NSCLC without correlation to any the following factors: gender, age or smoking history. Table 3.4 shows the analysed copy number changes in NSCLC.

PIK3CA and *SOX2* Gain (isochromosome 3q) was detected only in 4 cases of NSCLC at 95% CI (Figure 3.14), all of the cases were SCC and no gain was detected in ADC and LCC.

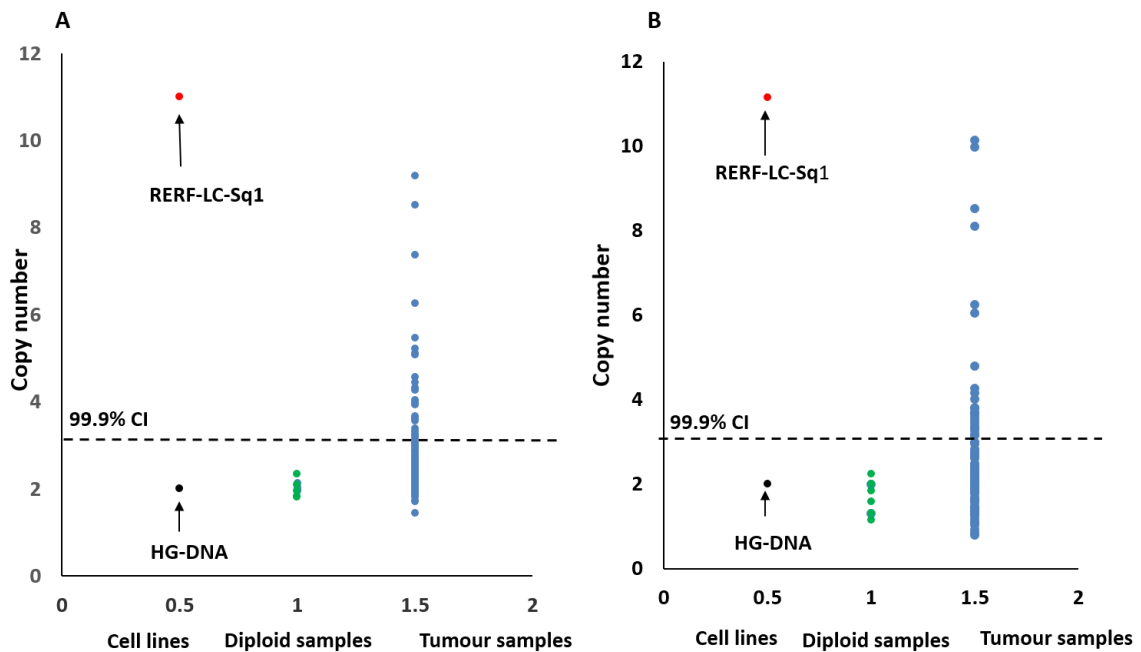


Figure 3.13 *PIK3CA* and *SOX2* amplifications in tumour samples. *PIK3CA* amplification was significant in 34% of tumour samples at a 99.9% confidence interval, diploid samples (tumour adjacent tissues) and HG-DNA did not show significant *PIK3CA* amplification, whereas the positive control DNA from the RERF-LC-Sq1 cell line showed significant *PIK3CA* amplification ($p < 0.001$) and showed about eleven copies of *PIK3CA* (A). *SOX2* was significant in 18% of tumour samples at a 99.9% confidence interval; control tumour samples and HG-DNA did not show significant *SOX2* amplification, whereas positive control DNA from the RERF-LC-Sq1 cell line showed very significant *SOX2* amplification ($p < 0.001$) (B).

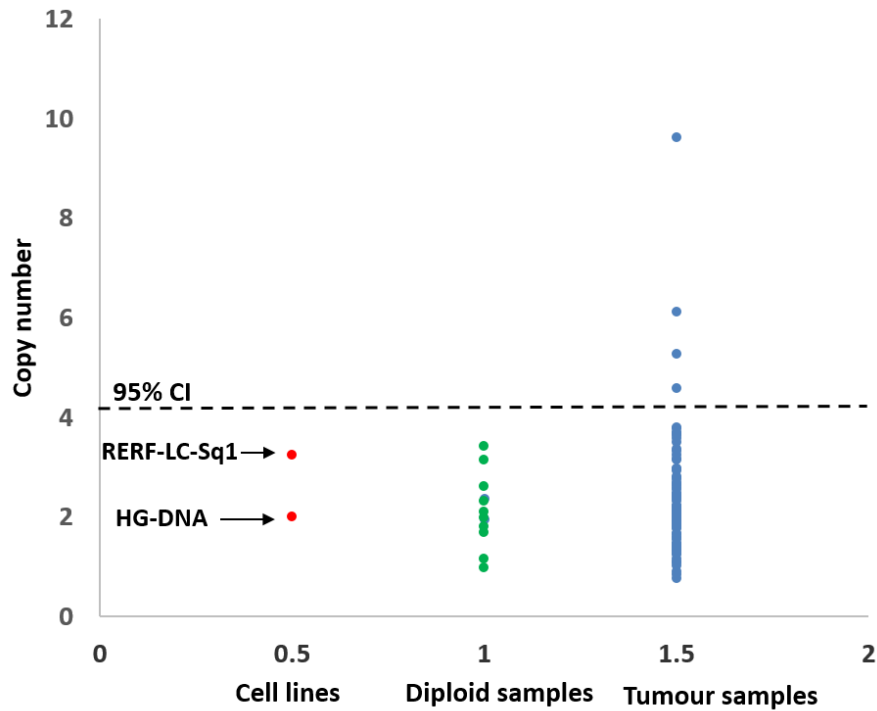


Figure 3.14 *PIK3CA* and *SOX2* gain in tumour samples. *PIK3CA* and *SOX2* gain was significant in tumour samples LT25, LT46, LT61 and LT82 at a 95% confidence interval ($p < 0.05$). Control tumour samples, RERF-LC-Sq1 cell line which is amplified for both (*PIK3CA* and *SOX2*) and HG-DNA did not show significant *PIK3CA* or *SOX2* gain.

Sample ID	Histology	Gender	Stage	gene	Copy number change	No of copies
LT2	SCC	F	IB	<i>PIK3CA</i>	Amplification	3
LT4	ADC	F	IA	<i>PIK3CA</i>	Amplification	3
LT5	SCC	M	IB	<i>MCL-1</i>	Amplification	6
LT7	SCC	F	IB	<i>MCL-1/SOX2</i>	Amplification	4/3
LT8	SCC	M	IIIA	<i>MCL-1</i>	Amplification	4
LT9	ADC	F	Unknown	<i>MCL-1</i>	Amplification	4
LT13	ADC	M	IIB	<i>PIK3CA/SOX2</i>	Amplification	3/3
LT17	SCC	M	IIA	<i>MCL-1</i>	Amplification/Gain	5/6
LT23	SCC	M	IIIA	<i>PIK3CA</i>	Amplification	5
LT24	SCC	M	IIIA	<i>PIK3CA</i>	Amplification	3
LT25	SCC	M	IB	<i>PIK3CA / SOX2</i>	Amplification	5 / 7
LT26	ADC	F	IB	<i>MCL-1</i>	Gain	6
LT27	ADC	M	IIIA	<i>PIK3CA</i>	Amplification	3
LT28	SCC	F	IIB	<i>PIK3CA/SOX2</i>	Amplification	4/4
LT29	ADC	M	Unknown	<i>PIK3CA</i>	Amplification	4

LT30	ADC	M	IIIA	<i>PIK3CA/SOX2</i>	Amplification	4/3
LT32	ADC	M	IB	<i>PIK3CA</i>	Amplification	3
LT33	ADC	F	IIB	<i>PIK3CA</i>	Amplification	3
LT38	SCC	M	IB	<i>MCL-1</i>	Amplification	5
LT42	SCC	F	IIB	<i>PIK3CA</i>	Amplification	5
LT46	SCC	F	Unknown	<i>PIK3CA/SOX2</i>	Amplification	6/3
LT52	SCC	M	IV	<i>PIK3CA</i>	Amplification	5
LT53	SCC	F	IA	<i>PIK3CA</i>	Amplification	4
TL54	SCC	F	IA	<i>PIK3CA</i>	Amplification	5
LT55	SCC	F	IIB	<i>PIK3CA</i>	Amplification	7
LT56	ADC	M	IA	<i>PIK3CA</i>	Amplification	9
LT59	ADC	F	IB	<i>SOX2</i>	Amplification	3
LT61	SCC	M	IB	<i>SOX2</i>	Amplification	9
LT63	SCC	F	IIB	<i>SOX2</i>	Amplification	3
LT64	ADC	F	IB	<i>PIK3CA</i>	Amplification	3
LT65	SCC	M	IB	<i>PIK3CA/SOX2</i>	Amplification	3/5
LT66	SCC	M	IB	<i>PIK3CA/SOX2</i>	Amplification	3/3
LT67	SCC	F	IIA	<i>SOX2</i>	Amplification	3
LT70	SCC	F	IA	<i>PIK3CA</i>	Amplification	3
LT71	SCC	M	IIB	<i>PIK3CA/SOX2</i>	Amplification	4/3
LT73	ADC	F	IB	<i>SOX2</i>	Amplification	3
LT74	SCC	M	IB	<i>PIK3CA/SOX2</i>	Amplification	3/6
LT76	SCC	F	IIIA	<i>PIK3CA/SOX2</i>	Amplification	4/9
LT82	SCC	F	Unknown	<i>PIK3CA/SOX2</i>	Amplification	4/7

Table 3.4 Copy number variation in NSCLC. *MCL-1*, *SOX2* and *PIK3CA* copy number changes were detected in NSCLC. Six cases were amplified for *MCL-1*; the LT5 showed six copies of *MCL-1*, LT17 and LT38 showed five copies, whereas LT7, LT8 and LT9 showed the lowest copy number (four copies). Massive amplification for *PIK3CA* was detected in the tumour sample LT56, *SOX2* high copy number was detected in T61 and T76 while the lowest copy number for both *PIK3CA* and *SOX2* (three copies) were detected in different tumour samples. *PIK3CA/SOX2* co-amplification was detected in nine cases of SCC and two cases of ADC.

3.4 Discussion

Both quantitative real time polymerase chain reaction (qRT-PCR) and next generation sequencing are used for mutation analysis; however, PCR is more sensitive than next generation sequencing (Tuononen *et al.*, 2013). The PNA-mediated PCR clamping technique is a sensitive method for mutation analysis. Tumour tissues are usually contaminated with DNA from different sources, such as inflammatory cells, and paraffin-embedded tissues also contain poor quality DNA. Therefore, we utilised a specific probe hybridization PNA clamping technique to detect mutations in NSCLC samples (Beau-faller *et al.*, 2009). Beau-faller and co-workers (2009) have applied this method to detect *KRAS* mutations in NSCLC and they demonstrated that the PNA clamping method is more sensitive than direct sequencing, which can show false negatives in resected surgical tissues containing a high number of inflammatory cells.

In this study, we applied the clamping technique to different cell line DNAs with *KRAS* mutations in codons 12 and 13 to detect the mutation status of the selected DNA before applying this to clinical samples. This study has supported the findings of Beau-faller *et al.* (2009) and highlighted the ability of this method to detect low frequency mutant alleles in a high wild-type background. Furthermore, several *KRAS* mutation hybridizing probes successfully detected the exact mutation with high specificity and sensitivity. The sensitivity of the reaction was increased in the presence of a PNA oligomer. This increased the sensitivity of the reaction (thereby lowering the limit of detection) by a factor of 64 and was able to detect mutants at a frequency of 0.001%. This study improved on previous experiments conducted by Oh *et al.* (2010) who detected *KRAS* mutants at an allele frequency of 0.1% in colorectal cancer samples. Another study (Luo *et al.*, 2006) has also shown the ability of the clamping technique to detect 10 pg of mutant allele in 100 ng of wild-type background (1:10000).

Because of the high cost of hybridizing probes, the quantitative allele-specific amplification method (QUASA) was used to detect base changes in codons 12 and 13. Our results have revealed a high-specificity to single base changes in different cell lines. Although the QUASA method is a cheap method of mutation analysis, the specific probe hybridizing method is the best technique for mutation screening, especially in fresh clinical samples. After validation and application of the PNA clamping qPCR technique, the analysed NSCLC specimens showed various types of somatic mutations including *KRAS*, *PIK3CA* and *EGFR* mutations. *KRAS* mutation was the most common type somatic mutation detected in NSCLC with a frequency of 18%, similar to that found by Arcangelo and co-workers (D’Arcangelo and Cappuzzo, 2012) . *PIK3CA* mutation frequency in this study was 10% in NSCLC, 15% in SCC and 5% ADC, respectively. Exon 9 mutation (77.7%) was more frequent than exon 20 (22.2%). Scheffler and colleagues (Scheffler *et al.*, 2015) have also demonstrated a high percentage of *PIK3CA* mutation in SCC (8.9%) compared to ADC (2.9%), 78.6% of *PIK3CA* mutations were exon 9 mutations and 16.8% were exon 20.

EGFR and *KRAS* mutations are mainly associated with ADC subtypes; several previous studies have also reported high proportions of *EGFR* and *KRAS* mutation in ADC compared to SCC, which shows a low incidence of *EGFR* and *KRAS* mutation (El-Telbany and Ma, 2012).

NSCLC is a disease of smokers (Proctor, 2012); our cohort showed that the majority of patients with NSCLC were smokers except for a few cases of ADC, indicating that ADC is a diseases of non-smokers (Yano *et al.*, 2011), in disagreement with a previous study conducted by Yang and co-workers (Yang *et al.*, 2002) that showed a strong correlation between adenocarcinoma and tobacco smoke. ADC is mainly detected in women with a

frequency of 60.7%, with a lower frequency in SCC. However, no significant difference was seen between males and females with the SCC subtype, a finding which is confirmed by a study conducted by Clancy and co-workers (Clancy *et al.*, 2008), which revealed a high incidence of ADC in women. In this study, *EGFR* and *KRAS* mutations were identified in a high proportion of females compared to males, a possible explanation for which is that these mutations are mainly linked to adenocarcinoma, which is very common in the female population.

Although G12D is the most common type of *KRAS* mutation in various types of cancer (Prior *et al.*, 2012), in this study G12C is the most frequent type of single nucleotide substitution in NSCLC. Prior and co-workers (2012) (Prior *et al.*, 2012) have also determined that the G12C mutation is more specific to lung malignancies, contrary to G12D, which is specific to other tumour types, such as colonic and pancreatic cancers. Moreover, despite the major causative agent of lung cancer, colonic cancer and pancreatic cancer being tobacco smoke, the selective properties of carcinogens in tissue results in a differential mutational status of *KRAS*.

Regarding *PIK3CA* mutations, E542K, E545K and H1047R were identified in NSCLC. E545K and H1047R mutations were found in NSCLC with a frequency of 25% for each mutation, whereas E542K was detected with a frequency of 50% and considered the most common among the three hotspots. This is in contrast to a previous study performed by Scheffler and co-workers (Scheffler *et al.*, 2015), which found a high prevalence of E545K (57.1%) compared to E542K (14.3%) and H1047R (16.7%).

MCL-1 is a critical gene, and has been implicated in cell survival and drug resistance. Amplification of *MCL-1* has been identified in different human malignancies (Leverson *et al.*, 2015), with a high frequency in breast and lung cancers (Beroukhi *et al.*, 2010).

In this study, we screened our clinical samples for *MCL-1* copy number variation, such as gene amplification and gain, and detected *MCL-1* amplification in different histological subtypes of NSCLC. Amplification of 1q26.2 on which *MCL-1* is located was detected in ADC in previous studies (Beroukhi *et al.*, 2010) with a frequency of 20% (Zhang *et al.*, 2015); by contrast, our study has found a frequency of only 2.5% *MCL-1* amplification in ADCs. *MCL-1* amplification was also identified in SCC (Chen *et al.*, 2014), and we have also detected *MCL-1* amplification at high frequency in SCC with *MCL-1* gain being mostly associated with ADC.

Because several factors contribute to somatic copy number alterations such as gender, age and a history of smoking, we determined the incidence of *MCL-1* amplification in both male and female smokers and non-smokers. This study is one of the first to indicate that *MCL-1* is commonly amplified in SCC, and gained in ADC (isochromosome), however there is not enough data in the literature to support our findings due to the limitations of similar previous studies.

PIK3CA copy number, including focal amplification and copy number gain, was also assessed in this study. A previous study (Okudela *et al.*, 2007) showed *PIK3CA* copy number change in the Western world at a frequency of 33%, of which 17% were ADC, 60% SCC and 25% LCC. *PIK3CA* copy number alteration in our study was found at a frequency of 34%, of which 25.9% were ADC, 74% SCC and was not detected in LCC. Massion and co-workers (Massion *et al.*, 2004) have indicated that *PIK3CA* amplification is an early event in tumourgenesis and found *PIK3CA* gain in both invasive and pre-invasive lesions of lung cancer. Our study agrees with this finding, as *PIK3CA* copy number gain or amplification was found in both early and late stages of our NSCLC cohort.

Frequent genetic alterations related to *SOX2*, such as copy number change has been previously detected in NSCLC, and Brcic and co-workers (Brcic *et al.*, 2012) have stated that *SOX2* amplification is a common event in SCCs including lung SCC. A previous study showed *SOX2* amplification in NSCLC with a frequency of 26.1%, with 31.6% being detected in SCC and 20% in ADC (Cai *et al.*, 2011). However, this study has identified *SOX2* copy number alteration in 18 % of NSCLC, with a frequency of 86.6% in SCC and 13.3% in ADC. Rare *SOX2* overexpression and amplification in ADC has been referred to as a major driver of tumour initiation, as SCC originates from the epithelial lining of the bronchus, which expresses *SOX2*, while pneumocytes, precursors of ADC lesions, are negative for *SOX2* expression (Wilbertz *et al.*, 2011). *SOX2* focal amplification was more common than gain in SCC as the screened samples of NSCLC showed only 5% *SOX2* gain.

3.5 Conclusions

This section has highlighted that the tumour histological subtype is a major determinant of both the oncogenic driver mutations and copy number aberrations seen in NSCLC apart from *PIK3CA* amplification, which is also associated with gender. However larger studies in bigger cohorts are required.

Chapter 4. Analysis of protein expression and gene transcription using immunohistochemistry and *in situ* hybridization, respectively

4.1 Introduction

Activation and overexpression of ERK proteins in lung cancer have previously been described, and generally activation of ERK is linked to advanced disease without significant correlation with patient outcome (Vicent *et al.*, 2004). Hyperactivation of AKT in NSCLC associated with chemo-resistance and poor outcome was observed in NSCLC patients (David *et al.*, 2004). Overexpression of MCL-1 correlated with chemo-resistance and reduced apoptosis in NSCLC cells was also identified (Song *et al.*, 2005), however there is no significant correlation between MCL-1 and patient outcome (Wesarg *et al.*, 2007). In this chapter we analysed protein expression in NSCLC as well as mRNA levels.

4.2 Aims and objectives

The aim of this study was to analyse the expression of proteins such as ERK, AKT and *MCL-1* mRNA in NSCLC to determine whether any correlation exists between gene expression and protein levels, as well as to find the relationship between the expression of these proteins and drug resistance. The specific objectives were:

1. To analyse expression of p-ERK in tumour samples.
2. To analyse levels of p-AKT in tumour specimens.
3. To measure expression of MCL-1 protein.
4. To measure expression of *MCL-1* mRNA.

4.3 Results

Samples of NSCLC were obtained from UHL, which consisted of different histological subtypes of NSCLC including adenocarcinoma, SCC and large cell lung carcinoma (Figure 4.1), which were categorised by pathologist using H&E staining. Specimens were stained for MCL-1, p-ERK and p-AKT as markers for *MCL-1* amplification, MAPK pathway and AKT/PI3K pathway activation, respectively. Normal adjacent tissues were also stained and compared to the tumour samples.

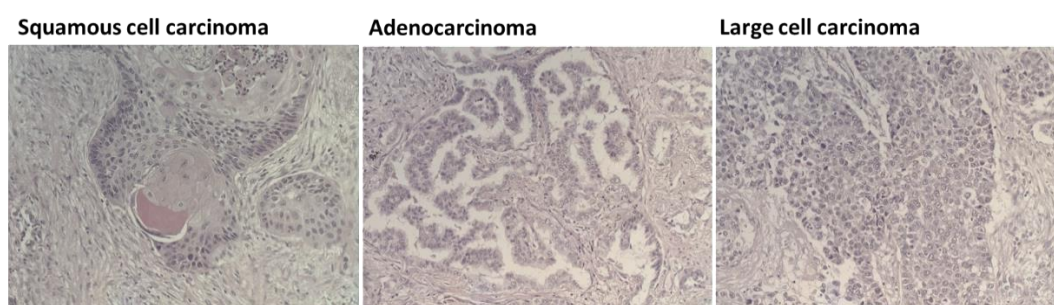


Figure 4.1 Histology of Lung cancer. This micrograph illustrates the histological features of adenocarcinoma with lepidic pattern. SCC is characterized by the presence of very clear pink keratin in the centre of the tumour. Large cell carcinoma appears as a nest of large polygonal cells, with predominant nucleoli and vesicular nuclei

4.3.1 Assessment of p-ERK expression in NSCLC

Immuno-staining of normal lung tissues showed mild to strong staining of p-ERK in the endothelial lining of blood vessels at median staining level of 93. Normally, pneumocytes type I and II did not express p-ERK. Hyperplastic alveolar cells or pneumocytes showed high expression of p-ERK. p-ERK expression was not detected in the epithelial lining of the air passages; sometimes a mild expression of activated ERK can be seen in the brush border of the ciliated cells in the airways (Figure 4.2). Positive nuclear and cytoplasmic staining of p-ERK was detected in a single cancer cell, with strong expression seen in the tumour periphery and stroma compared to the tumour centre (Figure 4.3).

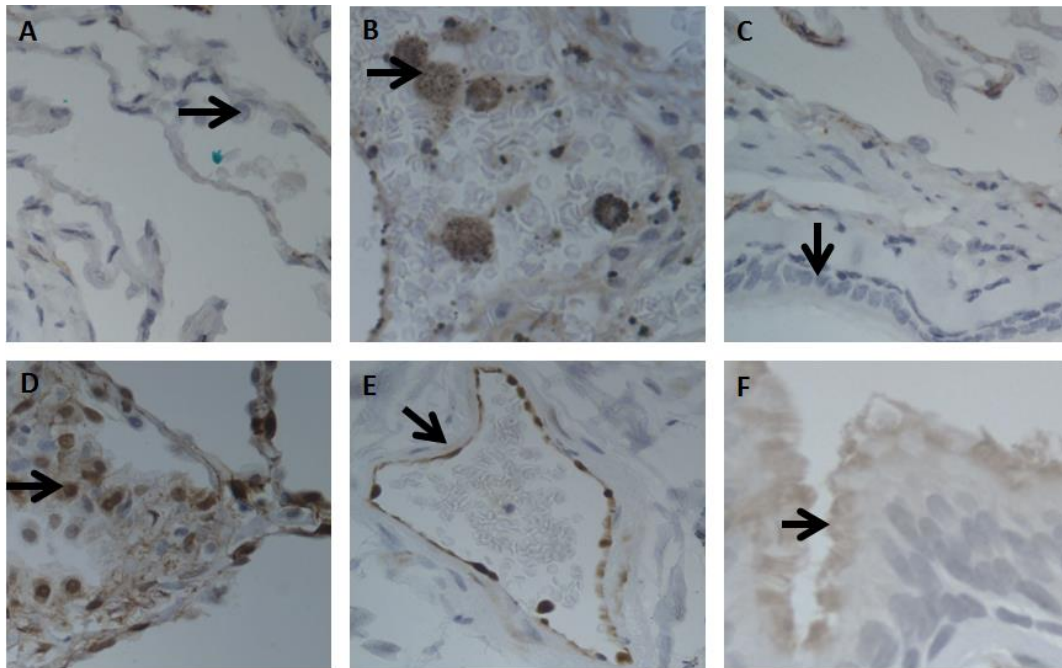


Figure 4.2 Expression of p-ERK across lung tissue. A high level of phosphorylated ERK was detected in the endothelial lining of blood vessels and some hyperplastic alveolar cells (E and D, respectively). Mild staining was seen in macrophages and the brush border of the ciliated cell (B and F, respectively). Normal pneumocytes and the epithelial lining of airways were negative for p-ERK (A and C, respectively).

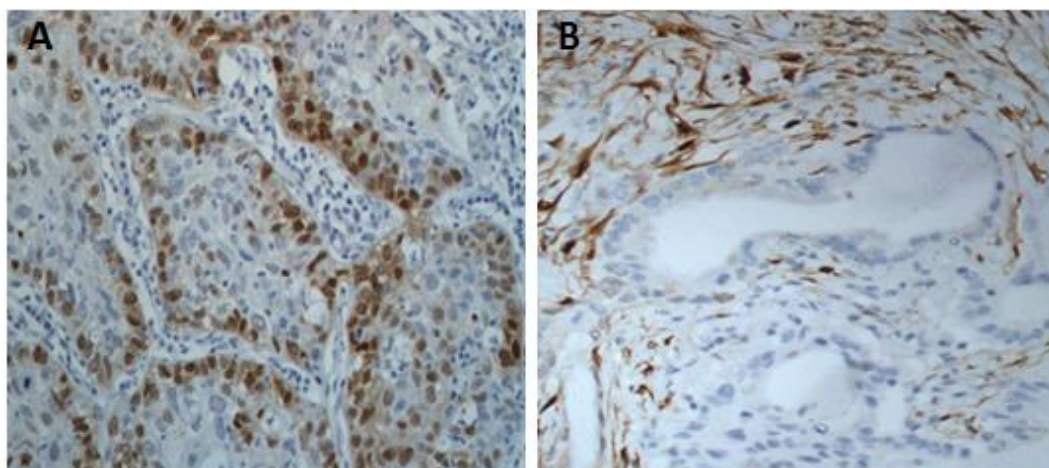


Figure 4.3 p-ERK expression in tumour microenvironment. This micrograph illustrates low expression of p-ERK in the tumour centre and overexpression of p-ERK in the tumour periphery (A). High level of p-ERK in tumour stroma was also detected (B).

There was a disparity in phospho-MAPK/ERK staining in cancer cells. Overexpression of p-ERK was detected in *EGFR* and *KRAS* mutated cells. Strong nuclear and cytoplasmic staining were identified in *KRAS* or *EGFR* mutant tumours. Not all tumours were positive for p-ERK in this study. p-ERK staining was observed in 72.1% of NSCLC with variable degrees of expression and detected in 70% of ADC tumours. 83% of ADC cases with p-ERK overexpression demonstrated oncogenic mutations in *KRAS* or *EGFR*. Although positive and negative staining for p-ERK was observed in both SCC and ADC in this study, high p-ERK expression was associated with ADC rather than SCC ($p = 0.0343$) and frequently seen in *KRAS* or *EGFR* mutant tumours compared to wild-type ($p < 0.0001$) (Figure 4.4). Strong positive staining of p-ERK was also correlated with late-stage ADC ($p < 0.0386$) (Figure 4.5).

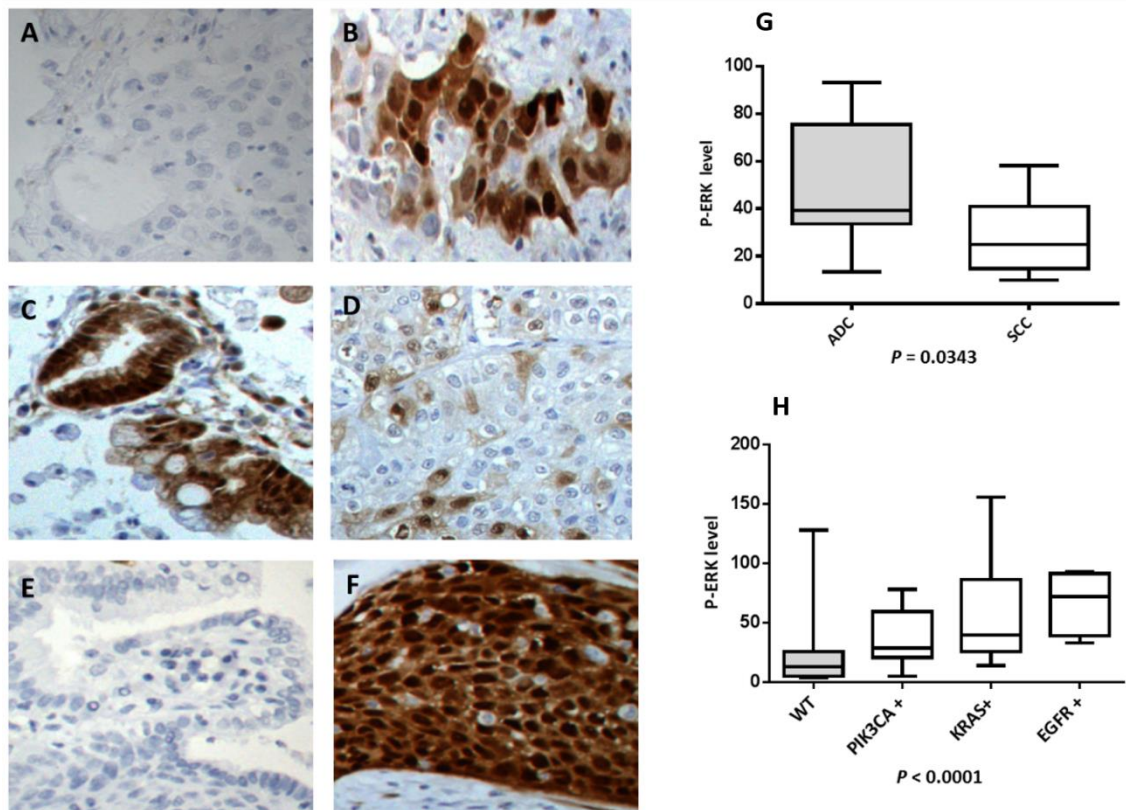


Figure 4.4 p-ERK expression in NSCLC. The *KRAS*, *EGFR* and *PIK3CA* wild-type tumour specimen was negative for p-ERK expression (A). Strong positive staining was identified in *KRAS*⁺ tumour (B) and *EGFR*⁺ tumours (C); a few cells with strong nuclear expression were also detected in a tumour sample with a *PIK3CA* mutation (D). Negative staining for p-ERK was seen in SCC (E); however, a rare strong positive staining was identified in SCC (F). p-ERK expression is seen in both SCC and ADC with an increased expression level in ADC compared with SCC (G). Expression of p-ERK in WT samples was lower than cases with oncogene driver mutations (H).

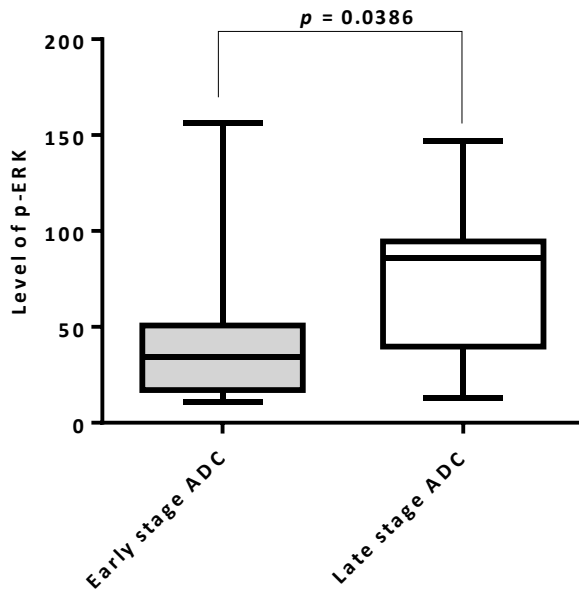


Figure 4.5 Expression of p-ERK according to stage of the disease. High expression of p-ERK was detected in the late stages of ADC compared to the early stages.

4.3.2 Assessment of p-AKT expression in NSCLC.

p-AKT is an important marker for recognition of a stimulated PI3K pathway (Baba *et al.*, 2011). Here, PI3K pathway activation was analysed using immunohistochemistry. Tonsil sections were first treated with several dilutions of the antibody and then a final dilution of 1:100 was selected to detect the signal of the target protein.

p-AKT expression was not identified in normal cells of the respiratory tract; however, overexpression of p-AKT was detected in blood vessels, hyperplastic pneumocytes and the epithelial lining of bronchioles. Macrophages revealed mild to strong expression of p-AKT in both normal and tumour samples. Overexpression of p-AKT was also seen in all histological subtypes of NSCLC; however, strong nuclear and cytoplasmic staining of p-AKT was detected in SCC (Figure 4.6).

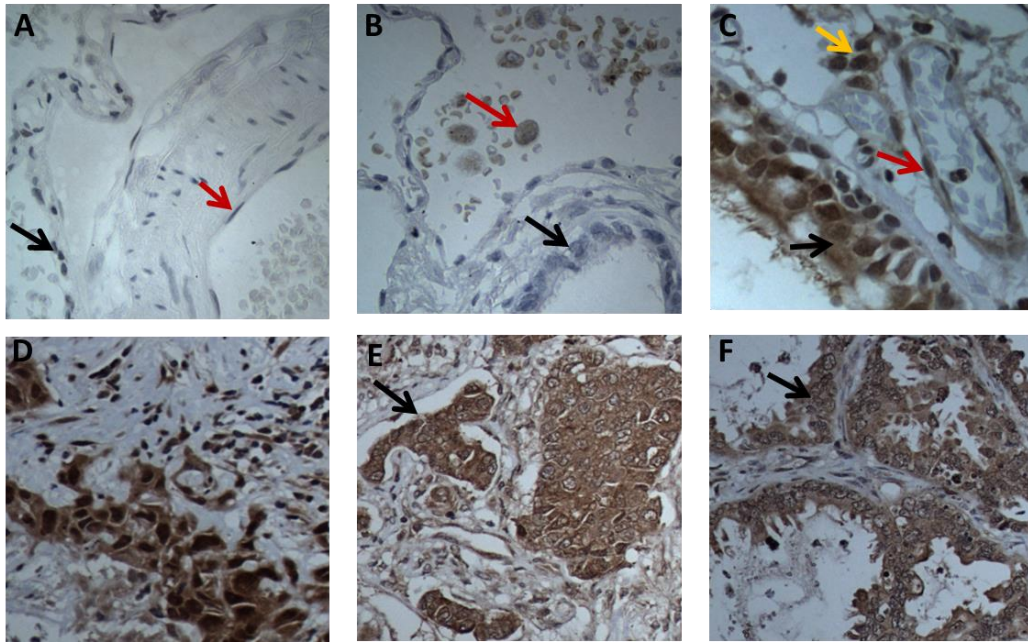


Figure 4.6 Expression of p-AKT in normal and tumour samples. Pneumocytes and endothelial cells from a normal lung were negative for p-AKT (A). Negative staining (black arrow) and mild expression of p-AKT (red arrow) were seen in the airway and macrophages of normal lung paranchyma, respectively (B). p-AKT was overexpressed in airways (black arrow), endothelial lining of blood vessels (red arrow), and hyperplastic alveolar cells (yellow arrow) of the tumour microenvironment (C). Overexpression of p-AKT was identified in ADC (F) and LCC (E). Overexpression of p-AKT associated with strong nuclear staining was detected in SCC (D).

Mild to strong staining was detected in several NSCLC samples, with 23 samples of NSCLC showing p-AKT overexpression. 56.5% (13/23) of the cases were SCCs, 8.6% (2/23) and 34.7 % (8/23) were LCCs and ADCs, respectively. The strongest positive staining was detected in two cases of SCC, one with a *PIK3CA* mutation (E545K) and the other with *PIK3CA* amplification (Table 4.1). Overexpression of p-AKT was also

associated with *PIK3CA*-amplified tumours, in particular those with significant amplification ($p = 0.0012$) (Figure 4.7).

Tumour	Histology	Gender	Age	Smoking	Stage	Mutations and amplifications	Staining levels
LT39	LCC	F	65	Unknown	IIIB	—	97
LT5	SCC	M	62	Smoker	IB	<i>MCL-1</i> amplification	138
IT40	LCC	M	62	Ex-smoker	IB	<i>KRAS</i> G12D	134
LT41	ADC	F	50	Smoker	IIIA	<i>EGFR</i> L858R	139
LT17	SCC	M	67	smoker	IIA	<i>PIK3CA/MCL-1</i> amplification	98
LT22	ADC	M	65	Ex-smoker	IB	—	96
TL23	SCC	M	81	Ex-smoker	IIIA	<i>PIK3CA</i> amplification	124
LT24	SCC	M	73	Smoker	IIIA	—	104
LT27	ADC	M	60	Never smoker	IIIA	<i>MCL-1</i> amplification	144
LT42	SCC	F	72	Ex-smoker	IIB	<i>PIK3CA</i> amplification	133
LT46	SCC	F	65	Unknown	Unknown	<i>PIK3CA</i> H1047R/ amplification	101
LT35	SCC	M	77	Smoker	IIB	<i>PIK3CA</i> E545K	193
LT53	SCC	F	63	Unknown	IA	<i>PIK3CA</i> amplification	115
LT54	SCC	F	77	Unknown	IA	<i>PIK3CA</i> amplification	83
LT55	SCC	F	73	Unknown	IIB	<i>PIK3CA</i> E542K/ amplification	103
LT56	ADC	M	84	Unknown	IA	<i>PIK3CA</i> amplification	153
LT61	SCC	M	86	Unknown	IB	<i>PIK3CA</i> amplification / <i>MCL-1</i> gain	202
LT76	SCC	F	63	Unknown	IIIA	<i>PIK3CA</i> amplification / <i>SOX2</i> gain	93
LT80	ADC	F	33	Unknown	IIB	—	96
LT81	ADC	M	70	Ex-smoker	IIB	<i>KRAS</i> G12C	93
LT88	ADC	F	75	Unknown	IIIA	—	123
LT92	ADC	F	72	Unknown	IIB	<i>KRAS</i> G12A	123
LT95	SCC	M	70	Unknown	IB	—	101

Table 4.1 Expression of p-AKT in NSCLC. p-AKT overexpression was seen in both SCC and ADC. The highest expression level of p-AKT was identified in SCC subtypes, in particular those that have alterations to the *PIK3CA* gene (LT35 and LT61).

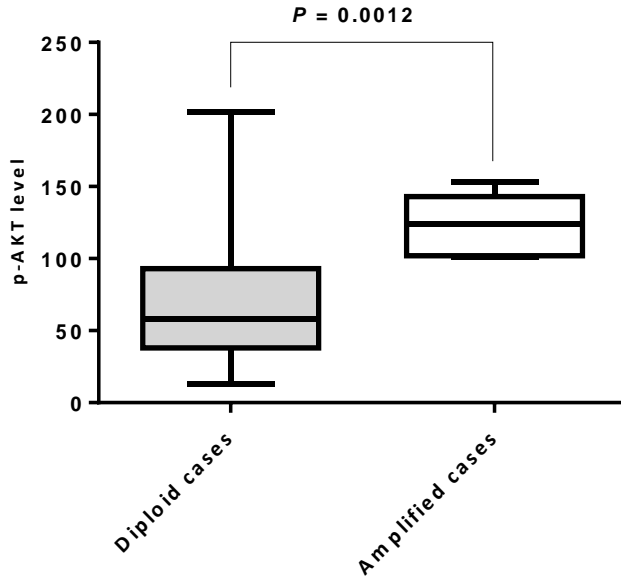


Figure 4.7 Expression of p-AKT in cancer cells. *PIK3CA*-amplified tumours have high p-AKT expression levels compared to normal diploid cases ($p = 0.0012$).

4.3.3 MCL-1 expression analysis

To optimise antibody staining, S-19 MCL-1 Ab was tested on tonsil tissue at different dilutions starting from 1:250-1:2000, and using TBS buffer as the antibody diluent with and without Triton X-100. Non-specific Ab binding was detected in samples treated without Triton X-100. Addition of Triton X-100 at a concentration of 0.1% reduced non-specific binding significantly. Clear MCL-1 signals in the germinal centre of the tonsil were observed, at a dilution of 1:1000, and squamous cells were negative for MCL-1 staining (Figure 4.8). Specificity of the antibody was also analysed using an MCL-1 amplified cell line (H1395), which showed overexpression of MCL-1 protein compared to the non-amplified cell line (H1355) (Figure 4.9).

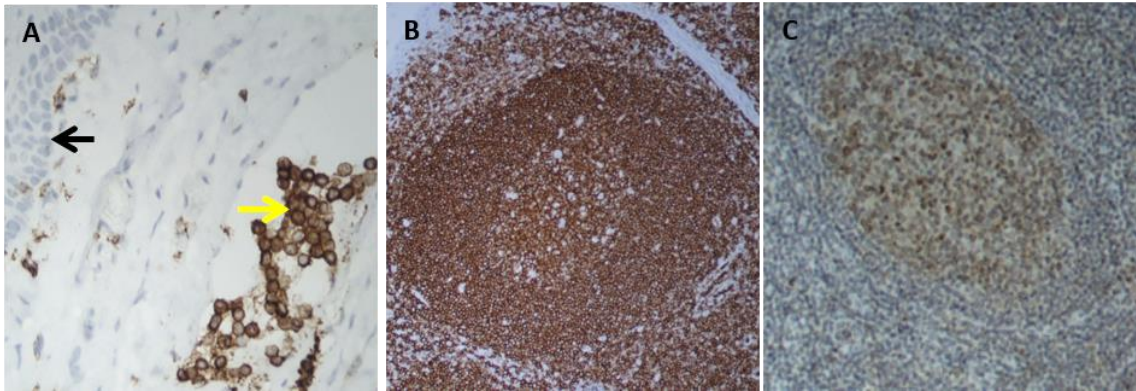


Figure 4.8 Assessment and optimisation of MCL-1 Ab (S-19) using tonsil specimens. Squamous epithelial cells were negative for MCL-1 staining as indicated by the black arrow. MCL-1 was highly expressed by lymphocytes as indicated by the yellow arrow (A). Non-specific staining for MCL-1 was detected at a dilution of 1:1000 (B), however addition of Triton X100 to the Ab diluent demonstrated specific staining to the active cells in the germinal centre of the lymphoid organ (C).

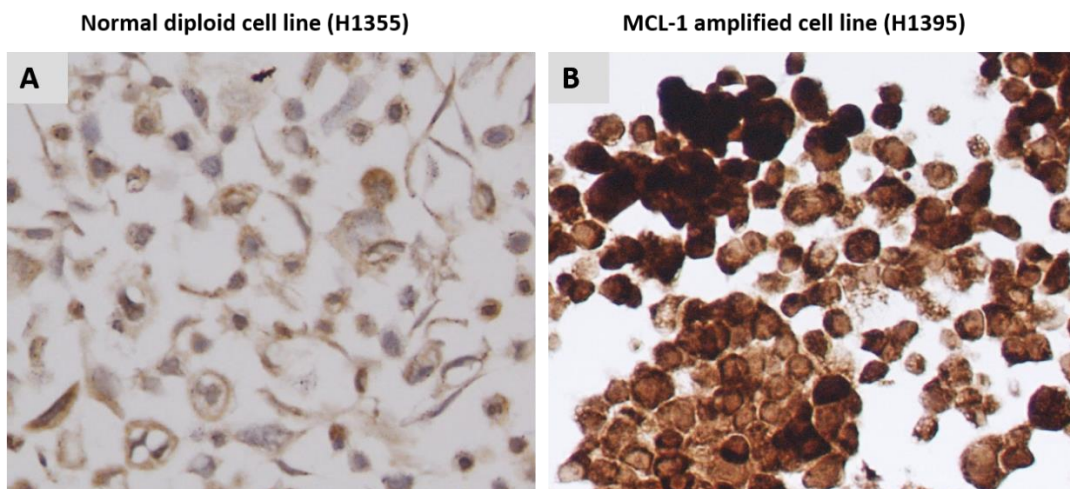


Figure 4.9 Assessment of MCL-1 Ab (S-19) specificity using MCL-1 amplified cell line. MCL-1 non-amplified cell line cells have low level of MCL-1 protein (A), compared to the MCL-1 amplified cell line which showed high expression level of MCL-1 (B).

The MCL-1 antibody was then applied to the tumour samples at a dilution of 1:1000 with overnight incubation at 4°C. Immuno-staining analysis showed mild, and medium to high expression of MCL-1 in normal lung tissue and tumour samples (SCC, LCC and ADC), respectively. Normal tissue revealed mild and moderate expression of MCL-1 in air passages and macrophages, respectively (Figure 4.9). Various levels of MCL-1

expression were identified in all samples of NSCLC. Table 4.2 summarizes the expression levels of MCL-1 in different histological subtypes of NSCLC.

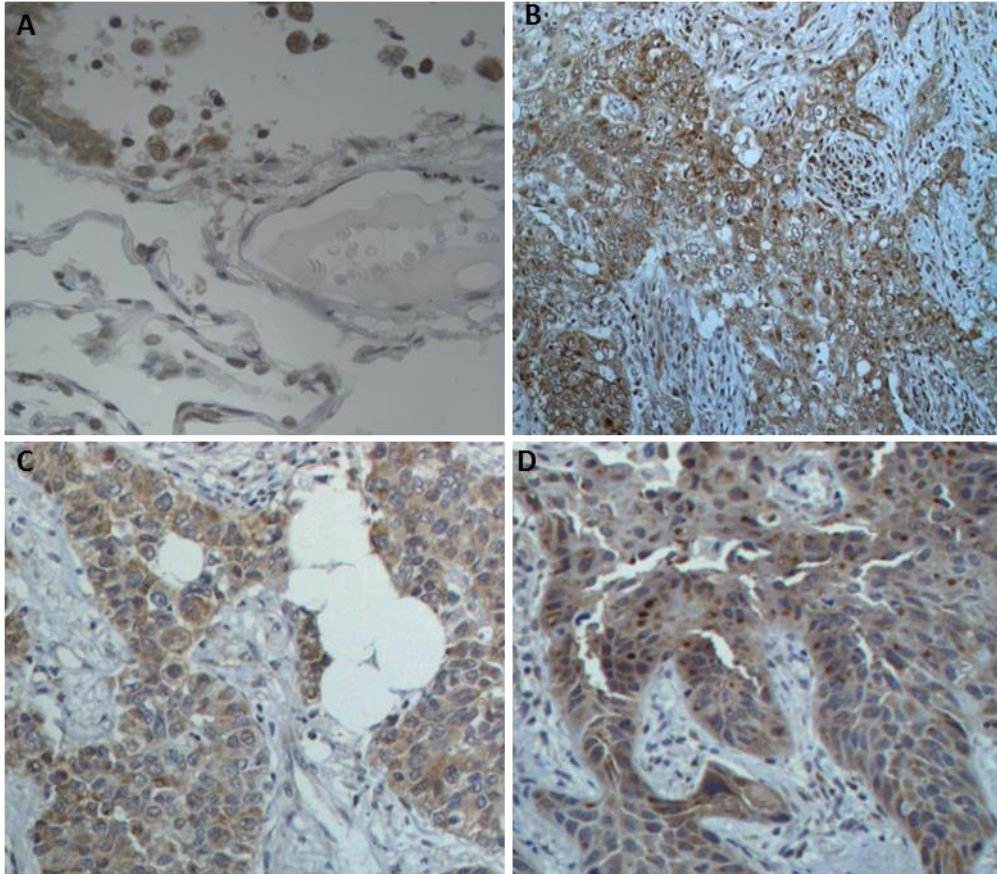


Figure 4.10 Expression of MCL-1 in normal and tumour lung tissue. MCL-1 was expressed by the epithelial lining of bronchioles and macrophages of normal lung (A). Strong positive staining of MCL-1 was detected in ADC (B) and SCC (D) samples with clear cytoplasmic location and a granular appearance of the MCL-1 protein in the mitochondria. Mild expression was detected in LCC (C).

Sample ID	Histology	MCL-1 level	Sample ID	Histology	MCL-1 level
LT2	SCC	48	LT48	ADC	45
LT4	ADC	95	LT49	ADC	43
LT5	SCC	67	LT51	ADC	34
LT6	SCC	108***	LT52	SCC	52
LT7	SCC	39	LT53	SCC	50
LT8	SCC	23	LT54	SCC	31
LT9	ADC	24	LT55	SCC	43
LT10	ADC	47	LT56	ADC	112***
LT12	SCC	32	LT57	ADC	150***
LT13	ADC	25	LT58	ADC	157***
LT14	SCC	70	LT59	ADC	156***
LT16	ADC	21	LT61	SCC	144***
LT17	SCC	31	LT63	SCC	105***
LT18	SCC	84	LT64	ADC	86
LT19	ADC	97	LT65	SCC	103***
LT20	ADC	40	LT66	SCC	200***
LT22	ADC	85	LT67	SCC	64
LT23	SCC	71	LT68	ADC	63
LT24	SCC	104***	LT70	SCC	107***
LT25	SCC	24	LT71	SCC	94
LT26	ADC	19	LT73	ADC	37
LT27	ADC	63	LT74	SCC	63
LT28	SCC	29	LT75	ADC	78
LT29	ADC	67	LT76	SCC	95
LT30	ADC	39	LT77	ADC	114***
LT32	ADC	50	LT78	ADC	76
LT33	ADC	37	LT80	ADC	172***
LT35	SCC	59	LT81	ADC	160***
LT36	ADC	76	LT82	SCC	78
LT37	ADC	55	LT83	SCC	124***
LT38	SCC	37	LT85	ADC	53
LT39	LCC	24*	LT88	ADC	162***
LT40	LCC	54*	LT89	SCC	71
LT41	ADC	21	LT90	SCC	59
LT42	SCC	21	LT92	ADC	129***
LT43	SCC	49	LT93	ADC	88
LT44	ADC	40	LT94	SCC	81
LT45	ADC	19	LT95	SCC	94
LT46	SCC	31	LT96	SCC	110***

Table 4.2. Expression of MCL-1 protein in NSCLC. Different expression levels of MCL-1 from mild to strong staining were detected in NSCLC. High expression levels (***) were detected in both ADC and SCC, whereas low expression levels (*) were detected in LCC.

4.3.4 *In situ* hybridization for *MCL-1* mRNA detection

4.3.4.1 *MCL-1* mRNA detection in cell lines

To analyse levels of *MCL-1* mRNA and optimise the target probe, ISH analysis was performed using an *MCL-1* probe obtained from Advanced Cell Diagnostics (ACD), designed specifically to target *MCL-1* mRNA. The probe was validated in *MCL-1*-amplified lung adenocarcinoma cells (H1395), and compared with the endogenous control gene *POLR2A* and the negative control *DapB*. Increased levels of mRNA were observed in H1395 cells compared to a non-amplified cell line (H1355) (Figure 4.10).

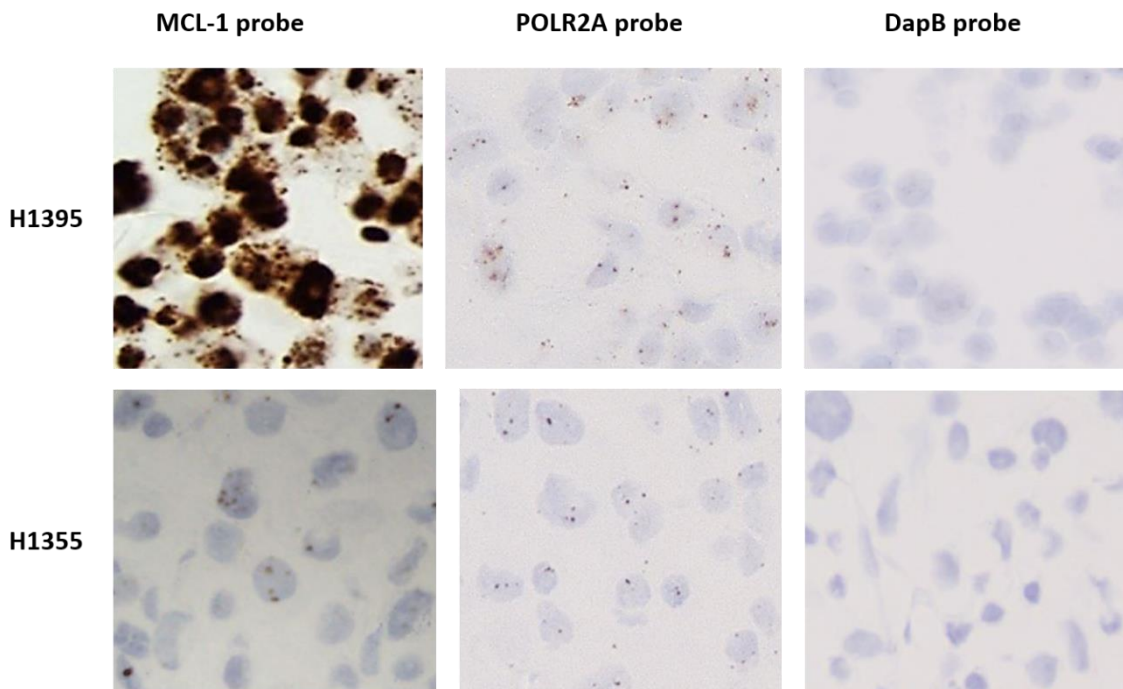


Figure 4.11 Expression of *MCL-1* mRNA in *MCL-1*-amplified cell line (H1395) and *MCL-1* non-amplified cell line (H1355). High levels of *MCL-1* mRNA were seen in the *MCL-1*-amplified cell line H1395, whereas normal expression was detected in the non-*MCL-1*-amplified cell line H1355.

4.3.4.2 MCL-1 mRNA detection in tumour sample

To detect mRNA levels of MCL-1 in tumour samples, the validated MCL-1 probe was applied to 79 NSCLC samples. *MCL-1* mRNA was detected at different levels from mild (0-93) to high (>93) across the 79 analysed samples. High levels were detected in 83% of the amplified cases. Figure 4.11 shows an example of mRNA levels in an *MCL-1*-amplified tumour, overall levels of *MCL-1* mRNA in *MCL-1*-amplified tumours were significantly higher than non-amplified tumours ($p = 0.0188$). Despite a significant correlation between *MCL-1* amplification and *MCL-1* mRNA expression being observed in tumour samples, expression of MCL-1 protein was not significantly correlated with *MCL-1* amplification (Figure 4.12)

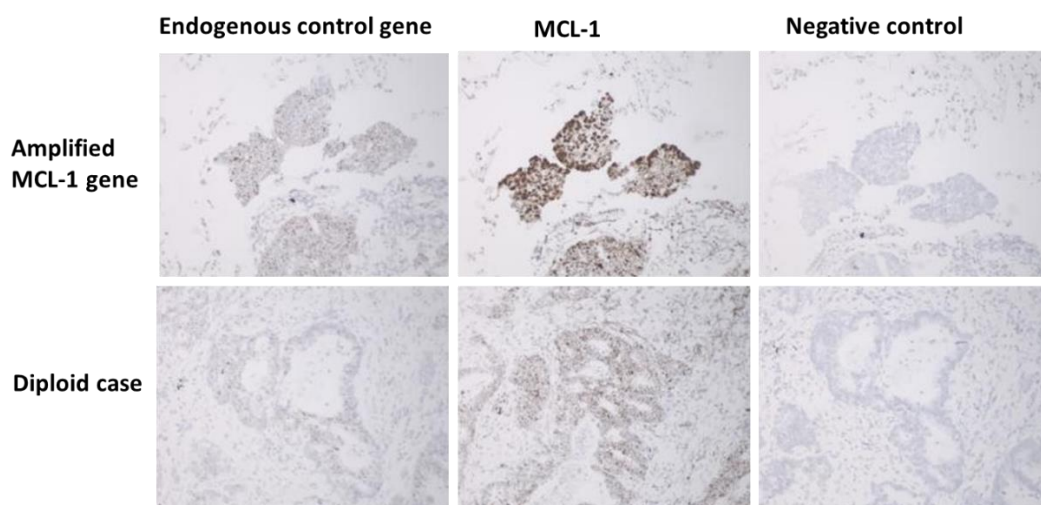


Figure 4.12 MCL-1 expression in tumour samples. The photomicrograph shows an increased amount of *MCL-1* mRNA in a tumour sample with *MCL-1* amplification, while the diploid case shows normal levels of *MCL-1* mRNA.

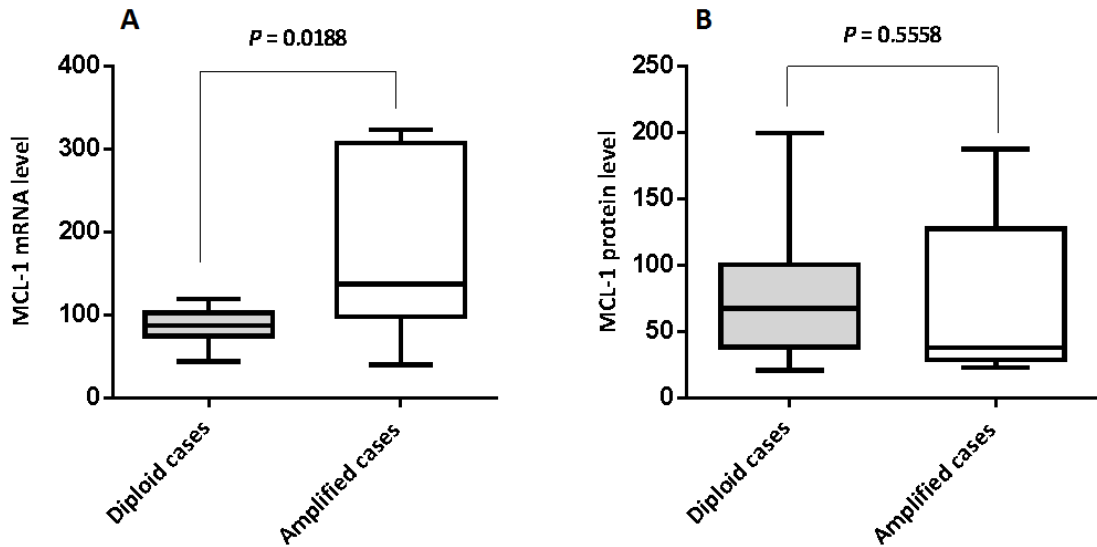


Figure 4.13 MCL-1 expression in normal diploid and amplified tumour cells. A significant increase of *MCL-1* mRNA was detected in *MCL-1*-amplified tumours compared to diploid samples ($p = 0.0188$) (A). However no significant increase of MCL-1 protein was detected in *MCL-1*-amplified tumours compared to diploid samples ($p = 0.5558$) (B).

Analysis of mRNA expression levels in patient samples showed different levels of mRNA in all age groups, histological subtypes, and all stages of the disease; however, no correlation was found between mRNA and other factors such as gender and smoking history (Table 4.3).

	Staining level	Number of cases with high expression level	Number of cases with low expression level
Histology	ADC	21	18
	SCC	19	19
	LCC	-	2
Gender	Males	19	20
	Female	19	21
Stages	I	15	12
	II	7	14
	III	6	8
	IV	1	1
	Unknown	3	10
Smoking	Smoker	5	5
	Ex-smoker	14	9
	Non-smoker	2	1
	Unknown	11	30
Age	0-44	2	-
	45-54	1	3
	55-64	14	5
	65+	33	29

Table 4.3. Expression levels of *MCL-1* mRNA in NSCLC. Mild to strong expression of mRNA was detected in tumour samples, though without any correlation between expression level and age, histology, gender, stage and smoking history.

4.4 Discussion

4.4.1 Analysis of p-ERK

Extracellular-regulating kinase (ERK) is one of the most important regulators of the MAPK pathway and plays a critical role in cell proliferation and survival. ERK is a key target of the upstream kinase MEK1 (Widmann *et al.*, 1999) and stimulates nuclear transcription factors. A previous study has reported negative staining of p-ERK in normal lung cells, in particular the two types of alveolar pneumocytes, bronchiolar epithelium and endothelial cells (Vicent *et al.*, 2004). This study also found negative staining of p-ERK in both types of alveolar pneumocytes; however, strong expression of p-ERK was detected in the endothelial lining of blood vessels of normal lungs. Furthermore, our study has found overexpression of p-ERK in hyperplastic pneumocytes and macrophages.

Uncontrolled stimulation of ERK through different oncogenes and contribution of phosphorylated ERK in malignant transformation has previously been described (Vicent *et al.*, 2004). This study has also identified active ERK in cancer cells with mutations in *EFGR* and *KRAS*. Mukohara and co-workers (Mukohara *et al.*, 2003) have stated that ERK is activated in approximately one-third of a total of 60 NSCLC samples. By contrast, our results showed activation of ERK in *more* than two-thirds of a total of 79 NSCLC samples (72.1%). Moreover, in this study, nuclear and cytoplasmic staining of p-ERK was identified in a single cell, and strong expression of p-ERK was frequently seen in the tumour periphery. This finding was also described by Albanell *et al.*, (2001) (Albanell *et al.*, 2001) in SCC of the head and neck, and they interpreted this staining pattern as a result of the presence of active proliferating cells in the tumour periphery. In this study, stromal expression of p-ERK was also detected. Previous studies have identified excessive expression of p-ERK in advanced stages of breast carcinoma (Zhang *et al.*, 2004). This study concurs with the findings of Zhang and co-workers, and showed that

strong staining of p-ERK is correlated with advanced stages of ADC. Increased levels of p-AKT and STAT3, but not p-ERK, has previously been detected in *EGFR* mutant cells (Sato *et al.*, 2006), with down-regulation of p-ERK seen after inhibition of *KRAS*, but not *EGFR* (Choi *et al.*, 2010). Moreover, Davies and co-workers (Davies *et al.*, 2011) have demonstrated that p-ERK activation is not correlated with *KRAS* mutation in colorectal cancer. In contrast to Sato and co-workers (2006), our study has found increased expression levels of p-ERK in samples with *EGFR* mutation and we also found increased levels of p-ERK in *KRAS* mutant cells, in agreement with Choi and co-workers (Choi *et al.*, 2010), but not with the finding of Davies and co-workers (Davies *et al.*, 2011).

4.4.2 Analysis of p-AKT

The PI3K-AKT pathway is a central regulatory pathway for cell survival, proliferation and differentiation (Liu *et al.*, 2009) and is involved in malignant transformation (Tsao *et al.*, 2003). In this study, we analysed p-AKT expression in NSCLC. Immunohistochemistry analysis of normal cells of the respiratory tract reported in the literature were negative for p-AKT expression (David *et al.*, 2004), which correlates with this study with the exception of macrophages, which showed mild to strong expression of p-AKT. By contrast, p-AKT staining in a study performed by Tsao and co-workers (Tsao *et al.*, 2003) showed expression of activated AKT in the normal bronchial epithelium, which can be explained by the epithelial cells under stimulating factors or at a critical point between normal and premalignant transformed cells. Hyperplastic pneumocytes, blood vessels, macrophages, and the epithelial lining of bronchioles in the tumour environment have shown p-AKT expression. Wu *et al.* (2007) (Wu *et al.*, 2007) demonstrated activation of VEGFR2 in lung cancer and tumour-associated endothelial cells. Overexpression of p-AKT was seen in all histological subtypes of NSCLC, and 59% of our cases have demonstrated overexpression of p-AKT. p-AKT is mainly seen in

SCC (56.5%) and to a lesser degree in ADCs (34.7%). However, a previous study by Lee *et al.* (2002) (Lee *et al.*, 2002) identified phosphorylated AKT in 67% of NSCLC, without significant differences between p-AKT expression level in SCC (68.2%) and ADC (61.5%). Massion *et al.* (2002) (Massion *et al.*, 2002) have found a correlation between high AKT and *PIK3CA* amplification; however, Massion and co-workers (2004) (Massion *et al.*, 2004) stated that AKT level is not correlated with *PIK3CA* amplification, whereas in our study, strong nuclear and cytoplasmic staining of p-AKT was significantly associated with *PIK3CA* mutation and *PIK3CA* amplification in SCC ($p = 0.0012$).

4.4.3 Analysis of MCL-1

The mitochondrial anti-apoptotic protein MCL-1 is essential for tumour survival in NSCLC and multiple myeloma (Zhang *et al.*, 2011). In previous studies, MCL-1 immunoreactivity was detected in epithelial cells of various tissues such as the epidermis, prostate, endometrium, breast, colon, intestine and respiratory system. Strong staining was detected in the apical layer of differentiated epithelial cells and in the germinal centre of tonsil cells, but not in the mantle zone (Krajewski *et al.*, 1995). In this study, we also detected strong immunostaining in several normal cell types such as macrophages, the epithelial lining of the respiratory tract and lymphoid cells in the germinal centre of tonsils cells, but not in the mantle or the stratified squamous epithelium of the blind crypt of the tonsil. As MCL-1 is expressed in all differentiated epithelial cells, almost all tumour samples have shown mild to strong staining of MCL-1 (Whitsett *et al.*, 2014). Strong positive and moderate staining of the MCL-1 protein with a clear granular cytoplasmic appearance in the mitochondria was detected. Intense immunoreactivity of MCL-1 was detected in 32.4% of NSCLC with a high proportion in ADC (56%) compared to SCC (44%). Previous studies have also demonstrated that expression of MCL-1 (moderate to strong) is high in ADC (80%) compared with SCC (58%) (Whitsett *et al.*, 2014). High

expression levels of MCL-1 were observed in metastatic melanoma but were not correlated to primary lesions (Zhuang *et al.*, 2007), and have also been observed in advanced clinical stages of ovarian cancer (Shigemasa *et al.*, 2002); however, there was no correlation between overexpressed MCL-1 and tumour stage in NSCLC.

The MCL-1 protein is known to have a short half-life (Wei *et al.*, 2012). As a result, mRNA analysis was added to this study. As well as *MCL-1* amplification being analysed using duplex qPCR, the RNA scope technique was used to measure the RNA levels. The advantage of this latter technique is that the RNA molecule is targeted by a specifically designed probe; previous studies have also shown the specificity of RNA scope target probes to different papilloma virus genotypes within different infected cell lines (Wang *et al.*, 2015). Moreover, simple conventional chromogenic staining, Haematoxylin dye and bright field microscopy can be used for signal detection. Prior to analysis of *MCL-1* mRNA in NSCLC samples, the ISH technique was applied to an *MCL-1*-amplified cell line (H1395), which showed high sensitivity and specificity. This finding has also been described by Wang and co-workers (Wang *et al.*, 2012). High levels of *MCL-1* mRNA (which is a good indicator of gene amplification) was detected in the H1395 cell line and, based on this finding, paraffin-embedded tissues of NSCLC were analysed for *MCL-1* gene expression, which also showed a clear granular appearance of mRNA in the specimens with different expression levels. MCL-1 expression was positively correlated with gene amplification in breast cancer; however, *MCL-1* amplification is not the only factor that controls MCL-1 regulation as several breast cancer tissues shown to be negative for *MCL-1* amplification have demonstrated MCL-1 overexpression (Balko *et al.*, 2014). In this study, no correlation was found between MCL-1 protein levels and *MCL-1* amplification. However, a strong correlation was found between *MCL-1* mRNA

and gene *MCL-1* amplification, the possible interpretation for which is that the mRNA half-life is longer than the protein half-life (Wei *et al.*, 2012).

4.5 Conclusion

This section has highlighted that expression of proteins (p-ERK, p-AKT and MCL-1) in normal tissues is cell-type dependent. p-ERK was mainly linked to endothelial cells of the normal lung unlike p-AKT and MCL-1, which were associated to normal epithelial lining of bronchioles and only to the endothelial cells of the tumour microenvironment. The major determinant of both protein and mRNA expression are oncogenic driver mutations and copy number alterations, and p-ERK overexpression is associated with advanced disease.

Chapter 5. MCL-1 status is linked to oncogene driver mutations, copy number variation and protein expression.

5.1 Introduction

Studies have speculated that epidermal growth factor (*EGFR*) is involved in stimulation of MCL-1 expression via the STAT signalling pathway, the MAPK pathway and the PI3K/AKT pathway (Song *et al.*, 2005). Stimulation of MCL-1 through *EGFR* in an ERK-dependent manner has been described in the literature (Song *et al.*, 2005), and controlling MCL-1 expression through phosphorylation of ERK has also been observed (Peddaboina *et al.*, 2012). Previous studies have demonstrated gene co-amplification in cancer cells including co-amplification of *MYC*, *EGFR* and *ERBB2*. Moreover, *EGFR* and *ERBB2* amplification might occur in *MYC*-amplified cells due to MYC-induced genomic instability (Ooi *et al.*, 2009).

5.2 Aims and objectives

The aim of this chapter was to study the link between *MCL-1* amplification and oncogene driver mutations (*KRAS*, *EGFR* and *PIK3CA*) and copy number variation of the commonly amplified genes in SCC (*SOX2* and *PIK3CA*). The specific objectives of this chapter are:

1. To identify co-amplification of *PIK3CA* and *SOX2* with *MCL-1* in NSCLC
2. To analyse *MCL-1* amplification in lung cancer cells with known oncogenic driver mutations.
3. To determine the effect of oncogene driver mutations on MCL-1 protein and mRNA levels.
4. To determine the effect of p-ERK and p-AKT overexpression on the MCL-1 protein and *MCL-1* mRNA.

5.3 Results

5.3.1 Concurrent *MCL-1* and *PIK3CA* /*SOX2* amplification in NSCLC

In this study, *MCL-1* amplification was identified in NSCLC, mainly in SCCs. *PIK3CA* and *SOX2* were also linked to SCC rather than ADC, and this study attempted to find if there is a correlation between *MCL-1* amplification and *PIK3CA* and/or *SOX2* amplification. All of the screened NSCLC samples with *MCL-1* amplification were negative for *PIK3CA* co-amplification. However one case with *MCL-1* amplification demonstrated *SOX2* amplification in NSCLC (Table 5.1).

Tumour ID	<i>MCL-1</i> status	<i>PIK3CA</i> status	<i>SOX2</i> status
LT5	Amplified	Diploid	Diploid
LT7	Amplified	Diploid	Amplified
LT8	Amplified	Diploid	Diploid
LT9	Amplified	Diploid	Diploid
LT17	Amplified	Diploid	Diploid
LT38	Amplified	Diploid	Diploid

Table 5.1 Co-existence of *MCL-1*, *PIK3CA* and *SOX2* amplification. No concurrent *MCL-1* and *PIK3CA* amplification was detected as tumour samples LT5, LT7, LT8, LT9, LT17 and LT38 were amplified for *MCL-1* and unamplified for *PIK3CA*. However one case (LT7) showed *MCL-1*/*SOX2* co-amplification.

5.3.2 Correlation between oncogene driver mutations and *MCL-1* amplification

Cell lines harbouring different oncogenic driver mutations were analysed for *MCL-1* copy number alteration. Comparative analysis of *MCL-1* against *CCT3* in cell lines harbouring *KRAS*, *EGFR* and *PIK3CA* mutations was performed. The *MCL-1*-amplified cell line H1395 and HG-DNA were used as positive and negative

controls for *MCL-1* amplification, respectively. None of the mutant cell lines showed significant *MCL-1* amplification compared to the normal control DNA. A low level gain in *MCL-1* was found in the *PIK3CA* mutant cell line CMF7; however, it was not significant compared to the H1395 cell line (Figure 5.1).

Analysis of NSCLC cases with the oncogene mutation for *MCL-1* amplification also showed the absence of any apparent correlation between oncogene driver mutations and *MCL-1* amplification. Only two cases with oncogene mutations (*KRAS* and *PIK3CA*) demonstrated *MCL-1* amplification among a total 25 cases harbouring *KRAS*, *PIK3CA* and *EGFR* mutations.

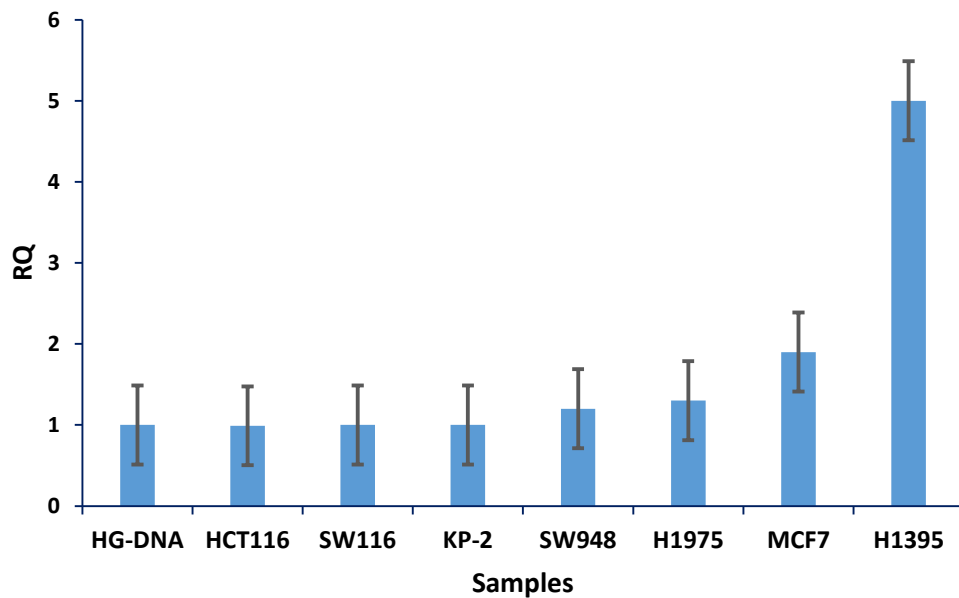


Figure 5.1 Analysis of *MCL-1* amplification in cell lines harbouring oncogene driver mutations. Significant amplification of *MCL-1* was only detected in the H1395 cell line; no amplification was identified in *KRAS* mutant cell lines (KP-2 and SW116), *EGFR* mutant cell line (H1975), *PIK3CA* mutant cell lines (SW948 and MCF7) and both a *PIK3CA* and *KRAS* mutant cell line (HCT116). HG-DNA was the negative control DNA for copy number analysis.

5.3.3 Expression levels of the MCL-1 protein and *MCL-1* mRNA in tumours harbouring mutations

MCL-1 protein and mRNA levels were measured in *KRAS*, *PIK3CA* and *EGFR* mutant cases and compared to wild-type. Although some individual cases harbouring oncogenic driver mutations demonstrated very high levels of *MCL-1* mRNA and moderate to high levels of MCL-1 protein (Table 5.2), these were not deemed significant when a one way ANOVA test was used to compare expression of both MCL-1 protein and *MCL-1* mRNA in WT vs mutant cases. Figure 5.2 shows expression levels of MCL-1 and *MCL-1* mRNA in mutant cases compared to wild-type.

Tumour ID	Histology	Mutation type	MCL-1 protein level	<i>MCL-1</i> mRNA level
LT12	SCC	WT	32	113
LT41	ADC	<i>EGFR</i>	21	112
LT48	ADC	WT	45	187
LT49	ADC	<i>EGFR</i>	43	207
LT52	SCC	<i>PIK3CA</i>	52	101
LT59	ADC	<i>KRAS</i>	156	96
LT92	ADC	<i>KRAS</i>	129	104
LT90	SCC	<i>PIK3CA</i>	59	107

Table 5.2 Expression levels of MCL-1 and MCL-1 mRNA in NSCLC cases. High levels of MCL-1 mRNA were detected in WT and mutant samples, whilst a high expression of MCL-1 protein was found in *KRAS* mutant cases compared to other cases.

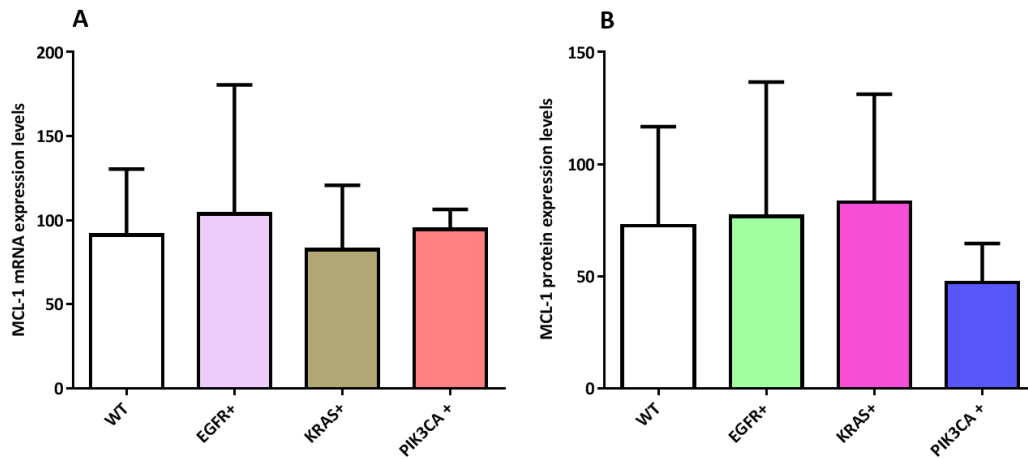


Figure 5.2 MCL-1 and MCL-1 mRNA expression level in mutant cases of NSCLC. A group analysis of NSCLC cases with different oncogene mutations compared to wild-type cases showed an absence of any apparent increase in expression levels of *MCL-1* mRNA (A) and MCL-1 protein (B) in mutant cases.

5.3.4 Comparison of MCL-1 protein and *MCL-1* mRNA levels with p-ERK and p-AKT levels

MCL-1 protein and mRNA expression were analysed in tumour samples. MCL-1 overexpression was observed in tumour samples with active MAPK and PI3K pathways. A t-test was used to compare expression levels of both MCL-1 protein and *MCL-1* mRNA in tumours with high levels of p-ERK and p-AKT vs. tumours with low levels. Tumour cells expressing high levels of p-ERK showed overexpression of both *MCL-1* mRNA and MCL-1 protein. High levels of *MCL-1* mRNA and MCL-1 protein were also identified in p-AKT overexpressing cancer cells (Figure 5.3). 19/23 (82.6%) cases with high expression levels of p-AKT revealed overexpression of *MCL-1* mRNA; however, MCL-1 protein overexpression was only found in 13/23 (56.5%) of cases. 4/10 (40%) p-ERK overexpressing tumours also showed high levels of the MCL-1 protein and 6/10 (60%) showed high mRNA overexpression. Importantly, MCL-1 protein and *MCL-*

l mRNA overexpression was significantly associated with high levels of p-ERK and p-AKT, ($p < 0.05$) (Figure 5.4).

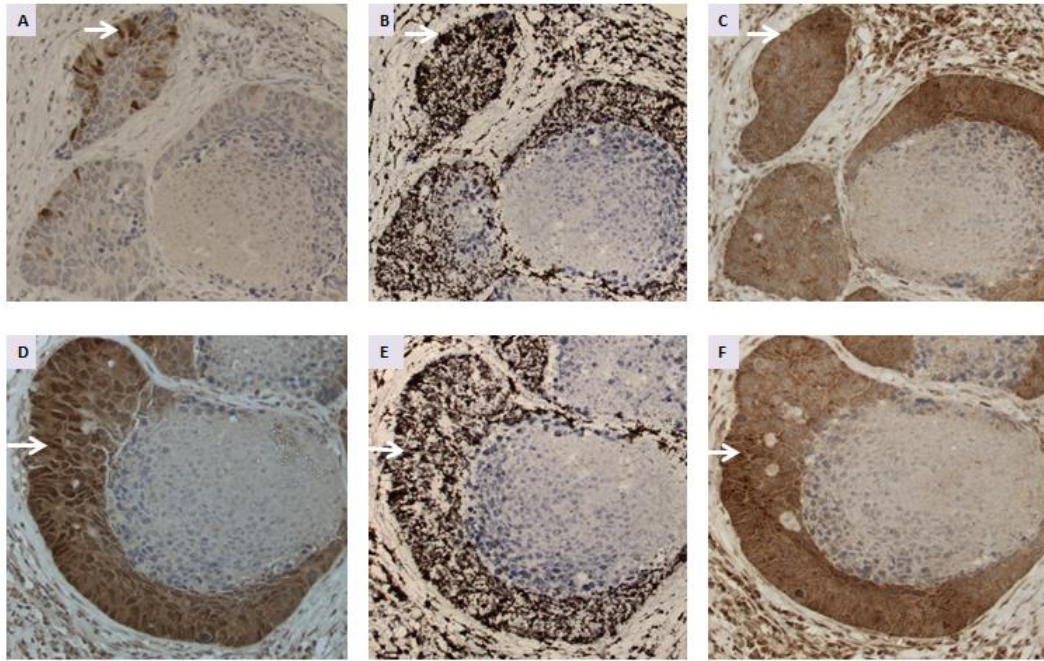


Figure 5.3 MCL-1 overexpression correlates with MAP and PI3K pathways in NSCLC. Tumour cells with high level of p-ERK (A) showed overexpression of *MCL-1* mRNA (B) and increased levels of MCL-1 protein (C). Cancer cells with high levels of p-AKT (D) revealed high levels of *MCL-1* mRNA (E) and MCL-1 protein (F).

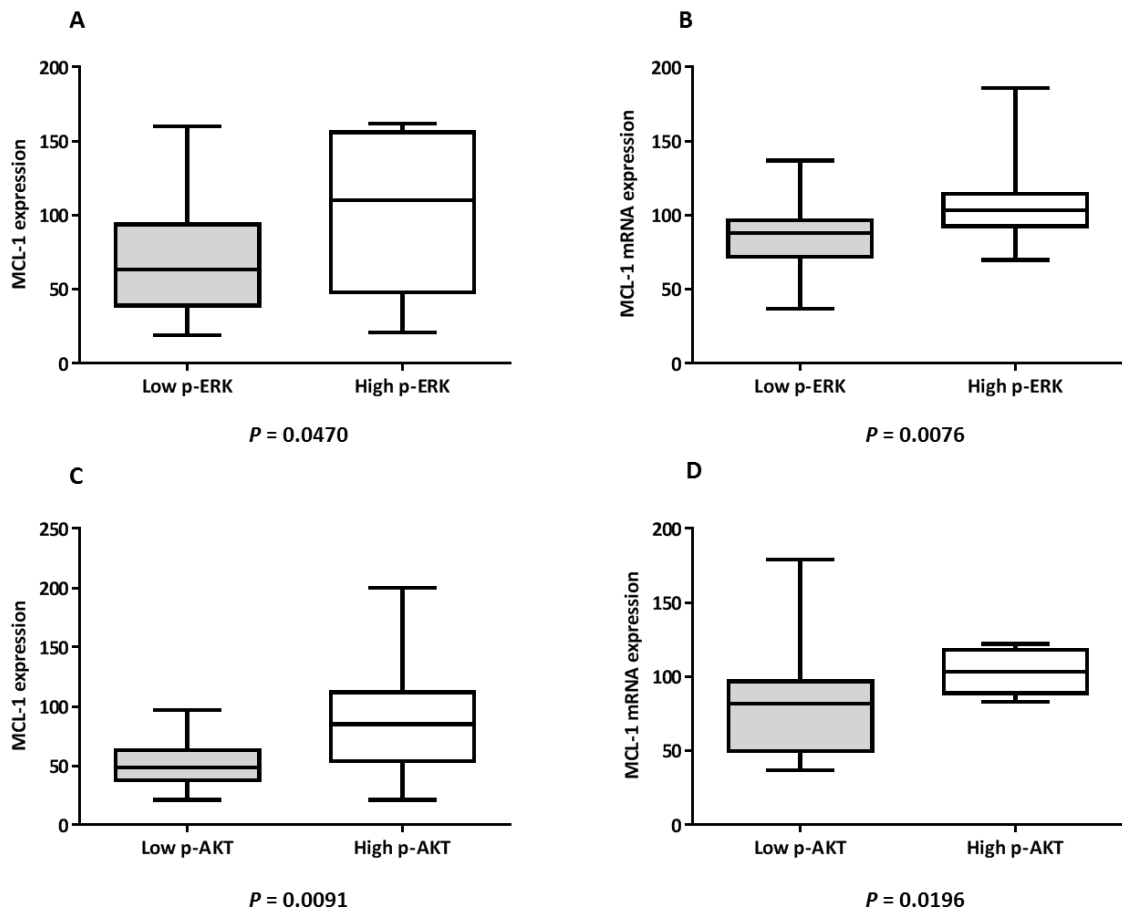


Figure 5.4 MCL-1 and *MCL-1* mRNA expression levels in NSCLC. A significant increase of MCL-1 was identified in NCSLC cases with p-ERK overexpression (A). *MCL-1* mRNA overexpression was also demonstrated in cancer cells with high levels of p-ERK (B). Strong positive staining of MCL-1 was found in p-AKT overexpressing cases (C). Cases with intense staining of p-AKT have revealed significant amounts of mRNA (D).

5.4 Discussion

Previous studies have demonstrated *MCL-1* and *MYC* co-amplification in breast cancer (Balko *et al.*, 2014) and *MCL-1/JUN* co-amplification in pseudomyxoma peritonei (Sio *et al.*, 2014). In this study, we analysed *MCL-1/PIK3CA* co-amplification and *SOX2/MCL-1* co-amplification. No co-amplification of *MCL-1* and *PIK3CA* was detected, and one concurrent amplification of *SOX2* and *MCL-1* was identified. The co-existence of *MCL-1* amplification with oncogene mutations

was also analysed. Only two NSCLC cases - one case harbouring *KRAS* mutation and one case with *PIK3CA* mutation showed *MCL-1* amplification, indicating that co-existence of *MCL-1* amplification and oncogene driver mutations in NSCLC samples could be a *de novo* event.

Studies demonstrated overexpression of both MCL-1 protein and *MCL-1* mRNA in MAPK up-regulated cutaneous metastatic melanoma harbouring the V600E mutation (McKee *et al.*, 2013), and up-regulation of MCL-1 via EGF (the upstream regulator of ERK) and the transcription activator Elk-1 was also described in breast cancer (Booy *et al.*, 2011). Furthermore, overexpression of MCL-1 has also been described in *EGFR* mutated NSCLC (Cetin *et al.*, 2010). In addition to the MAPK pathway, the PI3K pathway is also implicated in expression of MCL-1 as PI3K pathway inhibition causes suppression of MCL-1 in *EGFR* mutant NSCLC (Faber *et al.*, 2009). In accordance with these previous studies, we found overexpression of both MCL-1 protein and mRNA in tumours with active MAPK and PI3K pathways. The percentage of mRNA overexpressing tumours was higher than MCL-1 protein overexpressing tumours, which could be attributed to the short half-life of MCL-1.

5.5 Conclusion

This study has found no relationship between *MCL-1* amplification and oncogenic mutations or copy number alteration exists. The coexistence of oncogene mutation with *MCL-1* amplification was also identified as a random event. However, up-regulation of MCL-1 in cancer cells with activated PI3K and MAPK pathways suggests a possible association at the protein level but not at the genetic level.

**Chapter 6. *in vitro* study of MCL-1 regulation and
MCL-1-induced drug resistance**

6.1 Introduction

Patients with NSCLC are mainly diagnosed at an advanced stage, and the majority of patients show resistance to chemotherapies (Wesarg *et al.*, 2007). Platinum-based chemotherapies, such as cisplatin and carboplatin, are commonly used in NSCLC treatment and are cytotoxic by targeting cellular DNA and formation of DNA adducts. Moreover, it has been assumed that cisplatin targets cellular DNA and initiates apoptosis associated with other cellular parameter alterations (Cosaert and Quoix, 2002) such as activation of pathways involved in promotion and prevention of cell death (Basu and Krishnamurthy, 2010).

MCL-1 overexpression is implicated in drug resistance and cancer relapse, with cells expressing high levels of MCL-1 showing resistance to targeted therapies ABT-737 and ABT263, which prevent interaction between mitochondrial pro-apoptotic and anti-apoptotic proteins (Mojsa *et al.*, 2014). Activation of PI3K/AKT/mTOR pathways and MCL-1 up-regulation have also been implicated in acquired drug resistance (Choudhary *et al.*, 2015).

6.2 Aim and objectives

The aim of this chapter was to evaluate oncogenic MCL-1-induced drug resistance in NSCLC. The specific objectives were:

1. To culture cell lines harbouring genetic alterations including *KRAS* mutations, *MCL-1* amplification, *MCL-1* gain and *PIK3CA* amplification.
- 2 To target MCL-1-regulating pathways using different targeted therapies and evaluate *MCL-1* mRNA levels in the treated cell lines.

3. To evaluate the response of *MCL-1*-amplified cells to cisplatin compared to other cell lines.

4. To evaluate the response of an *MCL-1*-amplified cell line and other cell lines to inhibitors alone or combined with cisplatin.

6.3 Results

6.3.1 Culture of cell lines

The *MCL-1*-amplified cell line, H1395, and *MCL-1* non-amplified cell line, H1355, were cultured in complete medium containing RPMI-1640 containing 10% FCS combined with an antibiotic (penstrep) at a density of 2×10^4 for 24, 48, 78, and 92 hours in 96 well plates. Cells showed optimum growth at a density of 2×10^4 after the Alamar Blue assay was conducted to determine cell proliferation.

6.3.2 Inhibition of JAK/STAT, PI3K/AKT/mTOR and MAPK pathways

To assess the sensitivity of *MCL-1* amplified cells to a number of PI3K/AKT/mTOR pathway inhibitors, cell lines were grown to confluence and then treated with a PI3K/AKT/mTOR pathway inhibitor, AZD8055, with an IC₅₀ of 0.8 nM (Chresta *et al.*, 2010), and a MAPK inhibitor (U0126) with an IC₅₀ of 70 nM (Duncia *et al.*, 1998), respectively. The STAT inhibitor SH-4-54, which inhibits STAT3 at a concentration of 300 nM, and STAT5 at concentration of 464 nM (recommended doses from Selleckchem, USA) was also used to treat the cell line. The concentration of the specific STAT3 inhibitor niclosamide was 700 nM, because the IC₅₀ of niclosamide is 700 nM (Jung *et al.*, 2015). Cell lines were also treated with HSP90 inhibitor (STA9090; Selleckchem; IC₅₀ 4 nM) at a concentration of 4 nM.

The level of mRNA in the *MCL-1*-amplified cell line H1395 was 48-fold higher than the control non-amplified cell line, H1355. The *MCL-1*-amplified cell line was also resistant to all the inhibitors, with no significant reduction of mRNA detected in the treated samples compared to the DMSO-treated control sample ($p > 0.05$). However, a slight decrease in the amount of *MCL-1* mRNA was identified after treatment with the STAT5 inhibitor. A significant reduction of *MCL-1* mRNA was identified in the control cell line, H1355, when treated with the mTOR inhibitor AZD8055 ($p = 0.0001$). Up-regulation of *MCL-1* mRNA was seen in the H1355 cell line treated with both MEK and STAT3 inhibitors, whereas down-regulation of *MCL-1* mRNA was detected after treatment with niclosamide and STAT5 inhibitor ($p < 0.05$). Figure 6.1 shows the expression levels of mRNA in the control and the *MCL-1*-amplified cell line after treatment with different inhibitors.

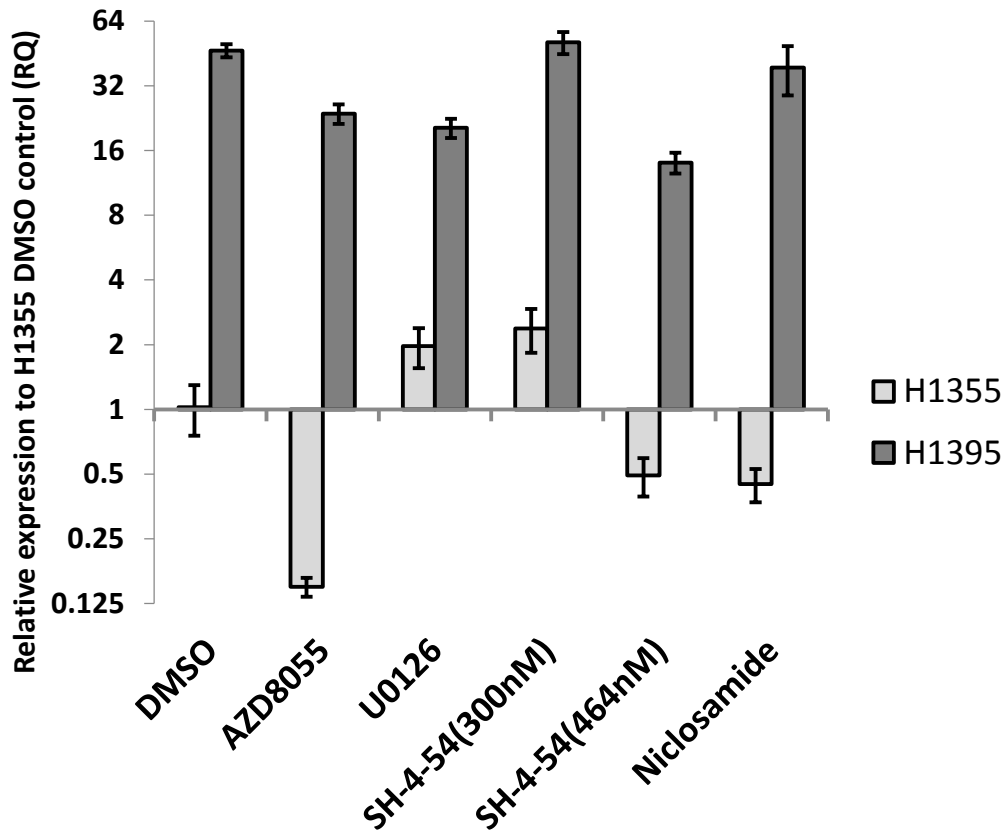


Figure 6.1 Expression levels of MCL-1 mRNA in cell lines treated with targeted therapies. *MCL-1* mRNA was highly expressed in the H1395 cell line compared to the H1355 cell line. The *MCL-1*-amplified cell line H1395 was resistant to the inhibitors, whereas the control cell line, H1355, was sensitive to AZD8055, niclosamide and SH-4-54 at a concentration of 464 nM, and resistant to U0126 and SH-4-54 at a concentration of 300 nM.

6.3.3 Targeting the MCL-1 regulatory pathways in KP-2 and RERF-LC-Sq1 cell lines

To assess the effects of oncogenic driver mutations on PI3K/AKT/mTOR inhibition, cells lines with known mutation status were subjected to various inhibitors and relative expression of MCL-1 analysed.

The control cell line H1355 which harbours a *KRAS* mutation (G13C) was very sensitive to AZD8055-induced *MCL-1* mRNA suppression. A pancreatic cell line KP-2 (which is also positive for *KRAS* mutation G12R) was included to determine

the sensitivity of a different *KRAS* mutant cell to the PI3K pathway inhibitor AZD8055. After treatment, KP-2 cells showed resistance to both AZD8055 and the STAT3 inhibitor niclosamide, indicating that each cell line has its own characteristics in response to the inhibitors. Furthermore, both cell lines harboured *KRAS* mutations that were active along the MAPK pathway, but were resistant to the MAPK inhibitor, U0126, unlike the PI3K inhibitor (Figure 6.2).

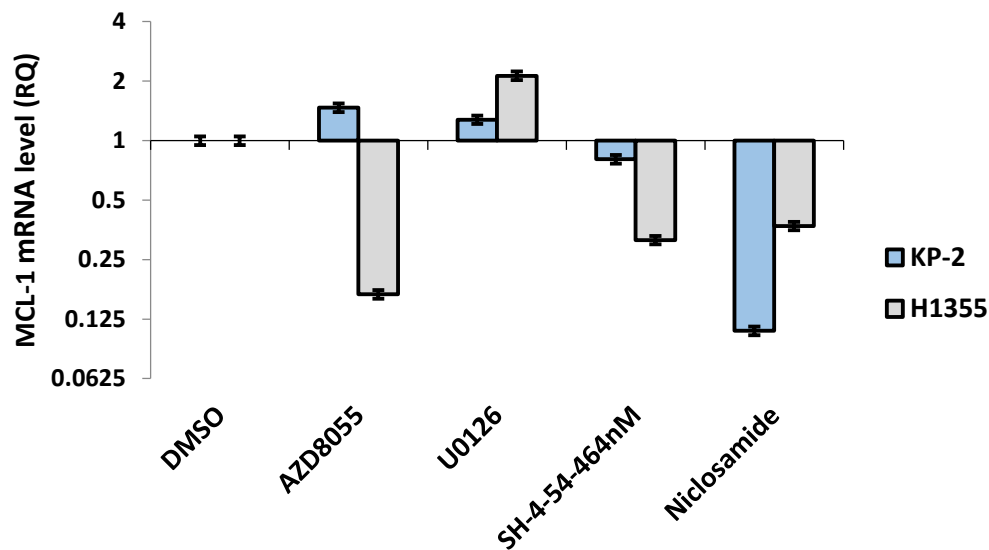


Figure 6.2 Response of *KRAS* mutant cell lines to the inhibitor. The *KRAS* mutant cell line KP-2 was more resistant to the inhibitors compared to the *KRAS* mutant cell line H1355. Both cell lines were resistant to U0126. The KP-2 cell line was sensitive to niclosamide; however, H1355 was sensitive to AZD8055, niclosamide and SH-4-54 at a concentration of 464 nM.

The *PIK3CA* mutant and amplified SCC cell line RERF-LC-Sq1 was also tested for response to inhibitors, and expression of *MCL-1* mRNA was analysed for the RERF-LC-Sq1 cell line and compared to that of the H1355 cell line. RERF-LC-Sq1 cells were also sensitive to niclosamide, AZD8055 and SH-4-54 at a concentration

of 464 nM, and showed decreased expression of *MCL-1* mRNA, as did the ADC cell line H1355. However, RERF-LC-Sq1 was more sensitive to the inhibitor SH-4-54 and niclosamide and less resistant to U0126 compared to H1355 (Figure 6.3).

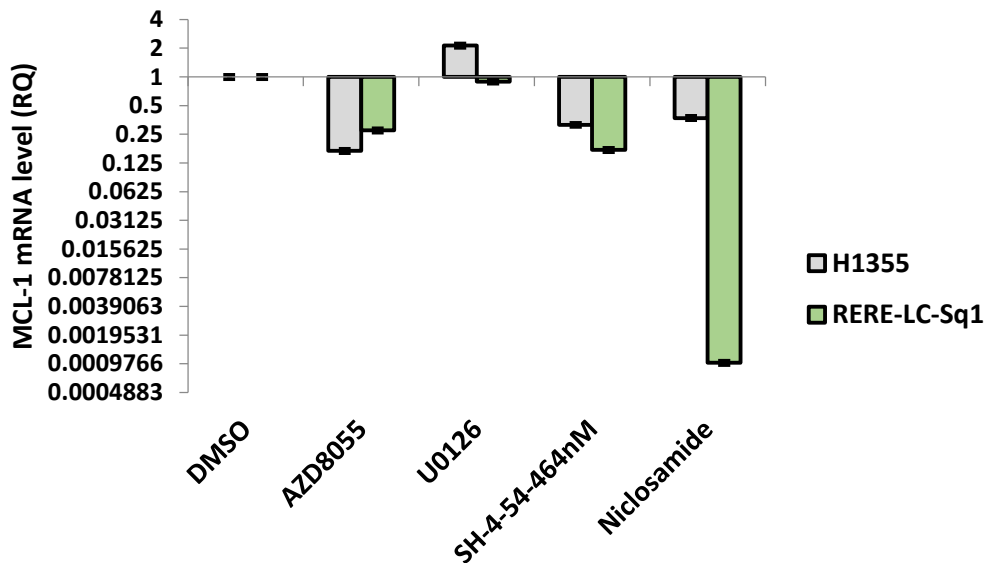


Figure 6.3 Response of the RERF-LC-Sq1 cell line to targeted therapies. The SCC cell line RERF-LC-Sq1 showed massive reduction of mRNA after treatment with SH-4-54 at a concentration of 464 nM, AZD8055 and niclosamide, and was resistant to U0126. H1355 was more resistant to U0126 than RERF-LC-Sq1.

6.3.4 Investigation of heat shock protein 90 (HSP90) effects on MCL-1mRNA expression

The H1395 and H1355 cell lines were further treated with the HSP90 inhibitor, STA9090, at a concentration of 4 nM and the response compared to the other inhibitors. The HSP90 inhibitor caused significant down-regulation of *MCL-1* mRNA in both control and amplified cell lines; however, the inhibitory effect of HSP90 on the amplified cell line was more significant ($p = 0.0076$) compared to

the normal control cell line ($p = 0.0158$). Figure 6.4 demonstrates the inhibitory effects of the STA9090 on MCL-1 mRNA expression in NSCLC.

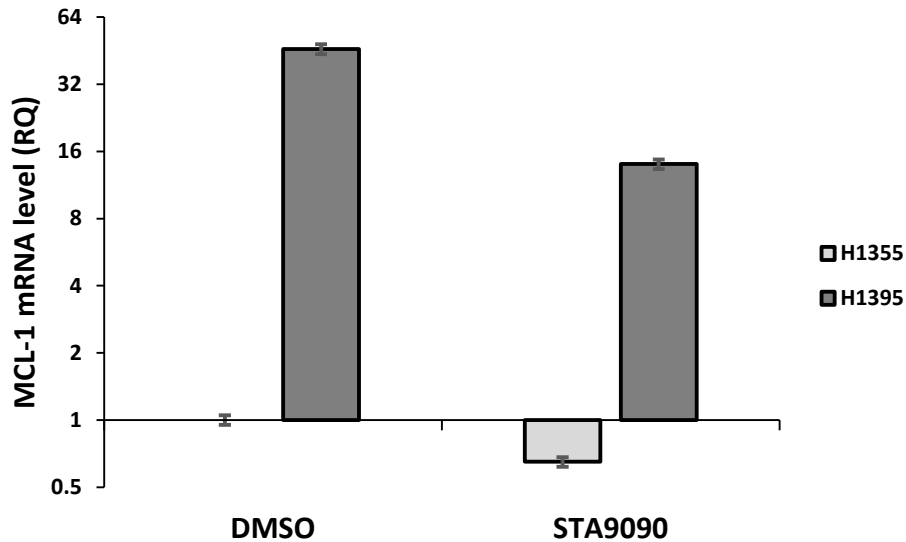


Figure 6.4 Effect of HSP90 on MCL-1 mRNA in normal control and *MCL-1*-amplified cell lines. The HSP90 inhibitor STA9090 showed inhibitory effects on mRNA in both cell lines, with a more significant reduction of mRNA in the *MCL-1*-amplified cell line (H1395) compared to the non-amplified cell line (H1355).

6.3.5 Response of *MCL-1*-amplified cell lines and other NSCLCs to cisplatin

To assess a potential role for *MCL-1* amplification in resistance to cisplatin cells were treated with cisplatin at concentrations of 500 nM, 1 μ M, 5 μ M, 10 μ M, 20 μ M, 50 μ M, and 100 μ M for 24 hours. The control cells were only treated with DMF. Alamar Blue cell viability assays were performed to analyse the response of the cell lines to cisplatin. 50% of the cells were killed at a concentration of 10 μ M. Both H1395 and H1355 cells were sensitive to cisplatin at a concentration of 10 μ M; however, the *MCL-1*-amplified cell line H1395 was more resistant than the non-amplified cell line H1355 at a concentration of 100 μ M, with $P = 0.0001$ (Figure 6.5).

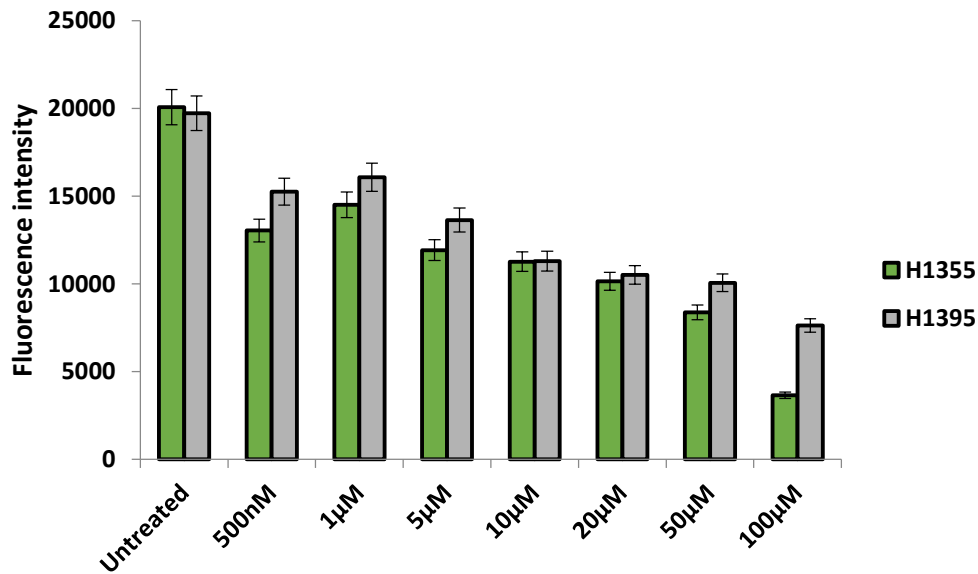


Figure 6.5 Response of NSCLC cell line to cisplatin. The two adenocarcinoma cell lines H1355 and H1395 showed sensitivity to cisplatin, whilst the amplified cell line H1395 was more resistant to cisplatin compared to H1355 ($p < 0.05$).

There was a disparity between SCC cell lines and ADC cell lines in response to cisplatin. Cell lines H1395, H1355, H2342 and RERF-LC-Sq1 were treated with two different concentrations (10 µM and 50 µM) of cisplatin for 24 hours, and viability assays showed that ADC cell lines H1395, H1355 and H2342 were more resistant to cisplatin compared to the SCC cell line RERF-LC-Sq1 ($P < 0.0001$) (Figure 6.6).

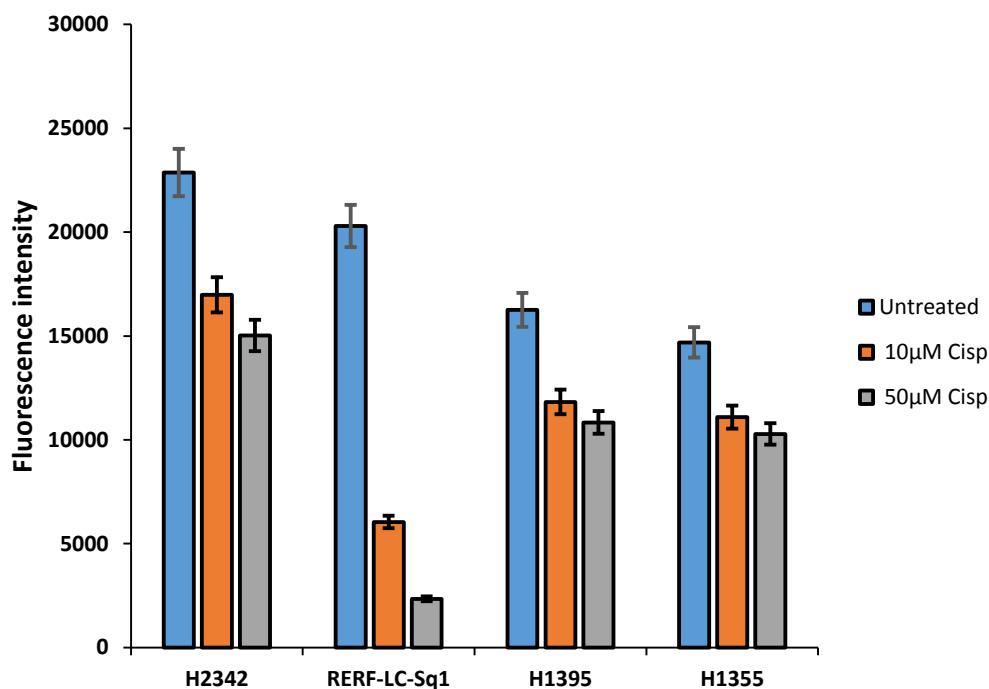


Figure 6.6 Responses of SCC cell line and ADC cell lines to cisplatin. The SCC cell line RERF-LC-Sq1 was sensitive to cisplatin compared to the ADC cell lines H1355, H1395 and H2342 at concentrations of 10 µM and 50 µM. The H1395 cell line harbouring *MCL-1* amplification and the H2342 cell line harbouring copy number gain were more resistant than the *KRAS* mutant cell line H1355.

6.3.6 Evaluation of cell viability in *MCL-1*-amplified and non-amplified cell lines after treatment with inhibitors for 24, 48 and 72 hours

NSCLC cell lines were treated with different inhibitors at concentrations of 0.8 nM, 70 nM, 464 nM 700 nM 4 nM and 300 nM for AZD8055, U0126, SH-4-54, niclosamide, STA9090 and SH-4-54, respectively, for 24 hours. DMSO-treated cells were used as a control. Both cell lines were resistant to the inhibitor at both concentrations, with no significant reduction in the number of viable cells observed. The treatment time was increased to 48 hours when the treated cell lines showed resistance upon exposure for 24 hours. Cells were treated with the same concentrations used for the 24 hour treatment. Surprisingly, cells treated for 48 hrs were more resistant to the inhibitors than those treated for 24 hours ($P = 0.021$).

Only niclosamide-treated cells (H1355) showed a slight decrease in viability, though this decrease was not significant. As no significant effect was observed in cells treated for 24 or 48 hours, cells were treated for 72 hours. Again, no significant effect was observed. Figure 6.7 shows the response of the H1355 and H1395 cell lines to the inhibitors after treatment for 24, 48 and 72 hours.

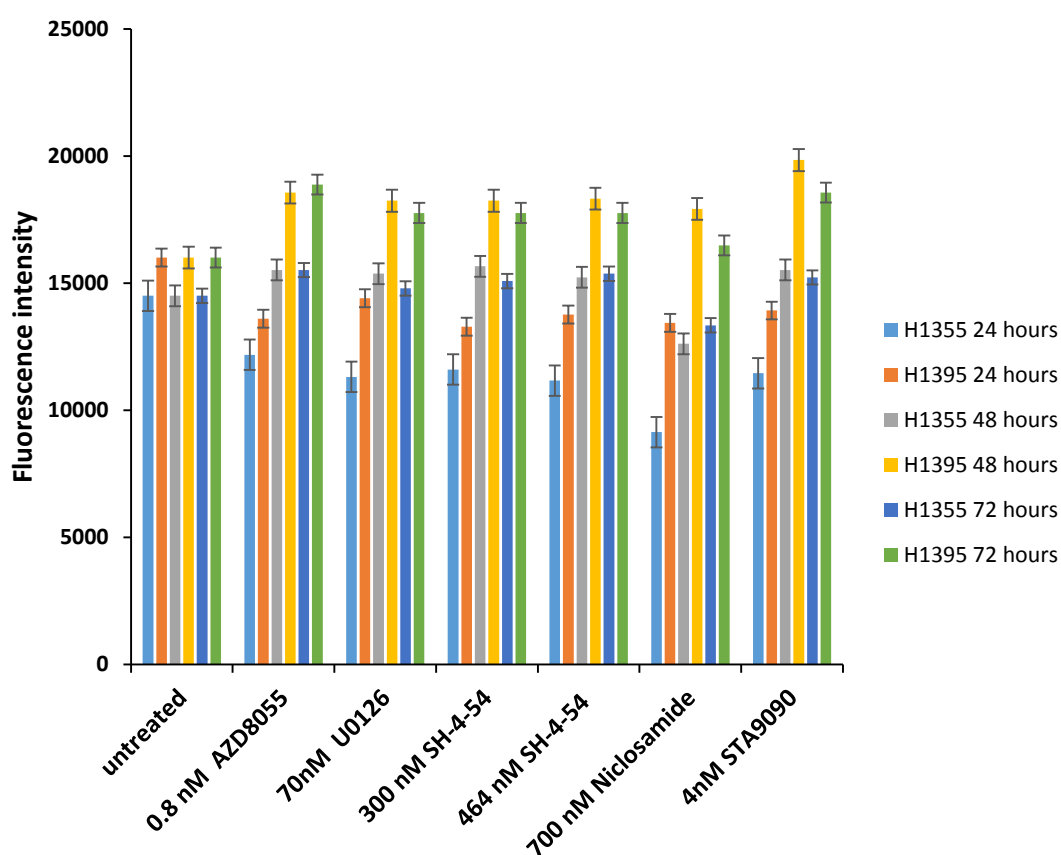


Figure 6.7 Responses of cell lines to inhibitors. 24 hour treatment of cell lines with the IC50 concentration of the inhibitors showed resistance of the cell to the inhibitors. A slight increase in cell viability was detected after 48 hours of treatment. No significant reduction was detected in the numbers of viable cells after incubation of the cells with the inhibitors for up to 48 hours; H1355 showed death of some viable cells, though this was not at any significant level. After 72 hours of treatment with inhibitors, cell viability was stable without any significant reduction in numbers of the cell lines.

6.3.7 Response of the cell lines to 5 μ M and 10 μ M of the inhibitors

Due to the resistance of the cell lines to treatment with each drug at standard concentration the dose of the inhibitors AZD8055, U0126, SH-4-54, niclosamide and STA9090 was increased to 5 μ M and incubated with the cells for 24 hours. The control cells were only treated with DMSO. Cell viability was measured after 24 hours. Cell lines were found to be resistant to 5 μ M of the inhibitors (Figure 6.8). Due to resistance of the cells to the inhibitors, even at a concentration of 5 μ M, the treatment dose was doubled to 10 μ M and a viability assay performed after 24 hours.

A dose of 10 μ M resulted in a significant reduction in viability of both cell lines. The reduction was very significant when SH-4-54-treated cells were compared to the untreated control cells ($P = 0.0001$). H1355 and H395 were also sensitive to niclosamide at a concentration of 10 μ M ($P = 0.0121$). Depending on these findings, the IC₅₀ of SH-4-54 in H1355 and H1395 could be $7.0 \pm 1.5 \mu\text{M}$, as 5 μ M of SH-4-54 inhibited only approximately 0.8% of the cells, whilst the 10 μ M concentration inhibited 99.2% of the cells. Figure 6.9 shows growth inhibition in cell lines H1355 and H1395 when treated with the inhibitors at a concentration of 10 μ M.

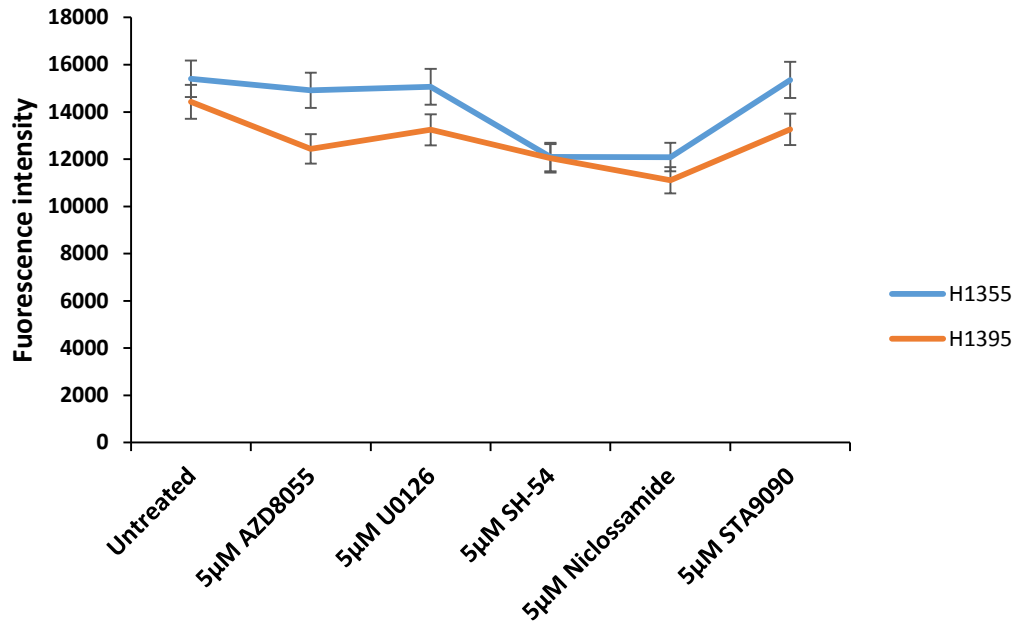


Figure 6.8 Response of the cell lines to a 5 μM concentration of the inhibitors. H1355 and H1395 were resistant to the inhibitor even at a concentration of 5 μM. A slight decrease in the number of viable cells was detected after treatment with niclosamide and SH-4-54.

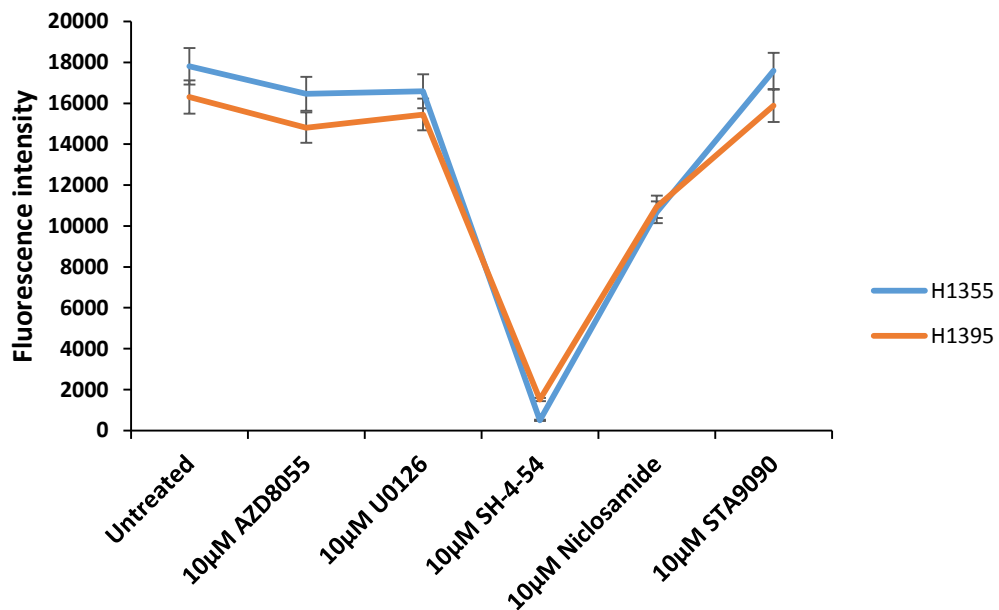


Figure 6.9 Response of the cell lines to a 10 μM concentration of the inhibitors. The cell lines were resistant to the inhibitors AZD855, U0126 and STA9090; however, sensitivity to niclosamide and SH-4-54 at a concentration of 10 μM was identified after 24 hours of treatment.

6.3.8 Response to combinations of inhibitor and cisplatin

As cells showed resistance to cisplatin (6.3.5), inhibitors were in combination to assess whether this increased cell lines sensitivity. Cells were treated using cisplatin combined with the inhibitors AZD8055, U0126, SH-4-54, niclosamide and STA9090. Cells were first treated with 10 μ M cisplatin combined with 0.8 nM, 70 nM, 300 nM, 700 nM, 4 nM and 464 nM of AZD8055, U0126, SH-4-54, niclosamide, STA9090 and SH-4-54, respectively. Growth inhibition was determined after 24 hours. Potentiation of cisplatin by the inhibitor was not detected (Figure 6.10), so the concentration of cisplatin was increased to 50 μ M and combined with the same concentrations of each inhibitor and incubated for 24 hours. Potentiation of cisplatin by the inhibitors was again not detected, and cell viability was found to be slightly *increased* by the combined therapy compared to cisplatin alone (Figure 6.11)

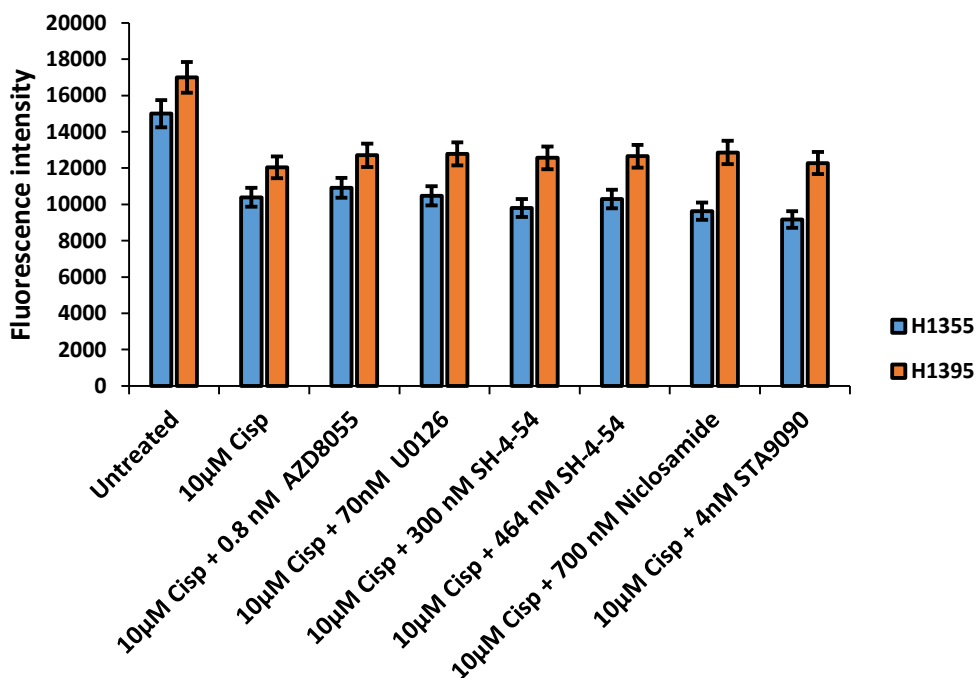


Figure 6.10 Responses of H1355 and H1395 cell lines to combined therapy. The cell lines were sensitive to cisplatin alone at a concentration of 10 μ M. The

inhibitors added did not sensitise the cell lines to cisplatin; indeed, a slight increase in cell viability was detected after application of the combined therapy.

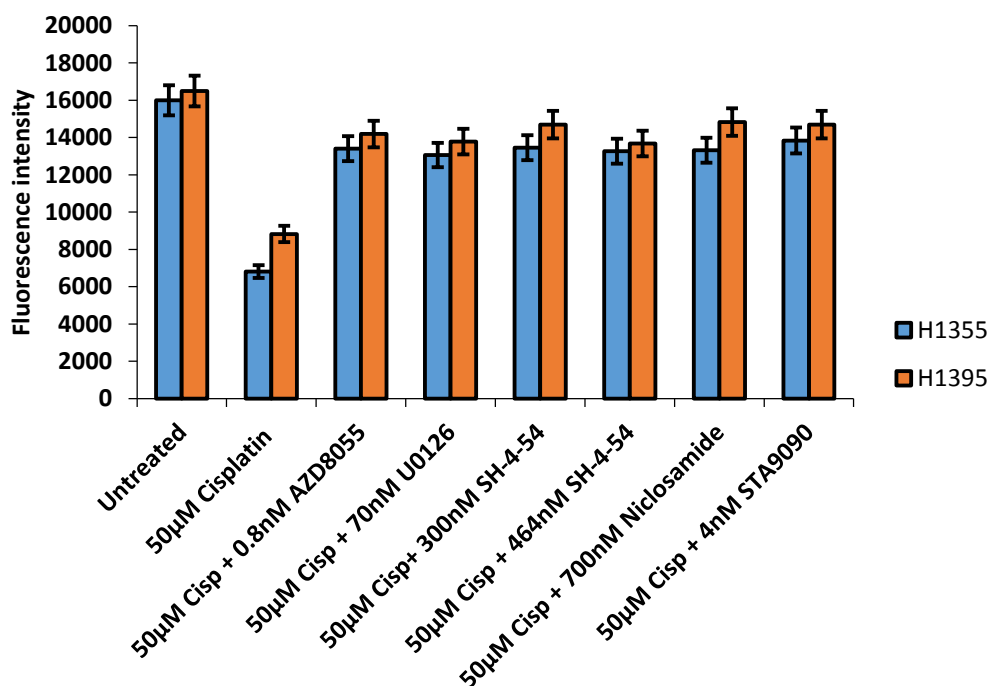


Figure 6.11 Response of the NSCLC cell line to combined therapy using 50 µM cisplatin. Cells became more resistant to the combined therapy when the dose of cisplatin was increased from 10 µM to 50 µM.

6.3.9 Evaluation of growth inhibition using 10 µM cisplatin with increased doses of inhibitors

Because all of the inhibitors combined with cisplatin lacked the ability to sensitise the treated cells to cisplatin, inhibitor concentrations were increased to 5 µM and 10 µM respectively, then combined with 10 µM cisplatin. Cell viability was assessed after 24 hours. No synergistic effect between cisplatin and the inhibitors was observed, even by increasing concentrations of the inhibitors to 5 µM (Figure 6.12).

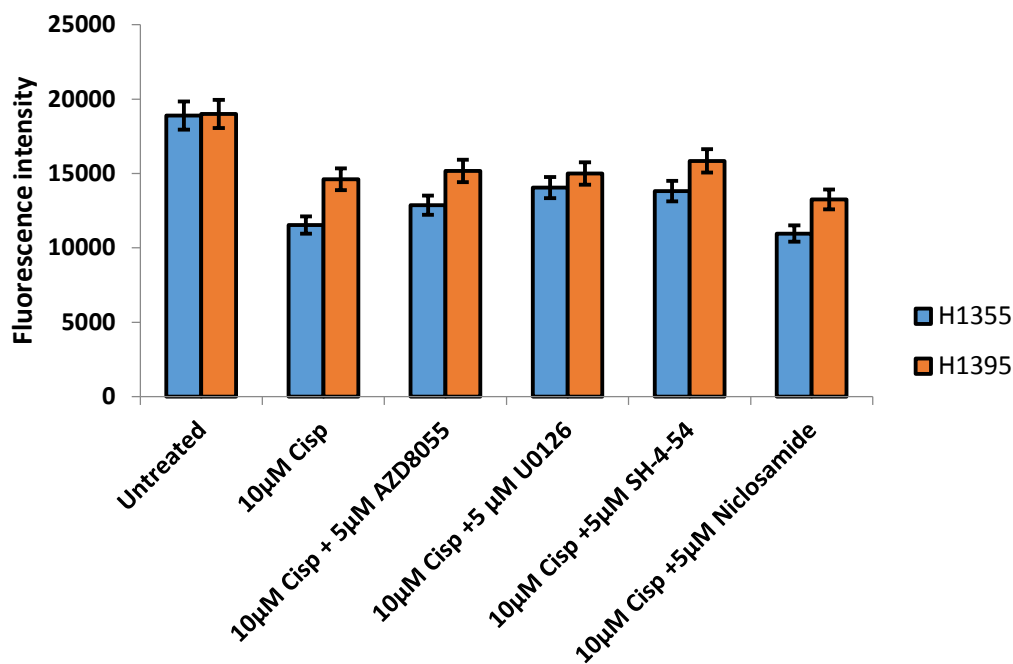


Figure 6.12 Growth inhibition at 5 µM inhibitor concentrations combined with cisplatin. The cells treated with cisplatin alone were more sensitive in comparison to the cells treated with cisplatin combined with 5 µM of inhibitor; a mild potentiation to cisplatin by niclosamide was detected in both H1355 and H1395 cell lines.

Next, 10 µM of each inhibitor combined with 10 µM of cisplatin was used to treat H1355 and H1395 cell lines when the 5 µM concentrations of the inhibitors failed to sensitise the cells to 10 µM of cisplatin. Growth inhibition was performed after 24 hours; significant inhibition of cells treated with a combination of cisplatin and SH-4-54 was detected in both cell lines, although growth inhibition was significant for both single agent treatment (10 µM SH-4-54) and combined treatment (10 µM SH-4-54 + 10 µM cisplatin). Increased cell viability was detected using the combined therapy, indicating a reduction in the number of viable cells occurred due to the inhibitory effect of SH-4-54. A mild additive effect of cisplatin by niclosamide was also identified (Figure 6.13).

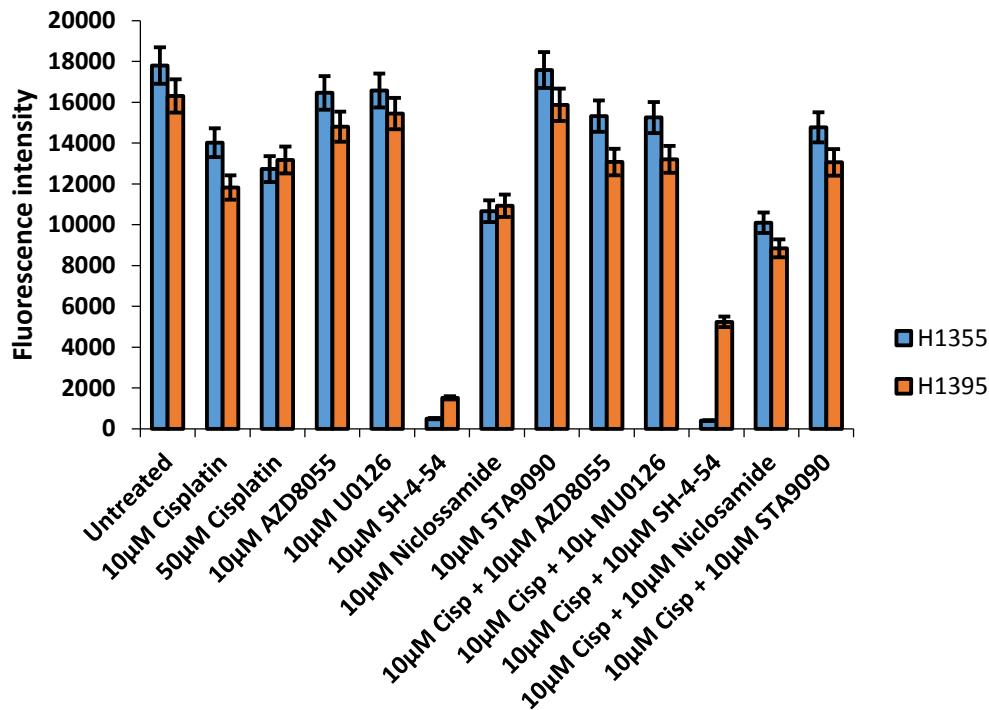


Figure 6.13 Response of cell lines to 10 µM inhibitor concentrations alone, and combined with 10 µM cisplatin. 10 µM of SH-4-54 caused significant cell death in both cell lines. However, the *MCL-1*-amplified cell line (H1395) was more resistant than the non-amplified cell line (H1355). The combination of cisplatin with SH-4-54 also reduced the number of viable cells, but significant reduction was seen when cells were exposed to SH-4-54 compared to cisplatin combined with SH-4-54, in particular in the H1395 cell line. Niclosamide also showed a reduction in cell viability, though this was less significant than that for SH-4-54.

6.4 Discussion

MCL-1 transcriptional regulation is varied from cell to cell and PI3K/AKT, JAK/STAT, and MEK/ERK pathways are implicated in *MCL-1* transcription (Gouill *et al.*, 2004). We also found that *MCL-1* transcriptional regulation is cell-type dependent: down-regulation of *MCL-1* mRNA in the H1355 cell line treated with AZD8055 was observed, but was not observed in H1395 cell lines treated with the same inhibitor. Moreover, targeting of the pancreatic cell line KP-2 and the lung

cancer cell line H1355 (both *KRAS* mutants) by AZD8055 demonstrated different responses of the cells to the inhibitor.

The JAK/STAT signalling pathway, rather than the MAPK or PI3K pathways, was the most important regulatory pathway for *MCL-1* transcription in *MCL-1*-amplified lung cancer cell lines. Inhibition of *MCL-1* mRNA after treating cells with 464 nM of SH-4-54 indicated that JAK/STAT5 was an important regulator for *MCL-1* transcription in *MCL-1*-amplified cells. Furthermore, Busacca *et al.* (2015) (Busacca *et al.*, 2015) have also reported down-regulation of *MCL-1* mRNA after targeting STAT5. This study demonstrated that targeting JAK/STAT3 in *KRAS* mutant cells using niclosamide led to suppression of *MCL-1* mRNA, in agreement with a previous (You *et al.*, 2014), where another *KRAS* mutant cell line, A549, showed a reduction in MCL-1 expression after treatment with niclosamide. Suppression of *MCL-1* mRNA via STA9090 in both the *MCL-1*-amplified cell line and *KRAS* mutant cell line was observed. Such a finding has previously been described by Busacca and co-workers (Busacca *et al.*, 2015), who found that the HSP90 inhibitor causes down-regulation of *MCL-1* mRNA in MCL-1 addicted cells via inhibition of STAT5.

Studies have demonstrated that the *MCL-1* transcriptional machinery is complicated as *MCL-1* is a direct target for numerous transcription factors such as STAT5, STAT3, c-MYC and NF- κ B (Balakrishnan *et al.*, 2014). Suppression of *MCL-1* mRNA after treatment with a STAT3 inhibitor (niclosamide) was observed in this study and has also been previously reported (You *et al.*, 2014). In this study, we found that STAT5 was the more critical transcription factor for *MCL-1* regulation compared to STAT3.

The PI3K/AKT/mTOR pathway was the key control for *MCL-1* transcription in the lung cancer cell line with the *KRAS* mutation (G13C). A previous study has also reported a sharp decrease in the level of *MCL-1* mRNA in a *KRAS* mutant cell line after treatment with the mTORC1/2 inhibitor (AZD8055). In contrast, down-regulation of MCL-1 protein in *KRAS* mutant colorectal cell lines by the mTORC1/2 inhibitor, AZD8055, has been observed without any apparent correlation with mRNA expression (Faber *et al.*, 2014).

Transcription of *MCL-1* via ERK/Elk-1 pathways has previously been observed (Townsend *et al.*, 1999). In this study, inhibition of the MAPK pathway via targeting the upstream effector of ERK (MEK) using U0126 led to up-regulation of *MCL-1* mRNA. Moreover, targeting of *KRAS* mutant pancreatic cell KP-2 with U0126 and the NSCLC cell line H1355 demonstrated up-regulation of MCL-1, indicating that transcription of *MCL-1* in *KRAS* mutant cancers is not MAPK dependent.

Cisplatin-based combination treatment has been used for several years as an effective and fundamental treatment for NSCLC (Andriani *et al.*, 2006). To identify and improve platinum-based combination therapy, in this study NSCLC cell lines were treated with cisplatin alone, inhibitors alone, and cisplatin combined with inhibitors to evaluate the most effective treatment for NSCLC, and in particular *MCL-1*-amplified cells. A variation in response of cell lines to cisplatin was observed (Barr *et al.*, 2013). In this study, cisplatin treatment showed varying responses according to treatment dose and the histological subtype of the cell. The *MCL-1*-amplified cell line was more resistant to cisplatin compared to *KRAS* mutant cells at a concentration of 100 μ M indicating that MCL-1 is involved in the

mechanism of drug resistance in NSCLC, in particular MCL-1 overexpressing ADC cases.

Previous studies have shown significant inhibition of lung cancer and colorectal cell lines by the mTORC1/2 inhibitor AZD8055 at a concentration of 500 nM-1 μ M, and inhibition by tamoxifen of oestrogen deprivation-resistant breast cancer cell line growth at concentrations of 18 nM and 24 nM, respectively (Jordan *et al.*, 2014). Moreover, targeting the hepatocellular carcinoma cell lines Hep3B, Huh-7 and HepG2 by AZD8055 revealed significant inhibition of growth at concentrations of 24.4 nM and 47.9 nM, respectively (Ewald *et al.*, 2015). However, in this study no growth inhibition was identified, even at concentrations of 5 μ M and 10 μ M in the lung cancer cell lines tested.

Toxic effects of U0126 on HeLa cells at concentrations of 5 μ M has been reported (McDaid and Horwitz, 2001) and treatment of the melanoma cell line A375 with U0126 for 24, 48, and 72 hours at concentrations of 5 μ M and 10 μ M showed significant suppression of growth, with an IC₅₀ of 5 μ M (Huang *et al.*, 2015). By contrast, no reduction in cell viability was detected in this study after treatment of cells for 24 hours with U0126 at concentrations of 5 μ M or 10 μ M, indicating that H1355 and H1395 cell lines are resistant to U0126.

The STAT3 inhibitor niclosamide was more potent than AZD8055, STA9090 and U0126 inhibitors at a concentration 5 μ M; 22% of lung cancer cell lines died after treatment with 5 μ M niclosamide, and 10 μ M niclosamide consistently induced cell death in 33% of lung cancer cell lines. A previous study has demonstrated apoptosis rates of 25.5% and 31.3% in a breast cancer cell line (4T1) at concentrations of 5 μ M and 10 μ M, respectively (Ye *et al.*, 2014).

Resistance to STA9090 at concentrations of 5 μ M and 10 μ M were observed in H1355 and H1395 cell lines. Reports have suggested that no effect due to long and short term exposure to STA9090 was observed after treatment of cell lines; the IC₅₀ of STA9090 in the H1355 cell line is 5 nM (Acquaviva *et al.*, 2012). Several STA9090 -resistant cell lines were observed in previous studies; Landman and co-workers (2014) (Landmann *et al.*, 2014) reported that HT29 is resistant to STA9090 and showed an IC₅₀ of 2000 nM, the gastric carcinoma cell line MKN-28 was also reported to be resistant to STA9090 at concentrations > 500 nM (Liu *et al.*, 2015), in agreement with Landman *et al.* (2014). No STA9090-induced cell death was identified after treatment with 5 μ M and 10 μ M for 24 hours, indicating that H1355 and H1395 cell lines are resistant to STA9090.

Targeting the JAK/STAT5 pathways is important in *MCL-1*-amplified tumours because STAT5 controls the MCL-1-regulating machinery (Sathe *et al.*, 2014); according to our findings, the IC₅₀ of SH-4-54 in H1355 and H1395 was $\sim 7 \pm 1.5$ μ M, as no significant reduction in the number of viable cells was detected after treatment with 5 μ M SH-4-54. However, a massive reduction was identified at a concentration of 10 μ M, depending on the inhibitory effects of the inhibitor used. In this study we found SH-4-54 was the most potent agent for targeting MCL-1 in order to overcome MCL-1-induced drug resistance in NSCLC. Although 7 ± 1.5 μ M of SH-4-54 might seem toxic to normal cells and thus that it is not possible to treat patients at such a toxic dose, one may consider that, until now, SH-4-54 has been considered to be the most effective targeted therapy for the chemotherapy-resistant *MCL-1*-amplified cell lines.

Combination therapy improves therapeutic response and decreases adverse effects and drug resistance (Wu *et al.*, 2014). Unfortunately, no significant effect was found after combination of cisplatin with any of the tested inhibitors; however, combination of 10 μ M cisplatin with 10 μ M SH-4-54 resulted in massive cell death.

As increased cell viability was seen in combined therapy compared to the single treatment with SH-4-54, this implies that single agent treatment using SH-4-54 was more promising than when SH-4-54 was combined with cisplatin. SH-4-54 treatment followed by cisplatin could be used as another strategy to target *MCL-1*-amplified tumours in future studies, as well as treatment for 72 hours possibly showing an IC₅₀ lower than $7 \pm 1.5 \mu$ M, but this possibility should also be the subject of future research.

6.5 Conclusion

We have shown that the JAK/STAT5 pathway is a key regulator for *MCL-1* transcription in NSCLC. Furthermore, while combined therapy is more potent than single agent treatment, some combination therapies actually reduce cell death and increase drug resistance in cancer cells. Finally, we have shown that STAT inhibitors may be considered the most effective targeted therapies for targeting cancer cells addicted to MCL-1 and future studies are required.

Chapter 7. Evaluation of drugs in NSCLC explants

7.1 Introduction

Ex vivo culture reflects the *in vivo* microenvironment of the patient tumour and is regarded as a more clinically relevant system to screen drug efficacy on tumour cells (Mitra *et al.*, 2013). This technique preserves cellular and organ architecture as well as maintaining stroma-tumour interactions (Vaira *et al.*, 2010), as well as faithfully reproducing the hallmarks of cancer cells including angiogenesis, proliferation, self-sufficiency in growth signals, anti-apoptotic mechanisms, invasion and metastasis (Godugu *et al.*, 2013). In this chapter, the treatment response of explants of NSCLC tumour tissue cultured and treated with cisplatin and inhibitors such as U0126 was studied. Cisplatin treatment and viability of the NSCLC explants were evaluated and the data provided by Ellie Karekla and Wen-Jing Liao.

The specific objectives were:

1. To evaluate responses of NSCLC explants harbouring mutations and copy number changes to cisplatin and inhibitors.
2. To evaluate the correlation between p-ERK, p-AKT, MCL-1 and *MCL-1* mRNA expressions and drug resistance.
3. To analyse any correlation between oncogenic mutations, copy number variation, protein expression and patient outcome.

7.2 Results

7.2.1 Response of NSCLC explants harbouring oncogene mutations to cisplatin

Cisplatin response was analysed in cases with different oncogenic mutations including *PIK3CA* (E542, E545 and H1047R) and *KRAS* (G12C, G12D, and G12A) mutations. Explants were treated with cisplatin and U0126, and compared to the untreated control. Resistance to cisplatin was detected in *KRAS* mutant explants at a concentration of 50 μ M. A *PIK3CA* mutant case was sensitive to cisplatin at the same concentration; however, cases harbouring both *KRAS* and *PIK3CA* mutations were resistant to 50 μ M cisplatin (Figure 7.1).

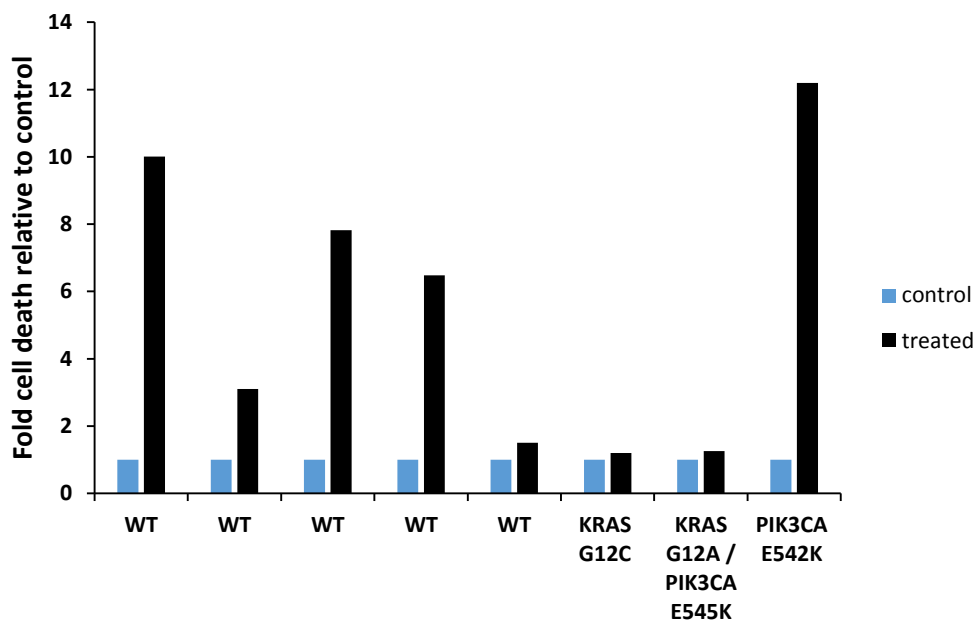


Figure 7.1 Response of NSCLC explants with oncogene mutations to 50 μ M cisplatin. All of the *KRAS* mutant explants were resistant to cisplatin treatment. The *PIK3CA* mutant case was sensitive to cisplatin. Some of the WT cases were resistant to cisplatin at a concentration of 50 μ M; however, the other WT cases were sensitive to cisplatin at this same concentration.

7.2.2 Response of NSCLC explants with copy number changes to cisplatin

To assess the effect of copy number alteration on response to treatment with cisplatin cells were treated with cisplatin at concentration of 50 μM . Cisplatin response was varied among the NSCLC explants treated according to their copy number changes. Cases with *MCL-1* gain (chromosome 1 polysomy) and a single case with *PIK3CA* amplification were resistant to cisplatin at a concentration of 50 μM , while SCC cases with *SOX2* and *MCL-1* amplifications showed sensitivity to cisplatin after treatment at a concentration of 50 μM (Figure 7.2).

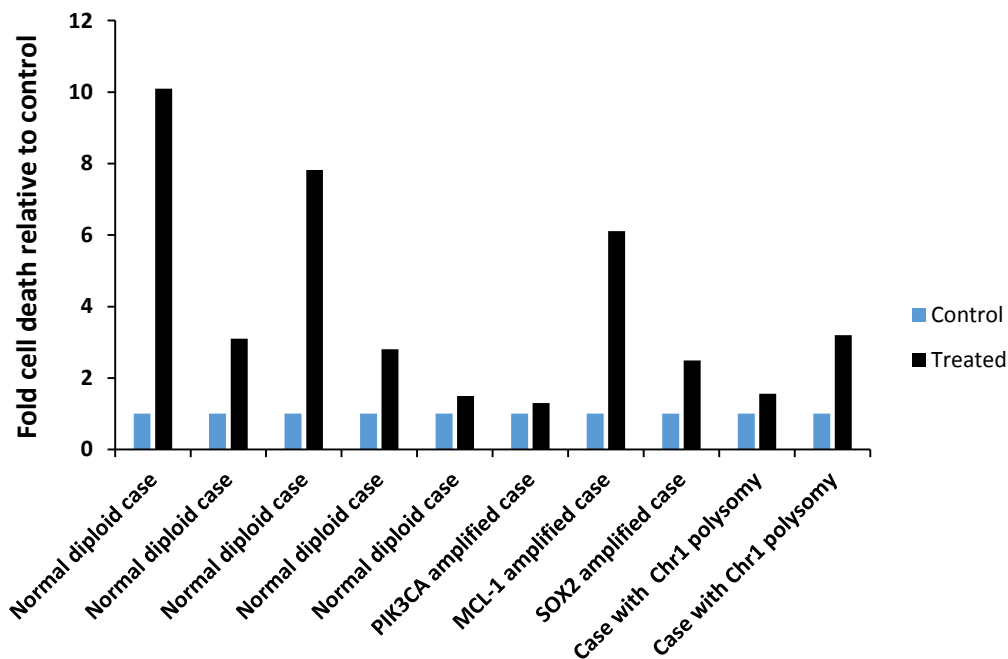


Figure 7.2 Response of NSCLC explants harbouring *PIK3CA* amplification, *MCL-1* amplification and *SOX2* amplification and chromosome 1 polysomy to 50 μM cisplatin. Cases with chromosome 1 polysomy and *PIK3CA* amplification were resistant to cisplatin. *SOX2*-amplified and *MCL-1*-amplified cases were sensitive to cisplatin.

7.2.3 Evaluating the effect of MEK inhibitor (U0126) on NSCLC explants with *MCL-1* gain

Two NSCLC explants (one WT and one with gain in *MCL-1*) were treated with the MEK inhibitor U0126 for 24 hours at a concentration of 10 μ M. Different responses to U0126 were identified; the WT case was sensitive to U0126 at a concentration of 10 μ M, whereas the sample harbouring a *MCL-1* gain was resistant to U0126 at the same concentration (Figure 7.3).

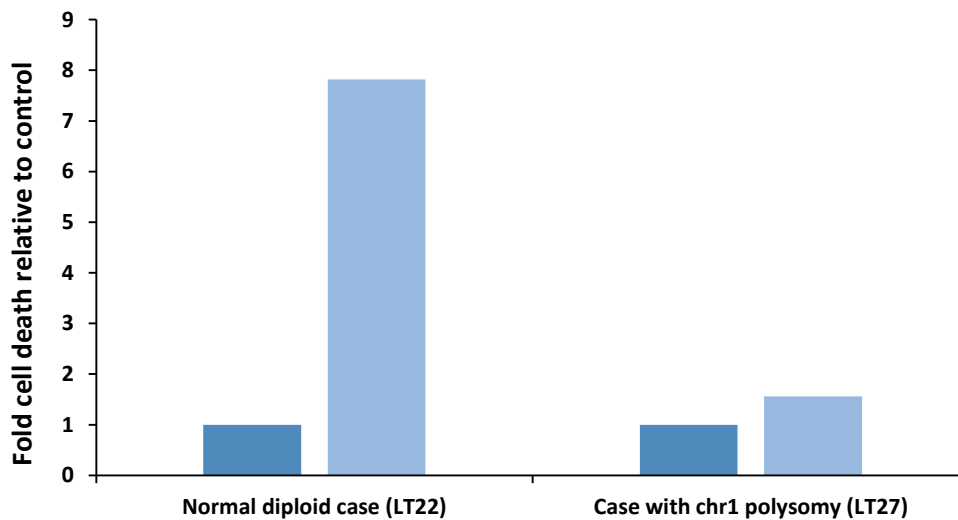


Figure 7.3 Response of NSCLC explants to U0126. The normal diploid case treated with 10 μ M U0126 showed a high rate of cell death compared to the case with increased *MCL-1* copy numbers (Chr1 polysomy).

MCL-1 protein expression and *MCL-1* mRNA levels were also linked to responses of NSCLC explants to cancer therapies. There was a variety of responses of the explants to cancer therapies according to their *MCL-1* protein and *MCL-1* mRNA levels. Some cases, with low levels of both *MCL-1* protein and mRNA, were resistant to cisplatin whilst others were sensitive. Resistance and sensitivity to cisplatin was also seen in certain cases

with high levels of MCL-1 protein (Figure 7.4) and *MCL-1* mRNA (Figure 7.5). A Mann-Whitney test analysis for correlation between MCL-1 protein and drug resistance, and *MCL-1* mRNA and drug resistance, showed no significant correlation (Figure 7.6). Intrinsic cell death was not correlated with levels of MCL-1 protein, low intrinsic cell death was detected in the LT90 and LT33 cases, which have high and low levels of MCL-1, respectively.

Next, there was variation in responses of the explants to cancer therapies according to their p-ERK and p-AKT levels. Some cases with low levels of both p-ERK and p-AKT were resistant to cisplatin, whilst others were sensitive. For example, the LT90 explant had a high level of p-ERK and was sensitive to cisplatin treatment; however, cases with high levels of p-ERK and *KRAS* mutations (LT36 and LT33) were resistant to cisplatin (Figure 7.7). Variations in response to cisplatin in cases with different levels of p-AKT were also observed; the majority of such cases (71%) with high p-AKT levels were resistant to cisplatin. Some cases with low levels of p-AKT, such as LT16, LT33 and LT36, have also shown drug resistance; however, these latter cases were positive for *KRAS* mutation (Figure 7.8). Several cases with p-AKT and p-ERK overexpression were resistant to cisplatin, but there was no significant correlation detected between drug resistance and p-AKT expression or between drug resistance and p-ERK expression (Figure 7.9).

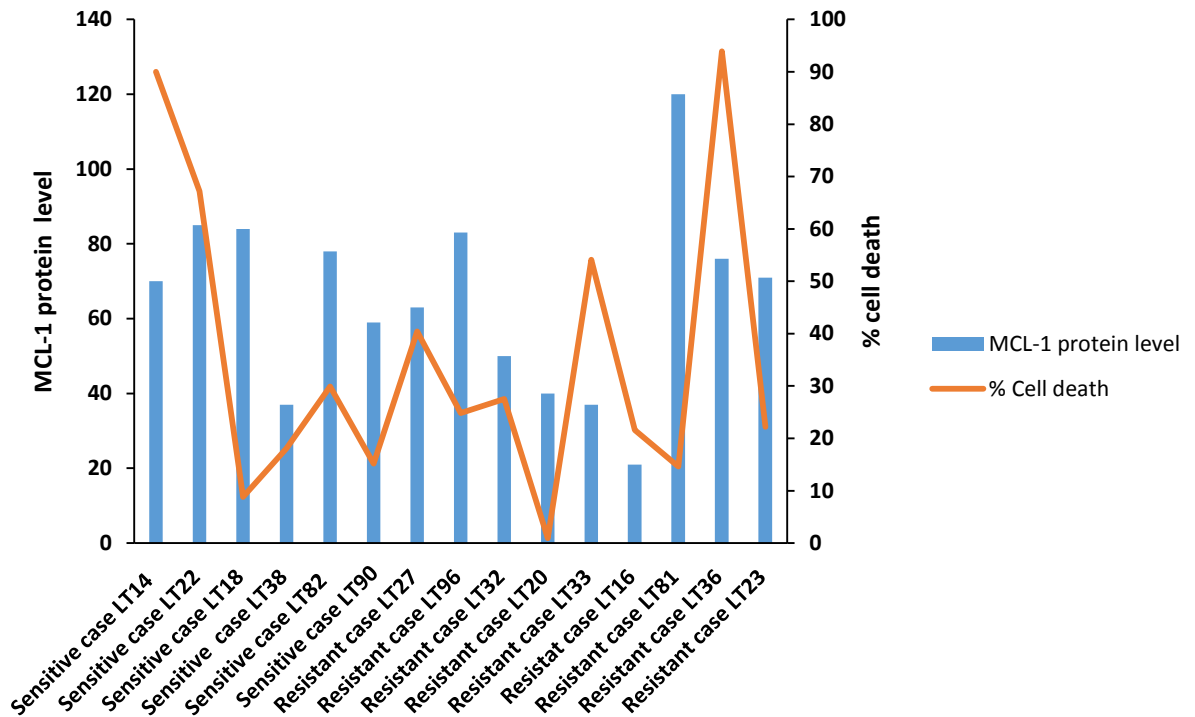


Figure 7.4 Responses of NSCLC explants to cisplatin according to MCL-1 status. LT81 represents a case with high levels of MCL-1 that was resistant to cisplatin. LT22 represents a case with high levels of MCL-1 but was sensitive to cisplatin. MCL-1 protein level is given on the left y-axis and is a score as defined in section 2.2.2.2 (page 56). Cell death is given on the right y-axis and is fold-change versus the untreated control explant.

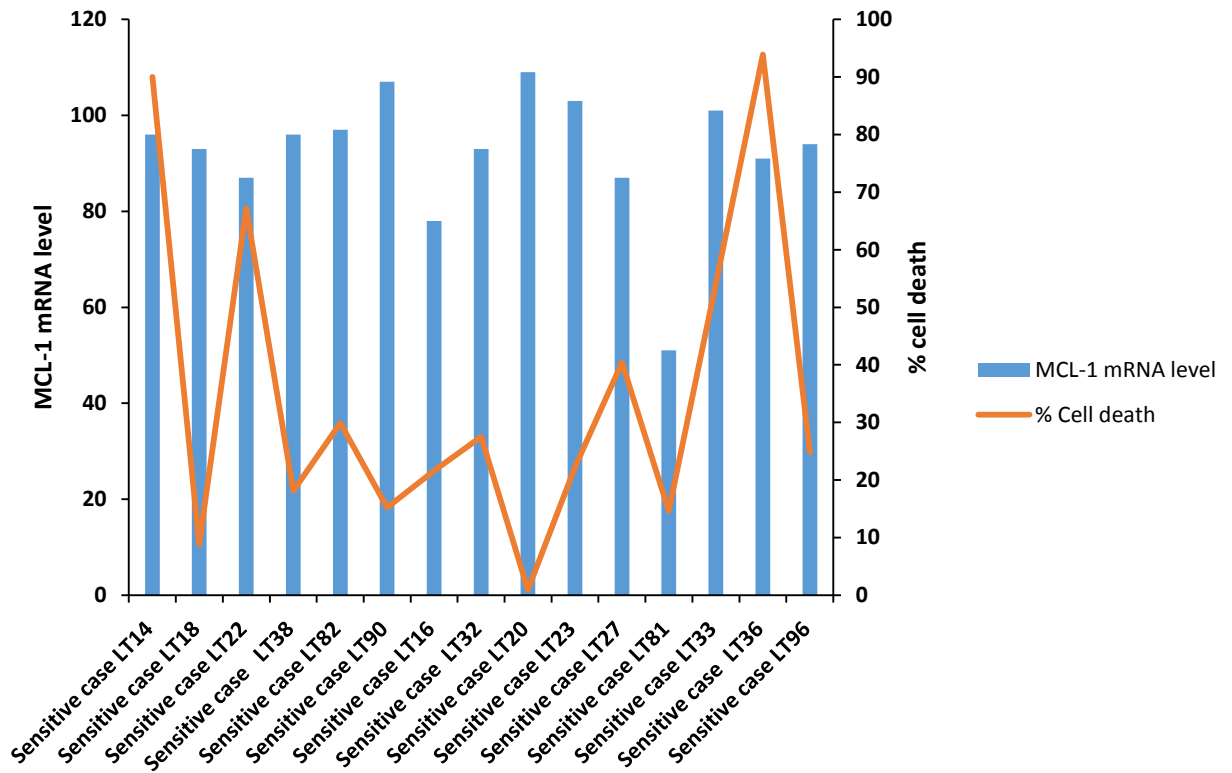


Figure 7.5 Responses of NSCLC explants to cisplatin according to MCL-1 status. LT20 represents a case with high levels of *MCL-1* mRNA that was resistant to cisplatin. LT90 represents a case with high levels of *MCL-1* mRNA but was sensitive to cisplatin. *MCL-1* mRNA level is given on the left y-axis and is a score as defined in section 2.2.2.2 (page 56). Cell death is given on the right y-axis and is fold-change versus the untreated control explant.

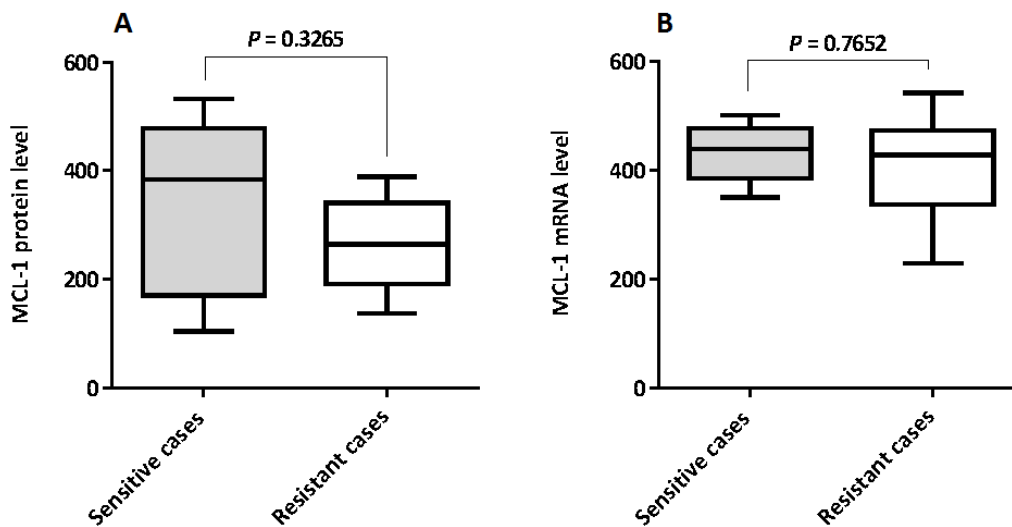


Figure 7.6 MCL-1 and MCL-1 mRNA are not associated to drug resistance in the explant system. No significant correlation was detected between MCL-1 protein

expression and drug resistance ($p = 0.3265$) (A), as well as no significant correlation was identified between *MCL-1* mRNA expression and drug resistance ($p = 0.7652$) (B).

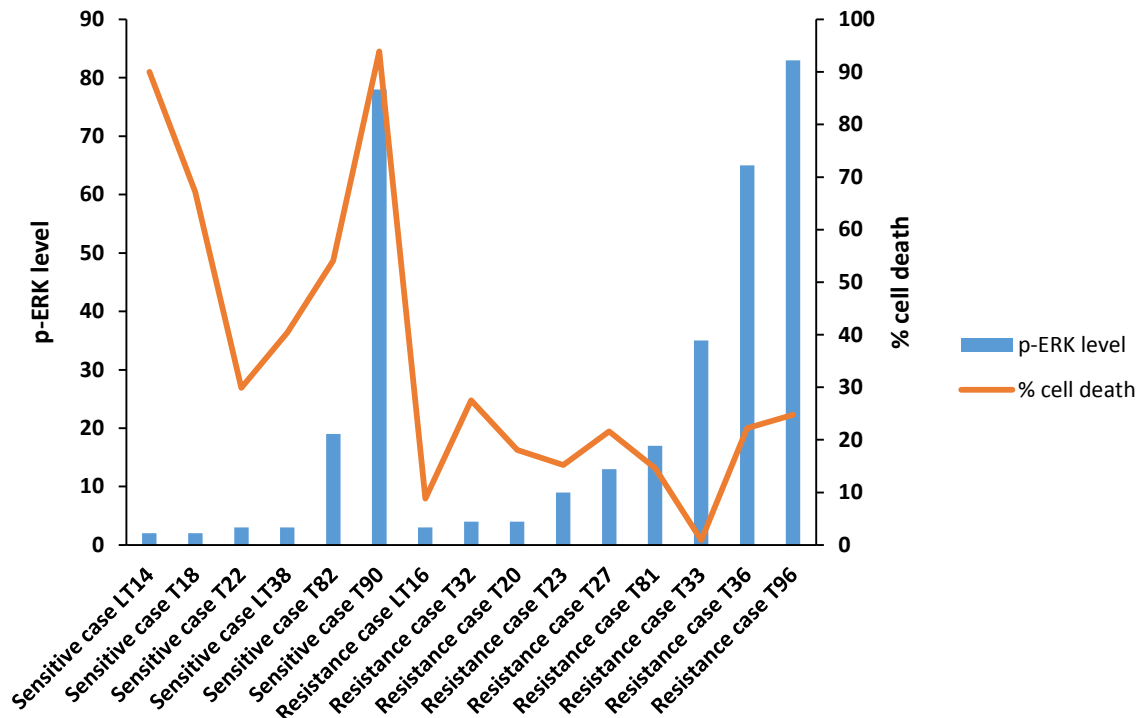


Figure 7.7 Response of NSCLC explants to cisplatin according to p-ERK expression. Cases with p-ERK overexpression with *RAS* oncogene mutations (LT33 and LT36) were resistant to cisplatin, whereas a WT *KRAS* case expressing a high level of p-ERK was sensitive to cisplatin (T90). p-ERK protein level is given on the left y-axis and is a score as defined in section 2.2.2.2 (page 56). Cell death is given on the right y-axis and is fold-change versus the untreated control explant.

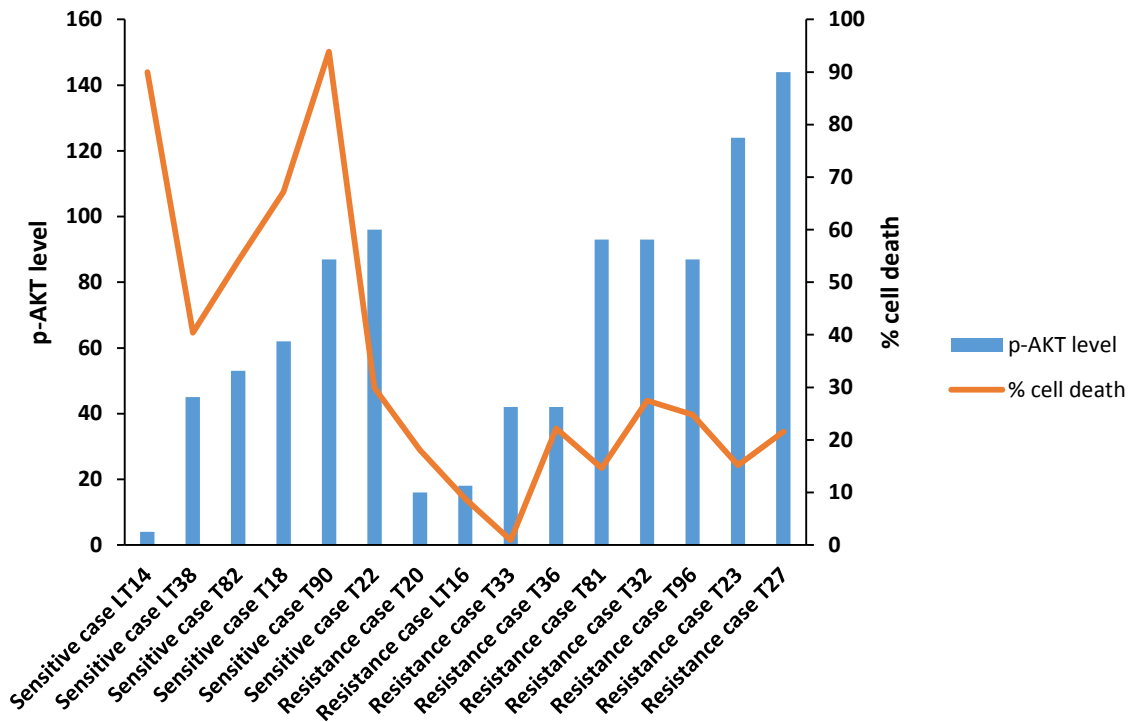


Figure 7.8 Response of NSCLC explants to cisplatin according to p-AKT expression. Cases with p-AKT overexpression were resistant to cisplatin except for, specifically, LT22, and LT90. Cases expressing low p-AKT were sensitive to cisplatin except LT16, LT33 and LT36, which have *KRAS* mutations. p-AKT protein level is given on the left y-axis and is a score as defined in section 2.2.2.2 (page 56). Cell death is given on the right y-axis and is fold-change versus the untreated control explant.

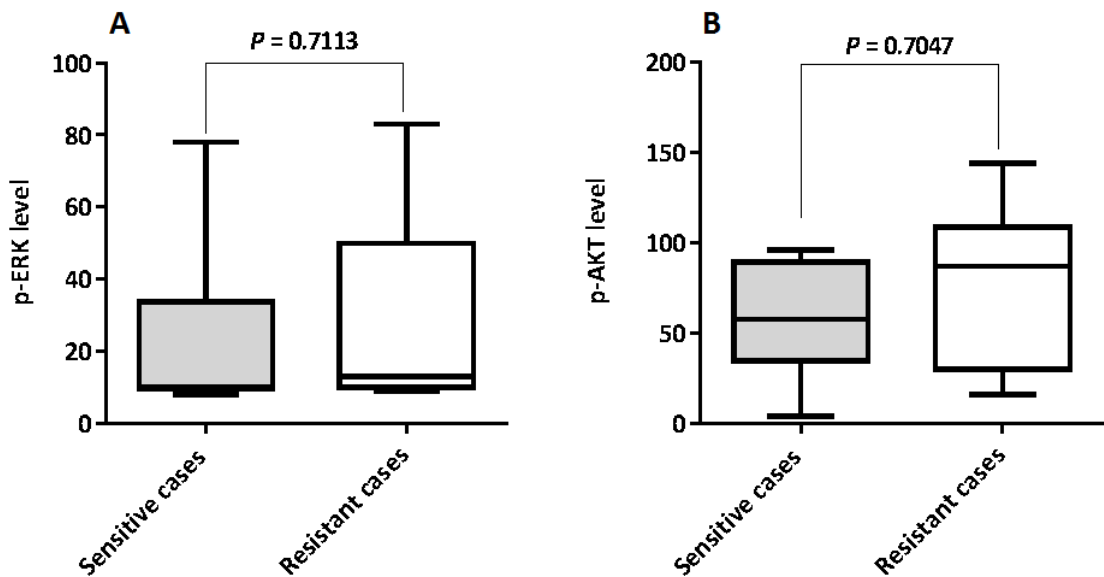


Figure 7.9 p-ERK and p-AKT not correlated to drug resistance. No correlation was detected between p-ERK expression and drug resistance ($p = 0.7113$) (A), or between p-

AKT expression and drug resistance ($p = 0.7047$) (B). p-ERK and p-AKT protein level are given on the left y-axis and is a score as defined in section 2.2.2.2 (page 56).

7.2.4 Evaluation of patient outcome

Patient outcome according to oncogene mutations, copy number changes, *MCL-1* mRNA levels and MCL-1 protein expression was analysed, and the correlation between patient outcome and p-ERK, p-AKT, MCL-1 and *MCL-1* mRNA was analysed using the Mann-Whitney test. Due to limited patient information, this study only analysed a small number of cases ($n = 15$). Patient information is reported in Table 7.1

Table 7.1 Patient characteristics and outcomes

patient	Histology	Mutation	Copy number	p-ERK	p-AKT	MCL-1	<i>MCL-1</i> mRNA	Drug response	Survival
LT14	SCC	-	-	9	7	70	96	Sensitive	Deceased
LT16	ADC	<i>KRAS/PIK3CA</i>	-	8	33	21	78	Resistant	Deceased
LT18	SCC	-	-	9	62	84	93	Sensitive	Deceased
LT20	ADC	-	-	8	16	40	109	Resistant	Deceased
LT22	ADC	-	-	7	96	85	87	Sensitive	Alive
LT23	SCC	-	<i>PIK3CA</i> amp	9	124	71	103	Resistant	Deceased
LT27	ADC	-	<i>PIK3CA</i> amp Chr1 polysomy	13	144	63	87	Resistant	Deceased
LT32	ADC	-	<i>PIK3CA</i> amp Chr1 polysomy	6	41	50	93	Resistant	Deceased
LT33	ADC	<i>KRAS</i>	<i>PIK3CA</i> amp Chr1 polysomy	35	42	37	101	Resistant	Alive
LT36	ADC	<i>KRAS/PIK3CA</i>	Chr1 polysomy	65	42	76	91	Resistant	Deceased
LT38	SCC	-	<i>MCL-1</i> amp	9	45	37	96	Sensitive	Deceased

LT81	ADC	<i>KRAS</i>		17	93	160	51	Resistant	Deceased
LT82	SCC		<i>PIK3CA</i> / <i>SOX2</i> gain	19	53	78	97	Sensitive	Alive
LT90	SCC	<i>PIK3CA</i>		78	87	59	107	Sensitive	Alive
LT96	SCC	-		83	87	110	94	Resistant	Deceased

Patient survival did not correlate with mutation status; poor survival rate was detected in cases with *KRAS* mutations, though patients with the *PIK3CA* mutation showed good outcomes. Decreased survival rate was identified in patients with both *KRAS* and *PIK3CA* mutations. There was a variation between patient outcome and drug resistance, SCC patients with stage 1 of the disease who displayed resistance markers such as *MCL-1* amplification showed sensitivity to cisplatin, but at the same time poor outcomes were seen in such patients. Patients with *SOX2* amplification have been shown to have a better prognosis and have survived for longer; however, patients with *PIK3CA*-amplified tumours have a poorer outcome, with a lower overall survival rate.

Despite sensitivity to cisplatin in patients with no amplification, a generally poor outcome for such patients could be demonstrated. Patients with chromosome 1 polysomy were resistant to cisplatin and showed poor outcomes. Among the cases studied, one patient with a *KRAS* mutation and chromosome 1 polysomy showed strong resistance to cisplatin (Table 7.1). Evaluation of *MCL-1* mRNA and MCL-1 protein in NSCLC patients showed the absence of any obvious correlation between either MCL-1 and *MCL-1* mRNA expression and patient survival ($P \geq 0.05$). Figure 7.10 shows the relationship between MCL-1 status and patient outcome. No strong correlation between p-ERK and patient survival was detected; furthermore, analysis of the link between p-AKT expression and

patient outcome showed no apparent association between patient survival and p-AKT expression level (Figure 7.11).

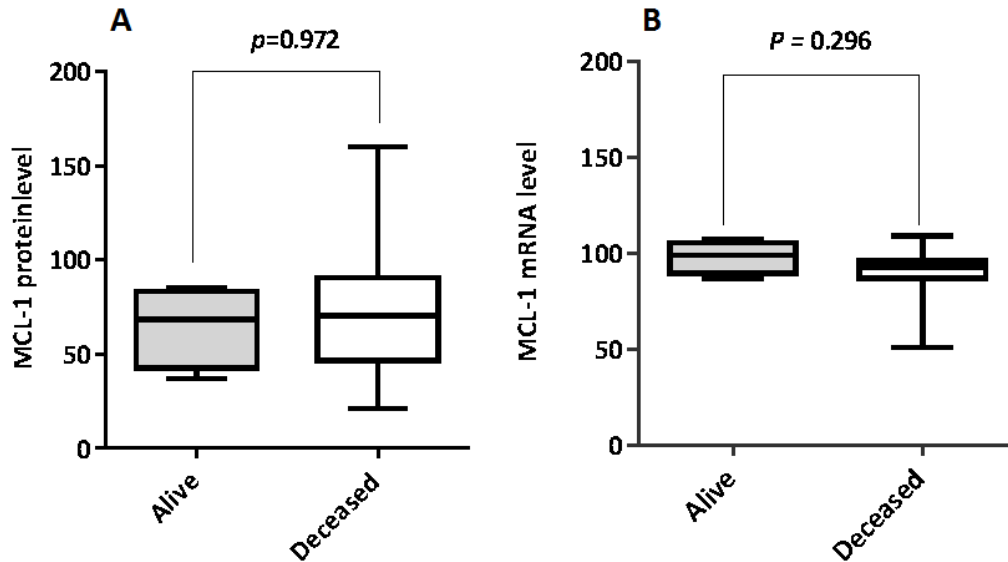


Figure 7.10 Correlation between patient survival and MCL-1 and *MCL-1* mRNA expression. No significant correlation between patient survival and MCL-1 at both the protein and mRNA level was observed ($p > 0.05$) (A and B), at median survival of 27 months.

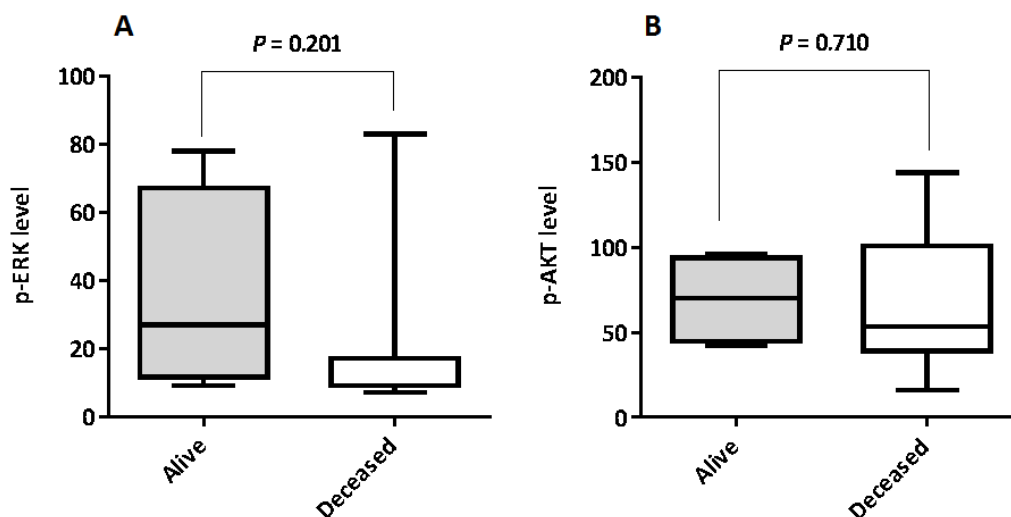


Figure 7.11 Correlation between patient survival and p-ERK and p-AKT expression. (A) The correlation between p-ERK expression and patient outcome was not significant ($p = 0.201$). (B) No correlation between p-AKT and patient outcome was observed ($p = 0.710$).

7.3 Discussion

Ex vivo studies of NSCLC response to cisplatin showed that cases harbouring *KRAS* mutations were resistant to cisplatin, in particular one case harbouring *KRAS* G12C. Furthermore, *KRAS* G12C mutant cell lines have previously been shown to have increased resistance to cisplatin compared to WT *KRAS*, *KRAS* G12D and *KRAS* G12V (Cataldo *et al.*, 2011, Garassino *et al.*, 2011). In this study, NSCLC explants demonstrated that cases with *KRAS* mutations were resistant to cisplatin; however, *KRAS* G12D explants were more resistant to cisplatin compared to *KRAS* G12C. This could be attributed to presence of chromosome 1 polysomy, which has been found to be a resistance factor in this study. There is not enough data in the literature to support our findings, however, studies have found unfavourable outcome in oligodendroglia patients with chromosome 1 polysomy (Wiens *et al.*, 2012). Despite *KRAS* G12D explants being more resistant than *KRAS* G12C, patients with *KRAS* G12D had a better prognosis, which is consistent with previous studies (Nadal *et al.*, 2013).

Cisplatin resistance has been observed in sub-clones of the ovarian cell line OVCAR-3/CDDP with activated PI3K-AKT, compared to the cisplatin-sensitive patient cell line OVCAR-3, which has low PI3K-AKT activity (Lee *et al.*, 2005). However, it is not necessarily the case that all tumours with active PI3K pathways are resistant to cisplatin. In this study, an explant of NSCLC with a *PIK3CA* mutation demonstrated sensitivity to cisplatin compared to *PIK3CA* wild-type cases. In agreement with a previous study (Lee *et al.*, 2005), a single case with *PIK3CA* amplification and p-AKT overexpression showed resistance to cisplatin, indicating that activation of the PI3K pathway is important with regards to drug resistance, though not in all cancer cells. Previous studies have speculated whether *PIK3CA* is correlated with a poor prognosis while other studies have suggested that *PIK3CA* is associated with a good outcome (Dumont *et al.*, 2012). In this study, we

found a better prognosis in a patient with mutant *PIK3CA* sensitive to cisplatin, and conversely a poor outcome was seen in a cisplatin-resistant patient with *PIK3CA* amplification. This observation has also been described in a previous study on gastric cancer (Shi *et al.*, 2012). However, overall survival in patients with *PIK3CA* mutations appeared to be conflicting. This disparity could indicate the presence of other genetic alterations that control tumour behaviour by different regulatory mechanisms.

Besides drug resistance and poor outcome in NSCLC harbouring *PIK3CA* amplification, *SOX2* amplification has also been suggested as a marker for drug resistance accompanied with poor patient outcome (Schröck *et al.*, 2014). By contrast, patients with *SOX2* amplification in this study that showed sensitivity to cisplatin had good outcomes, indicating that gene amplification can be also a marker for a good prognosis. Shimada *et al.* (2012) (Shimada *et al.*, 2012) found no correlation between *SOX2* amplification and patient outcome in oesophageal SCC. In addition, Wilbertz *et al.* (2011) (Wilbertz *et al.*, 2011) have confirmed that NSCLC patients harbouring *SOX2* amplification have better survival rates.

Despite MCL-1 being a resistance factor in lung cancer (Zhou *et al.*, 2013), a SCC case with *MCL-1* amplification demonstrated sensitivity to cisplatin, indicating that MCL-1 may be a resistance marker in ADC but not in SCC. Although the *MCL-1*-amplified SCC case was sensitive to cisplatin, a poor outcome was seen for the patient having SCC with *MCL-1* amplification, consistent with a previous study, which also demonstrated a poor outcome in breast cancer patients expressing high levels of MCL-1 (Ding *et al.*, 2007). Based on our results, gene amplification is not considered a marker for drug resistance and poor prognosis in all patients, but may possibly be a marker for drug resistance and poor outcome, or a marker for drug resistance and good outcome in patients with NSCLC.

Group analysis using the Mann-Whitney test showed the absence of any correlation between p-ERK and both drug resistance and patient outcome, and that p-AKT overexpression was not associated with drug resistance and patient outcome; however, some individual cases with both p-ERK and p-AKT expression were resistant to chemotherapy and showed poor outcomes, although this study cohort was small a previous study in the literature has also demonstrated the absence of any correlation between high levels of p-ERK chemoresistance and patient survival, and also showed that high p-AKT expression was not associated with chemoresistance and patient survival in rectal cancer (Davies *et al.*, 2011). Consistently, Wang *et al.* (2015) (Wang *et al.*, 2015) have also demonstrated that there is no correlation between patient survival and expression of p-AKT or p-ERK in oesophageal cancer. Although the findings of Davies *et al.* (2011) (Davies *et al.*, 2011) support our finding that patient outcome is not associated with levels of p-ERK or p-AKT, further studies in a larger cohort are required for more definite confirmation.

7.4 Conclusion

Cisplatin resistance was clearly observed in NSCLC cases with *KRAS* mutations and Chromosome 1 polysomy. Not all cases with *PIK3CA* mutations were resistant to cisplatin, and cisplatin resistance was observed in patients harbouring *PIK3CA* amplification but not *SOX2* amplification. SCC cases are sensitive to cisplatin, even those with *MCL-1* amplification. There is no apparent relationship between cisplatin resistance and protein expressions (p-ERK, p-AKT and MCL-1); however, further studies are required in this regard. A good outcome was observed in patients with *SOX2* amplification, in contrast to the poor outcome that was observed in patients with *PIK3CA/MCL-1* amplification, *KRAS* mutation and Chr1 polysomy. Both p-ERK and p-

AKT expression is not associated with patient outcomes, though future study using a larger population is required.

Chapter 8. Discussion and future work

8.1 Discussion

In this study, *KRAS*, *PIK3CA*, *BRAF* and *EGFR* mutation were analysed in NSCLC using the PNA clamping technique, which is a sensitive method of mutation analysis (Beau-Faller *et al.*, 2009). We found that *KRAS* and *EGFR* mutations were common in ADC, while *PIK3CA* was associated with SCC, and the incidence of both histological subtypes was correlated with tobacco smoke. Previous studies have also found a strong correlation between ADC and both *KRAS* and *EGFR* mutations, but not with SCC (El-Telbany and Ma, 2012). However, *PIK3CA* mutation is commonly associated with SCC compared to ADC, and tobacco carcinogens are the main risk factor for development of both SCC and ADC (Scheffler *et al.*, 2015, Yang *et al.*, 2002). Analysis of mutational statuses in NSCLC patients and identification of mechanisms of drug resistance via these oncogenes may give an insight into overcoming drug resistance and improving patient outcome.

Copy number analysis was also included in this study to give a broad insight into mechanisms of drug resistance in NSCLC. A duplex ratio test was used to analyse *MCL-1*, *SOX2* and *PIK3CA* amplification, focussing on *MCL-1* which has been described as a resistance factor in many human cancers (Stewart *et al.*, 2010). As *MCL-1* is a critical for survival and is a marker for drug resistance (Pei *et al.*, 2014), *MCL-1* copy number change was analysed in terms of gain, amplification and chromosome 1 polysomy. *MCL-1* protein and *MCL-1* mRNA levels were measured to find whether *MCL-1* was strongly correlated to drug resistance in NSCLC or otherwise. In this study, *PIK3CA*, *SOX2* and *MCL-1* amplification was identified in SCC. Previous studies have also demonstrated the frequency of *PIK3CA* and *SOX2* in SCC (Toschi *et al.*, 2014). Chen *et al.* (2014) reported that *MCL-1* is amplified in SCC, but Beroukhim *et al.* (2010) identified *MCL-1* amplification in ADC (Beroukhim *et al.*, 2010, Chen *et al.*, 2014). Interestingly, in this

study, *MCL-1* amplification was only linked to SCC subtype; however, *MCL-1* gain and chromosome 1 polysomy were linked to ADC.

Analysis of p-ERK and p-AKT was important in order to evaluate involvement of these proteins with regards to drug resistance, even in cases where *KRAS* mutations and *PIK3CA* mutations were absent, as these activated proteins are involved in cell proliferation and survival (Liu *et al.*, 2009, Widmann *et al.*, 1999), *MCL-1* regulation (Faber *et al.*, 2009, McKee *et al.*, 2013) and drug resistance (Abrams *et al.*, 2010). Another study has also reported the critical role of *MCL-1* among the BCL-2 family in inducing drug resistance in several types of human cancers (Pan *et al.*, 2015).

The *MCL-1* transcriptional pathway JAK/STAT (Gouill *et al.*, 2004) was studied here to evaluate the pivotal role of this pathway in *MCL-1* regulation in NSCLC. Our findings indicated that the JAK/STAT5 signalling pathway, rather than the PI3K pathway or MAPK pathway, is the most significant regulatory pathway for *MCL-1* transcription.

Cisplatin-based combination treatment has been used for decades as a first-line treatment for NSCLC (Andriani *et al.*, 2006). In this study, cisplatin responses were variable between NSCLC cell lines, in agreement with the results of a previous study in the literature (Barr *et al.*, 2013). Furthermore, *in vitro* analysis performed in this study showed that ADC subtype cell lines were more resistant to cisplatin than SCC cell lines. Previous studies have reported acquired resistance to cisplatin in *PIK3CA*-amplified cancer (Jiang, 2008); furthermore, *in vitro* analysis performed in this study showed that ADC subtype cell lines were more resistant to cisplatin than SCC cell lines. Previous studies have reported acquired resistance to cisplatin in *PIK3CA*-amplified cancer (Jiang, 2008); however, sensitivity to cisplatin was observed in the SCC cell line RERF-LC-Sq1 harbouring *PIK3CA* amplification. Cell lines with *MCL-1* amplification and *MCL-1* gain

were more resistant to cisplatin than non-amplified cell lines, even those harbouring *KRAS* mutations, indicating that MCL-1 is involved in a mechanism of cisplatin resistance in ADC cell lines. Treatment of NSCLC cell lines with AZD8055, U0126, SH-4-54, niclosamide and STA9090 showed that the STATs inhibitor SH-4-54 was the most potent agent that could be used to target MCL-1 in order to overcome MCL-1-induced drug resistance in NSCLC at a concentration of $7 \pm 1.5 \mu\text{M}$. Treatment of normal human foetal astrocytes at a concentration of $5\mu\text{M}$ has shown a mild toxicity (Haftchenary *et al.*, 2013), and that it is consequently might be possible to treat patients using $7 \pm 1.5 \mu\text{M}$ SH-4-54. Based on our findings, SH-4-54 could be one of the most effective targeted therapies used to target *MCL-1*-amplified cancer cells.

Previous studies have reported that combined therapy is more toxic than monotherapy, and a patient's treatment regime is dependent upon their status. For example, combined therapy may benefit patients with a high tumour burden and heterogeneity, rather than a patient with a low tumour burden or heterogeneity (Miles *et al.*, 2002). Unfortunately, in this study, no synergistic effect of the inhibitors with cisplatin was observed as unexpectedly increased cell viability was seen in combined therapy compared to single treatment, thus single agent treatment with SH-4-54 – but not AZD8055 and U0126, or niclosamide and STA9090 – could be a more effective therapy for NSCLC.

In vivo studies of NSCLC response to cisplatin showed that cases harbouring *KRAS* oncogene mutations are resistant to cisplatin (Caiola *et al.*, 2015). In this study, NSCLC *ex vivo* explants demonstrated that cases with *KRAS* mutation were resistant to cisplatin, and that chromosome 1 polysomy was also found as a resistance factor to cisplatin in NSCLC.

PIK3CA mutation has been suggested as a resistance marker in cancer cells (Lee *et al.*, 2005). In this study, not all tumours with active PI3K pathways were resistance to cisplatin; an explant of NSCLC with *PIK3CA* mutation demonstrated sensitivity to cisplatin. However, a *PIK3CA*-amplified case showed resistance to cisplatin, indicating that whilst activation of the PI3K pathway is an important mechanism in drug resistance, this is not the case for in all cancer cells. Previous studies have also indicated that *PIK3CA* is correlated with a poor prognosis, while other studies have suggested the opposite (Dumont *et al.*, 2012). In this study, a good outcome was observed in a patient with *PIK3CA* mutation, but another patient with *PIK3CA* amplification showed a poor outcome.

SOX2 amplification has been suggested as a marker for drug resistance linked with poor patient outcome (Schröck *et al.*, 2014); however, in this study, sensitivity to chemotherapy was observed in *SOX2*-amplified patients. Similarly, Shimada *et al.* (2012) and Wilbertz *et al.* (2011) (Shimada *et al.*, 2012, Wilbertz *et al.*, 2011) also failed to find any correlation between *SOX2* amplification and patient outcome. Poor outcome in patients with *MCL-1* copy number change was identified in this study. A previous study has demonstrated poor outcome in patients expressing high levels of MCL-1 protein (Ding *et al.*, 2007). Despite *MCL-1* copy number change being associated with drug resistance and poor outcome, in this study levels of both MCL-1 protein and *MCL-1* mRNA could not be correlated with patient outcome, though the reasons for this are unknown. Previous studies have demonstrated the absence of any correlation between high levels of p-ERK, chemoresistance and patient survival; similarly, high p-AKT expression could also not be associated with chemoresistance and patient survival in rectal cancer (Davies *et al.*, 2011). Consistently, Wang *et al.* (2015) have also demonstrated the absence of any correlation between patient survival and expression of

p-AKT and p-ERK in oesophageal cancer. Our results have also shown an absence of any significant correlation between p-ERK and p-AKT with both drug resistance and patient outcome, though individual cases with high p-ERK and p-AKT have showed drug resistance and poor outcome in NSCLC patients. Although previous studies have agreed with our findings that patient outcome was not associated with levels of p-AKT or p-ERK, a larger cohort is required to confirm the negative association between protein overexpression and patient outcome.

For studies of drug resistance in NSCLC, other factors, such as evolution of genotypes in cancer and changing resistance, should be considered. Drug resistance in cancer via evolutionary processes was observed, tumour heterogeneity due to evolution and production of different sub-clones may result in resistance to single agent treatments used to target mutations of the parent cell. This is not an indication of treatment failure, as cell free DNA analysis may resolve temporal and spatial dynamics of tumour evolution (Swanton, 2014). Therefore, analysis of a broad spectrum of oncogenes in cancer cells and finding related drug-resistant oncogenes, as well as analysis of the integration of different oncogenes, might be required to further our understanding of mechanisms of drugs resistance, and thus to find the optimum treatment for NSCLC.

8.2 Conclusion

This study has shown that important oncogenic drivers such as *KRAS* and *PIK3CA* are common in NSCLC. Furthermore, copy number alteration in *MCL-1* can be an important driver of resistance to chemotherapy, with the JAK/STAT pathway being a key regulator of *MCL-1* transcription. As a result, MCL-1 inhibition via the JAK/STAT pathway could be an important mechanism for overcoming drug resistance in NSCLC, and further study in a larger cohort is warranted.

8.3 Future directions

MCL-1 has been shown to have a critical role in drug resistance in several cancer types but not in NSCLC, therefore it is very important to analyse MCL-1 expression in NSCLC using Western blotting to confirm that immunohistochemistry assessment is reliable and was accurate for MCL-1 expression analysis.

Beside MCL-1 protein analyses, analysis of somatic mutations and copy number alterations in *MCL-1* is also required to give a broad insight about the role of MCL-1-induced chemo-resistance in NSCLC. Developing treatment strategies such as combinations of inhibitors or targeted therapy followed by chemotherapy, manipulation of treatment types, dose and treatment times in a much larger cohort is also required

Here, high sensitivity to the anti-STAT (SH-5-54) was observed in *MCL-1* amplified cell lines, indicating that drug resistance is induced in a STAT dependent manner. To support this hypothesis, creation of STAT overexpressing cell lines via transient transfection followed by treatment with anti-STATs is required. Theoretically, low sensitivity of the transfected cell to the anti-STAT will indicate the importance of the STAT signalling pathway in drug resistance through MCL-1 upregulation. Moreover, if knockdown of *MCL-1* using siRNA or targeting MCL-1 protein itself using small molecule MCL-1 inhibitors such as S63845 may increase toxicity of the drug, indicating the importance of MCL-1.

Finally, future studies could also develop next generation sequencing strategies for analysis of known oncogenic drivers, as well as amplification in *MCL-1* in cell free DNA, which is currently under intense investigation as a biomarker for real-time analysis and monitoring of many mutational events and acquisition of resistance to chemotherapy,

thereby paving the way for selection of the most appropriate treatment regimens once aberrant event occur.

Appendices

Table 0.1 Summary table of all cases

Tumour code	Histology	Gender	age	Smoking history	TNM Staging	Mutations	Copy number
LT1	ADC+SCC	M	62	smoker	PT1b.PN0,PMX		
LT2	SCC	F	73	ex-smoker	pT2, pN0, pMx, R0		<i>PIK3CA</i> amp
LT3	SCLC+LCC	M	45	smoker	pT2, pN0, pMx, R0		<i>SOX2</i> amp
LT4	ADC	F	66	ex-smoker	pT4, pN1(mi), pM1, Rx	<i>KRAS</i> G35>T	<i>PIK3CA</i> amp
LT5	SCC	M	62	smoker	pT2, pN0, pMx, R0		<i>MCL-1</i> amp
LT6	SCC	M	81	ex-smoker	Debatable. At least pT2a, possibly pT3, pN2, R2		
LT7	SCC	F	84	non-smoker	pT2a, pN0, pMx, R0	<i>PIK3CA</i> 1624	<i>MCL-1</i> / <i>SOX2</i> amp
LT8	SCC	M	52	ex-smoker 60 pack-years	pT3, pN1, pMx, R0		<i>MCL-1</i> amp
LT9	ADC	F	65	ex-smoker		<i>KRAS</i> G34>T	<i>MCL-1</i> amp
LT10	ADC	M	69	ex-smoker	pT3, pN0, pMx, R1		
LT12	SCC	M	74	Unknown	pT2a, pN0, pMx, R0		
LT13	ADC	M	69	smoker	pT3, pN0, pMx, R1		<i>PIK3CA</i> / <i>SOX2</i> amp
LT14	SCC	F	65	ex-smoker	pT1a, pN0, R0		
LT15	AC	M	69	ex-smoker			
LT16	ADC	F	69	ex-smoker	pT3, pN1, R0	<i>KRAS</i> G35>C <i>PIK3CA</i> 1633	
LTT17	SCC	M	67	smoker	pT2b, pN0, pMX, R0		<i>MCL-1</i> amp
LT18	SCC	M	84	ex-smoker	pT1b, pN0, R0		
LT19	ADC	M	72	ex-smoker	Larger: pT2a pN0 pMX RO Smaller: pT1a, pN0, pMx, RO		
LT20	ADC	F	77	Unknown	First pT3 pN0 pMx Second PT1a, pN0, pMx R2		
LT21	SCLC+ADC	M	82	ex-smoker	pT2b, pN1, pM1a	<i>PIK3CA</i> 1633	
LT22	ADC	M	65	ex-smoker	pT2a, pN0, R0		
LT23	SCC	M	81	ex-smoker	pT3,pN1,R0		<i>PIK3CA</i> amp
LT24	SCC	M	73	smoker	pT2b,pN2, pMx, R0		<i>PIK3CA</i> amp
LT25	SCC	M	74	Unknown	pT2b,pN0,pMX,R0		<i>PIK3CA</i> / <i>SOX2</i> gain
LT26	ADC	F	59	smoker	pT2b,pN0,pMX,R0		
LT27	ADC	M	60	never smoked	pT3, pN2, pMX,R0		<i>PIK3CA</i> amp Chr1 polysomy
LT28	SCC	F	83	ex-smoker	pT2b, pN1, pMX,R0		<i>PIK3CA</i> / <i>SOX2</i> amp

LT29	ADC	M	59	ex-smoker			<i>PIK3CA</i> amp Chr1 polysomy
LT30	ADC	M	79	ex-smoker	pT2a,pN2,pMX,R0		<i>PIK3CA</i> / <i>SOX2</i> amp
LT32	ADC	M	55	smoker	pT2a,pN0,pMX,R0		<i>PIK3CA</i> amp Chr1 polysomy
LT33	ADC	F	79	ex-smoker	pT3, pN0, pMx, R0	<i>KRAS</i> G35>A	<i>PIK3CA</i> amp Chr1 polysomy
LT35	SCC	M	77	smoker	pT2a,pN1,R0	<i>PIK3CA</i> 1633	
LT36	ADC	M	61	Unknown	pT2,pN0,pMX,R0	<i>KRAS</i> G34>T <i>PIK3CA</i> 3140	Chr1 polysomy
LT37	ADC	F	64	ex-smoker	pT2a, pN0,pMX,R0		
LT38	SCC	M	76	ex-smoker	pT2b,pN0,pMX,R0		<i>MCL-1</i> amp
LT39	LCC	F	65	Unknown	ypT4,ypN1		
LT40	LCC	M	62	ex-smoker	pT2a,pN0,pMX,R0	<i>KRAS</i> G35>A	
LT41	ADC	F	50	smoker	pT3,pN2,pMX,R0	<i>EGFR</i> L585R	
LT42	SCC	F	73	ex-smoker	pT2a,pN1,pMX,R0		<i>PIK3CA</i> amp
LT43	SCC	M	76	Unknown	pT2b,pN1,pMX,R0		
LT44	ADC	M	75	Unknown	pT2a,pN2,pMX,R0		<i>PIK3CA</i> amp
LT45	ADC	F	56	smoker	pT2a,pN2,pMX,R0		
LT46	SCC	F	65	Unknown		<i>PIK3CA</i> 3140	<i>PIK3CA</i> / <i>SOX2</i> gain
LT48	ADC	F	78	never smoked	pT2b, pN0,pMX, R0		
LT49	ADC	M	76	ex-smoker	pT2a, pN0,pMX, R0	<i>EGFR</i> L585R	
LT50	ADC+SCC	F	77	smoker	pT2a, pNx,pMX, R0		
LT51	ADC	F	70	smoker	pT2b, pN1,pMX, Rx	<i>KRAS</i> G34>T	
LT52	SCC	M	74	ex-smoker	pT2a,pN1,pM1a,R0	<i>PIK3CA</i> 1624	<i>PIK3CA</i> amp
LT53	SCC	F	63	Unknown	pT1b,pN0,pMX,PL0		<i>PIK3CA</i> amp
LT54	SCC	F	77	Unknown	pT1b, pN0,pMX, R0		<i>PIK3CA</i> amp
LT55	SCC	F	73	Unknown	pT2a,PN1,pMX,R1	<i>PIK3CA</i> 1624	<i>PIK3CA</i> amp
LT56	ADC	M	84	Unknown	pT1b, pN0,pMX, R0		<i>PIK3CA</i> amp
LT57	ADC	F	67	Unknown	pT3,pN2,pMX,R0	<i>KRAS</i> G34T	
LT58	ADC	F	59	Unknown	pT2a,pN2,pMX,pL0, R0	<i>EGFR</i> L585R	
LT59	ADC	F	72	Unknown	pT2a,pN0,pMX,R0	<i>KRAS</i> G35T	<i>SOX2</i> amp
LT60	ADC+SCC	M	76	Unknown	R0		
LT61	SCC	M	80	Unknown	pT2a,pN0,pMX,R0		<i>PIK3CA</i> / <i>SOX2</i> gain
LT63	SCC	F	72	Unknown	pT3,pN0,pMX,R0		<i>SOX2</i> amp
LT64	ADC	F	70	Unknown	pT2b,pN0,,R0	<i>EGFR</i> L585R	<i>PIK3CA</i> amp
LT65	SCC	M	72	Unknown	ypT2a,ypNX,ypMX		<i>PIK3CA</i> / <i>SOX2</i> amp
LT66	SCC	M	86	Unknown	pT2b,pNX,pMX,R0		<i>PIK3CA</i> / <i>SOX2</i> amp

							Chr1 polysomy
LT67	SCC	F	71	Unknown	pT1b,pN1,R0		<i>SOX2</i> amp
LT68	ADC	F	68	Unknown	pT3,R0(parietal pleura) and pT1b,R0(acinar)	<i>KRAS</i> G35A	
LT70	SCC	F	58	current smoker	pT1a,pN0,pMX,RX		<i>PIK3CA</i> amp
LT71	SCC	M	68	Unknown	pT2a,pN1,pMX,pL0, R0(LUL) and pT2apN0,pMX,pL1, R0		<i>PIK3CA</i> / <i>SOX2</i> amp
LT73	ADC	F	68	Unknown	pT2a,pN0, R0	<i>KRAS</i> G35C	<i>SOX2</i> amp
LT74	SCC	M	83	Unknown	pT2a,pN,R0		<i>PIK3CA</i> / <i>SOX2</i> amp
LT75	ADC	F	74	Unknown	pT2a,nN1,R0	<i>KRAS</i> G34T	
LT76	SCC	F	63	Unknown	pT3,pN1,pMX,R0		<i>PIK3CA</i> / <i>SOX2</i> amp
LT77	ADC	F	74	Unknown	pT2a,pN0,R0	<i>KRAS</i> G35A	
LT78	ADC	F	39	Unknown	pT3,pN0,pMX,R0		Chr1 polysomy
LT80	ADC	F	33	Unknown	pT3,pN0,pMX,R0		
LT81	ADC	M	70	ex-smoker	pT2(pL1)b,pN1,pMX	<i>KRAS</i> G34T	
LT82	SCC	F	75	Unknown	R0		<i>PIK3CA</i> / <i>SOX2</i> gain
LT83	SCC	M	78	ex-smoker	pT2b,pN2,pMX,pL0, R0		
LT84	ADC	M	71	smoker	pT2a,pN0,pMX,R0		
LT85	ADC	F	71	smoker	pT3,pN0,R0		
LT87	atypical	F	85	Unknown	pT2a,PL1,PN0,PMX, R0		
LT88	ADC	F	75	Unknown	pT2,PL1,PN2b,PMX, R0		
LT89	SCC	M	78	Unknown	pT1b,,PN0,PL0,R0		<i>SOX2</i> amp
LT90	SCC	F	62	Unknown	pT2b,,PN1,PL1,R1	<i>PIK3CA</i> 1624	
LT91	SCC +SCLC	M	78	Unknown	pT2a,,PN1,PMX,R0		
LT92	ADC	F	71	Unknown	pT3,,N0,,R0	<i>KRAS</i> G35C	
LT93	ADC	M	68	Unknown	pT3,,PN1,,R0		<i>SOX2</i> amp
LT94	SCC	M	67	Unknown	pT2b,(PL1)PN2,PM X,R0		
LT95	SCC	M	70	Unknown	pT2b,(PL0)PN0,,R0		
LT96	SCC	M	73	Unknown	pT3,(PL1)PN0,,R0		

Table 0.2 proteins and *MCL-1* mRNA expression levels

Tumour code	p-ERK level	MCL-1 level	p-AKT level	<i>MCL-1</i> mRNA level	Tumour code	p-ERK level	MCL-1 level	p-AKT level	<i>MCL-1</i> mRNA level
LT1	3	74	74	56	LT49	33	43	61	207
LT2	132	48	20	103	LT50	5	73	55	119
LT3	7	30	38	72	LT51	28	34	31	95
LT4	85	95	21	88	LT52	23	52	30	101
LT5	34	67	138	188	LT53	27	50	115	88
LT6	7	108	18	96	LT54	9	31	83	104
LT7	20	39	16	112	LT55	22	43	103	87
LT8	8	23	13	40	LT56	11	112	153	95
LT9	91	24	49	186	LT57	147	150	72	70
LT10	41	47	30	113	LT58	87	157	74	29
LT12	8	32	29	113	LT59	90	156	52	96
TL13	11	25	48	96	LT60	1	69	29	44
LT14	9	70	7	96	LT61	22	144	69	82
LT15	9	28	35	59	LT63	9	105	37	64
LT16	5	21	33	78	LT64	57	86	64	67
LT17	12	31	98	179	LT65	15	103	85	49
LT18	10	84	62	93	LT66	20	200	202	120
LT19	8	97	29	98	LT67	18	64	48	69
LT20	10	40	16	109	LT68	37	63	23	43
LT21	46	118	125	111	LT70	18	107	65	77
LT22	9	85	96	87	LT71	12	94	65	50
LT23	9	71	124	103	LT73	14	37	37	44
LT24	11	104	104	75	LT74	12	63	30	46
LT25	46	24	49	75	LT75	17	78	38	37
LT26	10	19	38	97	LT76	24	95	93	94
LT27	13	63	144	87	LT77	38	114	63	39
LT28	8	29	40	87	LT78	14	76*	46	54
LT29	7	67	51	79	LT80	54	172	96	51
LT30	48	39	65	179	LT81	17	160	93	51
LT32	10	50	41	93	LT82	19	78	53	97
LT33	35	37	42	101	LT83	12	124	38	98
LT35	42	59	193	83	LT84	3	5	10	17
LT36	65	76	42	91	LT85	14	53	20	48
LT37	18	55	67	137	LT87	66	185	118	98
LT38	8	37	45	96	LT88	95	162	123	122
LT39	24	24	97	87	LT89	128	71	99	99
LT40	59	54	134	82	LT90	78	59	87	107
LT41	93	21	139	112	LT91	67	218	90	107
LT42	58	21	133	74	LT92	156	129	123	104
LT43	6	49	30	114	LT93	4	88	82	118
LT44	37	40	46	98	LT94	7	81	81	89
LT45	2	19	45	81	LT95	6	94	101	93
LT46	26	31	101	98	LT96	83	110	87	94
LT48	34	45	47	187					

References

- ABRAMS, S. L., STEELMAN, L. S., SHELTON, J. G., WONG, E. W., CHAPPELL, W. H., BÄSECKE, J., STIVALA, F., DONIA, M., NICOLETTI, F. & LIBRA, M. 2010. The Raf/MEK/ERK pathway can govern drug resistance, apoptosis and sensitivity to targeted therapy. *Cell Cycle*, 9, 1781-1791.
- ACQUAVIVA, J., SMITH, D. L., SANG, J., FRIEDLAND, J. C., HE, S., SEQUEIRA, M., ZHANG, C., WADA, Y. & PROIA, D. A. 2012. Targeting KRAS-mutant non-small cell lung cancer with the Hsp90 inhibitor ganetespib. *Molecular cancer therapeutics*, 11, 2633-2643.
- ALBANELL, J., CODONY-SERVAT, J., ROJO, F., DEL CAMPO, J. M., SAULEDA, S., ANIDO, J., RASPALL, G., GIRALT, J., ROSELLÓ, J. & NICHOLSON, R. I. 2001. Activated extracellular signal-regulated kinases: association with epidermal growth factor receptor/transforming growth factor α expression in head and neck squamous carcinoma and inhibition by anti-epidermal growth factor receptor treatments. *Cancer research*, 61, 6500-6510.
- ALLEN, T. D., ZHU, C. Q., JONES, K. D., YANAGAWA, N., TSAO, M.-S. & BISHOP, J. M. 2011. Interaction between MYC and MCL1 in the genesis and outcome of non-small-cell lung cancer. *Cancer research*, 71, 2212-2221.
- ANDRIANI, F., PEREGO, P., CARENINI, N., SOZZI, G. & ROZ, L. 2006. Increased sensitivity to cisplatin in non-small cell lung cancer cell lines after FHIT gene transfer. *Neoplasia*, 8, 9-17.
- ATHEY, V. L., TOD, A. M., SUCKLING, R. & ROGERS, T. K. 2010. Diagnosis of lung cancer—improving survival rates. *European oncology*, 6, 26-30.
- BABA, Y., NOSHO, K., SHIMA, K., HAYASHI, M., MEYERHARDT, J. A., CHAN, A. T., GIOVANNUCCI, E., FUCHS, C. S. & OGINO, S. 2011. Phosphorylated AKT expression is associated with PIK3CA mutation, low stage, and favorable outcome in 717 colorectal cancers. *Cancer*, 117, 1399-1408.
- BAGNARDI, V., RANDI, G., LUBIN, J., CONSONNI, D., LAM, T. K., SUBAR, A. F., GOLDSTEIN, A. M., WACHOLDER, S., BERGEN, A. W. & TUCKER, M. A. 2009. Alcohol consumption and lung cancer risk in the Environment and Genetics in Lung Cancer Etiology (EAGLE) study. *American journal of epidemiology*, kwp332.
- BAIN, C., FESKANICH, D., SPEIZER, F. E., THUN, M., HERTZMARK, E., ROSNER, B. A. & COLDITZ, G. A. 2004. Lung cancer rates in men and women with comparable histories of smoking. *Journal of the National Cancer Institute*, 96, 826-834.
- BALAKRISHNAN, K., BURGER, J. A., FU, M., DOIFODE, T., WIERDA, W. G. & GANDHI, V. 2014. Regulation of mcl-1 expression in context to bone marrow stromal microenvironment in chronic lymphocytic leukemia. *Neoplasia*, 16, 1036-1046.
- BALKO, J. M., GILTNANE, J. M., WANG, K., SCHWARZ, L. J., YOUNG, C. D., COOK, R. S., OWENS, P., SANDERS, M. E., KUBA, M. G. & SÁNCHEZ, V. 2014. Molecular profiling of the residual disease of triple-negative breast cancers after neoadjuvant chemotherapy identifies actionable therapeutic targets. *Cancer discovery*, 4, 232-245.
- BARR, M. P., GRAY, S. G., HOFFMANN, A. C., HILGER, R. A., THOMALE, J., O'FLAHERTY, J. D., FENNELL, D. A., RICHARD, D., O'LEARY, J.

- J. & O'BYRNE, K. J. 2013. Generation and characterisation of cisplatin-resistant non-small cell lung cancer cell lines displaying a stem-like signature. *PloS one*, 8, e54193.
- BASS, A. J., WATANABE, H., MERMEL, C. H., YU, S., PERNER, S., VERHAAK, R. G., KIM, S. Y., WARDWELL, L., TAMAYO, P. & GATVIKS, I. 2009. SOX2 is an amplified lineage-survival oncogene in lung and esophageal squamous cell carcinomas. *Nature genetics*, 41, 1238-1242.
- BASU, A. & KRISHNAMURTHY, S. 2010. Cellular responses to cisplatin-induced DNA damage. *Journal of nucleic acids*, 2010.
- BEAU-FALLER, M., LEGRAIN, M., VOEGELI, A.-C., GUÉRIN, E., LAVAUX, T., RUPPERT, A.-M., NEUVILLE, A., MASSARD, G., WIHLM, J.-M. & QUOIX, E. 2009. Detection of K-Ras mutations in tumour samples of patients with non-small cell lung cancer using PNA-mediated PCR clamping. *British journal of cancer*, 100, 985-992.
- BEHN, M., THIEDE, C., NEUBAUER, A., PANKOW, W. & SCHUERMAN, M. 2000. Facilitated detection of oncogene mutations from exfoliated tissue material by a PNA-mediated 'enriched PCR' protocol. *The Journal of pathology*, 190, 69-75.
- BEROUKHIM, R., MERMEL, C. H., PORTER, D., WEI, G., RAYCHAUDHURI, S., DONOVAN, J., BARRETINA, J., BOEHM, J. S., DOBSON, J. & URASHIMA, M. 2010. The landscape of somatic copy-number alteration across human cancers. *Nature*, 463, 899-905.
- BESARATINIA, A. & PFEIFER, G. P. 2008. Second-hand smoke and human lung cancer. *The lancet oncology*, 9, 657-666.
- BOCH, C., KOLLMEIER, J., ROTH, A., STEPHAN-FALKENAU, S., MISCH, D., GRÜNING, W., BAUER, T. T. & MAIRINGER, T. 2013. The frequency of EGFR and KRAS mutations in non-small cell lung cancer (NSCLC): routine screening data for central Europe from a cohort study. *BMJ open*, 3, e002560.
- BOOY, E., HENSON, E. & GIBSON, S. 2011. Epidermal growth factor regulates Mcl-1 expression through the MAPK-Elk-1 signalling pathway contributing to cell survival in breast cancer. *Oncogene*, 30, 2367-2378.
- BOWMAN, T., GARCIA, R., TURKSON, J. & JOVE, R. 2000. STATs in oncogenesis. *Oncogene*, 19.
- BRAMBILLA, E. The histologic reclassification of adenocarcinoma of the lung: implications for diagnosis and therapy. *Am Soc Clin Oncol*, 2011. 1092-9118.
- BRAMBILLA, E., PUGATCH, B., GEISINGER, K., GAL, A., SHEPPARD, M., GUINEE, D., JIANG, S., LANTUEJOUL, S., CHANG, Y. & PETERSEN, I. 2004. Large cell carcinoma. *World Health Organization Classification of Tumours. Pathology and Genetics of Tumours of the Lung, Pleura, Thymus and Heart*, 48.
- BRCIC, L., SHERER, C. K., SHUAI, Y., HORNICK, J. L., CHIRIEAC, L. R. & DACIC, S. 2012. Morphologic and clinicopathologic features of lung squamous cell carcinomas expressing Sox2. *American journal of clinical pathology*, 138, 712-718.
- BROSE, M. S., VOLPE, P., FELDMAN, M., KUMAR, M., RISHI, I., GERRERO, R., EINHORN, E., HERLYN, M., MINNA, J. &

- NICHOLSON, A. 2002. BRAF and RAS mutations in human lung cancer and melanoma. *Cancer research*, 62, 6997-7000.
- BÜCHNER, F. L., BUENO-DE-MESQUITA, H. B., ROS, M. M., OVERVAD, K., DAHM, C. C., HANSEN, L., TJØNNELAND, A., CLAVEL-CHAPELON, F., BOUTRON-RUAULT, M.-C. & TOUILLAUD, M. 2010. Variety in fruit and vegetable consumption and the risk of lung cancer in the European prospective investigation into cancer and nutrition. *Cancer Epidemiology Biomarkers & Prevention*, 19, 2278-2286.
- BUETTNER, R., MORA, L. B. & JOVE, R. 2002. Activated STAT signaling in human tumors provides novel molecular targets for therapeutic intervention. *Clinical cancer research*, 8, 945-954.
- BUFFART, L. M., SINGH, A. S., VAN LOON, E. C., VERMEULEN, H. I., BRUG, J. & CHINAPAW, M. J. 2014. Physical activity and the risk of developing lung cancer among smokers: A meta-analysis. *Journal of Science and Medicine in Sport*, 17, 67-71.
- BUSACCA, S., LAW, E., POWLEY, I., PROIA, D., SEQUEIRA, M., LE QUESNE, J., KLABATSA, A., EDWARDS, J., MATCHETT, K. & LUO, J. 2015. Resistance to HSP90 inhibition involving loss of MCL1 addiction. *Oncogene*.
- BUSTIN, S. & NOLAN, T. 2004. Pitfalls of quantitative real-time reverse-transcription polymerase chain reaction. *Journal of biomolecular techniques: JBT*, 15, 155-166.
- CAI, Y.-R., ZHANG, H.-Q., QU, Y., MU, J., ZHAO, D., ZHOU, L.-J., YAN, H., YE, J.-W. & LIU, Y. 2011. Expression of MET and SOX2 genes in non-small cell lung carcinoma with EGFR mutation. *Oncology reports*, 26, 877-885.
- CAIOLA, E., SALLES, D., FRAPOLLI, R., LUPI, M., ROTELLA, G., RONCHI, A., GARASSINO, M. C., MATTSCHAS, N., COLAVECCHIO, S. & BROGGINI, M. 2015. Base excision repair-mediated resistance to cisplatin in KRAS (G12C) mutant NSCLC cells. *Oncotarget*, 6, 30072-30087.
- CANCER RESEARCH UK 2016. <http://www.cancerresearchuk.org/health-professional/cancer-statistics/statistics-by-cancer-type/lung-cancer/incidence#heading-One>.
- CAPPER, D., PREUSSER, M., HABEL, A., SAHM, F., ACKERMANN, U., SCHINDLER, G., PUSCH, S., MECHTERSHEIMER, G., ZENTGRAF, H. & VON DEIMLING, A. 2011. Assessment of BRAF V600E mutation status by immunohistochemistry with a mutation-specific monoclonal antibody. *Acta neuropathologica*, 122, 11-19.
- CATALDO, V. D., GIBBONS, D. L., PEREZ-SOLER, R. & QUINTAS-CARDAMA, A. 2011. Treatment of non-small-cell lung cancer with erlotinib or gefitinib. *N Engl J Med*, 364, 947-955.
- CETIN, Z., OZBILIM, G., ERDOGAN, A., LULECI, G. & KARAUZUM, S. B. 2010. Evaluation of PTEN and Mcl-1 expressions in NSCLC expressing wild-type or mutated EGFR. *Medical Oncology*, 27, 853-860.
- CHEN, Y., MCGEE, J., CHEN, X., DOMAN, T. N., GONG, X., ZHANG, Y., HAMM, N., MA, X., HIGGS, R. E. & BHAGWAT, S. V. 2014. Identification of druggable cancer driver genes amplified across TCGA datasets. *PLoS one*, 9, e98293.

- CHO, W. C. S. 2013. Targeting signaling pathways in lung cancer therapy. *Expert Opinion on Therapeutic Targets*, 17, 107-111.
- CHOI, E. J., RYU, Y. K., KIM, S. Y., WU, H. G., KIM, J. S., KIM, I. H. & KIM, I. A. 2010. Targeting epidermal growth factor receptor-associated signaling pathways in non-small cell lung cancer cells: Implication in radiation response. *Molecular Cancer Research*, 8, 1027-1036.
- CHOUDHARY, G., AL-HARBI, S., MAZUMDER, S., HILL, B., SMITH, M., BODO, J., HSI, E. & ALMASAN, A. 2015. MCL-1 and BCL-xL-dependent resistance to the BCL-2 inhibitor ABT-199 can be overcome by preventing PI3K/AKT/mTOR activation in lymphoid malignancies. *Cell death & disease*, 6, e1593.
- CHRESTA, C. M., DAVIES, B. R., HICKSON, I., HARDING, T., COSULICH, S., CRITCHLOW, S. E., VINCENT, J. P., ELLSTON, R., JONES, D. & SINI, P. 2010. AZD8055 is a potent, selective, and orally bioavailable ATP-competitive mammalian target of rapamycin kinase inhibitor with in vitro and in vivo antitumor activity. *Cancer research*, 70, 288-298.
- CLANCY, L., KABIR, Z. & CONNOLLY, G. N. 2008. Sex-differences in lung cancer cell-types? An epidemiologic study in Ireland.
- COHEN, D. A., DABBS, D. J., COOPER, K. L., AMIN, M., JONES, T. E., JONES, M. W., CHIVUKULA, M., TRUCCO, G. A. & BHARGAVA, R. 2012. Interobserver agreement among pathologists for semiquantitative hormone receptor scoring in breast carcinoma. *American journal of clinical pathology*, 138, 796-802.
- COOPER, W., YU, B., YIP, P., NG, C., LUM, T., FARZIN, M., TRENT, R., MERCORELLA, B., CLARKSON, A. & KOHONEN-CORISH, M. 2013. EGFR mutant-specific immunohistochemistry has high specificity and sensitivity for detecting targeted activating EGFR mutations in lung adenocarcinoma. *Journal of clinical pathology*, 66, 744-748.
- COSAERT, J. & QUOIX, E. 2002. Platinum drugs in the treatment of non-small-cell lung cancer. *British journal of cancer*, 87, 825-833.
- CZOGALA, J., GONIEWICZ, M. L., FIDELUS, B., ZIELINSKA-DANCH, W., TRAVERS, M. J. & SOBCZAK, A. 2014. Secondhand exposure to vapors from electronic cigarettes. *nicotine & tobacco research*, 16, 655-662.
- D'ARCANGELO, M. & CAPPUZZO, F. 2012. K-Ras mutations in non-small-cell lung cancer: prognostic and predictive value. *ISRN Molecular Biology*, 2012.
- DA CUNHA SANTOS, G., SHEPHERD, F. A. & TSAO, M. S. 2011. EGFR mutations and lung cancer. *Annual Review of Pathology: Mechanisms of Disease*, 6, 49-69.
- DAVID, O., JETT, J., LEBEAU, H., DY, G., HUGHES, J., FRIEDMAN, M. & BRODY, A. R. 2004. Phospho-Akt overexpression in non-small cell lung cancer confers significant stage-independent survival disadvantage. *Clinical Cancer Research*, 10, 6865-6871.
- DAVIES, J. M., TREMBATH, D., DEAL, A. M., FUNKHOUSER, W. K., CALVO, B. F., FINNEGAN, T., WECK, K. E., TEPPER, J. E. & O'NEIL, B. H. 2011. Phospho-ERK and AKT status, but not KRAS mutation status, are associated with outcomes in rectal cancer treated with chemoradiotherapy. *Radiation Oncology*, 6, 1.
- DAVIES, S. J., GOSNEY, J. R., HANSELL, D. M., WELLS, A. U., DU BOIS, R. M., BURKE, M. M., SHEPPARD, M. N. & NICHOLSON, A. G. 2007.

- Diffuse idiopathic pulmonary neuroendocrine cell hyperplasia: an under-recognised spectrum of disease. *Thorax*, 62, 248-252.
- DEARDEN, S., STEVENS, J., WU, Y.-L. & BLOWERS, D. 2013. Mutation incidence and coincidence in non small-cell lung cancer: meta-analyses by ethnicity and histology (mutMap). *Annals of Oncology*, 24, 2371-2376.
- DING, Q., HE, X., XIA, W., HSU, J.-M., CHEN, C.-T., LI, L.-Y., LEE, D.-F., YANG, J.-Y., XIE, X. & LIU, J.-C. 2007. Myeloid cell leukemia-1 inversely correlates with glycogen synthase kinase-3 β activity and associates with poor prognosis in human breast cancer. *Cancer research*, 67, 4564-4571.
- DUMONT, A. G., DUMONT, S. N. & TRENT, J. C. 2012. The favorable impact of PIK3CA mutations on survival: an analysis of 2587 patients with breast cancer. *Chinese journal of cancer*, 31, 327.
- DUNCIA, J. V., SANTELLA, J. B., HIGLEY, C. A., PITTS, W. J., WITYAK, J., FRIETZE, W. E., RANKIN, F. W., SUN, J.-H., EARL, R. A. & TABAKA, A. C. 1998. MEK inhibitors: the chemistry and biological activity of U0126, its analogs, and cyclization products. *Bioorganic & medicinal chemistry letters*, 8, 2839-2844.
- DUTTA, P., SABRI, N., LI, J. & LI, W. X. 2014. Role of STAT3 in lung cancer. *JAK-STAT*, 3, e999503.
- EBERHARD, D. A., JOHNSON, B. E., AMLER, L. C., GODDARD, A. D., HELDENS, S. L., HERBST, R. S., INCE, W. L., JÄNNE, P. A., JANUARIO, T. & JOHNSON, D. H. 2005. Mutations in the epidermal growth factor receptor and in KRAS are predictive and prognostic indicators in patients with non-small-cell lung cancer treated with chemotherapy alone and in combination with erlotinib. *Journal of Clinical Oncology*, 23, 5900-5909.
- EL-TELBANY, A. & MA, P. C. 2012. Cancer genes in lung cancer racial disparities: are there any? *Genes & cancer*, 3, 467-480.
- ERTEL, F., NGUYEN, M., ROULSTON, A. & SHORE, G. C. 2013. Programming cancer cells for high expression levels of Mcl1. *EMBO reports*, 14, 328-336.
- EWALD, F., NÖRZ, D., GROTTKE, A., BACH, J., HERZBERGER, C., HOFMANN, B. T., NASHAN, B. & JÜCKER, M. 2015. Vertical Targeting of AKT and mTOR as Well as Dual Targeting of AKT and MEK Signaling Is Synergistic in Hepatocellular Carcinoma. *Journal of Cancer*, 6, 1195.
- FABER, A. C., COFFEE, E. M., COSTA, C., DASTUR, A., EBI, H., HATA, A. N., YEO, A. T., EDELMAN, E. J., SONG, Y. & TAM, A. T. 2014. mTOR inhibition specifically sensitizes colorectal cancers with KRAS or BRAF mutations to BCL-2/BCL-XL inhibition by suppressing MCL-1. *Cancer discovery*, 4, 42-52.
- FABER, A. C., LI, D., SONG, Y., LIANG, M.-C., YEAP, B. Y., BRONSON, R. T., LIFSHITS, E., CHEN, Z., MAIRA, S.-M. & GARCÍA-ECHEVERRÍA, C. 2009. Differential induction of apoptosis in HER2 and EGFR addicted cancers following PI3K inhibition. *Proceedings of the National Academy of Sciences*, 106, 19503-19508.
- FREEDMAN, N. D., LEITZMANN, M. F., HOLLENBECK, A. R., SCHATZKIN, A. & ABNET, C. C. 2008. Cigarette smoking and

- subsequent risk of lung cancer in men and women: analysis of a prospective cohort study. *The lancet oncology*, 9, 649-656.
- FURQAN, M., AKINLEYE, A., MUKHI, N., MITTAL, V., CHEN, Y. & LIU, D. 2013. STAT inhibitors for cancer therapy. *Journal of hematology & oncology*, 6, 1-11.
- GALLICCHIO, L., BOYD, K., MATANOSKI, G., TAO, X. G., CHEN, L., LAM, T. K., SHIELS, M., HAMMOND, E., ROBINSON, K. A. & CAULFIELD, L. E. 2008. Carotenoids and the risk of developing lung cancer: a systematic review. *The American journal of clinical nutrition*, 88, 372-383.
- GARASSINO, M., MARABESE, M., RUSCONI, P., RULLI, E., MARTELLI, O., FARINA, G., SCANNI, A. & BROGGINI, M. 2011. Different types of K-Ras mutations could affect drug sensitivity and tumour behaviour in non-small-cell lung cancer. *Annals of oncology*, 22, 235-237.
- GARDIZI, M., SCHEFFLER, M., HEUKAMP, L. C., BOS, M. C. A., ALBUS, K., HAYN, B., KO, Y.-D., SCHLESINGER, A., BROCKMANN, M. & SERKE, M. H. Frequency and clinical characterization of NSCLC patients harboring PIK3CA mutations identified within a regional screening network. ASCO Annual Meeting Proceedings, 2012. 10526.
- GAZDAR, A. F. & MINNA, J. D. 2008. Deregulated EGFR signaling during lung cancer progression: mutations, amplicons, and autocrine loops. *Cancer Prevention Research*, 1, 156-160.
- GODUGU, C., PATEL, A. R., DESAI, U., ANDEY, T., SAMS, A. & SINGH, M. 2013. AlgiMatrix™ based 3D cell culture system as an in-vitro tumor model for anticancer studies. *PLoS One*, 8, e53708.
- GOUILL, S. L., PODAR, K., HAROUSSEAU, J.-L. & ANDERSON, K. C. 2004. Mcl-1 regulation and its role in multiple myeloma. *Cell Cycle*, 3, 1259-1262.
- GREULICH, H. 2010. The Genomics of Lung Adenocarcinoma Opportunities for Targeted Therapies. *Genes & cancer*, 1, 1200-1210.
- GUSTAVSSON, P., JAKOBSSON, R., NYBERG, F., PERSHAGEN, G., JÄRUP, L. & SCHÉELE, P. 2000. Occupational exposure and lung cancer risk: a population-based case-referent study in Sweden. *American journal of epidemiology*, 152, 32-40.
- HAFTCHENARY, S., LUCHMAN, H. A., JOUK, A. O., VELOSO, A. J., PAGE, B. D., CHENG, X. R., DAWSON, S. S., GRINSHTEIN, N., SHAHANI, V. M. & KERMAN, K. 2013. Potent targeting of the STAT3 protein in brain cancer stem cells: a promising route for treating glioblastoma. *ACS medicinal chemistry letters*, 4, 1102-1107.
- HALUSKA, P., DY, G. & ADJEI, A. 2002. Farnesyl transferase inhibitors as anticancer agents. *European Journal of Cancer*, 38, 1685-1700.
- HATZIVASSILIOU, G., LIU, B., O'BRIEN, C., SPOERKE, J. M., HOEFELICH, K. P., HAVERTY, P. M., SORIANO, R., FORREST, W. F., HELDENS, S. & CHEN, H. 2012. ERK inhibition overcomes acquired resistance to MEK inhibitors. *Molecular cancer therapeutics*, 11, 1143-1154.
- HAYAKAWA, F., SUGIMOTO, K., HARADA, Y., HASHIMOTO, N., OHI, N., KURAHASHI, S. & NAOE, T. 2013. A novel STAT inhibitor, OPB-31121, has a significant antitumor effect on leukemia with STAT-addictive oncocinases. *Blood cancer journal*, 3, e166.

- HECHT, S. S. 1999. Tobacco smoke carcinogens and lung cancer. *Journal of the national cancer institute*, 91, 1194-1210.
- HSIEH, C.-H., CHEN, Y.-D., HUANG, S.-F., WANG, H.-M. & WU, M.-H. 2015. The effect of primary cancer cell culture models on the results of drug chemosensitivity assays: the application of perfusion Microbioreactor system as cell culture vessel. *BioMed research international*, 2015.
- HUANG, Y. C., PAN, M., LIU, N., XIAO, J. G. & CHEN, H. Q. 2015. Effects of nuclear factor- κ B and ERK signaling transduction pathway inhibitors on human melanoma cell proliferation in vitro. *Oncology letters*, 10, 3233-3237.
- HUNCHAREK, M., MUSCAT, J. & GESCHWIND, J. F. 1999. K-ras oncogene mutation as a prognostic marker in non-small cell lung cancer: a combined analysis of 881 cases. *Carcinogenesis*, 20, 1507-10.
- HWANG, S.-J., CHENG, L. S.-C., LOZANO, G., AMOS, C. I., GU, X. & STRONG, L. C. 2003. Lung cancer risk in germline p53 mutation carriers: association between an inherited cancer predisposition, cigarette smoking, and cancer risk. *Human genetics*, 113, 238-243.
- IMIELINSKI, M., BERGER, A. H., HAMMERMAN, P. S., HERNANDEZ, B., PUGH, T. J., HODIS, E., CHO, J., SUH, J., CAPELLETTI, M. & SIVACHENKO, A. 2012. Mapping the hallmarks of lung adenocarcinoma with massively parallel sequencing. *Cell*, 150, 1107-1120.
- JÄNNE, P. A., SHAW, A. T., PEREIRA, J. R., JEANNIN, G., VANSTEENKISTE, J., BARRIOS, C., FRANKE, F. A., GRINSTED, L., ZAZULINA, V. & SMITH, P. 2013. Selumetinib plus docetaxel for KRAS-mutant advanced non-small-cell lung cancer: a randomised, multicentre, placebo-controlled, phase 2 study. *The lancet oncology*, 14, 38-47.
- JIANG, B.-H. 2008. PI3K/AKT signaling in tumorigenesis and angiogenesis. *Biomedicine & Pharmacotherapy*, 62, 422-423.
- JORDAN, N. J., DUTKOWSKI, C. M., BARROW, D., MOTTRAM, H. J., HUTCHESON, I. R., NICHOLSON, R. I., GUICHARD, S. M. & GEE, J. 2014. Impact of dual mTORC1/2 mTOR kinase inhibitor AZD8055 on acquired endocrine resistance in breast cancer in vitro. *Breast Cancer Res*, 16, R12.
- JUNG, I. H., CHOI, J. H.-K., CHUNG, Y.-Y., LIM, G.-L., PARK, Y.-N. & PARK, S. W. 2015. Predominant Activation of JAK/STAT3 Pathway by Interleukin-6 Is Implicated in Hepatocarcinogenesis. *Neoplasia*, 17, 586-597.
- KALEMKERIAN, G. P. 2011. Staging and imaging of small cell lung cancer. *Cancer Imaging*, 11, 253.
- KALINSKY, K., JACKS, L. M., HEGUY, A., PATIL, S., DROBNJAK, M., BHANOT, U. K., HEDVAT, C. V., TRAINA, T. A., SOLIT, D. & GERALD, W. 2009. PIK3CA mutation associates with improved outcome in breast cancer. *Clinical Cancer Research*, 15, 5049-5059.
- KARACHALIOU, N., MAYO, C., COSTA, C., MAGRI, I., GIMENEZ-CAPITAN, A., MOLINA-VILA, M. A. & ROSELL, R. 2013. KRAS mutations in lung cancer. *Clin Lung Cancer*, 14, 205-14.
- KAREKLA, E., LIAO, W., SHARP, B., PUGH, J., REID, H., LE QUESNE, J., MOORE, D., PRITCHARD, C., MACFARLANE, M. & PRINGLE, H. 2016. Ex-vivo explant culture of NSCLC provides a relevant preclinical

- model for evaluation of primary tumour response to anticancer therapies. *Cancer Research*, submitted.
- KHOO, C., ROGERS, T.-M., FELLOWES, A., BELL, A. & FOX, S. 2015. Molecular methods for somatic mutation testing in lung adenocarcinoma: EGFR and beyond. *Translational lung cancer research*, 4, 126.
- KIMURA, H., OHIRA, T., UCHIDA, O., MATSUBAYASHI, J., SHIMIZU, S., NAGAO, T., IKEDA, N. & NISHIO, K. 2014. Analytical performance of the cobas EGFR mutation assay for Japanese non-small-cell lung cancer. *Lung Cancer*, 83, 329-333.
- KRAJEWSKI, S., BODRUG, S., KRAJEWSKA, M., SHABAIK, A., GASCOYNE, R., BEREAN, K. & REED, J. C. 1995. Immunohistochemical analysis of Mcl-1 protein in human tissues. Differential regulation of Mcl-1 and Bcl-2 protein production suggests a unique role for Mcl-1 in control of programmed cell death in vivo. *The American journal of pathology*, 146, 1309.
- LANDMANN, H., PROIA, D., HE, S., OGAWA, L., KRAMER, F., BEIBBARTH, T., GRADE, M., GAEDCKE, J., GHADIMI, M. & MOLL, U. 2014. UDP glucuronosyltransferase 1A expression levels determine the response of colorectal cancer cells to the heat shock protein 90 inhibitor ganetespib. *Cell death & disease*, 5, e1411.
- LEE, H.-W., WANG, H.-T., WENG, M.-W., CHIN, C., HUANG, W., LEPOR, H., WU, X.-R., ROM, W. N., CHEN, L.-C. & TANG, M.-S. 2015. Cigarette side-stream smoke lung and bladder carcinogenesis: inducing mutagenic acrolein-DNA adducts, inhibiting DNA repair and enhancing anchorage-independent-growth cell transformation. *Oncotarget*, 6, 33226.
- LEE, S., CHOI, E.-J., JIN, C. & KIM, D.-H. 2005. Activation of PI3K/Akt pathway by PTEN reduction and PIK3CA mRNA amplification contributes to cisplatin resistance in an ovarian cancer cell line. *Gynecologic oncology*, 97, 26-34.
- LEE, S., KIM, H., PARK, W., KIM, S., LEE, K., KIM, S., LEE, J. & YOO, N. 2002. Non-small cell lung cancers frequently express phosphorylated Akt; an immunohistochemical study. *Apmis*, 110, 587-592.
- LEVERSON, J., ZHANG, H., CHEN, J., TAHIR, S., PHILLIPS, D., XUE, J., NIMMER, P., JIN, S., SMITH, M. & XIAO, Y. 2015. Potent and selective small-molecule MCL-1 inhibitors demonstrate on-target cancer cell killing activity as single agents and in combination with ABT-263 (navitoclax). *Cell death & disease*, 6, e1590.
- LI, T., KUNG, H.-J., MACK, P. C. & GANDARA, D. R. 2013. Genotyping and genomic profiling of non-small-cell lung cancer: implications for current and future therapies. *Journal of Clinical Oncology*, 31, 1039-1049.
- LI, X., WANG, J., XU, Z., AHMAD, A., LI, E., WANG, Y., QIN, S. & WANG, Q. 2012. Expression of sox2 and oct4 and their clinical significance in human non-small-cell lung cancer. *International journal of molecular sciences*, 13, 7663-7675.
- LIANG, Y., WANG, L., ZHU, Y., LIN, Y., LIU, H., RAO, H., XU, G. & RONG, T. 2012. Primary pulmonary lymphoepithelioma-like carcinoma. *Cancer*, 118, 4748-4758.
- LIU, H., LU, J., HUA, Y., ZHANG, P., LIANG, Z., RUAN, L., LIAN, C., SHI, H., CHEN, K. & TU, Z. 2015. Targeting heat-shock protein 90 with

- ganetespib for molecularly targeted therapy of gastric cancer. *Cell death & disease*, 6, e1595.
- LIU, L., BÄCKLUND, L. M., NILSSON, B. R., GRANDÉR, D., ICHIMURA, K., GOIKE, H. M. & COLLINS, V. P. 2005. Clinical significance of EGFR amplification and the aberrant EGFRvIII transcript in conventionally treated astrocytic gliomas. *Journal of molecular medicine*, 83, 917-926.
- LIU, P., CHENG, H., ROBERTS, T. M. & ZHAO, J. J. 2009. Targeting the phosphoinositide 3-kinase pathway in cancer. *Nature reviews Drug discovery*, 8, 627-644.
- LUK, P. P., YU, B., NG, C. C., MERCORELLA, B., SELINGER, C., LUM, T., KAO, S., O'TOOLE, S. A. & COOPER, W. A. 2015. BRAF mutations in non-small cell lung cancer. *Translational lung cancer research*, 4, 142.
- LUO, J.-D., CHAN, E.-C., SHIH, C.-L., CHEN, T.-L., LIANG, Y., HWANG, T.-L. & CHIOU, C.-C. 2006. Detection of rare mutant K-ras DNA in a single-tube reaction using peptide nucleic acid as both PCR clamp and sensor probe. *Nucleic acids research*, 34, e12-e12.
- MAIER, S., WILBERTZ, T., BRAUN, M., SCHEBLE, V., REISCHL, M., MIKUT, R., MENON, R., NIKOLOV, P., PETERSEN, K. & BESCHORNER, C. 2011. SOX2 amplification is a common event in squamous cell carcinomas of different organ sites. *Human pathology*, 42, 1078-1088.
- MARCHETTI, A., FELICIONI, L., MALATESTA, S., SCIARROTTA, M. G., GUETTI, L., CHELLA, A., VIOLA, P., PULLARA, C., MUCILLI, F. & BUTTITTA, F. 2011. Clinical features and outcome of patients with non-small-cell lung cancer harboring BRAF mutations. *Journal of clinical oncology*, 29, 3574-3579.
- MASSION, P. P., KUO, W.-L., STOKOE, D., OLSHEN, A. B., TRESELER, P. A., CHIN, K., CHEN, C., POLIKOFF, D., JAIN, A. N. & PINKEL, D. 2002. Genomic copy number analysis of non-small cell lung cancer using array comparative genomic hybridization implications of the phosphatidylinositol 3-kinase pathway. *Cancer research*, 62, 3636-3640.
- MASSION, P. P., TAFLAN, P. M., SHYR, Y., RAHMAN, S. J., YILDIZ, P., SHAKTHOUR, B., EDGERTON, M. E., NINAN, M., ANDERSEN, J. J. & GONZALEZ, A. L. 2004. Early involvement of the phosphatidylinositol 3-kinase/Akt pathway in lung cancer progression. *American journal of respiratory and critical care medicine*, 170, 1088-1094.
- MCCAUGHAN, F., POLE, J. C., BANKIER, A. T., KONFORTOV, B. A., CARROLL, B., FALZON, M., RABBITS, T. H., GEORGE, P. J., DEAR, P. H. & RABBITS, P. H. 2010. Progressive 3q amplification consistently targets SOX2 in preinvasive squamous lung cancer. *American journal of respiratory and critical care medicine*, 182, 83-91.
- MCD AID, H. M. & HORWITZ, S. B. 2001. Selective potentiation of paclitaxel (taxol)-induced cell death by mitogen-activated protein kinase kinase inhibition in human cancer cell lines. *Molecular pharmacology*, 60, 290-301.
- MCKEE, C. S., HILL, D. S., REDFERN, C. P., ARMSTRONG, J. L. & LOVAT, P. E. 2013. Oncogenic BRAF signalling increases Mcl-1 expression in cutaneous metastatic melanoma. *Experimental dermatology*, 22, 767-769.

- MICHELS, J., JOHNSON, P. W. & PACKHAM, G. 2005. Mcl-1. *The international journal of biochemistry & cell biology*, 37, 267-271.
- MILES, D., VON MINCKWITZ, G. & SEIDMAN, A. D. 2002. Combination versus sequential single-agent therapy in metastatic breast cancer. *The oncologist*, 7, 13-19.
- MITRA, A., MISHRA, L. & LI, S. 2013. Technologies for deriving primary tumor cells for use in personalized cancer therapy. *Trends in biotechnology*, 31, 347-354.
- MOJSA, B., LASSOT, I. & DESAGHER, S. 2014. Mcl-1 ubiquitination: unique regulation of an essential survival protein. *Cells*, 3, 418-437.
- MOLINA, J. R., YANG, P., CASSIVI, S. D., SCHILD, S. E. & ADJEI, A. A. Non-small cell lung cancer: epidemiology, risk factors, treatment, and survivorship. Mayo Clinic Proceedings, 2008. Elsevier, 584-594.
- MORI, M., RAO, S. K., POPPER, H. H., CAGLE, P. T. & FRAIRE, A. E. 2001. Atypical adenomatous hyperplasia of the lung: a probable forerunner in the development of adenocarcinoma of the lung. *Modern Pathology*, 14, 72-84.
- MUKOHARA, T., KUDOH, S., YAMAUCHI, S., KIMURA, T., YOSHIMURA, N., KANAZAWA, H., HIRATA, K., WANIBUCHI, H., FUKUSHIMA, S. & INOUE, K. 2003. Expression of epidermal growth factor receptor (EGFR) and downstream-activated peptides in surgically excised non-small-cell lung cancer (NSCLC). *Lung Cancer*, 41, 123-130.
- NADAL, E., SHIRATSUCHI, H., CHEN, G., SAM, C., KALEMKERIAN, G. P., BEER, D. G. & RAMNATH, N. 2013. Abstract C141: KRAS G12C mutation is prognostic of poor outcome in resected lung adenocarcinomas and predictive of poor response to MEK inhibition in vitro. *Molecular Cancer Therapeutics*, 12, C141-C141.
- NASSAR, A. A., JAROSZEWSKI, D. E., HELMERS, R. A., COLBY, T. V., PATEL, B. M. & MOOKADAM, F. 2011. Diffuse idiopathic pulmonary neuroendocrine cell hyperplasia: a systematic overview. *American journal of respiratory and critical care medicine*, 184, 8-16.
- NELSON, H. H., CHRISTIANI, D. C., MARK, E. J., WIENCKE, J. K., WAIN, J. C. & KELSEY, K. T. 1999. Implications and prognostic value of K-ras mutation for early-stage lung cancer in women. *Journal of the National Cancer Institute*, 91, 2032-2038.
- NEMERY, B. 1990. Metal toxicity and the respiratory tract. *European Respiratory Journal*, 3, 202-219.
- NESBITT, J. C., PUTNAM, J. B., WALSH, G. L., ROTH, J. A. & MOUNTAIN, C. F. 1995. Survival in early-stage non-small cell lung cancer. *The Annals of thoracic surgery*, 60, 466-472.
- NEUGUT, A. I., MURRAY, T., SANTOS, J., AMOLS, H., HAYES, M. K., FLANNERY, J. T. & ROBINSON, E. 1994. Increased risk of lung cancer after breast cancer radiation therapy in cigarette smokers. *Cancer*, 73, 1615-1620.
- NICKLAS, J. A. & BUEL, E. 2003. Development of an Alu-based, real-time PCR method for quantitation of human DNA in forensic samples. *Journal of forensic sciences*, 48, 936-944.
- NYBERG, F., GUSTAVSSON, P., JÄRUP, L., BELLANDER, T., BERGLIND, N., JAKOBSSON, R. & PERSHAGEN, G. 2000. Urban air pollution and lung cancer in Stockholm. *Epidemiology*, 11, 487-495.

- OKABE, T., OKAMOTO, I., TAMURA, K., TERASHIMA, M., YOSHIDA, T., SATOH, T., TAKADA, M., FUKUOKA, M. & NAKAGAWA, K. 2007. Differential constitutive activation of the epidermal growth factor receptor in non-small cell lung cancer cells bearing EGFR gene mutation and amplification. *Cancer research*, 67, 2046-2053.
- OKUDELA, K., SUZUKI, M., KAGEYAMA, S., BUNAI, T., NAGURA, K., IGARASHI, H., TAKAMOCHI, K., SUZUKI, K., YAMADA, T. & NIWA, H. 2007. PIK3CA mutation and amplification in human lung cancer. *Pathology international*, 57, 664-671.
- OOI, A., SUZUKI, S., NAKAZAWA, K., ITAKURA, J., IMOTO, I., NAKAMURA, H. & DOBASHI, Y. 2009. Gene amplification of Myc and its coamplification with ERBB2 and EGFR in gallbladder adenocarcinoma. *Anticancer research*, 29, 19-26.
- OSANN, K. E., LOWERY, J. T. & SCHELL, M. J. 2000. Small cell lung cancer in women: risk associated with smoking, prior respiratory disease, and occupation. *Lung Cancer*, 28, 1-10.
- PAEZ, J. G., JÄNNE, P. A., LEE, J. C., TRACY, S., GREULICH, H., GABRIEL, S., HERMAN, P., KAYE, F. J., LINDEMAN, N. & BOGGON, T. J. 2004. EGFR mutations in lung cancer: correlation with clinical response to gefitinib therapy. *Science*, 304, 1497-1500.
- PAGGI, M. G., VONA, R., ABBRUZZESE, C. & MALORNI, W. 2010. Gender-related disparities in non-small cell lung cancer. *Cancer letters*, 298, 1-8.
- PAL, S. K., FIGLIN, R. A. & RECKAMP, K. 2010. Targeted therapies for non-small cell lung cancer: an evolving landscape. *Molecular cancer therapeutics*, 9, 1931-1944.
- PAN, R., RUVOLO, V. R., WEI, J., KONOPLEVA, M., REED, J. C., PELLECCIA, M., ANDREEFF, M. & RUVOLO, P. P. 2015. Inhibition of Mcl-1 with the pan-Bcl-2 family inhibitor (-) BI97D6 overcomes ABT-737 resistance in acute myeloid leukemia. *Blood*, 126, 363-372.
- PAO, W. & GIRARD, N. 2011. New driver mutations in non-small-cell lung cancer. *The lancet oncology*, 12, 175-180.
- PARK, C. M., GOO, J. M., LEE, H. J., LEE, C. H., KIM, H.-C., CHUNG, D. H. & IM, J.-G. 2006. CT findings of atypical adenomatous hyperplasia in the lung. *Korean journal of radiology*, 7, 80-86.
- PARK, W. Y., KIM, M. H., SHIN, D. H., LEE, J. H., CHOI, K. U., KIM, J. Y., LEE, C. H. & SOL, M. Y. 2012. Ciliated adenocarcinomas of the lung: a tumor of non-terminal respiratory unit origin. *Modern Pathology*, 25, 1265-1274.
- PAYNE, S. N., MAHER, M. E., TRAN, N. H., VAN DE HEY, D. R., FOLEY, T. M., YUEH, A. E., LEYSTRA, A. A., PASCH, C. A., JEFFREY, J. J., CLIPSON, L., MATKOWSKYJ, K. A. & DEMING, D. A. 2015. PIK3CA mutations can initiate pancreatic tumorigenesis and are targetable with PI3K inhibitors. *Oncogenesis*, 4, e169.
- PAZ-ARES, L., SOULIÈRES, D., MELEZÍNEK, I., MOECKS, J., KEIL, L., MOK, T., ROSELL, R. & KLUGHAMMER, B. 2010. Clinical outcomes in non-small-cell lung cancer patients with EGFR mutations: pooled analysis. *Journal of cellular and molecular medicine*, 14, 51-69.
- PEARCE, M., NAKORCHEVSKY, A., NYGREN, A. & IRWIN, D. 2014. Targeted Mutation Profiling of Non-Small Cell Lung Cancer Samples

- using the Sequenom Lungcarta™ Panel* for Clinical Research. Sequenom.
- PEDDABOINA, C., JUPITER, D., FLETCHER, S., YAP, J. L., RAI, A., TOBIN, R. P., JIANG, W., RASCOE, P., ROGERS, M. K. N. & SMYTHE, W. R. 2012. The downregulation of Mcl-1 via USP9X inhibition sensitizes solid tumors to Bcl-xl inhibition. *BMC cancer*, 12, 1.
- PEI, X.-Y., DAI, Y., FELTHOUSEN, J., CHEN, S., TAKABATAKE, Y., ZHOU, L., YOUSSEFIAN, L. E., SANDERSON, M. W., BODIE, W. W. & KRAMER, L. B. 2014. Circumvention of Mcl-1-dependent drug resistance by simultaneous Chk1 and MEK1/2 inhibition in human multiple myeloma cells. *PloS one*, 9, e89064.
- PERCIAVALLE, R. M., STEWART, D. P., KOSS, B., LYNCH, J., MILASTA, S., BATHINA, M., TEMIROV, J., CLELAND, M. M., PELLETIER, S. & SCHUETZ, J. D. 2012. Anti-apoptotic MCL-1 localizes to the mitochondrial matrix and couples mitochondrial fusion to respiration. *Nature cell biology*, 14, 575-583.
- PFEIFER, G. P., DENISSENKO, M. F., OLIVIER, M., TRETYAKOVA, N., HECHT, S. S. & HAINAUT, P. 2002. Tobacco smoke carcinogens, DNA damage and p 53 mutations in smoking-associated cancers. *Oncogene*, 21, 7435-7451.
- PLEASANCE, E. D., STEPHENS, P. J., O'MEARA, S., MCBRIDE, D. J., MEYNERT, A., JONES, D., LIN, M.-L., BEARE, D., LAU, K. W. & GREENMAN, C. 2010. A small cell lung cancer genome reports complex tobacco exposure signatures. *Nature*, 463, 184.
- PRIOR, I. A., LEWIS, P. D. & MATTOS, C. 2012. A comprehensive survey of Ras mutations in cancer. *Cancer research*, 72, 2457-2467.
- PROCTOR, R. N. 2012. The history of the discovery of the cigarette–lung cancer link: evidentiary traditions, corporate denial, global toll. *Tobacco control*, 21, 87-91.
- QUINN, B. A., DASH, R., AZAB, B., SARKAR, S., DAS, S. K., KUMAR, S., OYESANYA, R. A., DASGUPTA, S., DENT, P., GRANT, S., RAHMANI, M., CURIEL, D. T., DMITRIEV, I., HEDVAT, M., WEI, J., WU, B., STEBBINS, J. L., REED, J. C., PELLECCCHIA, M., SARKAR, D. & FISHER, P. B. 2011. Targeting Mcl-1 for the therapy of cancer. *Expert Opin Investig Drugs*, 20, 1397-411.
- REGALES, L., GONG, Y., SHEN, R., DE STANCHINA, E., VIVANCO, I., GOEL, A., KOUTCHER, J. A., SPASSOVA, M., OUERFELLI, O. & MELLINGHOFF, I. K. 2009. Dual targeting of EGFR can overcome a major drug resistance mutation in mouse models of EGFR mutant lung cancer. *The Journal of clinical investigation*, 119, 3000-3010.
- REN, J. H., HE, W. S., YAN, G. L., JIN, M., YANG, K. Y. & WU, G. 2012. EGFR mutations in non-small-cell lung cancer among smokers and non-smokers: A meta-analysis. *Environmental and molecular mutagenesis*, 53, 78-82.
- ROSENBERGER, A., BICKEBÖLLER, H., MCCORMACK, V., BRENNER, D. R., DUELL, E. J., TJØNNELAND, A., FRIIS, S., MUSCAT, J. E., YANG, P. & WICHMANN, H.-E. 2012. Asthma and lung cancer risk: a systematic investigation by the International Lung Cancer Consortium. *Carcinogenesis*, 33, 587-597.

- ROUGE, T. D. L. M., GALLUZZI, L., OLAUSSEN, K. A., ZERMATI, Y., TASDEMIR, E., ROBERT, T., RIPOCHE, H., LAZAR, V., DESSEN, P. & HARPER, F. 2007. A Novel Epidermal Growth Factor Receptor Inhibitor Promotes Apoptosis in Non-Small Cell Lung Cancer Cells Resistant to Erlotinib. *Cancer research*, 67, 6253-6262.
- SAKURAI, H. & ASAMURA, H. 2014. Large-cell neuroendocrine carcinoma of the lung: surgical management. *Thoracic surgery clinics*, 24, 305-311.
- SAMUELS, Y., WANG, Z., BARDELLI, A., SILLIMAN, N., PTAK, J. & SZABO, S. 2004. High frequency of mutations of the PIK3CA gene in human cancers. *Science*, 304, 554.
- SASAKI, H., SHITARA, M., YOKOTA, K., OKUDA, K., HIKOSAKA, Y., MORIYAMA, S., YANO, M. & FUJII, Y. 2012. Braf and erbb2 mutations correlate with smoking status in lung cancer patients. *Experimental and therapeutic medicine*, 3, 771-775.
- SATHE, P., DELCONTE, R. B., SOUZA-FONSECA-GUIMARAES, F., SEILLET, C., CHOPIN, M., VANDENBERG, C. J., RANKIN, L. C., MIELKE, L. A., VIKSTROM, I. & KOLESNIK, T. B. 2014. Innate immunodeficiency following genetic ablation of Mcl1 in natural killer cells. *Nature communications*, 5.
- SATO, M., SHAMES, D. S., GAZDAR, A. F. & MINNA, J. D. 2007. A translational view of the molecular pathogenesis of lung cancer. *Journal of Thoracic Oncology*, 2, 327-343.
- SATO, M., VAUGHAN, M. B., GIRARD, L., PEYTON, M., LEE, W., SHAMES, D. S., RAMIREZ, R. D., SUNAGA, N., GAZDAR, A. F. & SHAY, J. W. 2006. Multiple oncogenic changes (K-RASV12, p53 knockdown, mutant EGFRs, p16 bypass, telomerase) are not sufficient to confer a full malignant phenotype on human bronchial epithelial cells. *Cancer research*, 66, 2116-2128.
- SCHEFFLER, M., BOS, M., GARDIZI, M., KÖNIG, K., MICHELS, S., FASSUNKE, J., HEYDT, C., KÜNSTLINGER, H., IHLE, M. & UECKEROTH, F. 2015. PIK3CA mutations in non-small cell lung cancer (NSCLC): Genetic heterogeneity, prognostic impact and incidence of prior malignancies. *Oncotarget*, 6, 1315.
- SCHRÖCK, A., BODE, M., GÖKE, F. J. M., BAREISS, P. M., SCHAIRER, R., WANG, H., FRANZEN, A., KIRSTEN, R., VAN BREMEN, T. & QUEISSER, A. 2014. Expression and role of the embryonic protein SOX2 in head and neck squamous cell carcinoma. *Carcinogenesis*, bgu094.
- SCHROEDL, C. & KALHAN, R. 2012. Incidence, treatment options, and outcomes of lung cancer in patients with chronic obstructive pulmonary disease. *Current opinion in pulmonary medicine*, 18, 131-137.
- SHACKELFORD, R. E., VORA, M., MAYHALL, K. & COTELINGAM, J. 2014. ALK-rearrangements and testing methods in non-small cell lung cancer: a review. *Genes Cancer*, 5, 1-14.
- SHAW, A. T., WINSLOW, M. M., MAGENDANTZ, M., OUYANG, C., DOWDLE, J., SUBRAMANIAN, A., LEWIS, T. A., MAGLATHIN, R. L., TOLLIDAY, N. & JACKS, T. 2011. Selective killing of K-ras mutant cancer cells by small molecule inducers of oxidative stress. *Proceedings of the National Academy of Sciences*, 108, 8773-8778.

- SHI, J., YAO, D., LIU, W., WANG, N., LV, H., ZHANG, G., JI, M., XU, L., HE, N. & SHI, B. 2012. Highly frequent PIK3CA amplification is associated with poor prognosis in gastric cancer. *BMC cancer*, 12, 50.
- SHIGAKI, H., BABA, Y., WATANABE, M., MURATA, A., ISHIMOTO, T., IWATSUKI, M., IWAGAMI, S., NOSHO, K. & BABA, H. 2013. PIK3CA mutation is associated with a favorable prognosis among patients with curatively resected esophageal squamous cell carcinoma. *Clinical cancer research*, 19, 2451-2459.
- SHIGEMASA, K., KATO, O., SHIROYAMA, Y., MIHARA, S., MUKAI, K., NAGAI, N. & OHAMA, K. 2002. Increased MCL-1 Expression Is Associated with Poor Prognosis in Ovarian Carcinomas. *Japanese journal of cancer research*, 93, 542-550.
- SHIMADA, Y., OKUMURA, T., SEKINE, S., MORIYAMA, M., SAWADA, S., MATSUI, K., YOSHIOKA, I., HOJO, S., YOSHIDA, T. & NAGATA, T. 2012. Expression Analysis of iPS Cell-Inductive Genes in Esophageal Squamous Cell Carcinoma by Tissue Microarray. *Anticancer research*, 32, 5507-5514.
- SHOLL, L. M., BARLETTA, J. A., YEAP, B. Y., CHIRIEAC, L. R. & HORNICK, J. L. 2010. Sox2 protein expression is an independent poor prognostic indicator in stage I lung adenocarcinoma. *The American journal of surgical pathology*, 34, 1193.
- SIO, T. T., MANSFIELD, A. S., GROTZ, T. E., GRAHAM, R. P., MOLINA, J. R., QUE, F. G. & MILLER, R. C. 2014. Concurrent MCL1 and JUN amplification in pseudomyxoma peritonei: a comprehensive genetic profiling and survival analysis. *Journal of human genetics*, 59, 124-128.
- SLATORE, C. G., GOULD, M. K., AU, D. H., DEFFEBACH, M. E. & WHITE, E. 2011. Lung cancer stage at diagnosis: Individual associations in the prospective VITamins and lifestyle (VITAL) cohort. *BMC cancer*, 11, 1.
- SLEBOS, R. J., KIBBELAAR, R. E., DALESIO, O., KOOISTRA, A., STAM, J., MEIJER, C. J., WAGENAAR, S. S., VANDERSCHUEREN, R. G., VAN ZANDWIJK, N. & MOOI, W. J. 1990. K-ras oncogene activation as a prognostic marker in adenocarcinoma of the lung. *New England Journal of Medicine*, 323, 561-565.
- SONG, L., COPPOLA, D., LIVINGSTON, S., CRESS, W. D. & HAURA, E. B. 2005. Mcl-1 regulates survival and sensitivity to diverse apoptotic stimuli in human non-small cell lung cancer cells. *Cancer biology & therapy*, 4, 267-276.
- SONG, L., RAWAL, B., NEMETH, J. A. & HAURA, E. B. 2011. JAK1 activates STAT3 activity in non-small-cell lung cancer cells and IL-6 neutralizing antibodies can suppress JAK1-STAT3 signaling. *Mol Cancer Ther*, 10, 481-94.
- STAAF, J., ISAKSSON, S., KARLSSON, A., JÖNSSON, M., JOHANSSON, L., JÖNSSON, P., BOTLING, J., MICKE, P., BALDETORP, B. & PLANCK, M. 2013. Landscape of somatic allelic imbalances and copy number alterations in human lung carcinoma. *International journal of cancer*, 132, 2020-2031.
- STEWART, M. L., FIRE, E., KEATING, A. E. & WALENSKY, L. D. 2010. The MCL-1 BH3 helix is an exclusive MCL-1 inhibitor and apoptosis sensitizer. *Nature chemical biology*, 6, 595-601.

- SWANTON, C. 2014. Cancer evolution: the final frontier of precision medicine? *Annals of Oncology*, 25, 549-551.
- TAIT, S. W. & GREEN, D. R. 2010. Mitochondria and cell death: outer membrane permeabilization and beyond. *Nature reviews Molecular cell biology*, 11, 621-632.
- TAKASHIMA, A. & FALLER, D. V. 2013. Targeting the RAS oncogene. *Expert Opin Ther Targets*, 17, 507-31.
- TO, K.-F., TONG, J. H., YEUNG, K. S., LUNG, R. W., LAW, P. P., CHAU, S. L., KANG, W., TONG, C. Y., CHOW, C. & CHAN, A. W. 2013a. Detection of ALK rearrangement by immunohistochemistry in lung adenocarcinoma and the identification of a novel EML4-ALK variant. *Journal of Thoracic Oncology*, 8, 883-891.
- TO, M. D., ROSARIO, R., WESTCOTT, P. M., BANTA, K. L. & BALMAIN, A. 2013b. Interactions between wild-type and mutant Ras genes in lung and skin carcinogenesis. *Oncogene*, 32, 4028-4033.
- TONG, M. & TAIRA, R. K. Improving the accuracy of therapy descriptions in clinical trials using a bottom-up approach. AMIA Annual Symposium Proceedings, 2012. American Medical Informatics Association, 1393.
- TOSCHI, L., FINOCCHIARO, G., NGUYEN, T. T., SKOKAN, M. C., GIORDANO, L., GIANONCELLI, L., PERRINO, M., SIRACUSANO, L., DI TOMMASO, L. & INFANTE, M. 2014. Increased SOX2 gene copy number is associated with FGFR1 and PIK3CA gene gain in non-small cell lung cancer and predicts improved survival in early stage disease. *PloS one*, 9, e95303.
- TOWNSEND, K. J., ZHOU, P., QIAN, L., BIESZCZAD, C. K., LOWREY, C. H., YEN, A. & CRAIG, R. W. 1999. Regulation of MCL1 through a serum response factor/Elk-1-mediated mechanism links expression of a viability-promoting member of the BCL2 family to the induction of hematopoietic cell differentiation. *Journal of Biological Chemistry*, 274, 1801-1813.
- TRAVIS, W., BRAMBILLA, E., NICHOLSON, A., YATABE, Y., AUSTIN, J., BEASLEY, M., CHIRIEAC, L., DACIC, S., DUHIG, E. & FLIEDER, D. 2015. The 2015 World Health Organization Classification of Lung Tumors: Impact of Genetic, Clinical and Radiologic Advances Since the 2004 Classification. *Journal of thoracic oncology: official publication of the International Association for the Study of Lung Cancer*, 10, 1243.
- TRAVIS, W. D. 2011. Pathology of lung cancer. *Clinics in chest medicine*, 32, 669-692.
- TRAVIS, W. D., BRAMBILLA, E., NOGUCHI, M., NICHOLSON, A. G., GEISINGER, K. R., YATABE, Y., BEER, D. G., POWELL, C. A., RIELY, G. J. & VAN SCHIL, P. E. 2011. International association for the study of lung cancer/american thoracic society/european respiratory society international multidisciplinary classification of lung adenocarcinoma. *Journal of Thoracic Oncology*, 6, 244-285.
- TSAO, A. S., MCDONNELL, T., LAM, S., PUTNAM, J. B., BEKELE, N., HONG, W. K. & KURIE, J. M. 2003. Increased phospho-AKT (Ser473) expression in bronchial dysplasia implications for lung cancer prevention studies. *Cancer Epidemiology Biomarkers & Prevention*, 12, 660-664.

- TSE, L. A., YU, I. T.-S., WANG, X.-R., QIU, H. & AU, J. S. K. 2012. Synergistic effect between alcohol consumption and familial susceptibility on lung cancer risk among Chinese men. *PLoS one*, 7, e40647.
- TUONONEN, K., MÄKI-NEVALA, S., SARHADI, V. K., WIRTANEN, A., RÖNTY, M., SALMENKIVI, K., ANDREWS, J. M., TELARANTA-KEERIE, A. I., HANNULA, S. & LAGSTRÖM, S. 2013. Comparison of Targeted Next-Generation Sequencing (NGS) and Real-Time PCR in the Detection of EGFR, KRAS, and BRAF Mutations on Formalin-Fixed, Paraffin-Embedded Tumor Material of Non-Small Cell Lung Carcinoma—Superiority of NGS. *Genes, Chromosomes and Cancer*, 52, 503-511.
- TURNER, M. C., KREWSKI, D., POPE III, C. A., CHEN, Y., GAPSTUR, S. M. & THUN, M. J. 2011. Long-term ambient fine particulate matter air pollution and lung cancer in a large cohort of never-smokers. *American journal of respiratory and critical care medicine*, 184, 1374-1381.
- VAIRA, V., FEDELE, G., PYNE, S., FASOLI, E., ZADRA, G., BAILEY, D., SNYDER, E., FAVERSANI, A., COGGI, G. & FLAVIN, R. 2010. Preclinical model of organotypic culture for pharmacodynamic profiling of human tumors. *Proceedings of the National Academy of Sciences*, 107, 8352-8356.
- VAN SCHIL, P. E., ASAMURA, H., RUSCH, V. W., MITSUDOMI, T., TSUBOI, M., BRAMBILLA, E. & TRAVIS, W. D. 2012. Surgical implications of the new IASLC/ATS/ERS adenocarcinoma classification. *European Respiratory Journal*, 39, 478-486.
- VICENT, S., LOPEZ-PICAZO, J. M., TOLEDO, G., LOZANO, M. D., TORRE, W., GARCIA-CORCHON, C., QUERO, C., SORIA, J., MARTIN-ALGARRA, S. & MANZANO, R. G. 2004. ERK1/2 is activated in non-small-cell lung cancer and associated with advanced tumours. *British journal of cancer*, 90, 1047-1052.
- VILLAFLORES, V. M. & SALGIA, R. 2013. Targeted agents in non-small cell lung cancer therapy: What is there on the horizon? *Journal of carcinogenesis*, 12, 7.
- VOGELSTEIN, B., PAPADOPOULOS, N., VELCULESCU, V. E., ZHOU, S., DIAZ, L. A. & KINZLER, K. W. 2013. Cancer genome landscapes. *science*, 339, 1546-1558.
- VOGLER, M. 2014. Targeting BCL2-proteins for the treatment of solid tumours. *Advances in medicine*, 2014.
- VOORTMAN, J., CHECINSKA, A., GIACCONE, G., RODRIGUEZ, J. A. & KRUYT, F. A. 2007. Bortezomib, but not cisplatin, induces mitochondria-dependent apoptosis accompanied by up-regulation of noxa in the non-small cell lung cancer cell line NCI-H460. *Molecular cancer therapeutics*, 6, 1046-1053.
- WANG, C.-Y., DENG, J.-Y., CAI, X.-W., FU, X.-L., LI, Y., ZHOU, X.-Y., WU, X.-H., HU, X.-C., FAN, M. & XIANG, J.-Q. 2015. High EGFR and low p-Akt expression is associated with better outcome after nimotuzumab-containing treatment in esophageal cancer patients: preliminary clinical result and testable hypothesis. *Oncotarget*, 6, 18674.
- WANG, F., FLANAGAN, J., SU, N., WANG, L.-C., BUI, S., NIELSON, A., WU, X., VO, H.-T., MA, X.-J. & LUO, Y. 2012. RNAscope: a novel in

- situ RNA analysis platform for formalin-fixed, paraffin-embedded tissues. *The Journal of Molecular Diagnostics*, 14, 22-29.
- WATANABE, H., MA, Q., PENG, S., ADELMANT, G., SWAIN, D., SONG, W., FOX, C., FRANCIS, J. M., PEDAMALLU, C. S. & DELUCA, D. S. 2014. SOX2 and p63 colocalize at genetic loci in squamous cell carcinomas. *The Journal of clinical investigation*, 124, 1636-1645.
- WEEDEN, C., SOLOMON, B. & ASSELIN-LABAT, M. 2015. FGFR1 inhibition in lung squamous cell carcinoma: questions and controversies. *Cell Death Discovery*, 1.
- WEI, D., ZHANG, Q., SCHREIBER, J. S., PARSELS, L. A., ABULWERDI, F. A., KAUSAR, T., LAWRENCE, T. S., SUN, Y., NIKOLOVSKA-COLESKA, Z. & MORGAN, M. A. 2015. Targeting Mcl-1 for Radiosensitization of Pancreatic Cancers. *Translational Oncology*, 8, 47-54.
- WEI, G., MARGOLIN, A. A., HAERY, L., BROWN, E., CUCOLO, L., JULIAN, B., SHEHATA, S., KUNG, A. L., BEROUKHIM, R. & GOLUB, T. R. 2012. Chemical genomics identifies small-molecule MCL1 repressors and BCL-xL as a predictor of MCL1 dependency. *Cancer cell*, 21, 547-562.
- WESARG, E., HOFFARTH, S., WIEWRODT, R., KRÖLL, M., BIESTERFELD, S., HUBER, C. & SCHULER, M. 2007. Targeting BCL-2 family proteins to overcome drug resistance in non-small cell lung cancer. *International Journal of Cancer*, 121, 2387-2394.
- WHITSETT, T. G., MATHEWS, I. T., CARDONE, M. H., LENA, R. J., PIERCEALL, W. E., BITTNER, M., SIMA, C., LOBELLO, J., WEISS, G. J. & TRAN, N. L. 2014. Mcl-1 mediates TWEAK/Fn14-induced non-small cell lung cancer survival and therapeutic response. *Molecular Cancer Research*, 12, 550-559.
- WIDMANN, C., GIBSON, S., JARPE, M. B. & JOHNSON, G. L. 1999. Mitogen-activated protein kinase: conservation of a three-kinase module from yeast to human. *Physiological reviews*, 79, 143-180.
- WIENS, A. L., CHENG, L., BERTSCH, E. C., JOHNSON, K. A., ZHANG, S. & HATTAB, E. M. 2012. Polysomy of chromosomes 1 and/or 19 is common and associated with less favorable clinical outcome in oligodendrogliomas: fluorescent in situ hybridization analysis of 84 consecutive cases. *Journal of Neuropathology & Experimental Neurology*, 71, 618-624.
- WILBERTZ, T., WAGNER, P., PETERSEN, K., STIEDL, A.-C., SCHEBLE, V. J., MAIER, S., REISCHL, M., MIKUT, R., ALTORKI, N. K. & MOCH, H. 2011. SOX2 gene amplification and protein overexpression are associated with better outcome in squamous cell lung cancer. *Modern Pathology*, 24, 944-953.
- WISTUBA, I. I. 2007. Genetics of preneoplasia: lessons from lung cancer. *Current molecular medicine*, 7, 3-14.
- WISTUBA, I. I. 2012. Molecular pathogenesis of non-small cell lung carcinomas. *Journal of Lung Cancer*, 11, 12-20.
- WISTUBA, I. I., MAO, L. & GAZDAR, A. F. 2002. Smoking molecular damage in bronchial epithelium. *Oncogene*, 21, 7298-7306.
- WU, M., SIROTA, M., BUTTE, A. & CHEN, B. Characteristics of drug combination therapy in oncology by analyzing clinical trial data on ClinicalTrials.gov. Pacific Symposium on Biocomputing. Pacific Symposium on Biocomputing, 2014. NIH Public Access, 68-79.

- WU, W., ONN, A., ISOBE, T., ITASAKA, S., LANGLEY, R. R., SHITANI, T., SHIBUYA, K., KOMAKI, R., RYAN, A. J. & FIDLER, I. J. 2007. Targeted therapy of orthotopic human lung cancer by combined vascular endothelial growth factor and epidermal growth factor receptor signaling blockade. *Molecular cancer therapeutics*, 6, 471-483.
- XU, W., ZHAI, Z., HUANG, K., ZHANG, N., YUAN, Y., SHANG, Y. & LUO, Y. 2012. A novel universal primer-multiplex-PCR method with sequencing gel electrophoresis analysis. *PLoS One*, 7, e22900.
- YANG, P., CERHAN, J., VIERKANT, R., OLSON, J., VACHON, C., LIMBURG, P., PARKER, A., ANDERSON, K. & SELLERS, T. 2002. Adenocarcinoma of the lung is strongly associated with cigarette smoking: further evidence from a prospective study of women. *American journal of epidemiology*, 156, 1114-1122.
- YANO, T., HARO, A., SHIKADA, Y., MARUYAMA, R. & MAEHARA, Y. 2011. Non-small cell lung cancer in never smokers as a representative 'non-smoking-associated lung cancer': epidemiology and clinical features. *International journal of clinical oncology*, 16, 287-293.
- YE, T., XIONG, Y., YAN, Y., XIA, Y., SONG, X., LIU, L., LI, D., WANG, N., ZHANG, L. & ZHU, Y. 2014. The anthelmintic drug niclosamide induces apoptosis, impairs metastasis and reduces immunosuppressive cells in breast cancer model. *PLoS one*, 9, e85887.
- YIP, P. Y. 2015. Phosphatidylinositol 3-kinase-AKT-mammalian target of rapamycin (PI3K-Akt-mTOR) signaling pathway in non-small cell lung cancer. *Translational lung cancer research*, 4, 165.
- YOU, S., LI, R., PARK, D., XIE, M., SICA, G. L., CAO, Y., XIAO, Z.-Q. & DENG, X. 2014. Disruption of STAT3 by niclosamide reverses radioresistance of human lung cancer. *Molecular cancer therapeutics*, 13, 606-616.
- YOULDEN, D. R., CRAMB, S. M. & BAADE, P. D. 2008. The international epidemiology of lung cancer: geographical distribution and secular trends. *Journal of Thoracic Oncology*, 3, 819-831.
- ZHANG, H., BEREZOV, A., WANG, Q., ZHANG, G., DREBIN, J., MURALI, R. & GREENE, M. I. 2007. ErbB receptors: from oncogenes to targeted cancer therapies. *Journal of Clinical Investigation*, 117, 2051.
- ZHANG, H., GUTTIKONDA, S., ROBERTS, L., UZIEL, T., SEMIZAROV, D., ELMORE, S., LEVERSON, J. & LAM, L. 2011. Mcl-1 is critical for survival in a subgroup of non-small-cell lung cancer cell lines. *Oncogene*, 30, 1963-1968.
- ZHANG, H., XUE, J., HESSLER, P., TAHIR, S. K., CHEN, J., JIN, S., SOUERS, A. J., LEVERSON, J. D. & LAM, L. T. 2015. Genomic analysis and selective small molecule inhibition identifies BCL-X L as a critical survival factor in a subset of colorectal cancer. *Molecular cancer*, 14, 1.
- ZHANG, X.-M., LI, B.-L., SONG, M. & SONG, J.-Y. 2004. Expression and significance of ERK protein in human breast carcinoma. *Chinese Journal of Cancer Research*, 16, 269-273.
- ZHANG, X., LU, F., WANG, J., YIN, F., XU, Z., QI, D., WU, X., CAO, Y., LIANG, W. & LIU, Y. 2013. Pluripotent stem cell protein Sox2 confers sensitivity to LSD1 inhibition in cancer cells. *Cell reports*, 5, 445-457.

- ZHANG, Y. & HE, J. 2013. The development of targeted therapy in small cell lung cancer. *Journal of thoracic disease*, 5, 538-548.
- ZHAO, J., XIN, M., WANG, T., ZHANG, Y. & DENG, X. 2009. Nicotine enhances the antiapoptotic function of Mcl-1 through phosphorylation. *Molecular Cancer Research*, 7, 1954-1961.
- ZHONG, C.-Y., ZHOU, Y.-M., DOUGLAS, G. C., WITSCHI, H. & PINKERTON, K. E. 2005. MAPK/AP-1 signal pathway in tobacco smoke-induced cell proliferation and squamous metaplasia in the lungs of rats. *Carcinogenesis*, 26, 2187-2195.
- ZHOU, L., QIU, T., XU, J., WANG, T., WANG, J., ZHOU, X., HUANG, Z., ZHU, W., SHU, Y. & LIU, P. 2013. miR-135a/b modulate cisplatin resistance of human lung cancer cell line by targeting MCL1. *Pathology & Oncology Research*, 19, 677-683.
- ZHUANG, L., LEE, C. S., SCOLYER, R. A., MCCARTHY, S. W., ZHANG, X. D., THOMPSON, J. F. & HERSEY, P. 2007. Mcl-1, Bcl-XL and Stat3 expression are associated with progression of melanoma whereas Bcl-2, AP-2 and MITF levels decrease during progression of melanoma. *Modern pathology*, 20, 416-426.